University of Alberta

Structural, Metamorphic, and Plutonic History of Rocks Adjacent to Shuswap Lake, British Columbia: Evidence of Early to Middle Paleozoic Deformation

by

Nadya Marie Slemko

A thesis submitted to the Faculty of Graduate Studies and Research in partial fulfillment

of the requirements for the degree of Master of Science

Department of Earth and Atmospheric Sciences

Edmonton, Alberta

Fall 2000

0-612-59880-2

University of Alberta

Library Release Form

Name of Author: Nadya Marie Slemko

Title of Thesis: Structural, Metamorphic, and Plutonic History of Rocks Adjacent to Shuswap Lake, British Columbia: Evidence of Early to Middle Paleozoic Deformation

Degree: Master of Science

Year this Degree Granted: 2000

N. Slemko

18419-82 Avenue
Edmonton, AB
T5T 1G2

Oct. 2, 2000

University of Alberta

Faculty of Graduate Studies and Research

The undersigned certify that they have read, and recommend to the Faculty of Graduate Studies and Research for acceptance, a thesis entitled Structural, Metamorphic, and Plutonic History of Rocks Adjacent to Shuswap Lake, British Columbia: Evidence of Early to Middle Paleozoic Deformation submitted by Nadya Marie Slemko in partial fulfillment of the requirements for the degree of Master of Science.

October 02, 2000

Philippe Erdmer

Larry Heaman

D. R. Schmitt

ABSTRACT

This study focuses on rocks of the southern Omineca Belt near Shuswap Lake, B.C., deposited at the margin of Ancestral North America. The contact between two different lithometamorphic assemblages, the Eagle Bay Formation and the Queest Mountain assemblage, and their contact relationships with a pluton, are studied to provide constraints on the Paleozoic tectonic history of the area.

The Queest Mountain assemblage is separated from the Eagle Bay Formation by the Queest Mountain fault, dipping 16 to 30 degrees north. Pressure and temperature differences across this fault suggest 14 to 25 km of normal displacement. The pluton, dated at 365.9 ± 2.7 Ma by U-Pb zircon geochronology, and correlated with the Mount Fowler Batholith, cuts foliation in the country rock, and cross-cuts the Queest Mountain fault, recording Early to Middle Paleozoic compressional deformation and margin-parallel extension, likely related to subduction and intra-arc tectonism, possibly correlative with the Antler orogeny.

ACKNOWLEDGMENTS

Fieldwork was supported by the Geological Survey of Canada and Natural Sciences and Engineering Research Council of Canada grants to Philippe Erdmer. The University of Alberta and NSERC provided life-supporting funding during this study.

I would like to thank my supervisors, Philippe Erdmer of the University of Alberta and Robert I. Thompson of the Geological Survey of Canada, who provided guidance throughout this project.

Wes Groome and Krista Walker provided assistance in the field, and worked diligently through floods and heatwaves. Ken Daughtry took the time to show me many key outcrops and to discuss various interpretations in the field.

Larry Heaman and the geochronology lab technicians at the University of Alberta provided substantial assistance with the U-Pb dating of zircons. Tom Chacko and Lang Shi helped with sample selection and microprobe analysis for geothermobarometry.

I would like to thank Karen Fallas for enduring hundreds of questions on everything from using computer programs to writing my thesis; her help is greatly appreciated.

Andrew Okulitch has provided numerous insightful comments on my work throughout the research and writing stages. Several e-mail discussions with Ken Daughtry and Paul Schiarizza, and also discussions with fellow grad students Jennifer Unterschutz and Paul Glombick, have helped with interpreting my data and fitting it into the regional perspective.

Several people have read and commented on parts of my thesis, and I would like to thank them all: Andrew Okulitch, Tom Chacko, Karen Fallas, Jennifer Unterschutz, and Kim Toope.

I would like to thank my managers and colleagues at Imperial Oil for their patience and support during the final stages of my thesis, and the drafting department for help with several figures.

Finally, I would like to thank my parents for their support throughout my university studies.

TABLE OF CONTENTS

LIST OF TABLES

LIST OF FIGURES

LIST OF PLATES

LIST OF MAPS

CHAPTER 1

Introduction

GEOLOGICAL SETTING

It has been suggested that the Canadian Cordillera is an orogenic belt formed by the accretion of two allochthonous superterranes, or compilations of several smaller terranes, to the western margin of Ancestral North America (Monger, 1977; Coney *et al.*, 1980; Monger *et al.*, 1982). Terranes are blocks of crust that preserve a different geological history to adjacent terranes (Jones *et al.*, 1983; Monger and Berg, 1984). These accreted terranes are interpreted to be allochthonous because they have geological histories that show they formed at some distance from Ancestral North America (Gabrielse *et al.*, 1991). The Intermontane Superterrane (Monger, 1977; Coney *et al.*, 1980; Monger *et al.*, 1982) was interpreted to have been accreted to the margin during mid-Jurassic to mid-Cretaceous time (Archibald *et al.*, 1983) (Figure 1-1). The Insular Superterrane (Monger, 1977; Coney *et al.*, 1980; Monger *et al.*, 1982) was proposed to have been accreted during the Late Cretaceous to Paleocene (Archibald *et al.*, 1984) (Figure 1-1). The accretion of these superterranes resulted in compressional orogenic events in rocks to the east. The older event has been termed the Columbian Orogeny and the younger event the Laramide Orogeny (Gabrielse *et al.*, 1991) (Figure 1-2). More recent work, however, has suggested that some terranes might not be as exotic as once thought, and that the accretion history may be more complex than previously believed; for example Nelson and Mihalynuk (1993) and Mihalynuk *et al.* (1994) propose that the exotic Cache Creek terrane (Figure 1-3) was enclosed between two arcs of pericratonic Quesnellia and Stikinia terranes (Figure 1-3) in the Middle Jurassic. Although the history of terrance accretion is being reevaluated, there is abundant evidence for Middle Jurassic to Middle Cretaceous and Late Cretaceous to Paleocene events in the Canadian Cordillera. During the Early Tertiary, post-orogenic extension formed several low angle and listric normal faults (e.g. Johnson, 1994).

The Canadian Cordillera is composed of five morphogeological belts, each with a unique geological character (Figure 1-4). From east to west, they are the Foreland, Omineca, Intermontane, Coast, and Insular belts. The area focused on in this study is part of the Omineca Belt, an uplifted area that comprises mainly metamorphic and granitic rocks (Gabrielse *et al.*, 1991). The area studied in this thesis lies within the part of the Omineca Belt that consists of rocks of the Kootenay terrane (Figure 1-4) that were considered pericratonic with respect to Ancestral North America (Gabrielse *et al.*, 1991). However, recent work (Thompson and Daughtry, 1997) has shown that these rocks have a strong affinity with Ancestral North America, and are therefore not as exotic as once thought.

PURPOSE OF THIS INVESTIGATION

This study focuses on an area in the southern Omineca Belt, near Shuswap Lake, in the northern part of the Vernon map area (82L), British Columbia (Figure 1-3). In the Omineca Belt at this latitude, there is abundant evidence for Mesozoic and Early Tertiary compressional orogenesis (e.g. Reesor, 1965; Read and Brown, 1981; Okulitch, 1984;

Johnson, 1994) and also for Eocene extension (e.g. Johnson, 1989, 1990, 1994; Johnson and Brown, 1996). However, there is also sporadic evidence for older tectonic events in the Kootenay Arc (Figure 1-5) (Read and Wheeler, 1976; Klepacki, 1985; Gehrels and Smith, 1987) and the Purcell anticlinorium (Figure 1-5) (Root, 1987, 1993) to the east of the study area.

This study is part of a major Geological Survey of Canada initiative to study the Ancestral North American margin, and was suggested by R.I. Thompson (personal communication, 1997) because his preliminary investigations suggested that the geology of the area needed to be reexamined, and that Paleozoic deformation may be preserved. It is important to document this older deformation and to understand it with respect to the younger deformation that has also taken place. This area was specifically chosen for this study because it may be one of the few areas where the older deformation is preserved.

In the Vernon map area, the Eagle River Tertiary extension fault has been mapped (Johnson, 1989, 1990, 1994; Johnson and Brown, 1996). This fault juxtaposes high-grade rocks in the footwall to the east of the fault with lower-grade rocks in the hanging wall to the west. This thesis focuses on metasedimentary and metavolcanic rocks in the hanging wall of the Eagle River Fault. These rocks include the Mount Ida Group of Jones (1959) and the Mount Fowler suite granitoid gniess mapped by Okulitch *et al.* (1975).

In the study area, there are two different lithometamorphic assemblages, the Eagle Bay Formation (Jones, 1959) of the Mount Ida Group and an assemblage of mica schist and calcsilicate, called the Queest Mountain assemblage (Slemko and Thompson, 1998). The Queest Mountain assemblage was previously (Johnson, 1994) mapped as part of the

Eagle Bay Formation, but lithological differences indicated (Thompson and Daughtry, 1997) that the Queest Mountain assemblage may have a different affinity. This thesis examines the contact between the Eagle Bay Formation and the Queest Mountain assemblage, which is interpreted as a fault, termed the Queest Mountain fault. The nature, geometry, and extent of the Queest Mountain fault is studied in this thesis. As well, the regional affinity of the Queest Mountain assemblage is examined, and the possibility that the Queest Mountain assemblage may be correlative to Neoproterozoic rocks in the area (Thompson and Daughtry, 1997) is evaluated.

The age and nature of the Mount Fowler suite has not been well documented. The granitoid pluton within the study area was dated (Okulitch *et al.*, 1975) using U-Pb geochronological techniques of 25 years ago, which had limitations on the accuracy and precision attainable. Many recent advances in geochronological techniques have been made, so the age of the pluton and the correlation of the pluton to the Mount Fowler batholith need to be reevaluated using current geochronological methods. Also, Okulitch *et al.* (1975) only dated the pluton at one location within the study area, and it is important to confirm that all the granitoid rocks belong to a single pluton, as suggested by mapping. By studying the contact relationship between the pluton and the rocks it intrudes as well as the internal deformation of the pluton, constraints on the timing of deformation and metamorphism of the country rock, including motion on the Queest Mountain fault, can be evaluated. Study of the pluton has aided in finding evidence of a pre-Late Devonian tectonic event in the study area.

Specifically, this thesis focuses on five aspects:

(1) the internal stratigraphy of the Mount Ida Group;

(2) the nature and regional affinity of the rocks, termed the Queest Mountain assemblage, that do not fit within the Eagle Bay Formation as previously mapped, and the nature of the contact between the Queest Mountain assemblage and the Eagle Bay Formation;

(3) the nature of the contact relationship of the pluton with the country rock and a comparison of the deformation of the pluton with that of the country rock;

(4) confirmation of the age of the granitoid intrusion and its relationship with the Mount Fowler batholith; and

(5) the structural and metamorphic history of the study area and how it relates to regional studies.

Chapter 1 of this thesis provides definitions and a summary of previous work. Geological field mapping focused on details of the internal stratigraphy and contact relationships of units of the Mount Ida Group, which are described in Chapter 2. The nature and extent of the Queest Mountain assemblage is also discussed, as well as the contact between the Queest Mountain assemblage and the Mount Ida Group. This study incorporates petrography and structural analysis to document lithologic and structural differences between the Mount Ida Group and the Queest Mountain assemblage, in order to demonstrate that the Queest Mountain assemblage is not part of the Eagle Bay Formation and to aid in identifying possible regional correlatives of the Queest Mountain assemblage. The Mount Ida Group and the Queest Mountain assemblage are intruded by a granitoid pluton; detailed petrography of the pluton and contact relationships between it and the host rocks are also discussed. Fabrics in the pluton are compared to those of the host rock. Chapter 3 documents geothermobarometry, undertaken to establish possible metamorphic differences between the Mount Ida Group and the Queest Mountain assemblage, which, if present, would aid in showing that the Queest Mountain assemblage is separate from the Eagle Bay Formation and in finding regional correlatives of the Queest Mountain assemblage. Geochronology, described in Chapter 4, is used to confirm the age of the granitoid pluton and confirm its correlation (Okulitch *et al.*, 1975) with the Mount Fowler batholith. Chapter 5 provides a summary of this thesis and relates this work to regional geology and Cordilleran tectonic evolution.

The evidence presented in this thesis shows that the Eagle Bay Formation and the Queest Mountain assemblage are lithologically and metamorphically distinct units separated by a probable normal fault, termed the Queest Mountain fault. The granitoid pluton is Late Devonian in age and is correlative with the Mount Fowler batholith. Contact relationships between the pluton and the country rocks show that the pluton clearly cuts foliation in the Eagle Bay Formation and the Queest Mountain assemblage and therefore a record of pre-Late Devonian deformation is preserved. As well, the pluton likely cuts the Queest Mountain normal fault, preserving a record of probable pre-Late Devonian extension. These are important findings because they provide evidence for an Early to Middle Paleozoic tectonic event, supporting evidence found elsewhere in the southern Canadian Cordillera (e.g. Read and Wheeler, 1976; Klepacki, 1985; Root, 1987).

PREVIOUS WORK

Geological mapping in the Vernon map area began with Dawson (1898), who termed the metamorphic rocks in most of the northern part of the Vernon map area the 'Shuswap Series' and proposed, based on lithologic similarities, that they were correlative with Archean rocks of the Canadian Shield. Daly (1915) suggested that the rocks were part of a 'Shuswap Terrane' (Figure 1-6) of "Beltian" (Proterozoic) to Paleozoic age. Daly (1915) proposed that these rocks were metamorphosed in the Precambrian, whereas Brock (1934) suggested that the metamorphism was associated with the intrusion of Mesozoic plutons. The presence of more than one metamorphic event was established, and both authors were subsequently proven correct (Okulitch, 1984).

Jones (1959) published a comprehensive map and report of the Vernon map area at 4 mile = 1 inch scale. The rocks of the 'Shuswap Terrane' near Shuswap Lake were divided by Jones (1959) into the Monashee Group in the east and the Mount Ida Group in the west, separated by a fault, the Eagle River Fault of Johnson (1990), that follows the Eagle River and Mara Lake and can be traced south down the Okanagan Valley to Vernon (Jones, 1959) (Figure 1-7 and Figure 1-8). The Monashee Group includes gneiss, schist, quartzite, marble, dolomite, slate, and phyllite (Jones, 1959). The Mount Ida Group consists of schist, limestone, and quartzite, and has been subdivided into several formations based on lithology (Jones, 1959).

The Monashee Group

Read and Brown (1981) subdivided the Monashee Group of Jones (1959), in the footwall of the Eagle River Fault, into the Monashee Complex and the Shuswap Complex (Figure 1-7 and Figure 1-8). This subdivision is based on lithologic differences and position below or above a west-dipping zone of mylonite up to 1 km thick, which is termed the Monashee Décollement. Within the Monashee Décollement, mylonitic fabrics show northeast-directed displacement, consistent with northeast-directed thrusting (McNicoll and Brown, 1995). The Monashee Décollement is interpreted as a crustal-scale ductile thrust fault with at least 100 km of northeasterly-directed thrust displacement (Brown *et al.*, 1992). Rocks of the Shuswap Complex in the hanging wall of the Monashee Décollement are interpreted to be thrust over the underlying rocks of the Monashee Complex during Mesozoic to Paleocene compression associated with the Laramide Orogeny (Brown *et al.*, 1986). The upper plate of the Monashee Décollement, which includes the Shuswap Complex as well as rocks of the Mount Ida Group in the hanging wall of the Eagle River Fault, is termed the Selkirk allochthon (Read and Brown, 1981).

The Monashee Complex, which lies below the Monashee Décollement, is divided into core zones in the structural highs or culminations of Frenchman Cap, Thor-Odin, and Valhalla domes, which are stratigraphic windows of older rock, and a younger cover sequence (Reesor, 1970). The core zones contain paragneiss intruded by 2000 - 2100 Ma plutons (Wanless and Reesor, 1975; Okulitch *et al.*, 1981; Parrish and Armstrong, 1983; Duncan, 1984; Carr, 1991; Parkinson, 1992). Deformation (gneissosity) in the core zones is found in 2077 ± 2 Ma orthogneiss, and is therefore younger than the orthogneiss, but is older than a 2051 ± 12 Ma amphibolite dyke which cuts the foliation (Crowley, 1999). Monazite from pelitic schist gives a metamorphic age of 2060 ± 1 Ma and titanite from amphibolite gneiss provides a metamorphic age of 1854 ± 13 Ma, suggesting that the core gneisses were metamorphosed twice in the Paleoproterozoic (Crowley, 1999). Details of the deformation or the metamorphic grade are unknown because of overprinting by Mesozoic and/or Tertiary orogenesis (Crowley, 1999). These core gneisses of the Monashee Complex are interpreted as Paleoproterozoic basement of Ancestral North America upon which younger rocks were deposited (Okulitch, 1984; Armstrong *et al.*, 1991; Crowley, 1999).

The overlying rocks, quartzite, metapelite, calcsilicate gneiss, marble, and amphibolite, are interpreted as a continental platform and rift succession (McMillan, 1973; Scammell and Brown, 1990). These rocks are of Neoproterozoic to mid-Paleozoic age (Parrish and Scammell, 1988; Höy and Godwin, 1988; Scammell and Parrish, 1993). These rocks are younger than 1862 ± 1 Ma orthogneiss on which the sediments were deposited, but older than a 1852 ± 4 Ma pegmatite that intrudes the cover sequence (Crowley, 1999). The cover sequence contains 1.99 Ga detrital zircons, interpreted to have been derived from rocks of a similar age in the Alberta basement, providing a link between rocks of the Monashee Complex and Ancestral North American basement rocks (Crowley, 1999). It has been suggested based on U-Pb data (Parrish, 1995; Crowley, 1997) that metamorphism of the cover sequence of the Monashee Complex occurred in the early Tertiary.

The rocks of the Shuswap Complex, which lie above the Monashee Décollement but still in the footwall of the Eagle River Tertiary extensional fault, are composed mostly of migmatitic gneiss and pegmatite, divided into the Three Valley and the Hunters Range assemblages based on lithological differences and structural position (Johnson, 1994; Johnson and Brown, 1996) (Figure 1-8). The Three Valley assemblage is composed of semipelitic paragneiss with boudins of amphibolite and less abundant pelitic schist and calcareous psammite (Johnson and Brown, 1996). The Hunters Range assemblage structurally overlies the Three Valley assemblage and comprises migmatitic garnet-sillimanite-biotite schist, quartzofeldspathic paragneiss, amphibolite, marble, calcsilicate gneiss, and biotite-hornblende granodioritic to dioritic gneiss (Johnson and Brown, 1996). The Hunters Range assemblage is correlated (Johnson, 1994), based on lithologic similarities and similar Sm-Nd and Sr data (Parkinson, 1992), with the Neoproterozoic Windermere Supergroup to the east. The Three Valley assemblage is interpreted (Johnson, 1994) to be pre-Windermere in age based on U-Pb zircon dating of amphibolite boudins at Three Valley Gap that suggests an age of at least 1.5 Ga, and a Sm-Nd model age of 2.0 Ga and high initial $^{87}Sr/^{86}Sr$ ratio that indicate crustal contamination or a crustal source (Parkinson, 1992; Armstrong *et al.*, 1991). Rocks of the Shuswap Complex preserve at least three episodes of penetrative deformation with peak metamorphic mineral growth during D_2 (Johnson, 1994). U-Pb geochronology suggests that the deformation ranges in age from Early Cretaceous (Scammell, 1993; Carr *et al.*, 1997) to Late Cretaceous or younger (Johnson, 1994), associated with the Laramide Orogeny and motion on the Monashee Décollement.

The Mount Ida Group

Based on lithology, the Mount Ida Group was subdivided by Jones (1959) into several formations of Precambrian age, although the reasons for the assigned ages are not mentioned. Jones (1959) mapped the structurally lowest formation of the Mount Ida Group that crops out in the study area, the Silver Creek Formation (Figure 1-8), as Precambrian mica schist and mica gneiss. The mica schist is intruded by numerous aplite and pegmatite sills and dykes, which prompted Daly (1915) to term it the 'sill-sediment complex.' The Tsalksom Formation is present regionally above the Silver Creek Formation (but is not observed cropping out in the study area) and includes chlorite schist, slate, and hornblende gneiss of possible Precambrian age (Jones, 1959). The Mara Formation, mapped by Jones (1959) as argillite, slate, sericite schist, chlorite schist, and limestone of Precambrian age, was proposed to overlie the Tsalkom Formation. Jones (1959) characterized the Precambrian Sicamous Formation as a flaggy or platy impure limestone, with white layers of calcite and black layers of graphite-sericite schist, that conformably overlies the Silver Creek and Tsalkom formations. The Eagle Bay Formation, which conformably overlies the Sicamous Formation, is composed mainly of chlorite schist and limestone (Jones, 1959). This is the uppermost formation in the Mount Ida Group of Jones (1959). Dawson (1899) and Daly (1915) both suggested that most of the Eagle Bay was volcanic in origin, whereas Jones (1959) proposed a combination of sedimentary rocks, limestone, and volcanic rocks of Precambrian age. The sedimentary and volcanic rocks are altered to chlorite-sericite schists (Jones, 1959).

The rock descriptions and terminologies of Jones (1959) are, with a few revisions and debates about ages and regional affinities, agreed upon by more recent authors (Campbell and Okulitch, 1973; Okulitch, 1974, 1979, 1989; Preto, 1981; Preto and Schiarizza, 1985; Schiarizza and Preto, 1987; Johnson, 1989, 1990, 1994). This work has been summarized in Figure 1-9. Major revisions and recent conclusions are discussed here.

U-Pb dating (R. Friedman and A.V. Okulitch, personal communication, 1999) of the Little Shuswap Gneiss that intrudes the Silver Creek Formation shows that the age of the gneiss is Devonian, implying a pre-Devonian age for the Silver Creek Formation. The Silver Creek Formation has been correlated based on lithological similarities (Okulitch, 1979; Johnson, 1990) with either the Broadview Formation of the Lardeau Group or the Windermere Supergroup and Hamill Group of Neoproterozoic to Early Cambrian age. Johnson (1994) prefers the latter correlation because restoration of approximately 30 km of normal dip-slip displacement on the Eagle River fault juxtaposes the Silver Creek Formation with rocks of presumed Windermere age in the Hunters Range assemblage, implying that the latter correlation is more likely. Lithological similarities also exist between the Silver Creek Formation and Hunters Range assemblage, supporting this correlation (Johnson, 1994). Thompson and Daughtry (1996) also suggest a correlation between the Silver Creek Formation and the Hunters Range assemblage.

Okulitch (1989) correlated the Tsalkom Formation with the Jowett Formation of the Lardeau Group to the east and proposed that it was Early Paleozoic in age.

The Mara Formation is no longer mapped as a separate unit, because the Tsalkom Formation sits directly above the Silver Creek Formation and below the Sicamous

Formation (Campbell and Okulitch, 1973). Rocks previously assigned to the Mara Formation are placed in the Silver Creek and Sicamous formations.

Correlation with the lithologically similar Index Formation of the Lardeau Group implies that the Sicamous Formation may be Cambrian to Ordovician in age (Okulitch, 1989; Johnson, 1994). Crinoid stems have been found in the Larch Hills, between Salmon Arm and Mara Lake, in rocks interpreted (personal communication from K.L. Daughtry to B.J. Johnson in Johnson, 1994) to be part of the Sicamous Formation; however the exact age of these fossils remains undetermined (Johnson, 1994), and therefore provides only an approximate age for the Sicamous Formation.

Mississippian conodonts collected from the Eagle Bay Formation near Adams Lake implied that the Eagle Bay Formation is at least partly Mississippian in age (Campbell and Okulitch, 1973). Okulitch *et al.* (1975) showed that the Eagle Bay Formation is intruded by a Late Devonian pluton, implying a pre-Late Devonian age for at least part of the Eagle Bay Formation. Acid metavolcanic rocks from Squaam Bay on Adams Lake, dated between 367 and 379 Ma by U-Pb zircon geochronology (Preto, 1981; Preto and Schiarizza, 1985), are also interpreted to be part of the Eagle Bay Formation. These metavolcanic rocks can be traced stratigraphically (P. Schiarizza, personal communication, 1999) into rocks that contain Mississippian fossils (Campbell and Okulitch, 1973) that were also interpreted to be part of the Eagle Bay Formation. Archaeocyathids collected from the Tshinakin Limestone member of the Eagle Bay Formation provided an Eocambrian age (B.S. Norford, unpublished internal report, Geological Survey of Canada, 1985). These data imply that the Eagle Bay Formation ranges in age from Cambrian to Mississippian. Johnson (1994) correlated the Eagle Bay Formation with the Lower Cambrian Badshot Formation and with the Hamill and Lardeau groups on the basis of lithological similarities and the occurrence of Lower Cambrian archaeocyathid fossils in a marble unit of the Eagle Bay Formation near Adams Lake to the northwest of the present study area (Schiarizza and Preto, 1987). This archaeocyathid fauna is representative of Lower Cambrian miogeoclinal strata, linking the Eagle Bay Formation to Ancestral North America (Schiarizza and Preto, 1987). Johnson (1990, 1994) interpreted a possible structural contact between the Sicamous and Eagle Bay formations, and placed the Silver Creek and Sicamous formations in the Mount Ida assemblage and termed the overlying rocks the Eagle Bay assemblage. Johnson (1990, 1994) subdivided the Eagle Bay assemblage into three units on the basis of lithological differences: Em, a marble; Ec, consisting of calcsilicate schist, marble, phyllite, quartzite, and schist; and Eq, comprising micaceous quartzite and schist.

Rocks of the Silver Creek, Sicamous, and Eagle Bay formations are interpreted to have undergone three phases of deformation (Johnson, 1994). According to Johnson (1994), the oldest of these three phases of deformation produced a gneissosity (S_1) in rocks of the Mount Fowler orthogneiss and a parallel schistosity (S_1), parallel to primary layering (S_0), in the metasedimentary rocks that the orthogniess intrudes, and must therefore be younger than the Late Devonian intrusion. Johnson's (1994) second phase of deformation folded S_0S_1 into F_2 folds and produced a schistosity (S_2) that is parallel or nearly parallel to S_0S_1 except in the hinges of F_2 folds, and is the most prominent fabric in the area. The youngest, or third, phase of deformation folded S_0S_1 and S_2 into broad open folds and pre-dates the intrusion of the Baldy batholith west of Adams Lake (Schiarizza and Preto, 1987), which has been dated at 116 ± 5 Ma (Calderwood *et al.*, 1990). Study of metamorphic mineral growth has indicated that peak metamorphism was syntectonic with the latest phase of deformation (Johnson, 1994). These data imply that the deformation and metamorphism preserved in rocks in the hanging wall of the Eagle River fault is older than that preserved in rocks of the Shuswap Complex in the footwall (Johnson, 1994). Deformation and metamorphism of the Silver Creek, Sicamous, and Eagle Bay formations is interpreted to have occurred during the Middle Jurassic to Early Cretaceous Columbian Orogeny (Schiarizza and Preto, 1987), whereas metamorphism preserved in the Shuswap Complex is Early to Late Cretaceous (see details on page 11 of this thesis).

Mount Fowler granitoid

An elongate pluton of granitoid gneiss, 3 to 5 km across, strikes at about 300 degrees for 70 km between Shuswap and Adams Lakes (Okulitch *et al.*, 1975) (Figure 1-10). This pluton, the Mount Fowler batholith, includes medium to coarse-grained granite, quartz monzonite, and granodiorite, with biotite, hornblende, and epidote as mafic minerals (Okulitch *et al.*, 1975). Foliation, defined by the alignment of biotite, and pencil lineation, defined by rods of quartz and feldspar, are locally present (Okulitch *et al.*, 1975). Sharp intrusive contact relationships are observed between the Mount Fowler batholith and the country rocks on Mount Fowler and east of Shuswap Lake (Okulitch *et al.*, 1975). Okulitch *et al.* (1975) also observed contact metamorphism, defined by changes in composition and a coarsening of grain size, accompanied by alkali metasomatism, defined by an increase in microcline and orthoclase in the country rocks near contacts with the pluton, within 100 m of the pluton. Okulitch *et al.* (1975) suggested that this contact metamorphism may be partly obscured by regional metamorphism that occurred during the Columbian and Laramide orogenies. Johnson (1994) observed quartz-calcite-actinolite-epidote skarn zones, interpreted to be related to contact metamorphism, in calcsilicate rocks adjacent to the Mount Fowler orthogneiss.

Okulitch *et al.* (1975) dated four zircon fractions, one from each of four locations of the Mount Fowler batholith, one to the east of Shuswap Lake within the area of the present study, and three to the west between Shuswap Lake and Adams Lake (Figure 1-10). The four U-Pb zircon dates plot on a single concordia diagram with an upper intercept of 372 ± 6 Ma, which is interpreted as the crystallization age of the pluton (Okulitch *et al.*, 1975). The fraction from within the study area of this thesis has a $^{207}Pb/^{206}Pb$ age of 376 ± 6 Ma. The age obtained for the pluton by Okulitch *et al.* (1975) cannot be considered precise by modern geochronologic standards, but does provide a Late Devonian age for the intrusion. The pluton intrudes Eagle Bay Formation rocks, thereby providing a constraint on the age of the Eagle Bay Formation (Okulitch *et al.*, 1975).

Eagle River Fault

Jones (1959) mapped lithologic differences between the Monashee Group and the Mount Ida Group, specifically the absence of schist, limestone, and basic volcanic rocks in the Monashee Group, which are abundant in the Mount Ida Group. It was also recognized that the Monashee Group is at a higher metamorphic grade than the Mount Ida

Group (Jones, 1959). For these reasons, Jones (1959) inferred a fault, along the valley between Sicamous and Vernon, that separates the Monashee Group from the Mount Ida Group (Figure 1-7).

Johnson (1989, 1990, 1994) and Johnson and Brown (1996) mapped the presence of high-grade rocks in the footwall of the fault to the east of the valley and lower-grade rocks in the hanging wall to the west, as well as the presence of mylonites in the Eagle River valley and near Mara Lake. The mylonites were interpreted to represent a low- to moderately-dipping shear zone, termed the Eagle River Fault (Johnson, 1989, 1990, 1994; Johnson and Brown, 1996). Mylonites in the footwall have shear-sense indicators which consistently show relative westward down-dip movement of the hanging wall, and the fault was interpreted as a west-dipping normal detachment (Johnson, 1990).

$^{40}Ar/^{39}Ar$ dating of amphiboles, from twelve samples of amphibolite and hornblende gneiss, was undertaken to determine cooling ages for the rocks (Johnson, 1994). Seven samples were from various locations within the Shuswap Complex in the footwall of the Eagle River Fault, east of the valley, and five samples were from various locations in the hanging wall, west of the valley but east of Adams Lake. Samples from the footwall yielded Late Paleocene to earliest Middle Eocene (50 to 59 Ma) plateau ages, while hanging wall samples yielded Mesozoic plateau ages ranging from 74 to 202 Ma (Johnson, 1994). Johnson (1994) interpreted these ages to mean that exhumation of the footwall, associated with normal faulting, occurred in the Paleocene to Eocene.

Footwall rocks are interpreted to have equilibrated at about 700 °C and 8 kbar during the Late Cretaceous (Nicholls *et al.*, 1991). In comparison, hornblende $^{40}Ar/^{39}Ar$

and K-Ar dates for hanging wall rocks show that these rocks cooled below 500 °C by about the same time (Johnson, 1994). Middle Eocene biotite and muscovite K-Ar dates suggest that the hanging wall rocks were above 280-300 °C at that time (Wanless *et al.*, 1978). Based on surface mapping (Johnson, 1994) and Lithoprobe seismic studies (Cook *et al.*, 1992), Johnson (1994) mapped the Eagle River fault as having a dip of ~14° to the west at the surface and flattening out into the middle crust. These geometric constraints and the metamorphic differences across the fault suggest 32 km of down to the west dip slip displacement on the Eagle River Fault (Johnson, 1994).

EVALUATION OF PREVIOUS WORK

Previous studies in the northern part of the Vernon map area have resulted in a greater understanding of the tectonic history of the southern Omineca Belt. However, several topics required clarification or further study, and are addressed in this thesis.

The fact that the Eagle Bay Formation ranges in age from Cambrian to Mississippian but is intruded by a Late Devonian pluton is a paradox that must be addressed. This thesis confirms the age of a pluton belonging to the Mount Fowler suite, implying a pre-Late Devonian age for the Eagle Bay Formation within the study area. It is possible that enough regional diversity exists that within the study area the older Eagle Bay Formation rocks were intruded by the Mount Fowler batholith, while regionally the Eagle Bay Formation continued to be deposited. Alternatively, the rocks that have been assigned to the Eagle Bay Formation may not belong to a single unit. Schiarizza and Preto (1987) suggested that a significant unconformity may be present between Cambrian

Eagle Bay Formation rocks and Devonian and Mississippian Eagle Bay Formation rocks, because contact relationships suggest that the younger package overlies different older units in different areas, and because parts of the Eagle Bay Formation are intruded by the Late Devonian Mount Fowler gneiss. Therefore, the Eagle Bay should be divided into two units, one that is Cambrian in age and is intruded by a Late Devonian pluton, and another that is Devonian and Mississippian. This thesis confirms that within the study area, the Eagle Bay Formation is older than Late Devonian, as proposed by Okulitch *et al.* (1975), so these rocks should be assigned to the Cambrian "Eagle Bay Formation."

Initial study also suggested that some rocks previously mapped as Eagle Bay Formation may have a different affinity. These rocks, termed the Queest Mountain assemblage, are described in this thesis. The contact between the Eagle Bay Formation and the Queest Mountain assemblage is interpreted as a fault. The Queest Mountain assemblage may be correlative to the Lichen assemblage of Johnson (1994), the Silver Creek Formation, the Hunters Range assemblage, and/or the Monashee Complex.

Previous studies of the Eagle Bay Formation and other units of the Mount Ida Group have provided evidence for Mesozoic deformation and metamorphism, which is compatible with other studies from the southern Canadian Cordillera. Preliminary investigations by R.I. Thompson suggested that Early to Middle Paleozoic deformation may be preserved in the area adjacent to Shuswap Lake, and therefore this study was undertaken to evaluate this possibility. Early to Middle Paleozoic deformation has been described by studies to the east in the Kootenay Arc (Read and Wheeler, 1976; Klepacki, 1985; Gehrels and Smith, 1987) and the Purcell Anticlinorium(Root, 1987, 1993), but would mean that a reevaluation of the geology of the Shuswap Lake area is needed. A pluton correlated with the Late Devonian Mount Fowler batholith intrudes the Eagle Bay Formation. Contact relationships between this pluton and the country rock were studied, and geochronology of the pluton was undertaken, to provide age constraints on deformation and metamorphism in the study area.

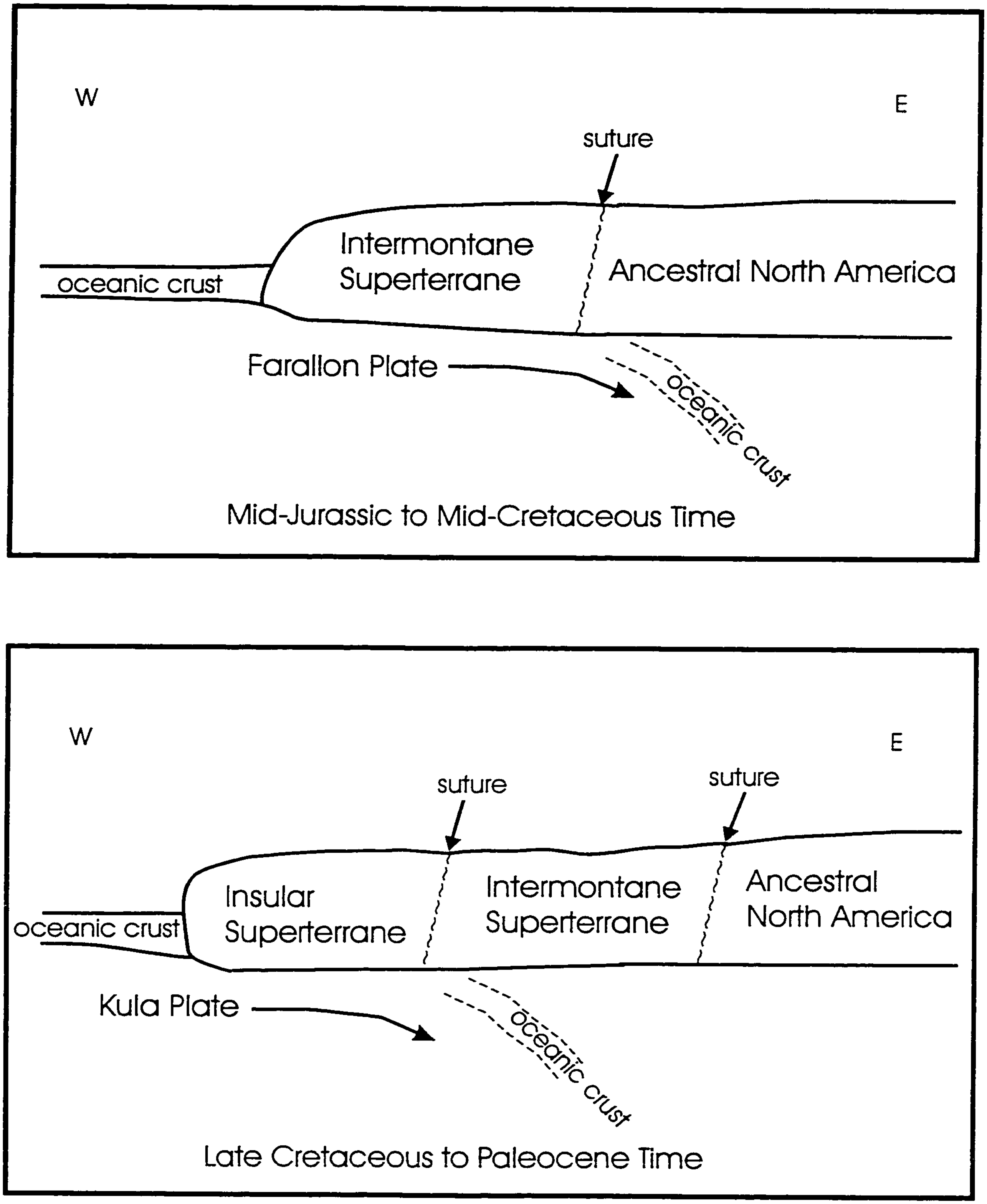

Figure 1-1: Schematic diagrams of the accretion of the Intermontane and Insular Superterranes to Ancestral North America

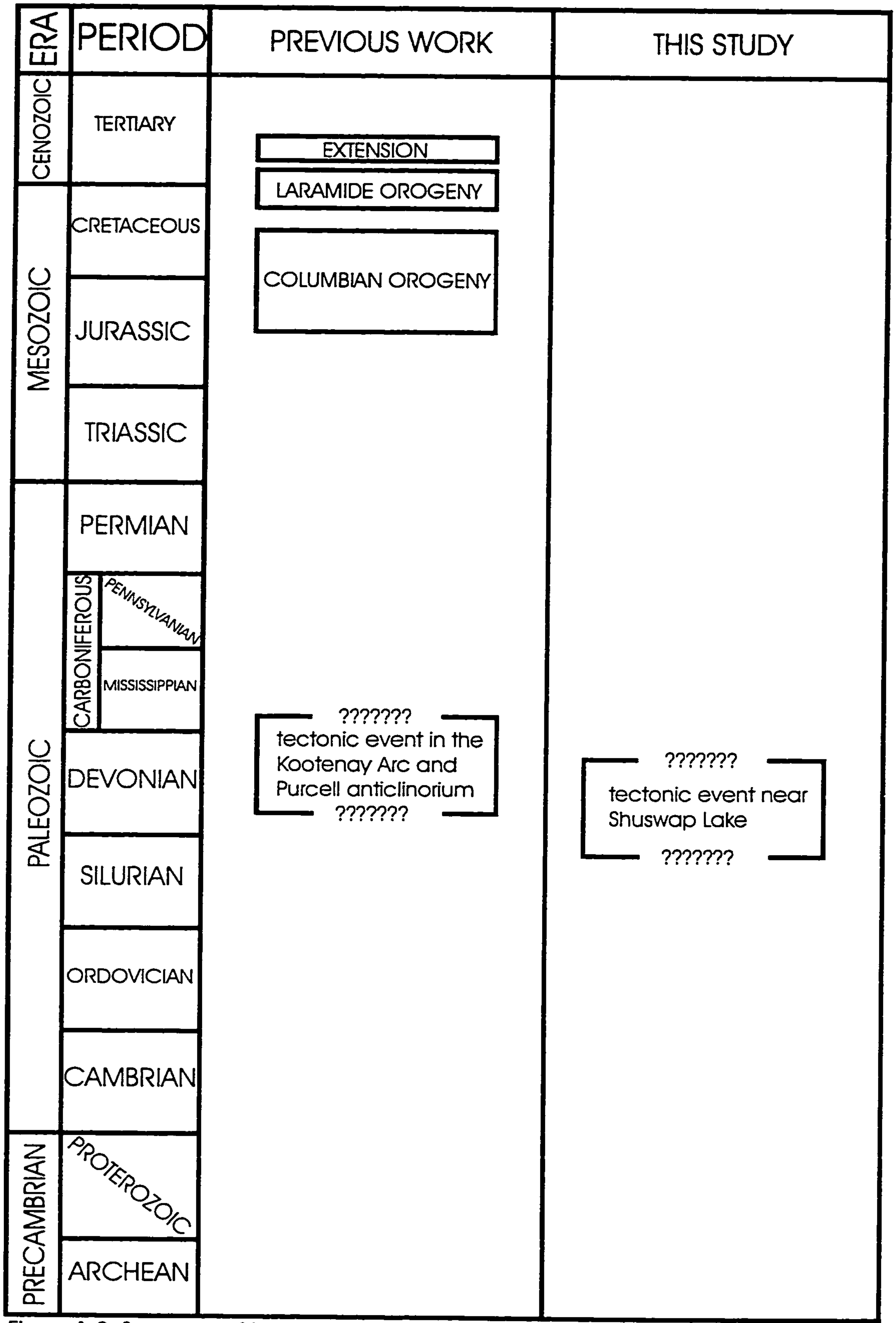

Figure 1-2: Summary of tectonic events in the southern Canadian Cordillera.

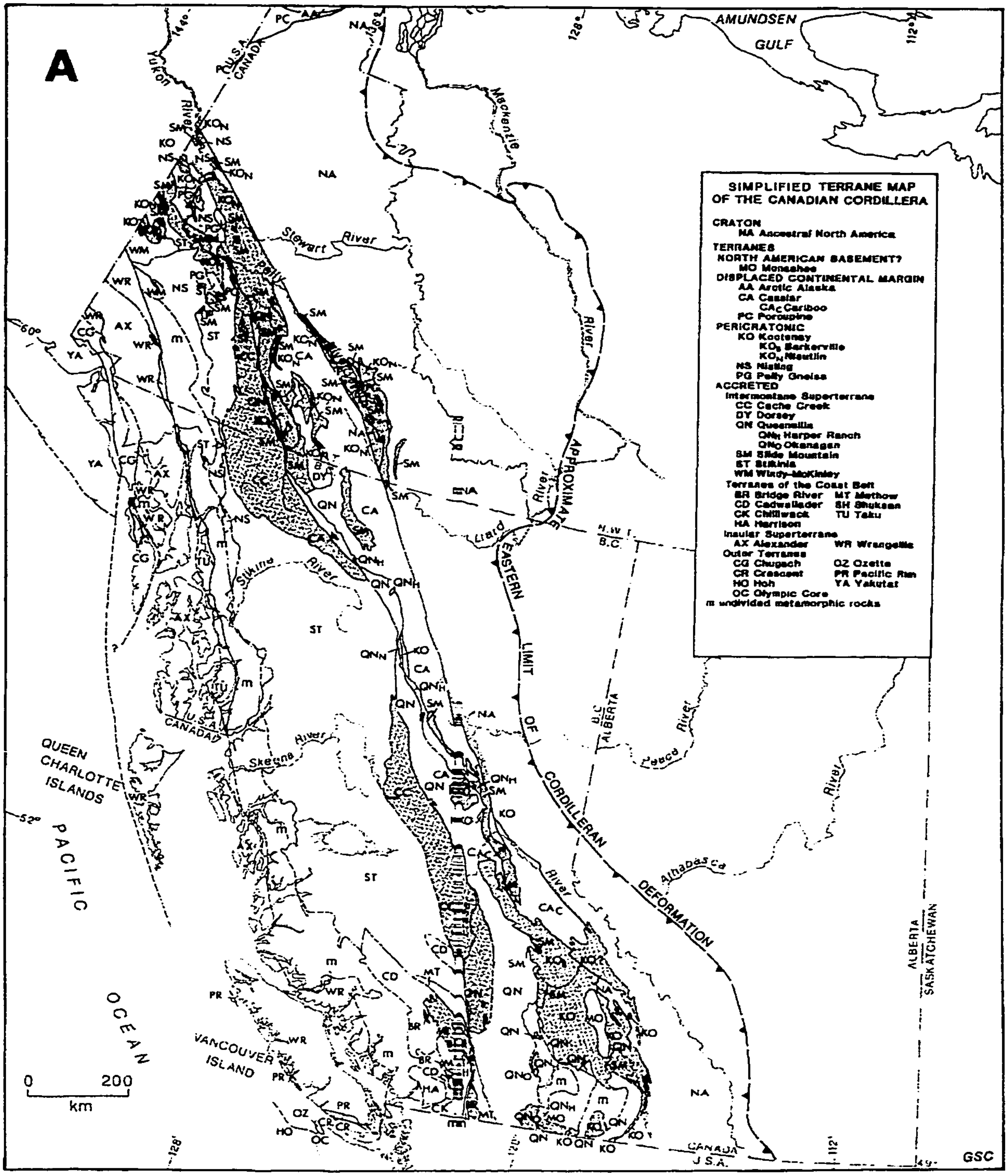

Figure 1-3: Simplified terrane map of the Canadian Cordillera. Grey shading represents oceanic and pericratonic terrane. From Gabrielse *et al.* (1991).

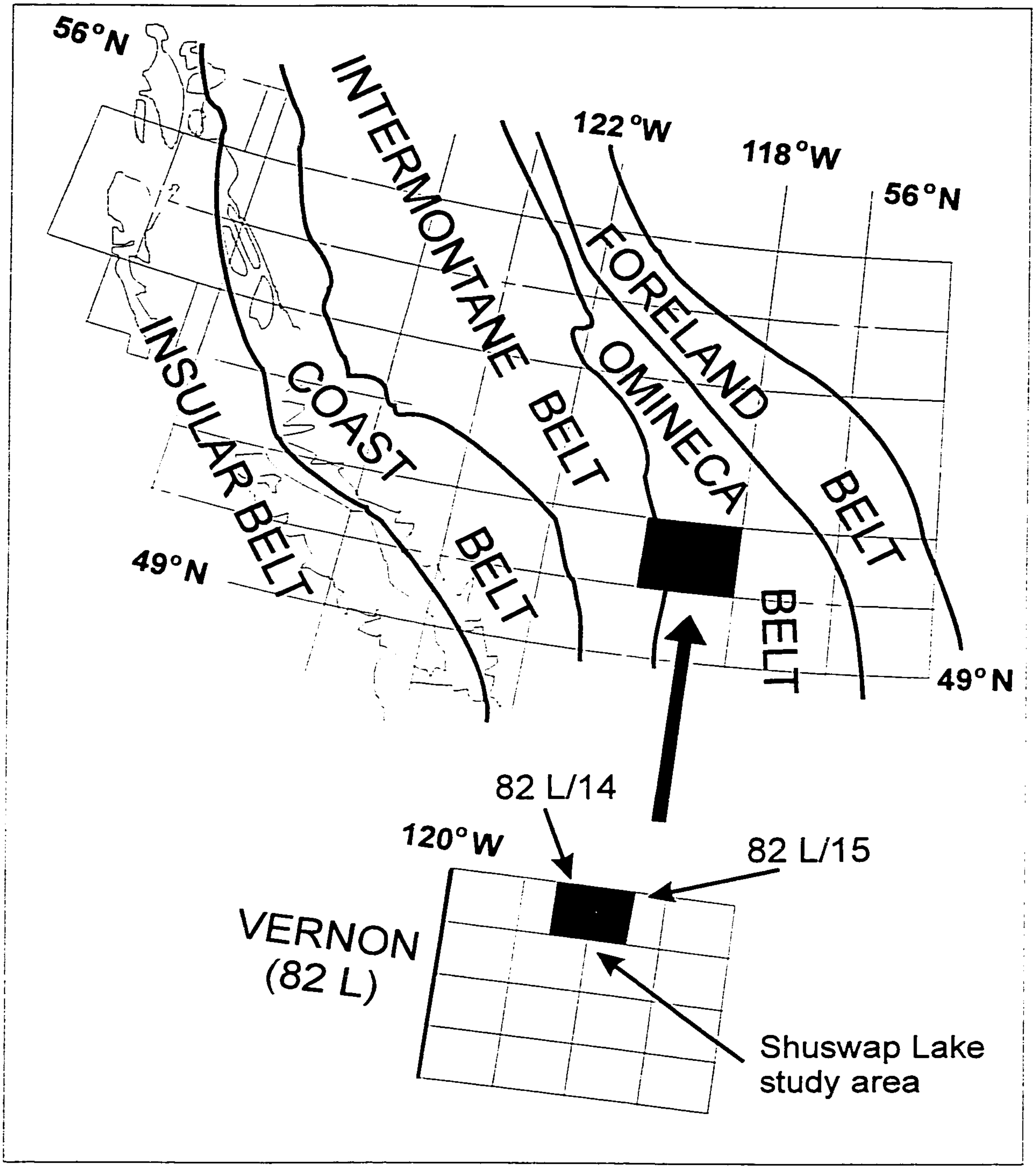

Figure 1-4: Location of NTS 1: 250 000 scale Vernon map area and study area for this study.
(modified from Gabrielse et al. (1991))

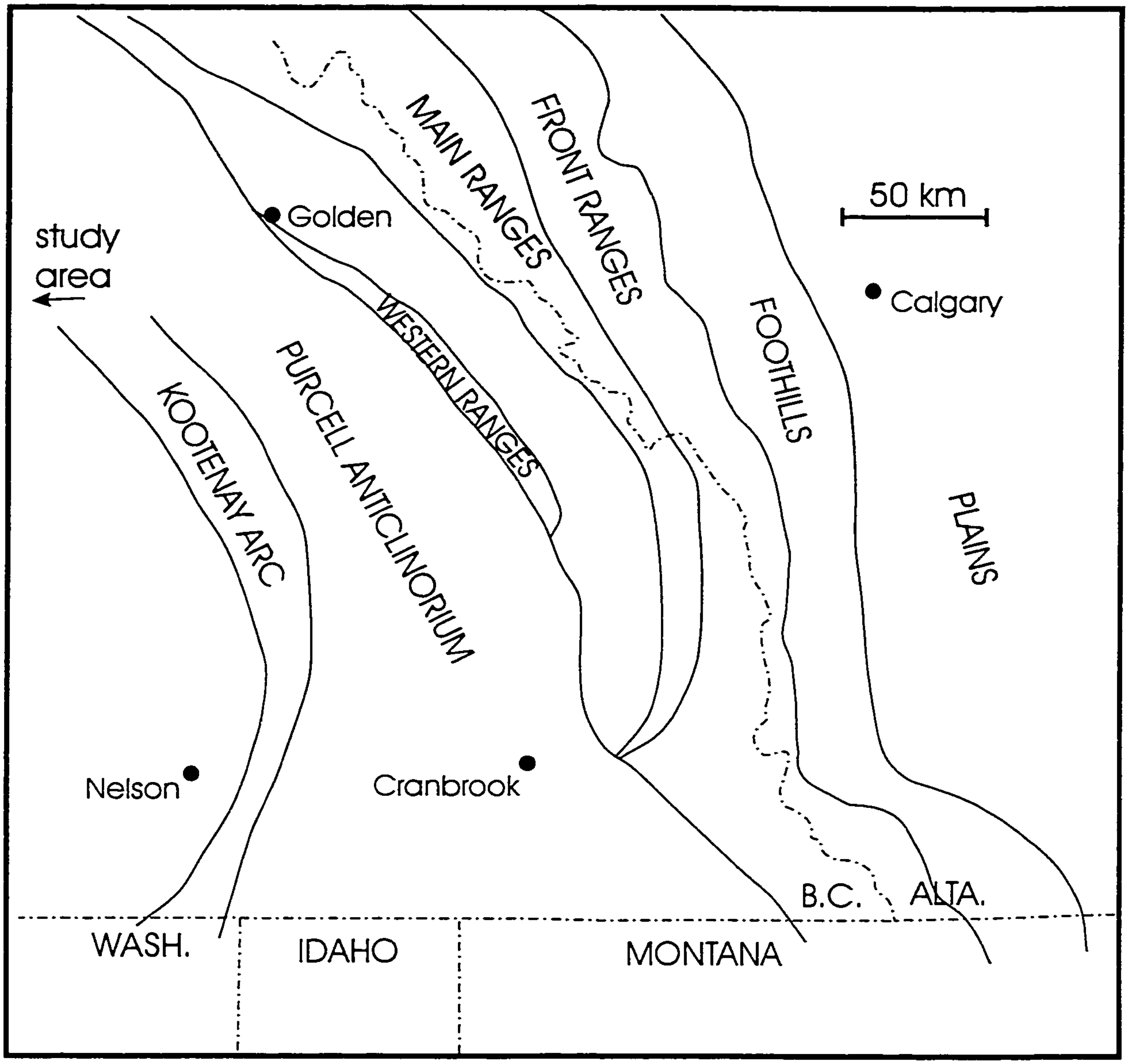

Figure 1-5: Structural elements of the southeastern Canadian Cordillera. Modified from Root (1993).

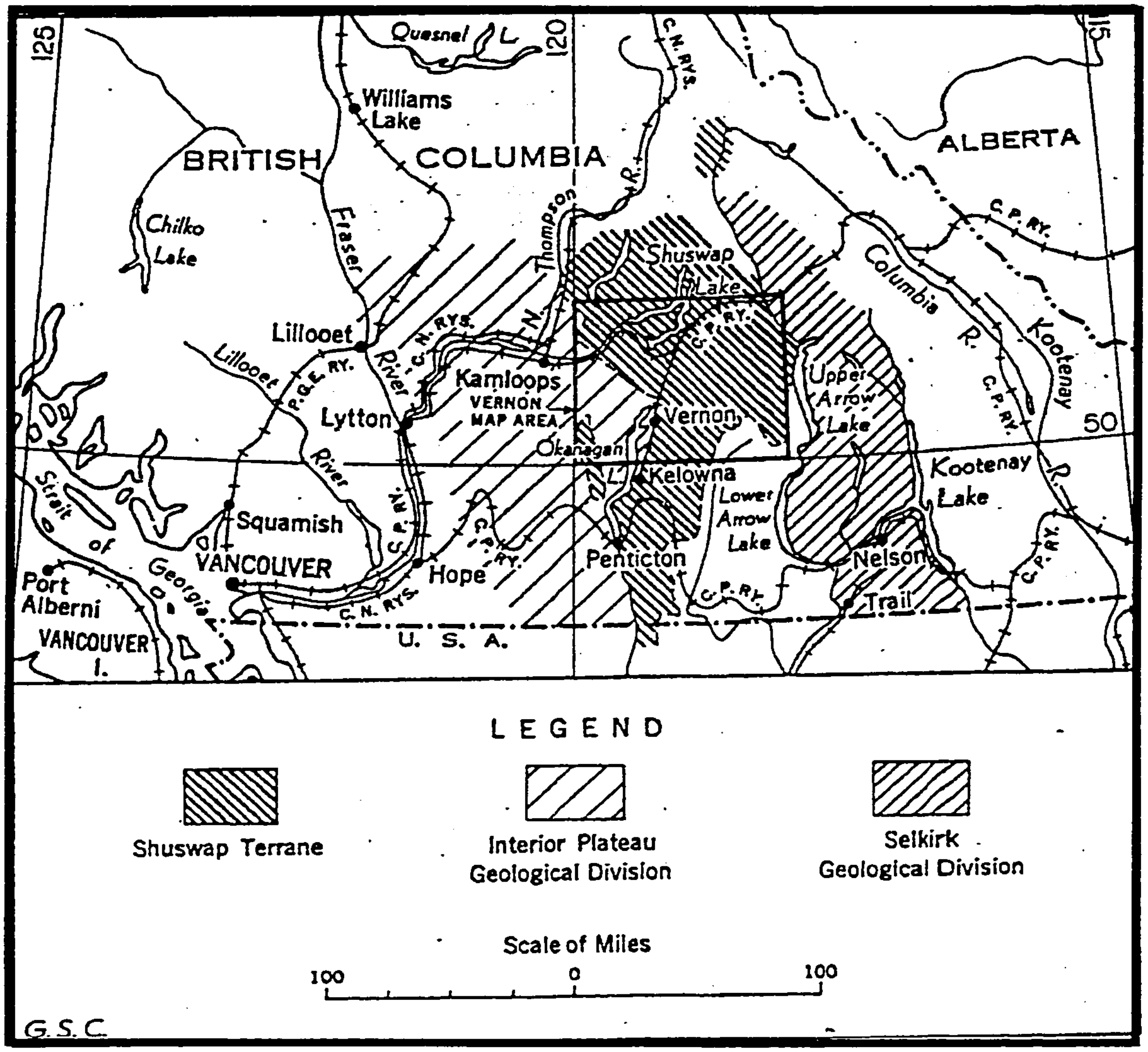

Figure 1-6: Distribution of Shuswap terrane.
(from Jones (1959))

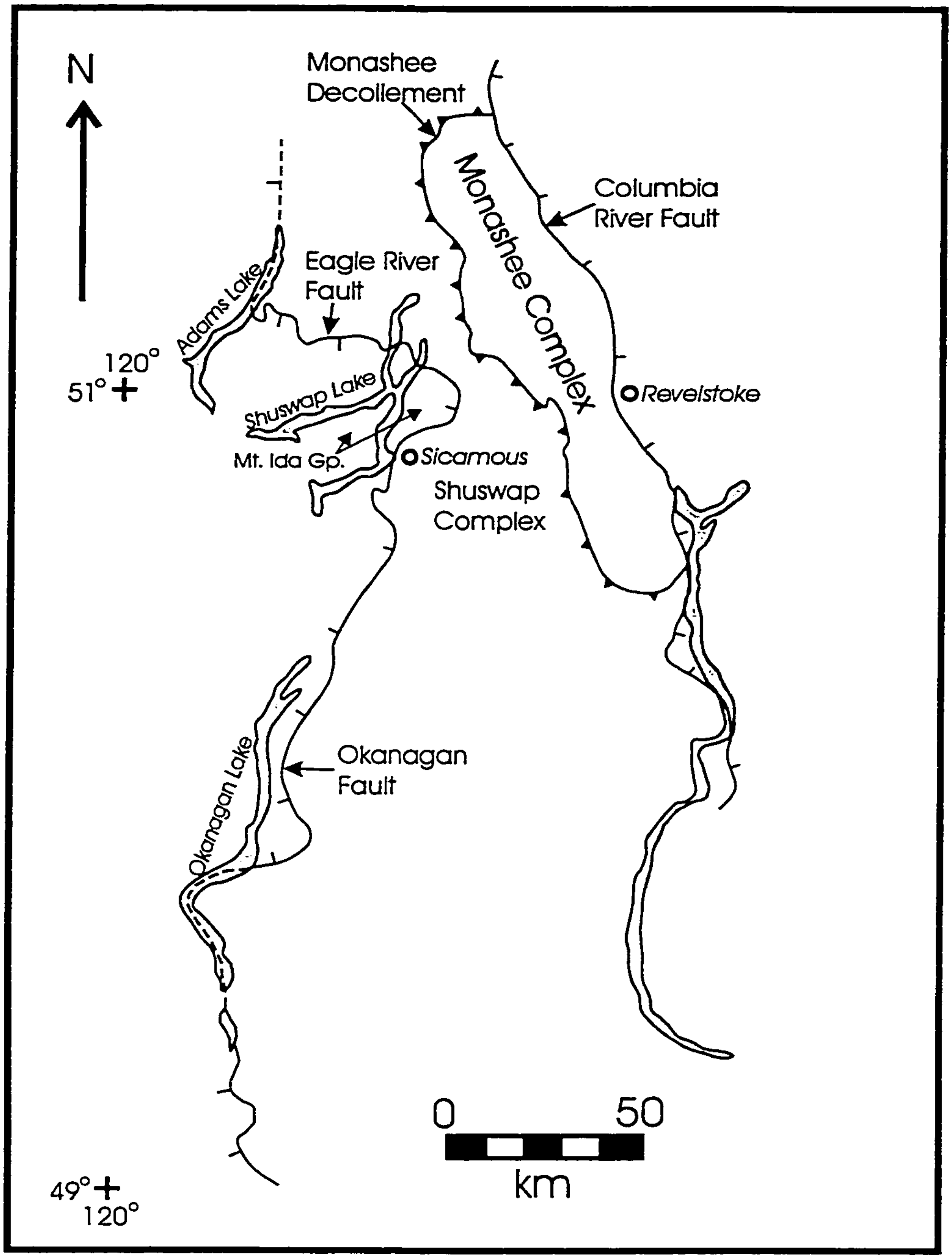

Figure 1-7: Tectonic map of the southern Omineca Belt.
(modified from Parrish *et al.* (1988) and Johnson (1989))

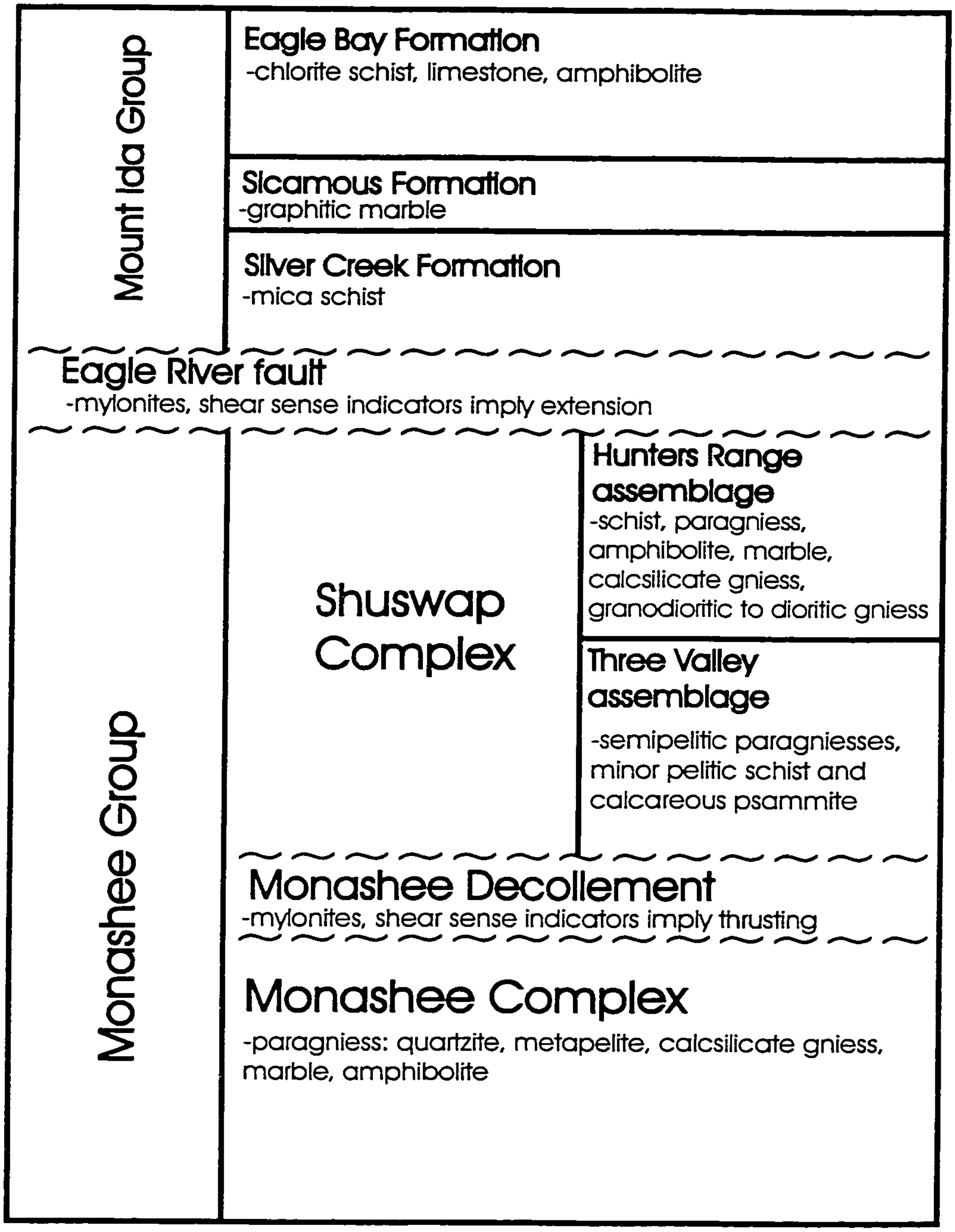

Figure 1-8: Schematic relationships of the Monashee Group and the Mount Ida Group. From Johnson (1990, 1994).

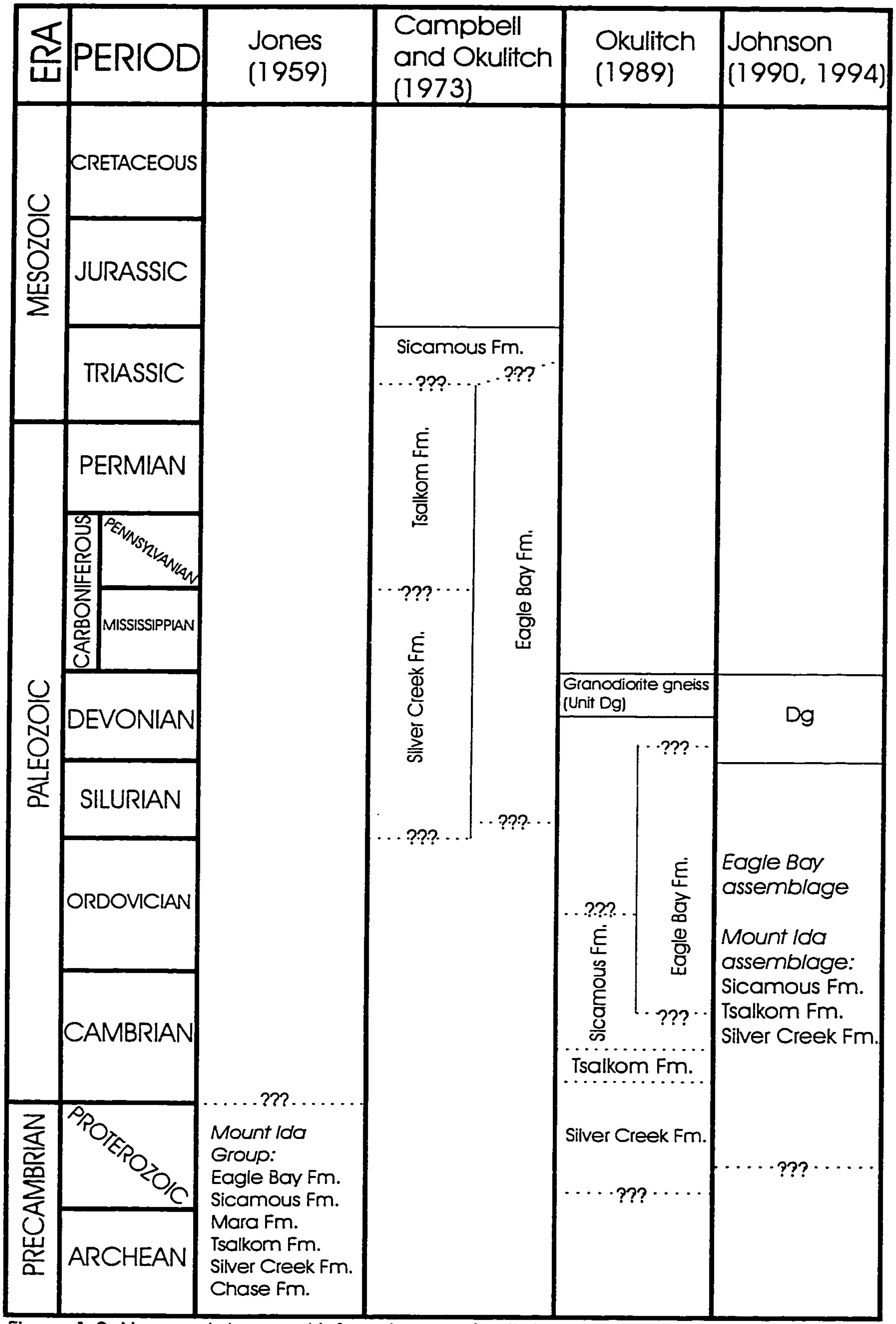

Figure 1-9: Nomenclature and inferred ages of units by prominent authors.

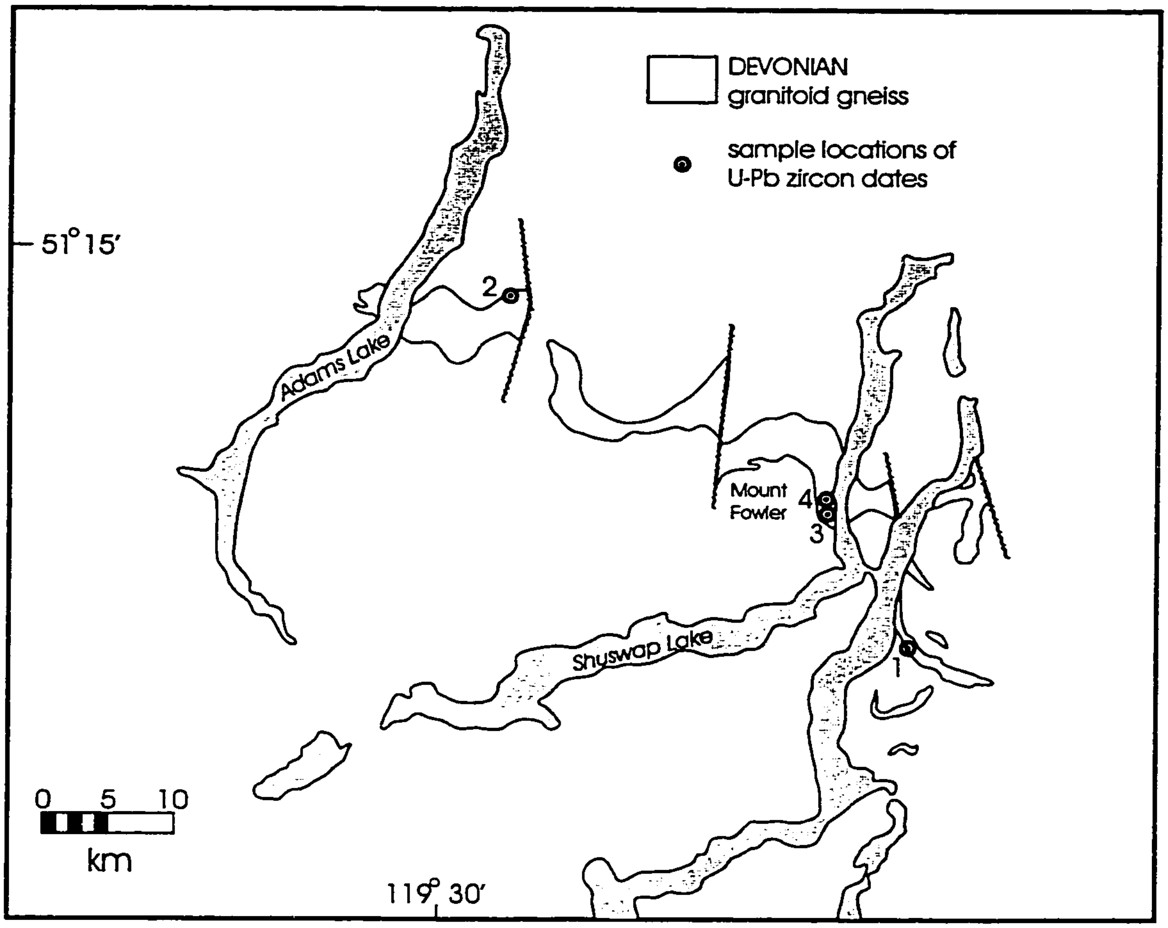

Figure 1-10: Location of previous U-Pb zircon dates from the Mount Fowler gneiss. (modified from Okulitch *et al.* (1975))

CHAPTER 2

Geology of the Study Area

INTRODUCTION

This chapter discusses the results of four months of geological field work and subsequent petrographic and structural analysis of rocks adjacent to Shuswap Lake. The region was mapped at 1:20 000 scale and drafted on a 1:50 000 map for inclusion with this thesis (Map 2-1). Mapping and petrography of the rocks in the study area provide detailed descriptions of the Silver Creek, Sicamous, and Eagle Bay formations and a granitoid pluton (Mount Fowler suite), and the first detailed documentation of an assemblage of metamorphic rocks, termed the Queest Mountain assemblage. The composition and the metamorphic and structural character of metasedimentary and intrusive units, as well as contact relationships between units, are discussed. This chapter provides details of the internal stratigraphy and contact relationships of the Silver Creek, Sicamous, and Eagle Bay formations of the Mount Ida Group, in order to better understand their depositional environment(s) and relationship to Ancestral North America. Lithologic and structural differences between the Eagle Bay Formation and the Queest Mountain assemblage are described, and the contact between these two units is discussed. As well, the granitoid pluton and its contacts with the host rocks are described, and evidence of deformation and metamorphism both before and after the intrusion of the pluton is provided. Outcrop locations and descriptions are provided in Appendix A and thin section descriptions are in Appendix B.

STRATIGRAPHY AND PETROLOGY

Silver Creek Formation

The Neoproterozoic (Johnson, 1994) Silver Creek Formation is exposed within the map area along the Trans-Canada Highway west of Sicamous and along the northern shore of Salmon Arm on Shuswap Lake (Slemko and Thompson, 1998) (Map 2-1). Its thickness is unknown as the lower contact is not present within the map area, but a minimum of several thousand meters is observed within the map area. In the study area, the Silver Creek Formation is composed mainly of fine- to medium-grained biotite-muscovite-quartz schist (unit SCs), with layers of fine- to medium-grained calcareous mica schist (unit SCc) tens to hundreds of meters thick. This formation is characteristically intruded by numerous granite pegmatite and aplite sills and dykes, ranging in thickness from a few millimeters to several tens of centimeters (Plate 2-1). Units SCs and SCc are generally pale brown on weathered surfaces and off-white to pale brown on fresh surfaces.

Unit SCc ranges from calcareous mica schist to almost pure marble with minor epidote and actinolite. Unit SCs contains at least 50% quartz and feldspar. Plagioclase is commonly seriticized. Retrogression of biotite to chlorite varies from minor alteration around the rims to almost complete alteration of the entire grain (Plates 2-3a, 2-3b).

A metaconglomerate layer, approximately a meter thick, crops out along the Trans-Canada Highway; the cobbles are composed predominantly of fine-grained hornblende with minor diopside, while the matrix is composed of fine-grained, randomly-oriented microcline and quartz. The clasts range in size from few centimeters to ten centimeters. The clasts are elongate in the same orientation as the foliation in surrounding Silver Creek Formation schist, implying that the conglomerate was likely deformed at the same time as the schist. The edges of the clasts are irregular, and it appears that the hornblende is partially resorbed, possibly implying metamorphic disequilibrium. The contacts of the metaconglomerate layer with the surrounding rock are not exposed. This metaconglomerate is lithologically different than the rest of the Silver Creek Formation, and may have originally formed as a mafic volcaniclastic layer before being metamorphosed.

In the area mapped, the Silver Creek Formation contains chlorite, biotite, muscovite, quartz, and feldspar, and is therefore at greenschist grade. Regionally, rocks mapped as Silver Creek Formation (Okulitch, 1974; Thompson and Daughtry, 1997) additionally contain garnet and sillimanite and are therefore at amphibolite grade. The apparent difference in grade could be due to differences in bulk composition, i.e., rocks in the study area may not have the right composition to form garnet and sillimanite, or to an actual difference in metamorphic grade. Detailed study of the Silver Creek between the study area and the higher grade rocks to the west (Thompson and Daughtry, 1997) is needed to distinguish between these possibilities. It is possible that there is a metamorphic gradient within the Silver Creek Formation or that there is a contact and not all these rocks are part of the Silver Creek Formation.

The aplite sills that intrude the Silver Creek Formation contain minor (<10%) hornblende and biotite, and have a primary igneous crystallization texture with undeformed randomly oriented grains. The sills commonly have the same orientation as foliation planes, and are interpreted to have intruded along these planes of weakness after foliation development. Therefore, the sills are younger than the foliation along which they intrude.

The Silver Creek Formation displays moderately- to well-developed foliation. In outcrop, two fabrics are commonly observed: mica schistosity and parallel transposed original compositional layering. The schistosity and compositional layering are parallel to the contact with the Sicamous Formation (described below). In thin section, alignment of micas parallel to a compositional layering of quartzofeldspathic layers and more micaceous layers can be clearly seen (Plate 2-2). In mica-rich samples, a crenulation can also be seen, defined by the folding of the first schistosity. This crenulation is typically slightly asymmetrical and the amplitude ranges from 1 to 5 mm. The crenulation is oriented at a high angle (almost perpendicular) to the schistosity, implying that the Silver Creek Formation has been subjected to at least two stress fields of different orientations.

Sicamous Formation

The Silver Creek Formation is overlain by the early (?) Paleozoic (Johnson, 1994) Sicamous Formation. The Sicamous Formation (unit Sm) is exposed along the Trans-Canada Highway near Sicamous, along the adjacent shore of Shuswap Lake on the north shore of Old Town Bay, and along the west shore of Shuswap Lake north of Canoe Point (Slemko and Thompson, 1998) (Map 2-1). This unit is a fine- to medium-grained carbonaceous marble, and is about 1500 m thick. Outcrop, both fresh and weathered, has distinctive black and white layers 5 to 10 mm thick (Plate 2-4). The white layers are almost pure calcite, while the black layers contain graphite.

In thin section, it can be seen that the Sicamous Formation is composed mainly of calcite, with dark layers containing up to 25% graphite. The graphite-rich layers have a finer grain size than the pure calcite layers (Plate 2-5). Some samples have minor quartz and/or muscovite layers that were only observed in thin section. The Sicamous Formation does not contain metamorphic minerals that are indicative of grade, because its bulk composition does not allow the formation of such minerals.

The Sicamous Formation typically displays foliation defined by the alignment of elongate calcite grains and compositional layering of graphite-rich layers. Foliation is parallel to unit contacts, so it may be transposed original sedimentary layering. In muscovite-rich layers, a weak, asymmetric crenulation with an amplitude of < 4 mm can be seen in thin section. Crenulation is at a high angle to foliation, and thus, like the Silver Creek Formation, the Sicamous Formation has been subjected to at least two different stress fields.

The contact between the Sicamous Formation and the underlying Silver Creek Formation, well-exposed along the Trans Canada Highway west of Sicamous, consists of layers, several centimeters to several meters thick, of alternating mica schist of the Silver Creek Formation and marble of the Sicamous Formation. This contact could be depositional, caused by a change in the bulk composition of the original sediments, or tectonic, resulting in a structural interleaving of rock types. Contacts between rock types appear gradational where exposed, and therefore a depositional contact is more likely.

Eagle Bay Formation

The early (?) Paleozoic (Johnson, 1994) Eagle Bay Formation, which overlies the Sicamous Formation, consists of metavolcanic and metaclastic strata. This formation is well exposed to the north of Old Town Bay and near Aline Hill (Slemko and Thompson, 1998) (Map 2-1). The thickness of the Eagle Bay Formation is unknown as the upper contact is not present within the study area, but it has a structural thickness of at least 4000 m. The Eagle Bay Formation is subdivided in this thesis into three units, based on lithologic contrasts. Unit EBg consists of 'greenstones': chlorite schist, chlorite-sericite schist, and amphibolite, has a characteristic green colour on both fresh and weathered surfaces (Plate 2-6), shows well developed foliation, and locally shows well developed crenulation. This unit commonly contains abundant pyrite, which weathers to a rust colour. Unit EBg is the most common rock type in the Eagle Bay Formation and in places comprises almost the entire thickness of the Eagle Bay Formation. Unit EBq is composed of biotite-muscovite-feldspar-quartz schist ± garnet and impure quartzite. This unit is typically light brown or light grey coloured on fresh and weathered surfaces. Unit EBm consists of several (up to 25) marble marker horizons, 100 to 200 m thick, which sometimes contain graphite. The marble layers are white (Plate 2-7) or have black and white layers 5 to 10 mm thick (Plate 2-8) on fresh surfaces, and commonly weather to a buff and/or grey colour. Some marble layers within the Eagle Bay Formation are lithologically similar to the Sicamous Formation; these can be distinguished based on stratigraphic position as the Eagle Bay Formation marbles form only thin layers within units EBg and EBq.

Pelitic samples of the Eagle Bay Formation (unit EBq) typically contain biotite and muscovite (Plates 2-9a, 2-9b). Quartz and feldspar are also present, comprising up to 50% of schists. Almandine garnet is commonly a minor (<10%) constituent. Sillimanite is present in minor (<10%) amounts in samples with sufficiently aluminous compositions. Feldspar is commonly seriticized (Plate 2-9a). In thin section it can be seen that biotite is commonly partially retrograded to chlorite (Plate 2-10); however, a few samples do not show any retrogression. Quartzites of unit EBq are typically impure, usually containing quartz and up to 20% graphite. Mafic samples (unit EBg) contain hornblende, quartz, and feldspar, with epidote present in minor (<10%) amounts in rocks of the correct bulk composition (Plate 2-11). Marble layers are ≥90% calcite, locally with minor (<10%) amounts of phlogopite or graphite.

Lateral variations in metamorphic grade occur, over distances of 1 to 2 km, from lower greenschist-grade chlorite schist to amphibolite-grade sillimanite-garnet-biotite-muscovite schist. This is likely caused by a combination of variations in the amount of retrogression and variations in original bulk composition, meaning that only some rocks have the correct bulk composition to form high grade minerals. All the minerals except chlorite appear to be in equilibrium with each other, as mineral overgrowths are not observed and no reactions appear to be taking place at grain boundaries. Chlorite is interpreted to be retrograde as it is only present as alteration on the rims of biotite grains. Thus, the peak metamorphic assemblage did not contain chlorite, but did contain sillimanite, garnet, biotite, muscovite, quartz, and feldspar (unit EBq) or hornblende, quartz, and feldspar (unit EBg).

The Eagle Bay Formation has well-developed foliation, typically defined by the alignment of micas and/or amphiboles, parallel to compositional layering, that can be seen in outcrop and thin section. This compositional layering may be transposed original compositional layering, since it is parallel to contacts with other units. In marble layers this foliation is defined by compositional layering and the alignment of elongate calcite grains, and is strongest in marbles that contain graphite. A weak to strong crenulation is also observed in micaceous or amphibole-rich samples (Plate 2-11). This crenulation can commonly be seen in outcrops of unit EBg. In some samples, micas are kinked, indicating that brittle deformation also occurred. Foliation wraps around garnet porphyroblasts, so the porphyroblasts are pre-tectonic. The growth of micas, amphibole, quartz, feldspar, and calcite is pre- or syn-tectonic to the foliation and crenulation development. This metamorphism and deformation are the result of a regional tectonic event.

Near Old Town Bay, the contact between the Eagle Bay Formation and the underlying Sicamous Formation is well exposed. The contact consists of layers, several centimeters thick, of graphitic marble of the Sicamous Formation alternating with layers, also several centimeters thick, of Eagle Bay mica-quartz schist. Contacts between layers are gradational and the contact is therefore inferred to be depositional. Compositional layering and mica schistosity in both the Sicamous and Eagle Bay formations are parallel to this contact. The Sicamous and Eagle Bay Formations are inferred to have been deposited at the outer margin of the North American craton

(Thompson and Daughtry, 1997). The contact represents a change from carbonate sedimentation to a time of increased volcanic activity.

Queest Mountain assemblage

Mica schist and calcsilicate rocks located in the northeast corner of the study area, were previously (Okulitch, 1974; Johnson, 1990) mapped as part of the Eagle Bay Formation. However, on the basis of differences in protolith composition (eg. lack of calcsilicate in the Eagle Bay Formation, discussed below), metamorphic grade (which is higher in the Eagle Bay Formation, see Chapter 3), and structural history (differences in orientation data discussed later in this chapter), these rocks have been (Slemko and Thompson, 1998) assigned to their own assemblage, or group of metamorphic rocks, termed the Queest Mountain assembalge.

The Queest Mountain assemblage includes fine- to medium-grained biotite-muscovite schist (unit QMs), commonly with coarse-grained garnets (Plate 2-12), and fine- to medium-grained marble and calcsilicate schist (unit QMmc) (Plate 2-13). Unit QMmc forms a layer 200 to 500 m thick (Map 2-1). The pelitic schist (unit QMs) is typically light brown and pink on fresh and weathered surfaces. The marble and calcsilicate (unit QMmc) are typically white and pink on fresh surfaces but weather to buff and rust colours. The calcsilicate displays a characteristic pitted weathering pattern with layers of resistant silicate minerals and layers of recessive calcite.

The pelitic schist (unit QMs) contains biotite, muscovite, quartz, and feldspar. Some samples also contain garnet and sillimanite, or staurolite. In thin section it can be seen that some pelitic samples of biotite-muscovite schist (Plates 2-14a, 2-14b) show retrogression of biotite to chlorite. Marble and calcsilicate samples (unit QMmc) contain calcite, tremolite to actinolite, grossular, and diopside, (Plates 2-15a, 2-15b) locally with minor quartz and/or feldspar and/or phlogopite and/or sphene.

Most minerals in units QMmc and QMs, except for chlorite, do not show overgrowths of other minerals or reactions at grain boundaries, and thus appear to be in equilibrium. In a few samples, garnet has irregular grain boundaries and appears to be somewhat resorbed, meaning that the garnets are not in equilibrium. However, in most samples the garnet is euhedral and pristine, and therefore is in equilibrium with other minerals. This indicates that two episodes of garnet growth probably occurred. The peak metamorphic mineral assemblage is indicative of amphibolite facies metamorphism, although some parts have been retrograded to chlorite grade.

Thin section textures show a schistosity defined by the alignment of micas parallel to compositional layering. An asymmetric crenulation, with amplitude between 0.5 and 5 cm, is also observed in some samples. Some micas are kinked, the result of a later brittle deformation. Garnet and staurolite porphyroblasts appear to have grown pre- or syn-tectonically, as the foliation is wrapped around them. Growth of micas, quartz, feldspar, and sillimanite is pre- or syn-tectonic to the foliation and crenulation development. Crenulated micas appear recrystallized, and are therefore synkinematic to crenulation development. Chlorite formed by later retrograde reactions.

The contact between the Eagle Bay Formation and the Queest Mountain assemblage is obscured by vegetation and glacial deposits, however its approximate location can be estimated within 200 to 500 m. The contact was originally defined based on a change in rock type from mica schist and greenstones in the south to mica schist and calcsilicate in the north (Slemko and Thompson, 1998). While both units contain mica schist, the Queest Mountain Formation does not contain amphibolite, which is abundant in the Eagle Bay Formation. The Eagle Bay Formation does not contain calcsilicate rocks, which are prevalent in the Queest Mountain assemblage; marble in the Eagle Bay Formation is composed almost entirely (>90%) of calcite. The approximate position of the contact suggests a moderately north-northeast dipping contact. Rocks of the Queest Mountain assemblage are located on the east side of Shuswap Lake, but along strike, across the lake to the west, rocks of the Eagle Bay Formation are present. Also, south of Cinnemousun Narrows the Eagle Bay Formation is present while north of Cinnemousun Narrows (north of the mapped area) the Queest Mountain assemblage is present on land between the northern two arms of Shuswap Lake. Sharp differences in lithology along strike, differences in structural style (discussed in the latter part of this chapter), and differences in metamorphic grade (discussed in Chapter 3) between the two units imply a structural and metamorphic break suggestive of an unconformity or a fault. The contact strikes approximately east-west on land east of Shuswap Lake, and appears to strike north beneath Shuswap Lake and strike west through Cinnemousun Narrows (Map 2-1). The location of the contact to the west of Shuswap Lake is unknown as the area was not mapped for this study. Due to the shape of the contact and the presence of a structural and metamorphic break, the contact is interpreted as a fault. The geometry is suggestive of two east-west striking faults, one east of Shuswap Lake and one through Cinnemousun Narrows, joined by a north-south striking tear fault (Map 2-1). It is also possible that this is a single fault that has been subsequently folded; however the sharp angles (< 90°) at which the parts of the fault meet and the lack of similar folding of the schistosity or unit contacts adjacent to the fault means that a tear fault is more likely. The surface trace of the fault to the east of Shuswap Lake is approximately straight, also implying that the fault has not been substantially deformed.

The orientation of the fault on the east side of Shuswap Lake has been estimated by examining the limits placed on the location of the contact by outcrop locations (Map 2-1). Using outcrop locations and elevations at these outcrops, two three-dimensional three-point-problems were constructed to provide maximum and minimum strikes and dips for the fault. These estimates of the orientation of the fault provide a strike of between 223 and 258 degrees and a dip of between 16 and 30 degrees to the northeast. This fault, termed the Queest Mountain fault (Slemko and Thompson, 1998), would place the Queest Mountain assemblage on the Eagle Bay Formation. Based on the mineral assemblages described above, both the Queest Mountain assemblage and at least parts of the Eagle Bay Formation are at amphibolite grade. However, geothermometry and geobarometry (Chapter 3) show that the Eagle Bay Formation is at a higher metamorphic grade than the Queest Mountain assemblage, implying a normal sense of motion on the Queest Mountain fault. Structural data, shown later in this chapter, also suggest differences between the Queest Mountain assemblage and the Eagle Bay Formation.

In the northeast corner of the map area, an outcrop of Eagle Bay Formation chlorite schist, mica schist, and amphibolite was observed; another fault, similar to the Queest Mountain fault, may separate this from the Queest Mountain assemblage. Further mapping is needed to determine the presence and location of this possible fault and whether it is linked, spatially or genetically, to the Queest Mountain fault. Depending on the orientation of this second fault, it could be the other half of a graben structure (if it is south-dipping), or it and the Queest Mountain fault could be part of a series of imbricate normal faults (if it is north-dipping like the Queest Mountain fault).

Granitoid Gneiss Pluton (Mount Fowler suite)

An intrusion of biotite-hornblende, equigranular to megacrystic granite to granodiorite, 15 km across, included by Okulitch *et al.* (1975) in the Devonian Mount Fowler suite, cuts the Eagle Bay Formation and the Queest Mountain assemblage on the east side of Shuswap Lake (Map 2-1). The intrusion crosses the mapped trace of the Queest Mountain fault on the east side of Shuswap Lake without offset. Map patterns suggest that the Queest Mountain assemblage is folded into a broad open syncline. The intrusion also appears to cut this fold. Within the study area, the intrusion is light brown on weathered surfaces and black and white on fresh surfaces (Slemko and Thompson, 1998). The granitoid gneiss intrusion is resistant and commonly forms distinctive cliffs.

Quartz, plagioclase, and alkali feldspar are everywhere present in rocks of the Mount Fowler suite. One or both of biotite and hornblende are present. Some samples contain minor (<5%) epidote or sphene. The pluton has four phases of different composition and grain size. Medium-grained (2 to 5 mm sized crystals) biotite-hornblende granite (Dg) comprises most of the pluton. Phase Dg typically contains between 25 and 40 percent each of quartz, alkali feldspar, and plagioclase, with up to 25% mafic minerals (biotite and hornblende). Fine-grained (crystals ≤ 1mm) mafic biotite-hornblende granite to granodiorite (Dgm), felsic biotite-hornblende granite (Dgf), and pegmatitic biotite-hornblende granite (Dgp) comprise the remainder of the pluton. Phase Dgm contains at least 50% mafic minerals (hornblende and biotite) and is much finer-grained than Dg. Phase Dgf is medium-grained granite and contains less than 20% mafic minerals. Phase Dgp is pegmatitic granite with less than 20% mafic minerals.

Irregularly-shaped inclusions (ranging in size from a few centimeters to a meter long) and dykes and sills of one phase intruding another phase are observed in several outcrops (Plate 2-16). Inclusions of Dg within Dgm are observed, implying that Dgm is older than Dg. A sill of Dgp intrudes into Dgm, implying that Dgm is also older than Dgp. Not all phases are present in a single outcrop; this, combined with a lack of exposure in some areas, makes it difficult to determine the relative ages of the different phases. However, geochronological work (Chapter 4) on phases Dg (the most extensive and possibly youngest phase) and Dgm (possibly the oldest phase) shows that these phases are essentially the same age. These two phases constitute the majority of the intrusion, meaning that most of the pluton was likely intruded at the same time.

In some samples, biotite has been chloritized, interpreted to be the result of post-intrusion retrogression. In some samples mineral grains are somewhat recrystallized and therefore some areas are interpreted to have been weakly metamorphosed during the Columbian and/or Laramide orogenies.

Fabrics range from massive igneous texture in some of the undeformed samples (Plate 2-17) to mica schistosity or gneissosity in other regions. This indicates that strain is heterogeneous, varying from none to strongly penetrative. The foliation is more strongly penetrative near the edges of the pluton, which implies either that the foliation resulted during emplacement or that the foliation is post-emplacement but the edges provided a buffer zone that prevented the center of the pluton from becoming as greatly foliated. Syn-emplacement foliation would consist of flow foliation, not the schistosity that is seen in rocks of the Mount Fowler suite, so post-emplacement foliation is more likely.

The contact between the granitoid pluton and the rocks it intrudes is observed in only one outcrop. Foliation in the host rock is generally uniformly oriented, whereas foliation in the pluton is not uniform. Initial field work (Slemko and Thompson, 1998) suggested that the pluton may cut foliation in the country rock, because at map scale, foliation in the pluton near its contact with the host rock appears discordant with regional foliation. Also, inclusions, several tens of centimeters to meters long, of mica schist were observed within the pluton in an outcrop along a logging road north of Sicamous. This schist is lithologically similar to nearby outcrops of the Eagle Bay Formation and is therefore inferred to be rafts of Eagle Bay Formation included within the pluton. The schistosity in these rafts is discordant with respect to the foliation in the pluton.

One outcrop shows the pluton cutting compositional banding in calcsilicate rock of the Queest Mountain assemblage (Plate 2-18, Figure 2-1). A weak schistosity seen in this outcrop, but not observed in other Queest Mountain assemblage rocks, has the same orientation in both granitoid gneiss and the calcsilicate. Peak metamorphic mineral growth in the Queest Mountain assemblage is pre- or syn-tectonic with respect to the development of the compositional banding. This relationship implies that the Eagle Bay Formation and the Queest Mountain assemblage were deformed and metamorphosed prior to the intrusion of the Mount Fowler suite. As well, the pluton appears to cross the proposed Queest Mountain fault without offset, implying that the fault may also pre-date the intrusion. It has been proposed (Johnson, 1994) that all deformation in the study area is Mesozoic and younger, associated with the Columbian and Laramide orogenies. However, there is evidence of Middle Paleozoic events in the Kootenay Arc and Purcell Anticlinorium (Read and Wheeler, 1976; Klepacki, 1985; Gehrels and Smith, 1987; Root, 1987, 1993). Evidence presented in this thesis suggests that an Early to Middle Paleozoic tectonic history is preserved near Shuswap Lake as well.

ORIENTATION DATA

Foliation (schistosity and/or compositional layering) was measured at outcrops throughout the field area, and plotted on stereonets for structural analysis to determine any differences in orientation of fabrics between units and hence any differences in tectonic histories.

Initially, data from each unit were plotted on separate stereonets. From this, it could be seen that foliations from the formations of the Mount Ida Group (Silver Creek, Sicamous, and Eagle Bay formations) all have a similar orientation, with the averages of the clusters being within a few degrees of each other both in azimuth and dip. Therefore these three units were combined onto a single stereonet. The foliation from the Queest Mountain assemblage has a different orientation than the foliation of Mount Ida Group, and shows two distinct clusters instead of a single cluster. Also, the foliation from the granitoid pluton is different in orientation than any of the metasedimentary units, and is separated from the metasedimentary units because the pluton has not experienced any pre-Late Devonian strain, whereas the metasedimentary units have been deformed prior to the intrusion of the pluton. Thus, the area was subdivided into three structural domains based on separate fabric orientations and possibly separate tectonic histories.

The first structural domain encompasses the Silver Creek, Sicamous, and Eagle Bay formations of the Mount Ida Group. A plot of poles to foliation (Figure 2-2) shows that the poles cluster around a point but have some scatter along a girdle. From the pattern of foliations plotted on the geology map (Map 2-1) it can be seen that the Mount Ida Group forms an essentially homoclinal panel in the southern part of the map area. Some folding of marble marker layers is observed in the northern part of the map area near Aline Hill. These folds are open folds, with a wavelength of several hundred meters. The points that do not cluster, which lie in the far northeast or southwest quadrants of the stereonet, are all from near Aline Hill where the rocks have been folded. Eigenvector 3 (Figure 2-2), the statistical mean of the measurements, represents the average pole to foliation. It has a trend and plunge of 199, 68, so the dip direction and dip of the foliation in the homoclinal portion is approximately 19, 22. The elliptical 95% confidence cone for eigenvector 3 has a maximum angle (major axis) of 7.66° and a minimum angle (minor axis) of 5.84°, which means that the point distribution of the data significantly departs from orthorhombic symmetry, due to a substantial degree of scatter. Therefore, eigenvector 3 is an inexact estimate of the orientation of the Eagle Bay Formation.

In the second structural domain, which comprises the Queest Mountain assemblage, poles to foliation plot as two clusters with trends and plunges of 17, 38 and 228, 47 (Figure 2-3). These two clusters could either represent foliations of two different ages or two limbs of a fold that folded the foliation. The map pattern (Map 2-1) shows calcsilicates and marbles of the Queest Mountain assemblage present in a layer that is folded into a large (5 km wavelength) open, upright, syncline, with a gently northwest-plunging fold axis. Poles to foliation from the north limb of the fold cluster at eigenvector 3 (Figure 2-3), while poles to foliation from the southern limb of the fold cluster at eigenvector 2, which suggests that the two clusters represent the two limbs of this fold. The average of each cluster represents the average orientation of the pole to each limb of the fold. Therefore, the two limbs would have orientations of 197, 52 and 48, 43 (dip direction, dip), which corresponds to the fold pattern observed on the map. The interlimb angle of the fold is 90 degrees. The pole to the best-fit great circle, eigenvector 1 (Figure 2-3), represents the fold axis of this fold, which is oriented 120, 16 (trend and plunge). The axial plane of the fold strikes approximately west-northwest. The azimuth of maximum stress needed to produce a fold of this orientation would be approximately north-northeast and south-southwest.

Poles to foliation in the third domain, the granitoid pluton, show a weak cluster with considerable scatter (Figure 2-4). Field observations of foliation in the pluton also show considerable scatter. The scatter could be associated with syn-emplacement foliation development and/or the warping of foliation at the edges of the pluton, possibly by post-Devonian strain. Mesozoic orogenesis, during the Columbian and Laramide orogenies, is well documented in the Omineca Belt (Gabrielse *et al.*, 1991), so the pluton has likely been deformed and metamorphosed after its emplacement.

These data highlight the differences between the three domains. The Mount Ida Group forms a homoclinal panel in the southern part of the map area, with folding in the northern part, while the Queest Mountain assemblage is folded into an open syncline. These differences could be due to separate tectonic histories or to rheological differences between the units. Metamorphic differences presented in the next chapter show that a fault contact between the Mount Ida Group and the Queest Mountain assemblage is likely, implying that these units could also have been deformed separately before being juxtaposed by the Queest Mountain fault. Therefore, the observed differences in foliation orientation are proposed to be due to separate tectonic histories.

The foliation in the granitoid pluton is more variable in strength and more scattered than the foliations in the metasedimentary rocks. This could mean that the metasedimentary rocks were foliated before the intrusion of the pluton, or that post-emplacement tectonism affected the metasedimentary rocks more than the pluton due to rheological differences. As previously discussed, the pluton cuts foliation in the Queest Mountain assemblage and foliated rafts of Eagle Bay Formation schist are present within the granitoid, so at least some of the deformation occurred prior to the intrusion of the pluton. Post-emplacement deformation also occurred, but did not affect the entire pluton, as parts of the pluton are unfoliated. Also, there are differences in foliation orientation between the metasedimentary rocks and the pluton, and because the pluton cuts foliation in the metasedimentary rocks it is apparent that post-emplacement tectonism did not overprint the first foliation in the metasedimentary rocks. This means that two episodes of deformation have occurred in the area: one before the emplacement of the pluton in the Late Devonian, and one afterwards, likely associated with the Columbian and Laramide orogenies. Details of the tectonic history of the region will be discussed in Chapter 5.

SUMMARY

Detailed mapping in the Shuswap Lake region focused on the internal stratigraphy of the Silver Creek, Sicamous, and Eagle Bay formations and the contacts between them. The Queest Mountain assemblage, recognized on the basis of lithologic differences, was documented in this thesis. The postulate that the Queest Mountain assemblage should be separated from the Eagle Bay Formation is supported by the descriptions of its lithology provided in this section. Contact relationships between all units were studied. The Silver Creek, Sicamous, and Eagle Bay formations appear to have stratigraphic contacts between units where observed within the map area. Based on the nature of the contact and lithological and structural evidence, as well as metamorphic differences presented in the next chapter, the contact between the Eagle Bay Formation and the Queest Mountain assemblage is interpreted as a fault termed the

Queest Mountain fault. A granitoid pluton intrudes the Eagle Bay Formation and the Queest Mountain assemblage. The intrusion cuts the Queest Mountain fault and foliation and a fold in the host rocks, and pre-dates metamorphic mineral growth in the host rocks. Foliation in the host rocks is more pervasive than foliation in the pluton, and foliation in the pluton is discordant to that of surrounding rocks. This evidence shows that pre-Devonian tectonism is likely preserved in the region.

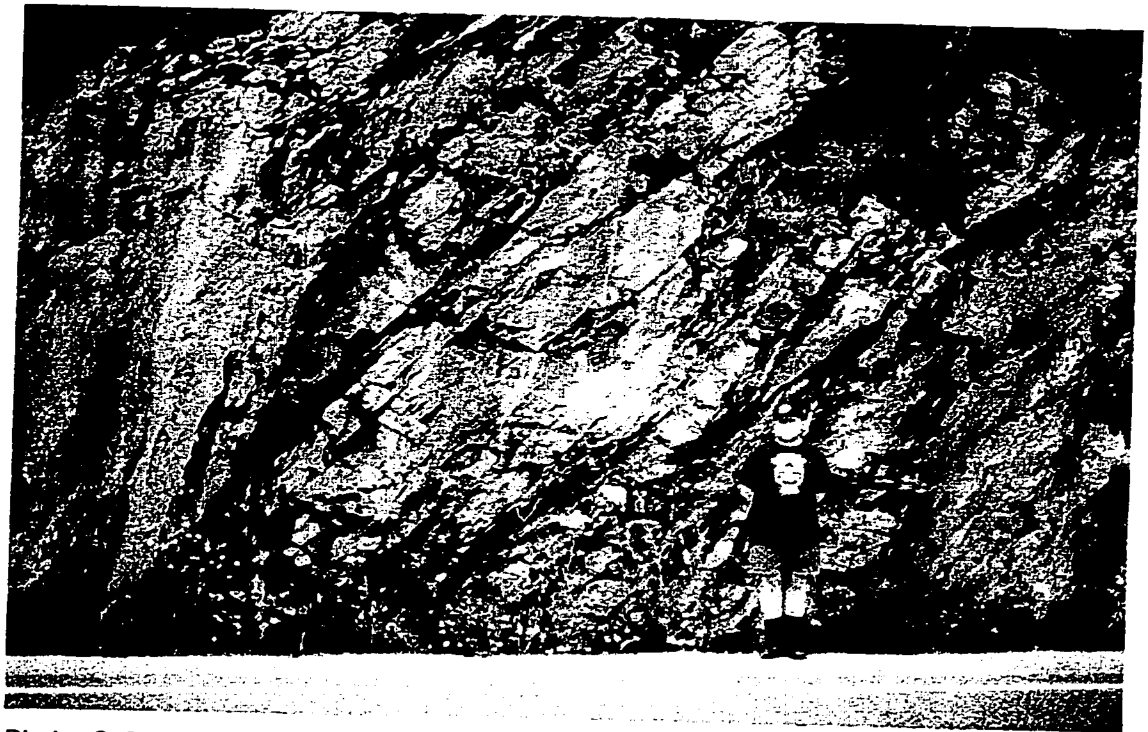

Plate 2-1: Photo of typical Silver Creek Formation mica schist, intruded by abundant aplite and pegmatite sills and dykes, beside the Trans-Canada Highway west of Sicamous.

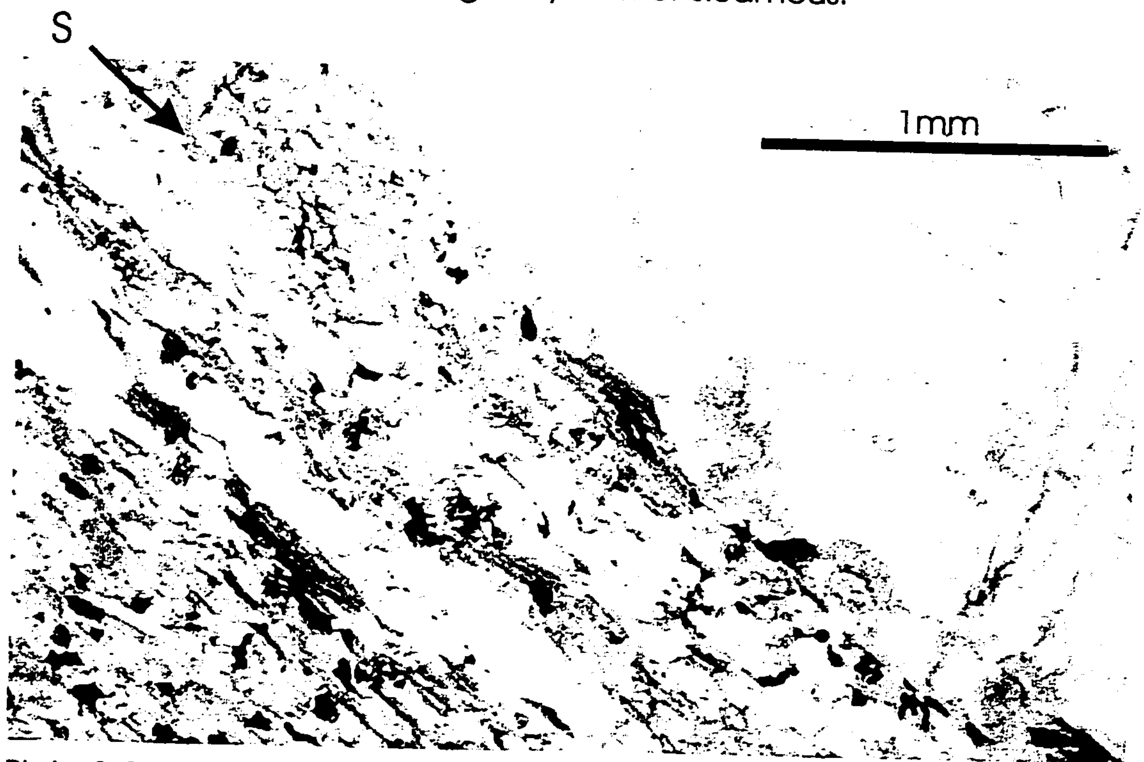

Plate 2-2: Photomicrograph of Silver Creek Formation mica schist showing typical foliation (S) defined by the alignment of micas. (Sample NS97-205; plane-polarized light)

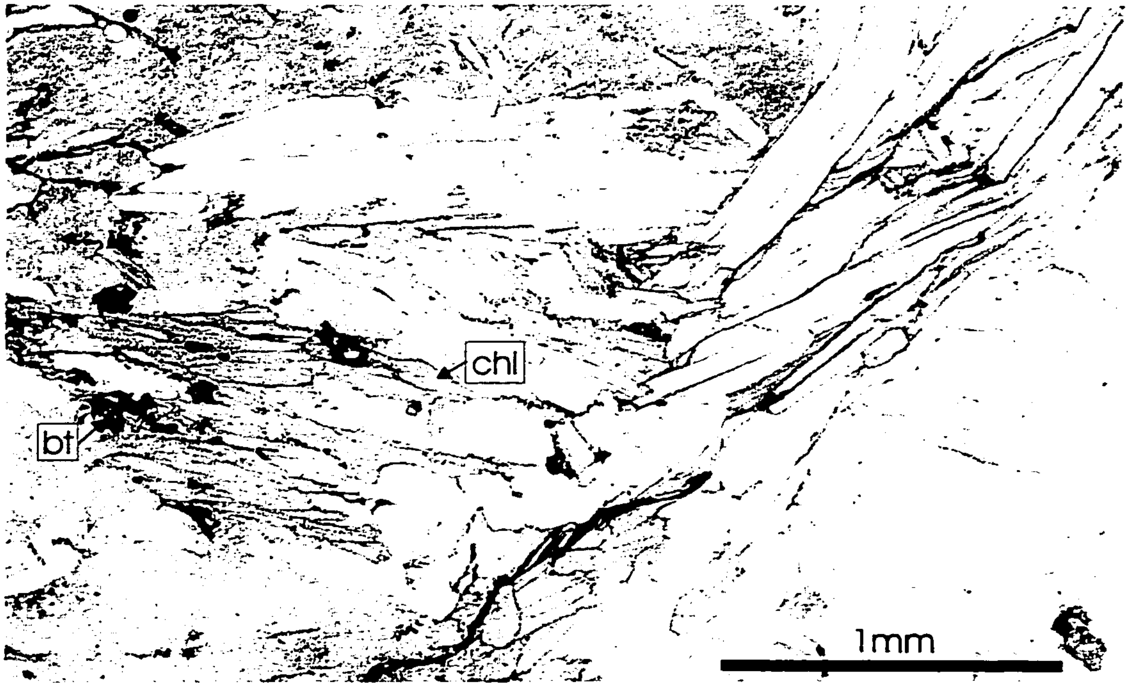

Plate 2-3a: Photomicrograph of Silver Creek Formation mica schist with biotite (bt) partly retrograded to chlorite (chl).
(Sample NS97-198; plane-polarized light)

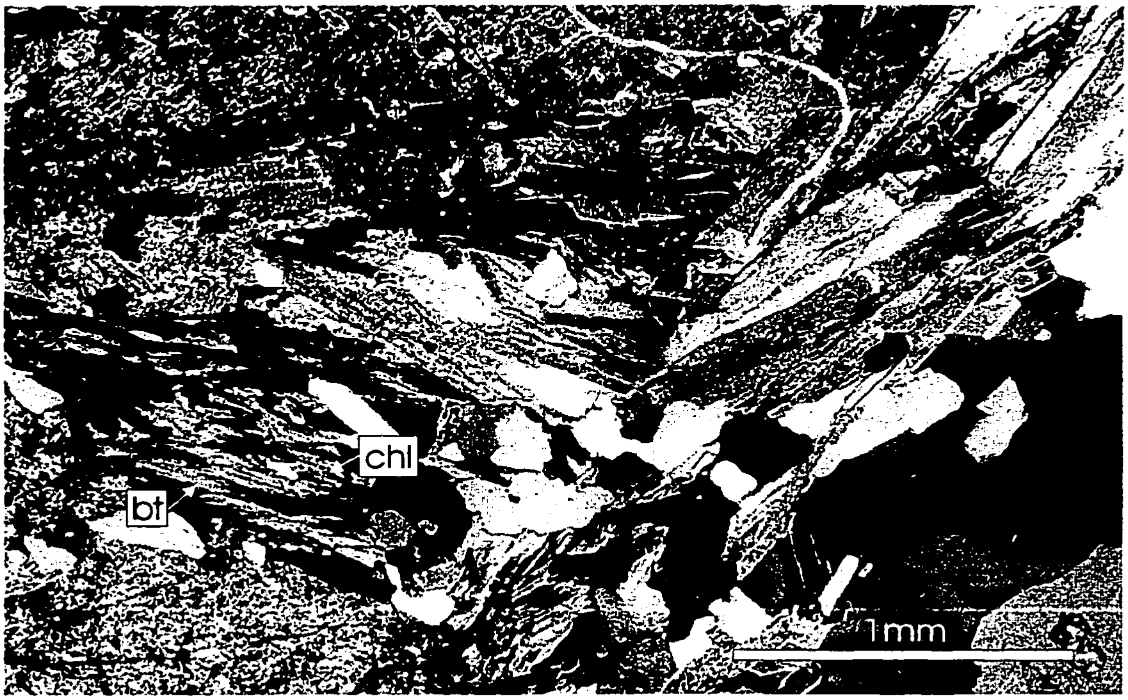

Plate 2-3b: Photomicrograph of Silver Creek Formation mica schist with biotite (bt) partly retrograded to chlorite (chl). Note blue interference colour of chlorite. (Sample NS97-198; crossed-polarized light)

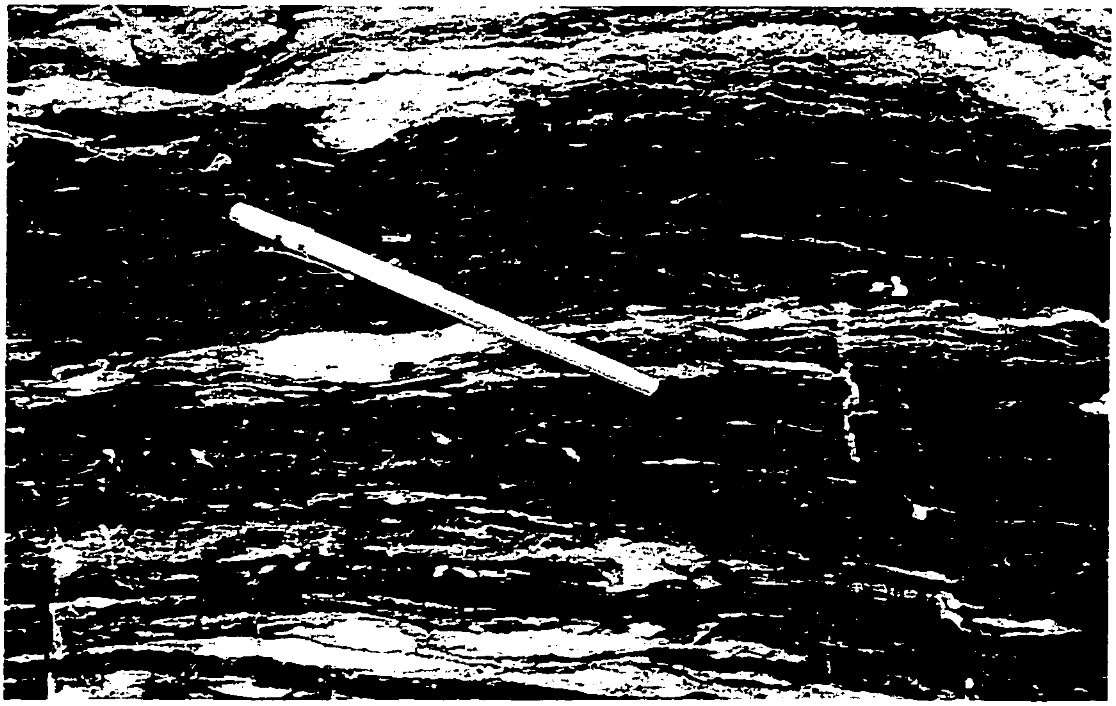

Plate 2-4: Photo of the Sicamous Formation showing typical black and white layering of the marble. (Outcrop NS97-289, north of Old Town Bay; pen for scale ~14cm long)

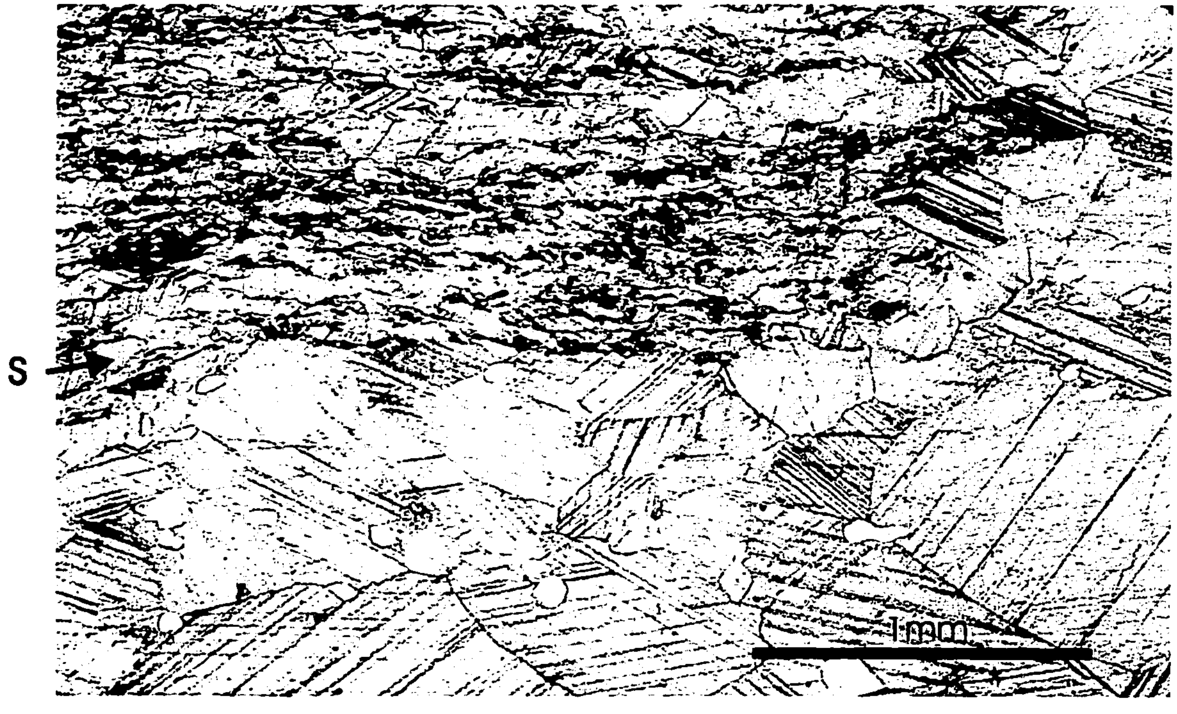

Plate 2-5: Photomicrograph of the Sicamous Formation showing typical foliation (S) defined by grain size, compositional changes, and alignment of elongate calcite grains. Note presence of graphite in finer-grained layer at the top. (Sample NS97-5;plane-polarized light)

Plate 2-6: Photo of an Eagle Bay Formation amphibolite showing the typical green colour seen in outcrop. (Outcrop NS97-33; hammer for scale ~30cm long)

Plate 2-7: Photo of an Eagle Bay Formation white marble marker horizon. (Outcrop NS97-366; hammer for scale ~30cm long)

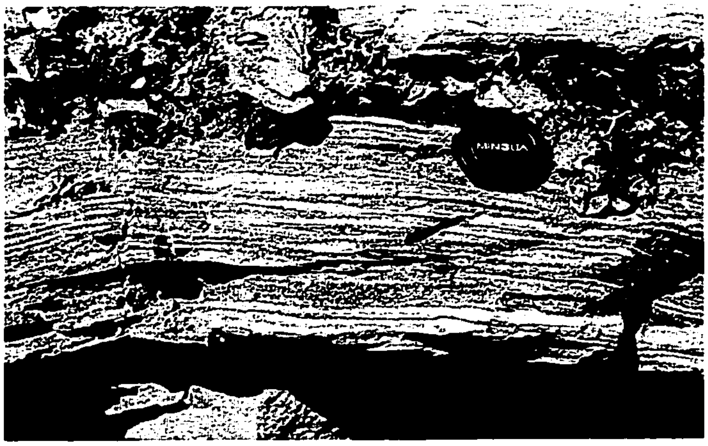

Plate 2-8: Photo of an Eagle Bay Formation black and white marble marker horizon. Note similarity to Sicamous Formation, Plate 2-4. (Outcrop NS97-313; lens cap for scale ~5cm diameter)

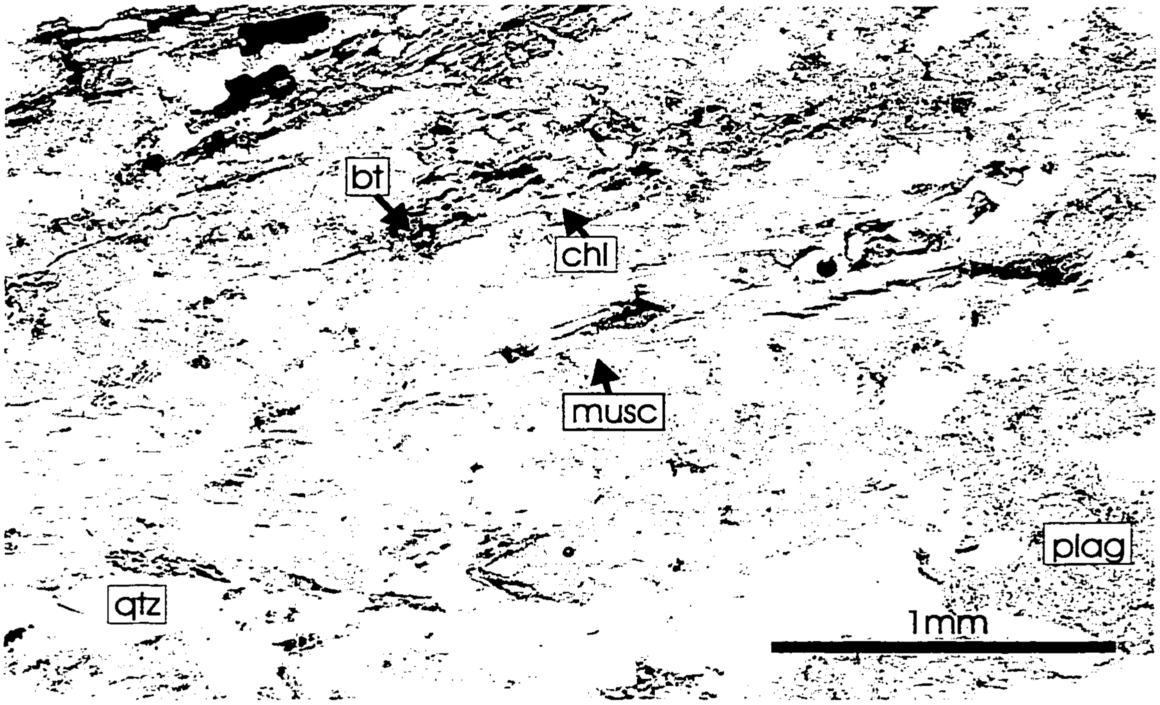

Plate 2-9a: Photomicrograph of typical Eagle Bay Formation pelitic schist showing muscovite (musc), biotite (bt) partly retrograded to chlorite (chl), seriticized plagioclase (plag), quartz (qtz), and opaque pyrite.
(Sample NS97-151A; plane-polarized light)

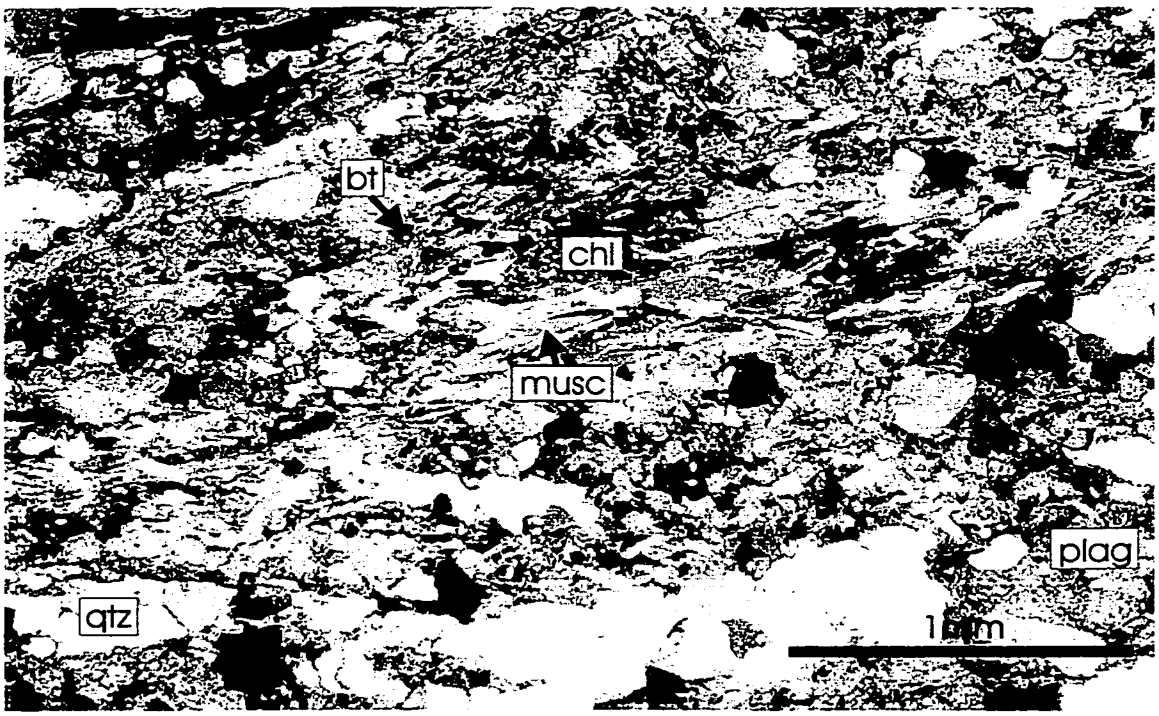

Plate 2-9b: Same as 2-9a (crossed-polarized light)

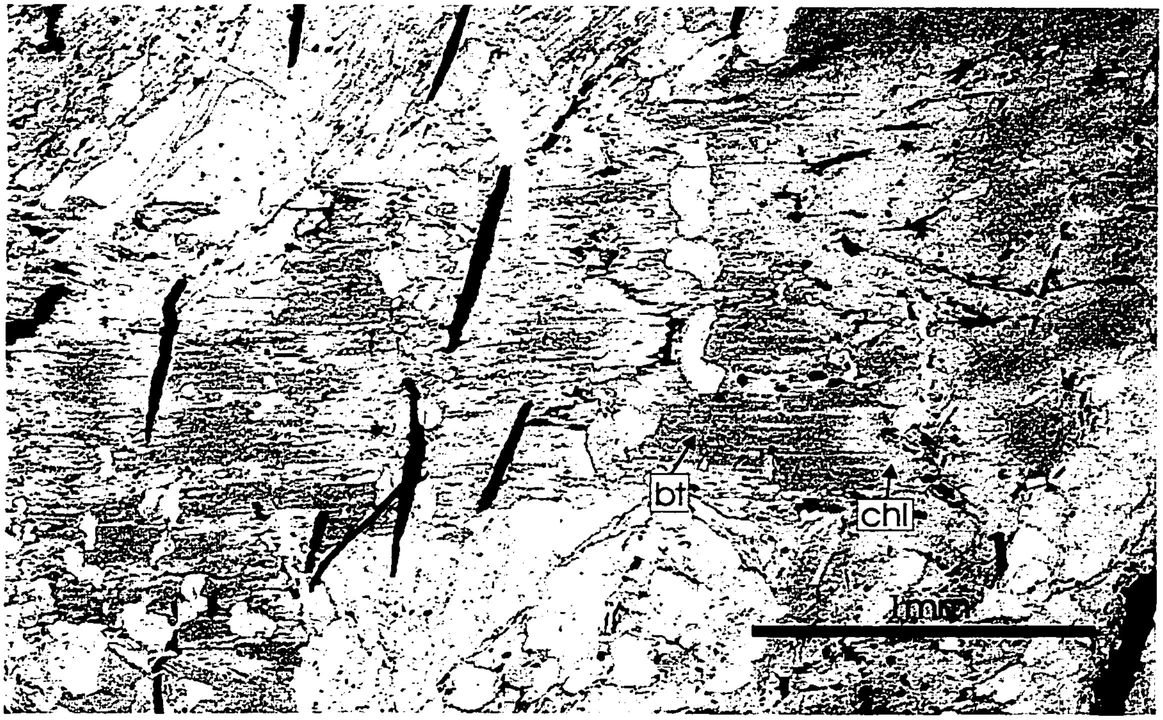

Plate 2-10: Photomicrograph of Eagle Bay Formation mica schist showing biotite grains retrograded to chlorite.
(Sample NS97-8; plane-polarized light)

Plate 2-11: Photomicrograph of Eagle Bay Formation amphibolite, also showing foliation (S) and crenulation.
(Sample NS97-145; plane-polarized light)

Plate 2-12: Photo of Queest Mountain assemblage pelitic schist.
(Outcrop NS97-91A)

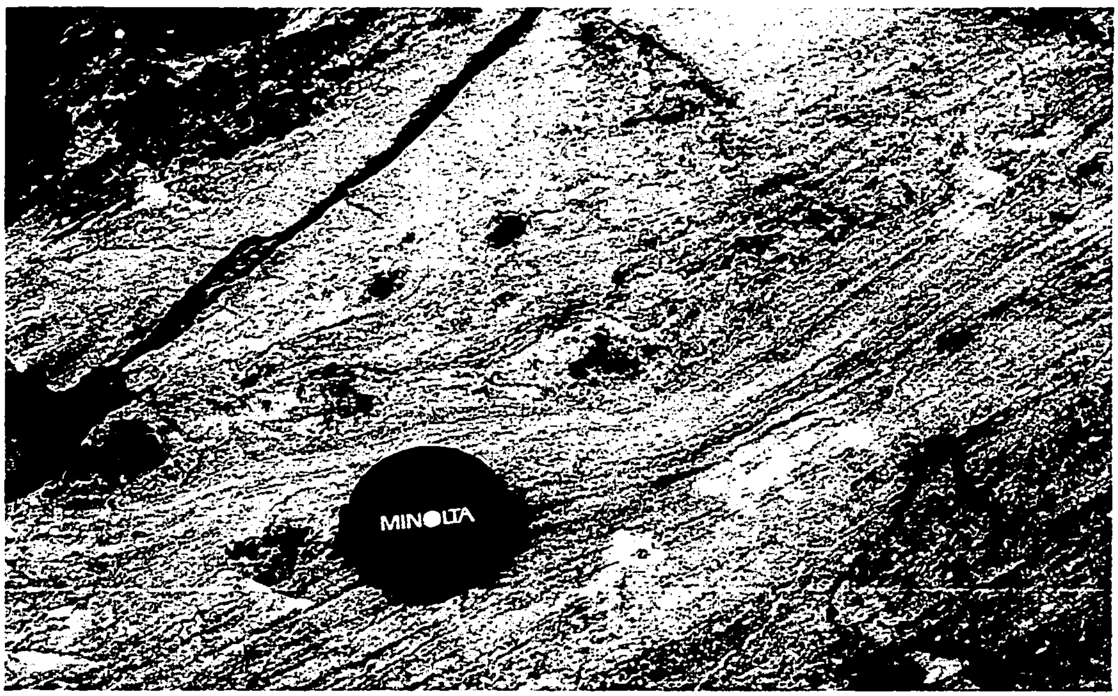

Plate 2-13: Photo of Queest Mountain calcsilicate schist showing clots of calcsilicate minerals (grossular, tremolite, diopside).
(Outcrop NS97-107; lens cap for scale ~5cm diameter)

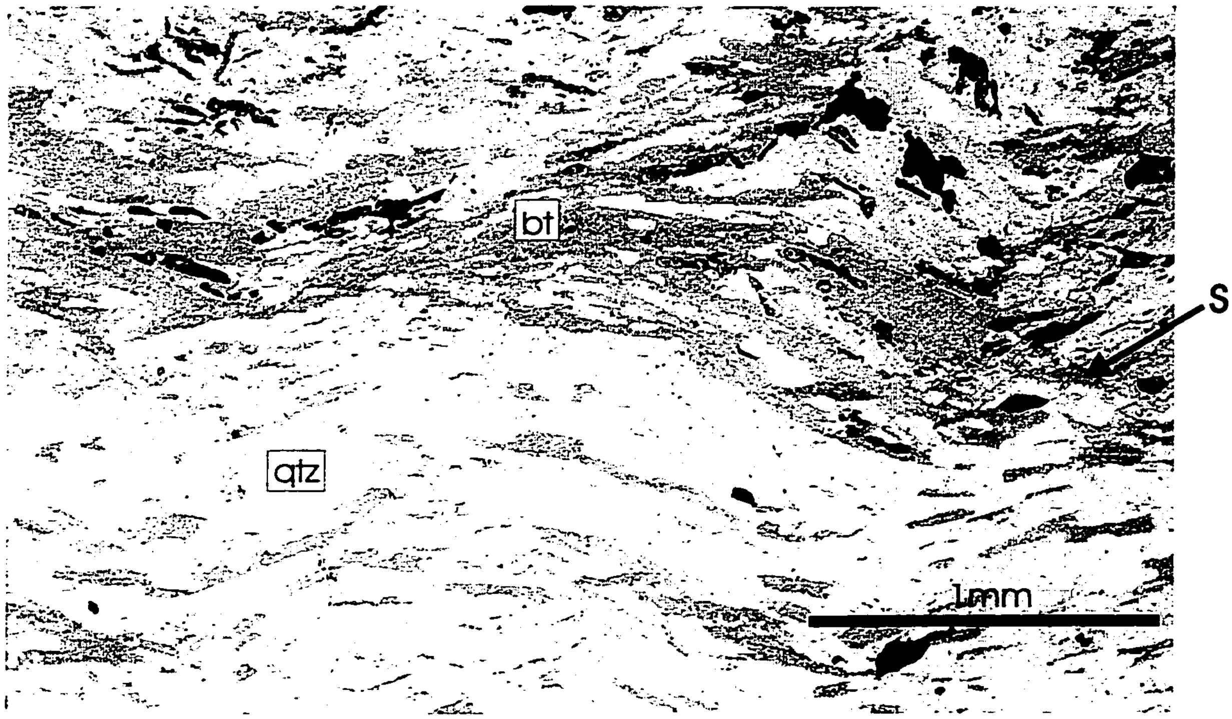

Plate 2-14a: Photomicrograph of Queest Mountain assemblage pelitic schist showing biotite (bt)-rich and quartz (qtz)-rich layers and foliation (S) and crenulation. (Sample NS97-84A; plane-polarized light)

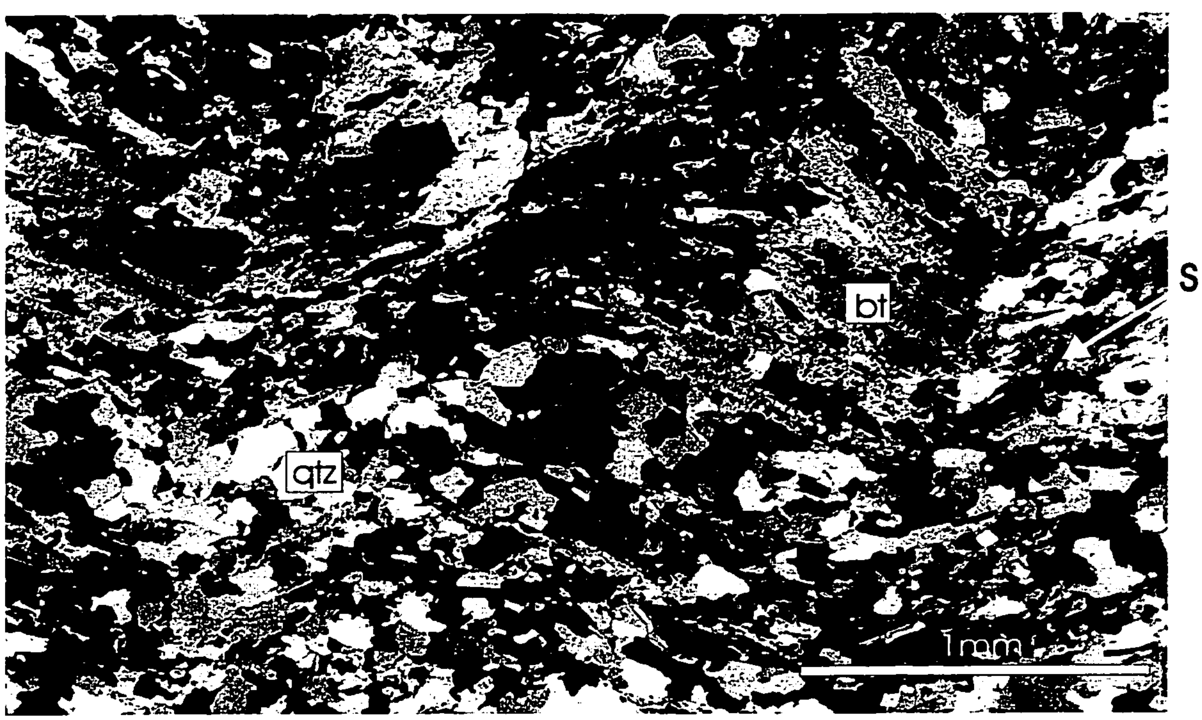

Plate 2-14b: Same as above (crossed-polarized light)

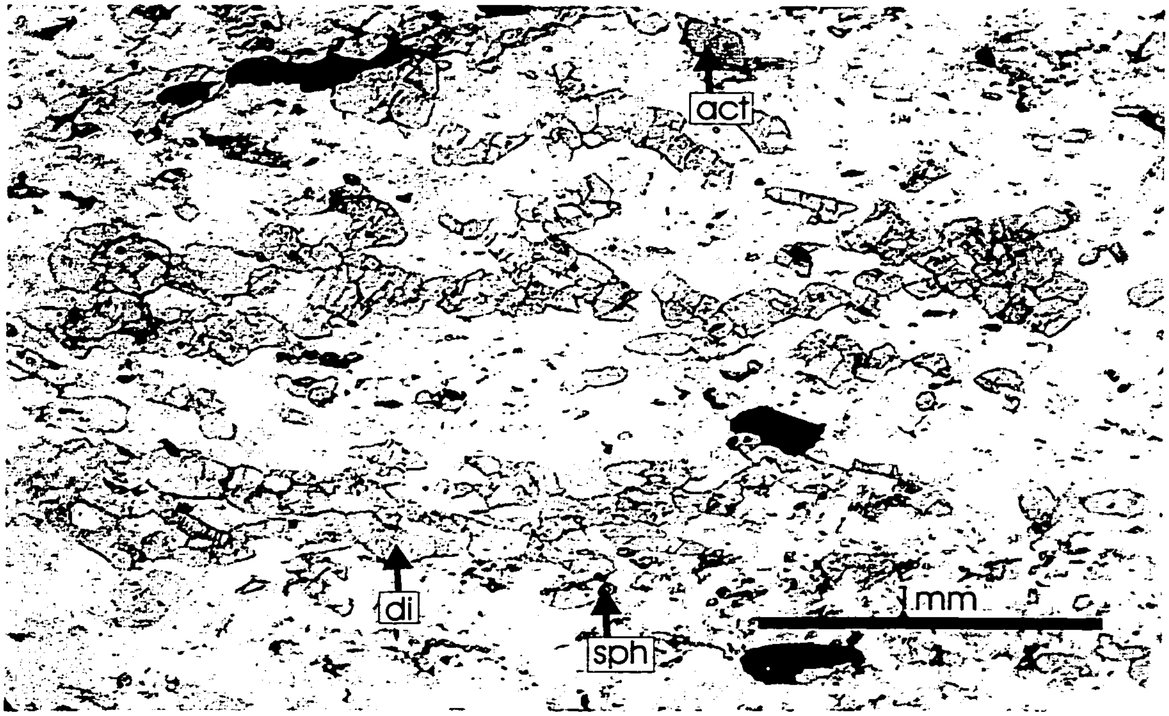

Plate 2-15a: Photomicrograph of Queest Mountain assemblage calcsilicate. High relief minerals are diopside (di), sphene (sph), and actinolite (act). Lower relief minerals are quartz, plagioclase, and calcite. (Sample NS97-107; plane-polarized light)

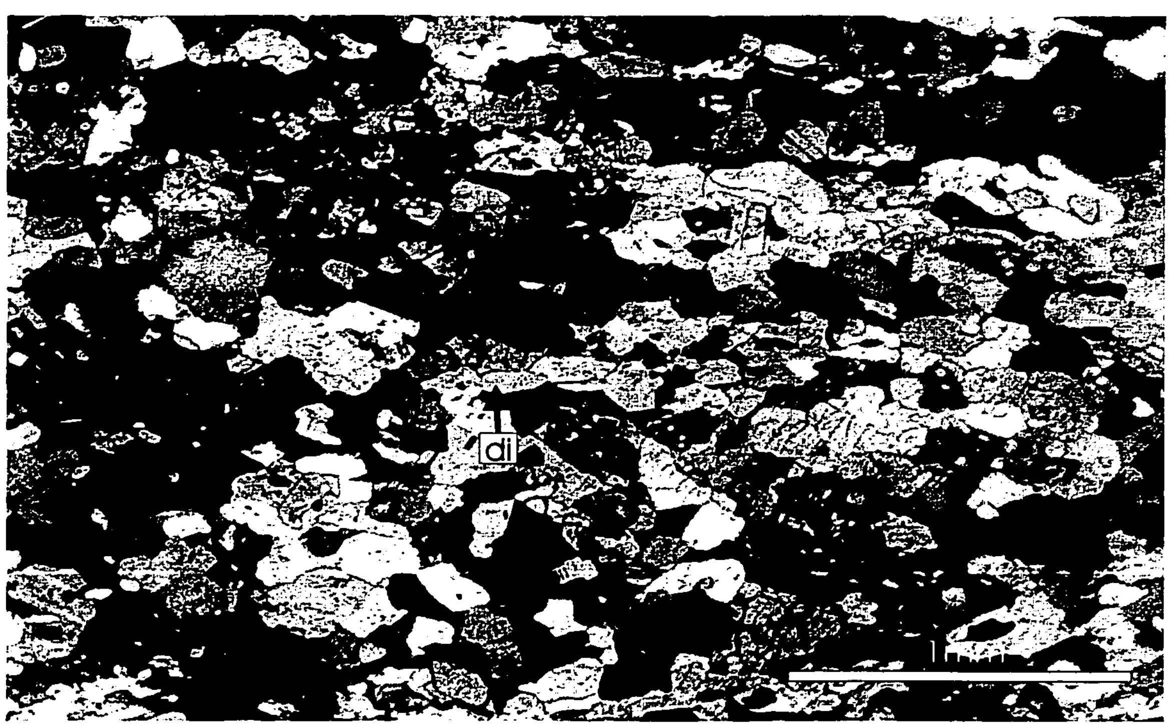

Plate 2-15b: Same as above (crossed-polarized light).

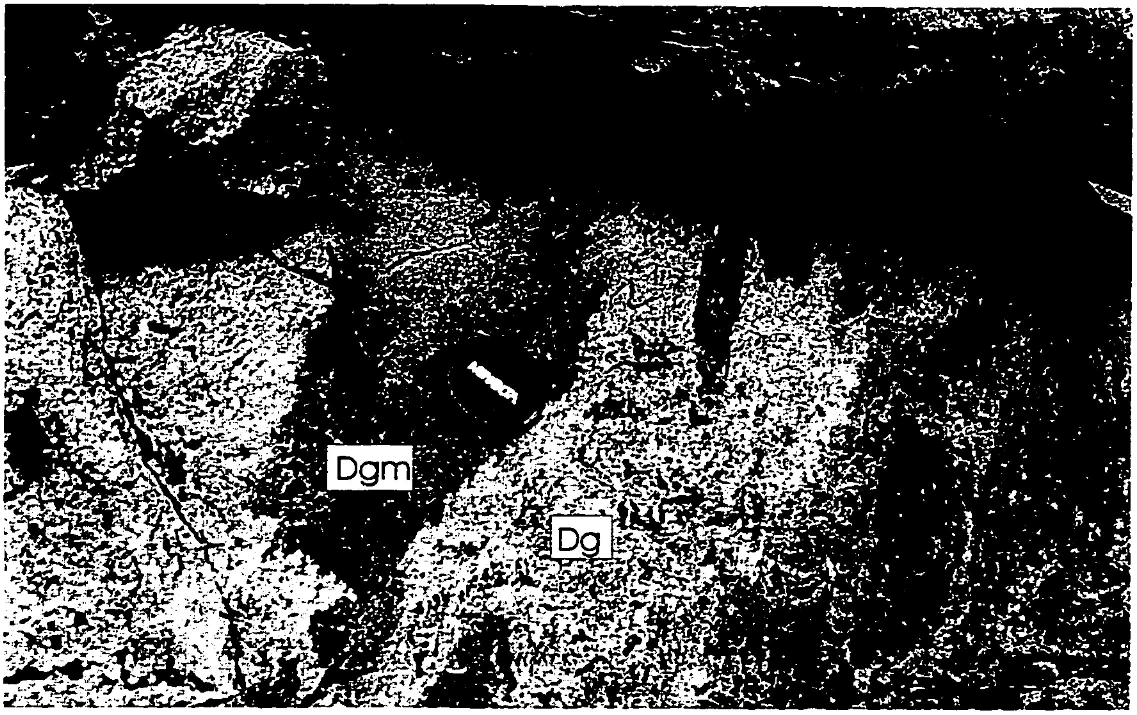

Plate 2-16: Photo of the Mount Fowler pluton showing Dg intruding Dgm. (Outcrop NS97-83; lens cap for scale ~5cm diameter).

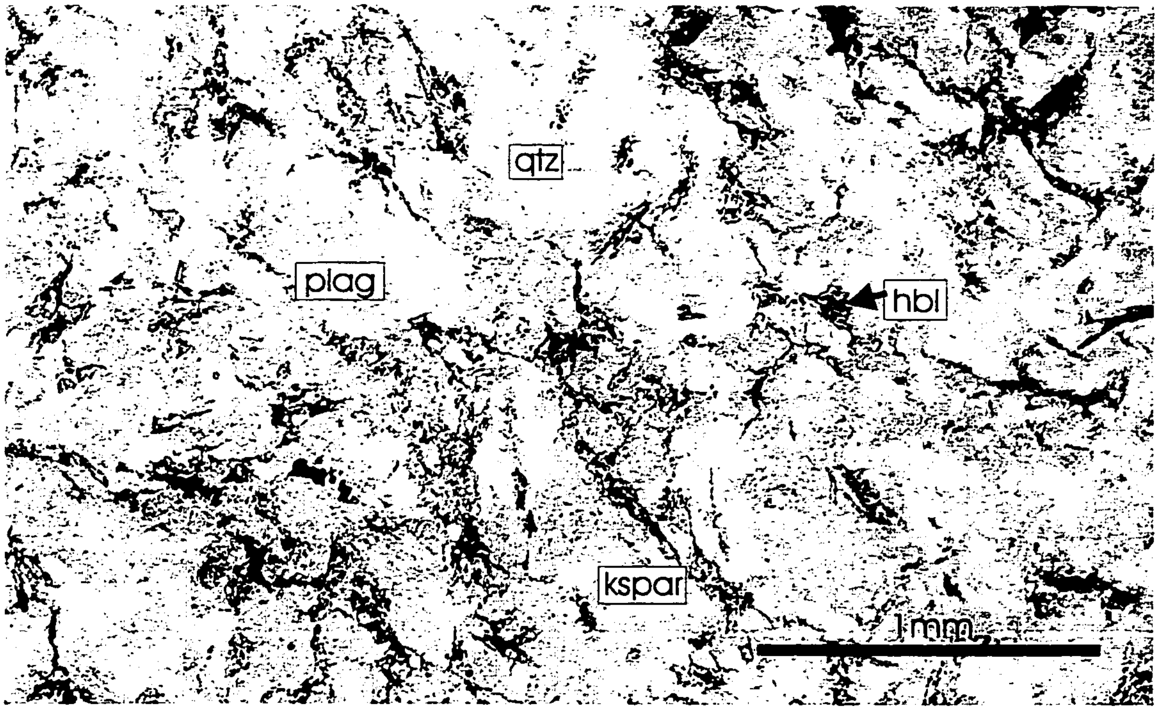

Plate 2-17: Photomicrograph of undeformed Dg containing quartz (qtz), seriticized plagioclase (plag), k-feldspar (kspar), and hornblende (hbl). (Sample NS97-11; plane-polarized light)

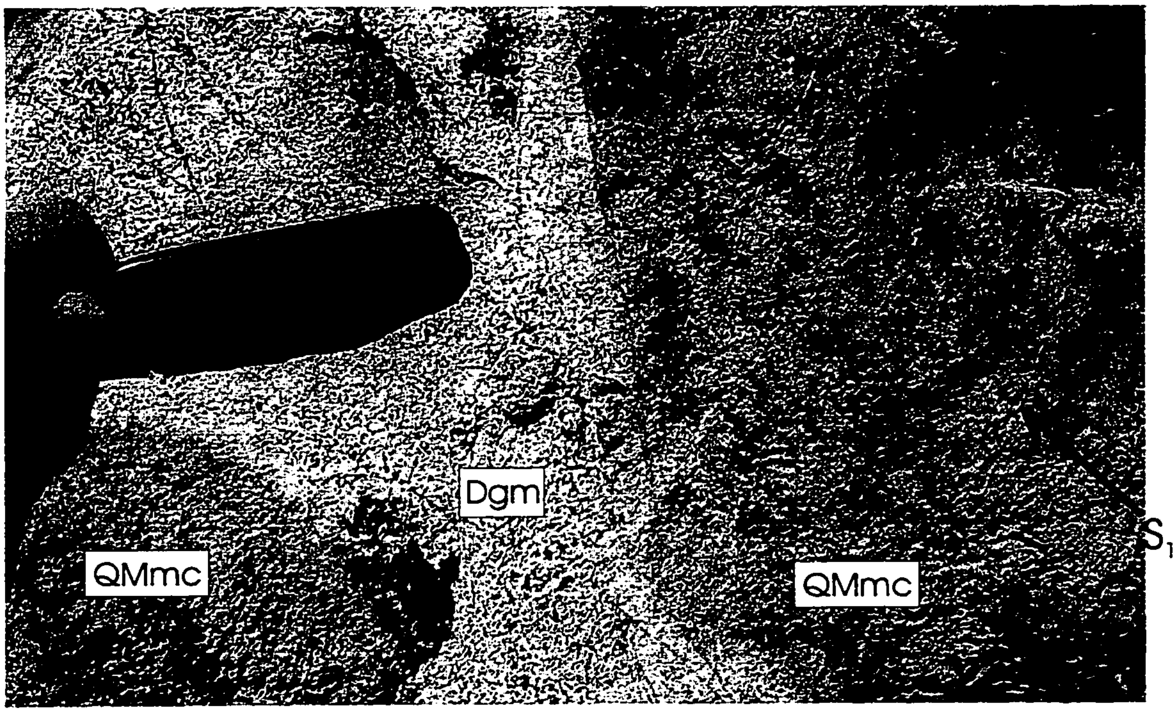

Plate 2-18: Photo of Dgm intruding Queest Mountain assemblage calcsilicate (QMmc). The intrusion cuts foliation (S_1) in the Queest Mountain assemblage. (Outcrop NS98-13; red scale ~8cm long).

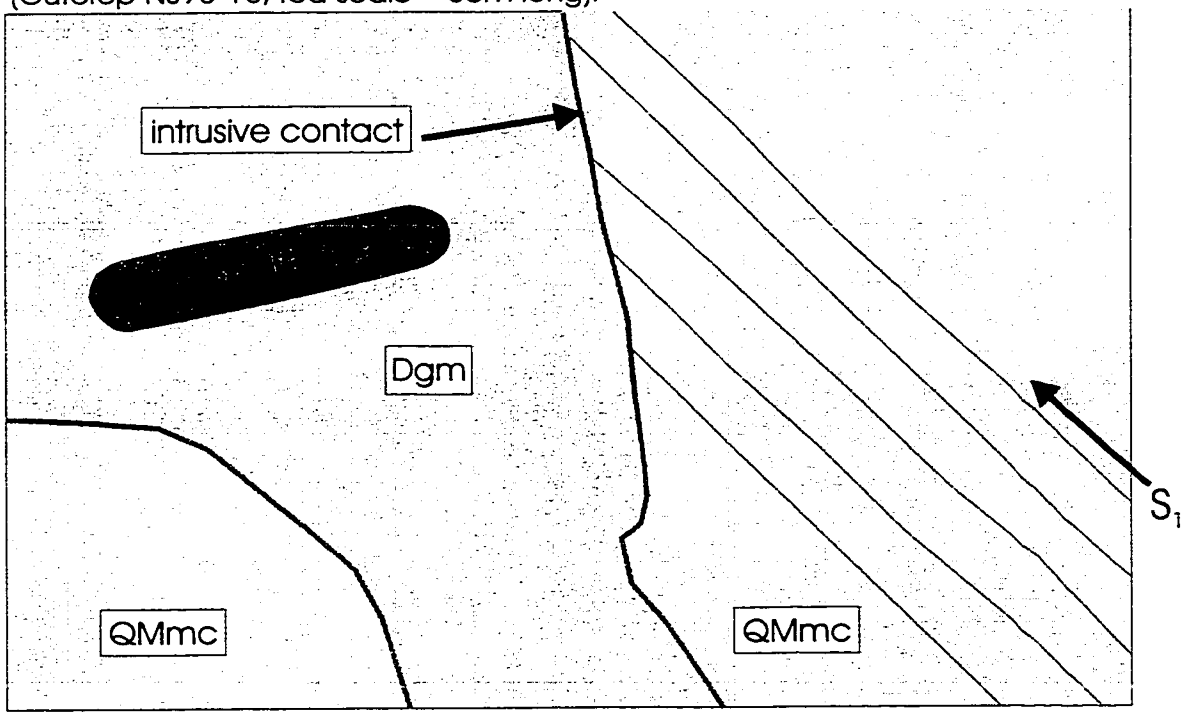

Figure 2-1: Sketch of Outcrop NS97-83 showing the intrusive contact of Dgm and the Queest Mountain assemblage (QMmc). Older (S_1) foliation is shown, younger (S_2) foliation is parallel to the page. S_1 is cut by the intrusive contact and it therefore pre-intrusion. S_2 is present in Dgm and QMmc, and is therefore post-intrusion.

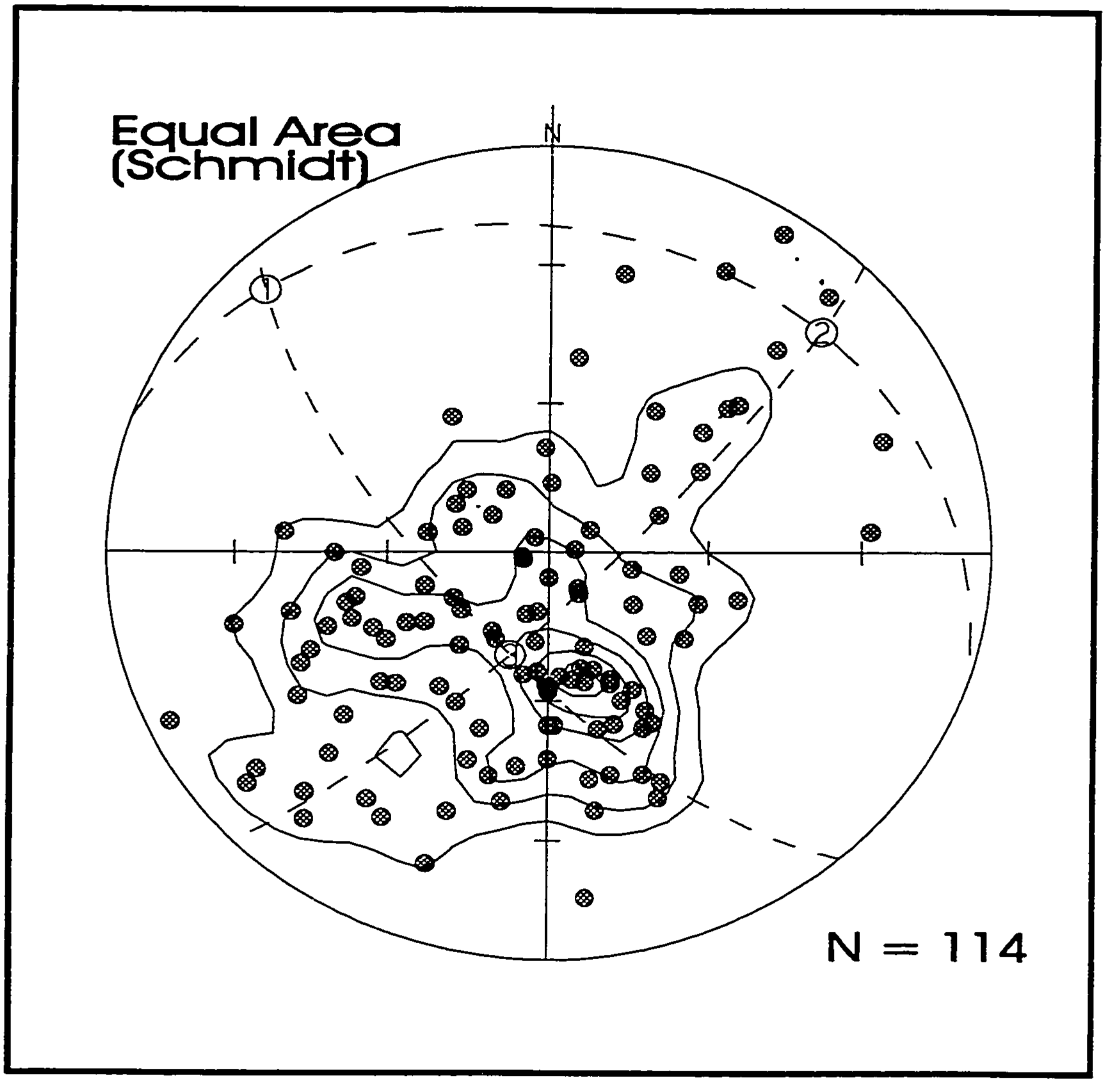

Eigenvectors	Trend	Plunge	Value
1	315	10	12.189
2	49	19	23.629
3	199	68	78.182

Figure 2-2: Poles to schistosity of the Mount Ida Group.
Numbers on the diagram correspond to eigenvectors listed above.

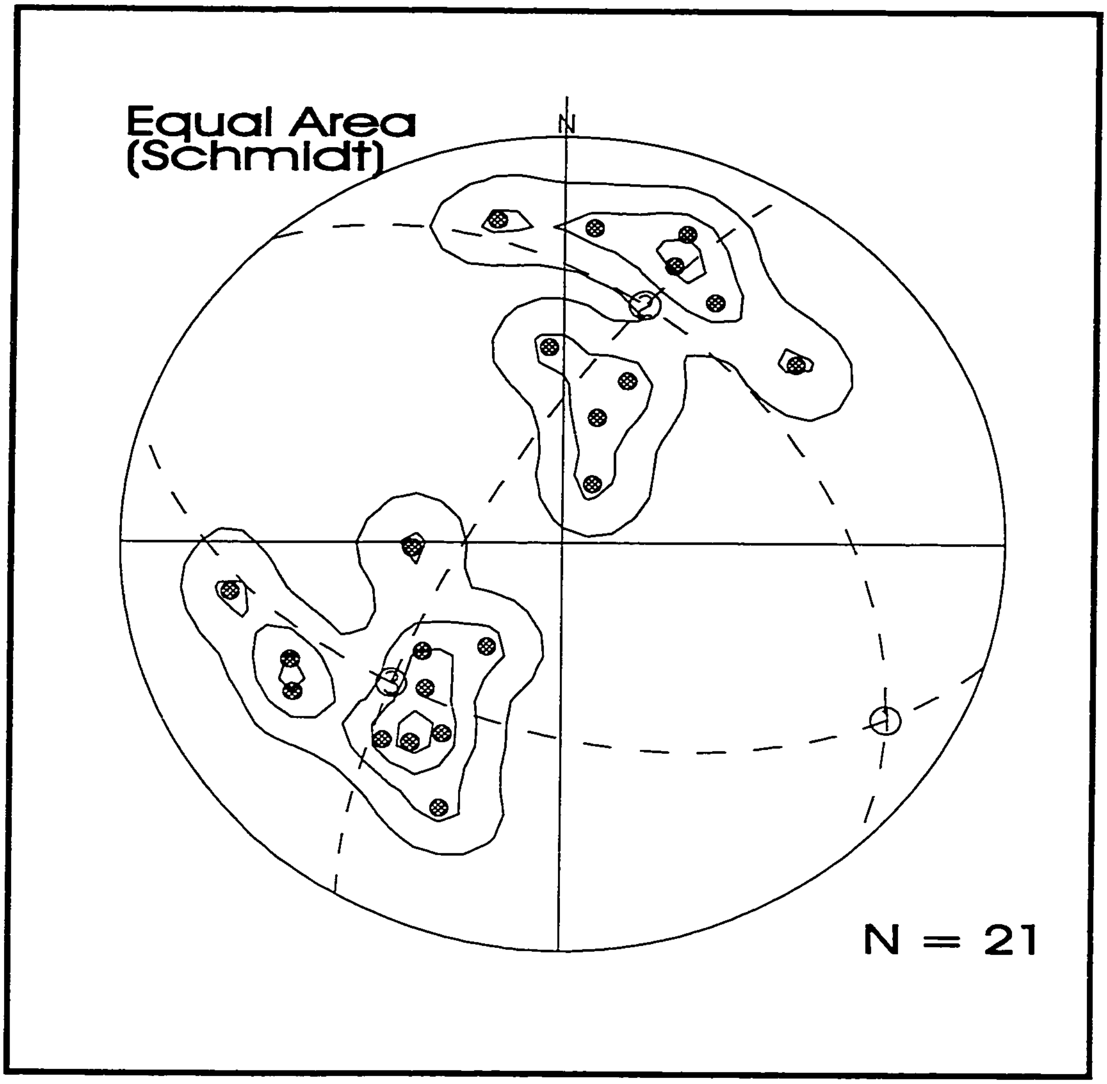

Eigenvectors	Trend	Plunge	Value
1	120	16	1.3112
2	17	38	9.0113
3	228	47	10.678

Figure 2-3: Poles to schistosity in the Queest Mountain assemblage. Number on the diagram correspond to eigenvectors listed above.

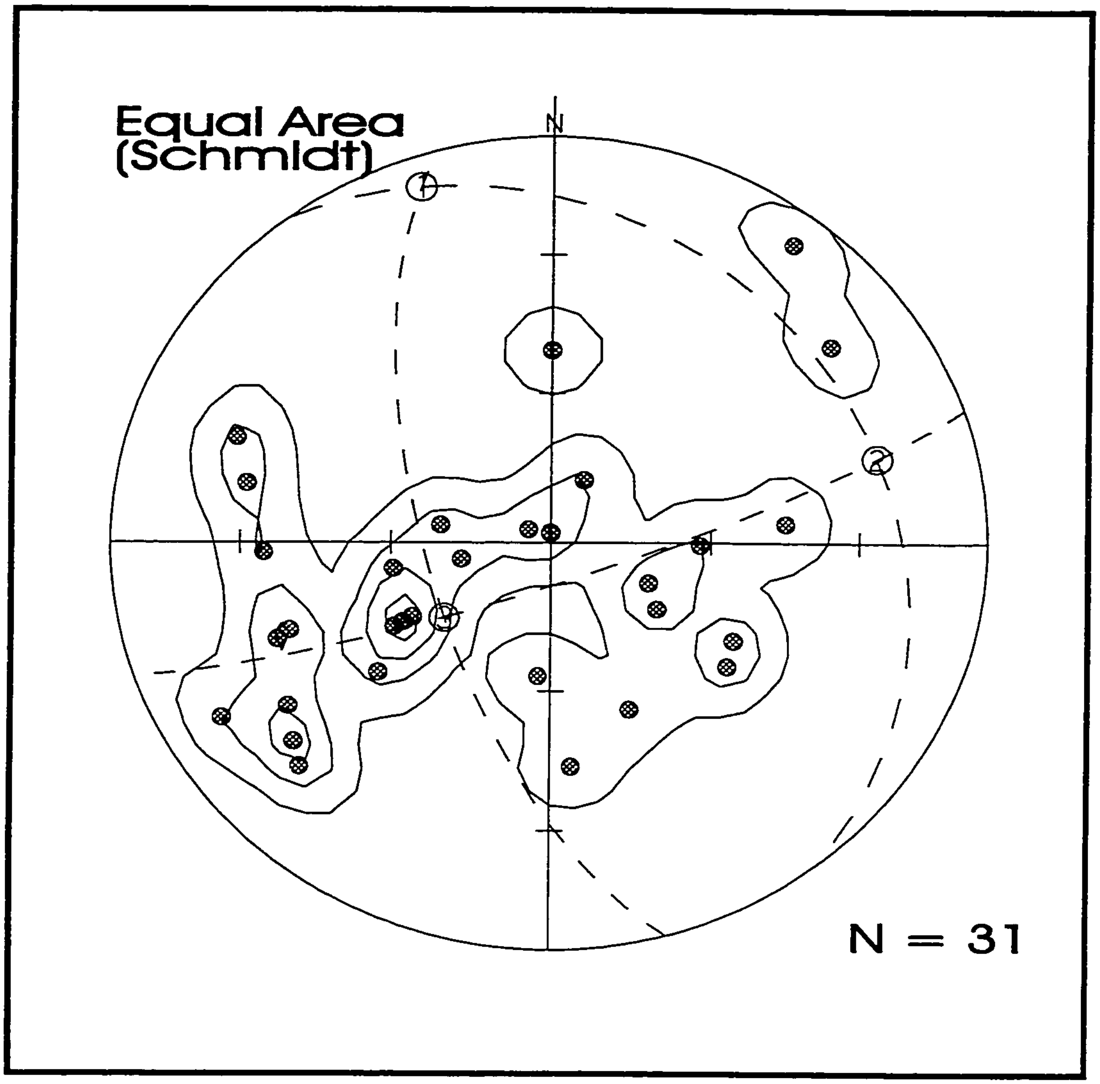

Eigenvectors	Trend	Plunge	Value
1	341	8	3.3110
2	74	23	8.6898
3	233	65	18.999

Figure 2-4: Poles to foliation in the Mount Fowler Batholith.
Numbers on the diagram correspond to eigenvectors listed above.

CHAPTER 3

Geothermometry and Geobarometry of Metamorphic Rocks

INTRODUCTION

As discussed in the previous chapter, the Queest Mountain assemblage has been separated from the Eagle Bay Formation based on lithological and structural differences. Due to changes in rock type across the contact between the Queest Mountain assemblage and the Eagle Bay Formation, the contact is interpreted as a fault or an unconformity. The orientation of the contact and the lithological differences across Shuswap Lake are suggestive of a fault. Geothermobarometry was undertaken to test this hypothesis. If a pressure and temperature difference exists between the two units, a fault contact, termed the Queest Mountain fault, is likely, because if the older unit was metamorphosed before being unconformable overlain by the younger unit, the older unit would likely have been reequilibrated during metamorphism of the younger unit, resulting in the same pressure and temperature for both units. Quantitative pressure-temperature estimates will also establish the sense of motion and amount of displacement on the proposed Queest Mountain fault. As many of the rocks in this area are pelitic, the minerals garnet, biotite, plagioclase, muscovite, and locally sillimanite are present and can be used for geothermobarometry.

Garnet and biotite form an Fe-Mg exchange geothermometer using the equation:

phlogopite + almandine = annite + pyrope.

The corresponding equilibrium curve, plotted on a P-T graph, represents the conditions under which garnet and biotite of a specific composition can co-exist. Because this equilibrium curve has a steep gradient in P-T space, temperature changes relatively little over wide pressure variations, and hence it can be used as a geothermometer (Spear, 1995).

The garnet-plagioclase-muscovite-biotite net transfer equilibrium:

pyrope + muscovite + grossular = 3 anorthite + phlogopite

is sensitive to pressure and therefore makes a good geobarometer (Spear, 1995).

If garnet, biotite, plagioclase, and muscovite all co-exist in a sample, three equilibria can be calculated, two of which are linearly independent. On a pressure vs. temperature plot, these two equilibrium curves will intersect at a point, which represents the only pressure and temperature at which minerals with those specific compositions can co-exist.

When garnet, biotite, plagioclase, muscovite, and sillimanite all exist at equilibrium, three more equilibria can be plotted in P-T space:

grossular + α-quartz + 2 sillimanite = 3 anorthite

almandine + muscovite = 2 sillimanite + α-quartz + annite

pyrope + muscovite = phlogopite + α-quartz + 2 sillimanite.

In principle, the six equilibrium curves should intersect in a single point where all the minerals are estimated to co-exist at equilibrium. For this to happen, the thermodynamic and compositional data must be accurate and the minerals must have last equilibrated at the same temperature and pressure (Berman, 1991). Commonly these conditions are not met, and the equilibrium curves intersect in three points, forming a triangle of estimate of possible P-T conditions.

ANALYTICAL METHODS

Ten samples were analysed, five from the Queest Mountain assemblage and five from the Eagle Bay Formation, to establish differences in the pressure and temperature of metamorphism between the two units. The minerals used for this analysis include garnet, biotite, plagioclase, muscovite (where present), and sillimanite (where present). Samples were chosen that had a maximum number of these phases present. Mineral grains that appeared to be in textural equilibrium (i.e. no reactions at grain boundaries, no mineral overgrowths) with each other were chosen for this study, as their compositions should represent equilibrium compositions and therefore provide an accurate estimate of metamorphic pressure and temperature. This meant selecting grains that were close to each other within a single thin section and avoiding grains such as biotite that had been extensively retrograded to chlorite. As described in Chapter 2, most textures indicate that the minerals are at equilibrium.

The samples were analysed using a JEOL JXA-8900R electron microprobe at the University of Alberta. A 15 kV accelerating voltage, a 15 nÅ beam current, and a beam size of 5 μm were used. Standards used for calibration are shown in Table 3-1.

Several grains of each mineral were analysed in each sample. As well, each grain was analysed across several traverses, from the center to the rim of the grain, to determine homogeneity. Biotite and muscovite were typically homogeneous. Garnet showed a small amount of zoning in some grains, usually by an increase of up to 10 weight percent in the amount of almandine towards the rims, accompanied by an equivalent decrease in the amount of grossular. In these cases, rim compositions were used for pressure and temperature estimates, as it is assumed that rim compositions are most likely at equilibrium with adjacent grains. Larger garnets were typically more zoned than small garnets, as small garnets were likely completely homogenized during metamorphism. Plagioclase was commonly inhomogeneous, with variations of up to 10 weight percent in the amount of albite and anorthite, usually becoming slightly more anorthite-rich at the rims; average or typical rim compositions were used in calculations. These zonation patterns for garnet and plagioclase imply a decrease in pressure and/or an increase in temperature as the minerals formed.

The computer programs and data base TWEEQU (Thermobarometry With Estimation of EQUilibrium state) consists of a computer program for calculating phase equilibrium curves (Berman, 1991), a thermodynamic database for minerals (Berman, 1988, 1990), and additional programs for plotting and printing (Berman, 1991). The program TWQ202 (Berman, 1991) was used to calculate reaction boundaries and estimate a pressure and temperature of metamorphism for selected samples. The range of data obtained from the microprobe, as well as the data chosen for use in the following calculations, are shown in Appendix C.

Sample locations and P-T determinations are plotted on Figure 3-12.

EAGLE BAY FORMATION

Sample NS97-340 is from Unit Eq of the Eagle Bay Formation, from near Quartzite Point on the east shore of Shuswap Lake. This sample was chosen because it contains garnet, plagioclase, biotite, and muscovite, all of which appear to be in equilibrium with each other. The P-T plot for this sample shows an intersection of reactions corresponding to a pressure of ~ 7.2 kbar and a temperature of ~ 700 °C (Figure 3-1).

Sample NS97-82, from the Eagle Bay Formation Unit Eq, in the northeastern part of the study area, also contains the assemblage garnet, plagioclase, biotite, and muscovite. The P-T plot for this sample gives a pressure of ~ 7.6 kbar and a temperature of ~ 650 °C (Figure 3-2).

Sample NS97-8 was chosen from the southern part of the Eagle Bay Formation. This sample, from Unit Eg, did not contain muscovite, and so only the garnet-biotite geothermometer could be used. A temperature of ~ 610 °C was obtained for this sample (Figure 3-3), which is slightly lower than the temperatures derived for the other Eagle Bay Formation samples.

Sample NS97-162 is from Unit Eq of the Eagle Bay Formation in an area near the Queest Mountain fault and contains sillimanite in addition to garnet, biotite, plagioclase, and muscovite. Three linearly independent equilibria can be plotted, resulting in a triangle of possible pressures and temperatures (Figure 3-4). The pressure range is from ~ 4.0 to 6.8 kbar and the temperature range is from 600 to 700 °C.

Sample NS97-387 is also from Unit Eq, west of sample NS97-162, adjacent to the

Queest Mountain fault. This sample also contains sillimanite, garnet, biotite, plagioclase, and muscovite. The triangle on the P-T plot for this sample has a pressure range of ~ 4.0 to 6.0 kbar and a temperature range of 600 to 680 °C (Figure 3-5).

The four samples for which both pressure and temperature estimates were obtained are plotted on Figure 3-11. For the two samples (NS97-162 and NS97-387) that contain sillimanite, the higher limit of the pressure and temperature range was used for this plot, as the higher temperature and pressure is derived from the same geothermobarometer as the temperature and pressures from samples that do not contain sillimanite. In order to eliminate calibration uncertainties and allow direct comparison of pressures and temperatures, the same geothermobarometer must be used for all samples (Spear, 1995). Error bars of ± 25°C and ± 200 bars, which is the uncertainty associated with only analytical errors and geological uncertainty caused by compositional heterogeneities in minerals (Spear, 1995), are shown. For the procedure undertaken for this thesis, calibration uncertainties are negligible as they will cancel out when looking at a pressure difference rather than an actual pressure (Spear, 1995).

From Figure 3-11 it can be seen that the temperatures are the same within error. Although the pressures are not the same within error, they appear to form a separate cluster from the Queest Mountain assemblage samples. The average pressure and temperature of the Eagle Bay Formation is 6.9 kbar and 682.5 °C. This falls within the amphibolite metamorphic facies, and also falls within the stability range of the mineral assemblages present in these samples.

QUEEST MOUNTAIN ASSEMBLAGE

Sample NS97-75, from Unit Qs of the Queest Mountain assemblage, contains garnet, plagioclase, biotite, and muscovite in textural equilibrium. This sample is from north of the Queest Mountain fault. Equilibria intersect in a point that corresponds to a pressure of ~ 4.1 kbar and a temperature of ~ 590 °C (Figure 3-6).

Sample NS97-91A, from an outcrop of Unit Qs along Shuswap Lake just north of the Queest Mountain fault, also contains garnet, plagioclase, biotite, and muscovite in equilibrium. The P-T plot for this sample shows a pressure of ~ 2.8 kbar and a temperature of ~ 580 °C (Figure 3-7). The pressure and temperature estimated for this sample are lower than other Queest Mountain assemblage samples because the garnet is very manganese-rich (12 weight percent MnO compared to < 6 weight percent MnO in other samples) and therefore its composition is near the limits of accuracy of the thermodynamic database used by the program TWQ202 (Berman, 1990).

Sample NS97-74, from an outcrop of Unit Qs west of NS97-75, contains garnet, plagioclase, biotite, and muscovite in textural equilibrium. The P-T plot for this sample (Figure 3-8) shows a pressure of ~ 5.1 kbar and a temperature of ~ 540 °C.

Sample NS97-326, from Unit Qs just north of Sample NS97-75, also contains garnet, plagioclase, biotite, and muscovite in equilibrium. The equilibria curves for this sample intersect in a point corresponding to a pressure of 5.2 kbar and a temperature of 550 °C (Figure 3-9).

The final sample from the Queest Mountain assemblage, sample NS97-119, is from west of sample NS97-326 and north of sample NS97-74. Garnet in this sample has irregular grain boundaries and appears to have undergone resorption, and therefore is not in textural equilibrium. This sample was analysed due to a lack of other samples from the Queest Mountain assemblage and to see what the effects of possible disequilibrium might be. This sample yielded a pressure of 8.1 kbar and a temperature of 680 °C (Figure 3-10), which is different from other Queest Mountain assemblage samples. Therefore, the assumption that the garnet in this sample is not in equilibrium may be correct, and data obtained from this sample is therefore not considered accurate.

The four samples from the Queest Mountain assemblage that display equilibrium textures are plotted on Figure 3-11. Sample NS97-119 is not included as its minerals are not considered to be at equilibrium. The four samples plotted on Figure 3-11 have all been analysed using the same geothermobarometer, so calibration uncertainties are negligible and a direct comparison of the data is possible.

For the Queest Mountain assemblage samples, it can be seen that the temperatures are the same within error, while the pressures have a spread of 2.4 kbar. The average of the four samples is 4.3 kbar and 565 °C. As discussed above, sample NS97-91A may have an anomalously low pressure due to the high manganese content of the garnets; if this sample is not included, the spread is 1.1 kbar and the average pressure and temperature is 4.8 kbar and 560 °C. Both of these pressure and temperature averages are within amphibolite facies and fall within the P-T space defined by petrogenetic grid constraints determined from the mineral assemblages present in these samples.

DISCUSSION

With one exception, described above, the samples used for this analysis have textures that indicate that the minerals are at equilibrium. Pressures and temperatures estimated from geothermobarometry fit within the pressure and temperature range defined by petrogenetic grid constraints (Yardley, 1989). The samples were all analysed using the same geothermobarometer, which eliminates calibration uncertainties and allows for the direct comparison of data between samples. For these reasons, the pressures and temperatures obtained for these samples accurately estimate the pressure and temperature of peak metamorphism. The pressure and temperature difference between the Eagle Bay Formation and the Queest Mountain assemblage is real.

The average pressures and temperatures (6.9 kbar and 682.5 °C for the Eagle Bay Formation and 4.8 kbar and 560 °C for the Queest Mountain assemblage) differ by 2.1 kbar and ~ 123 °C. As can be seen from Figure 3-12, the closest samples on either side of the Queest Mountain fault are 2.5 km apart on the map. The closest two samples (NS97-387 and NS97-91A) have a pressure difference of 3.2 kbar and a temperature difference of 100°C over the 2.5 km. A normal pressure gradient for regionally metamorphosed continental crust is about 3 kbar/10 km (Yardley, 1989). This pressure difference between the closest two samples is 12.8 kbar/10 km, over four times is too great to be a normal pressure gradient. Geothermal gradients for continental crust are typically in the range 15 to 30 °C/km (Yardley, 1989); the temperature difference between the units is 40°C/km, also too great to be a normal geothermal gradient. The presence of a pressure and temperature difference between the Eagle Bay Formation and the Queest Mountain assemblage suggests that a fault contact is more likely than an unconformity, because if one unit was metamorphosed before being unconformably overlain by the other, the metamorphism that affected the younger rocks would have reequilibrated the older rocks, resulting in the same pressure and temperature of metamorphism for both units. The pressure and temperature difference suggests that the Eagle Bay Formation and the Queest Mountain assemblage were metamorphosed separately before being juxtaposed by the Queest Mountain fault.

Field relations indicate that the Queest Mountain fault dips to the north, which would place the lower-pressure Queest Mountain assemblage over the higher-pressure Eagle Bay Formation, implying a normal sense of motion on the fault. From Chapter 2, the Queest Mountain fault is estimated to have a dip between 16° and 30°. An average pressure difference of 2.1 kbar between the Eagle Bay Formation and the Queest Mountain assemblage, assuming a normal pressure gradient of 3 kbar/10 km, implies a difference in depth of 7 km between the two units. As shown in Figure 3-13, this implies a normal displacement of between 14 and 25 km on the fault, depending on the dip of the fault.

Since the pluton cuts the Queest Mountain fault, the juxtaposition of the Eagle Bay Formation and the Queest Mountain assemblage must have occurred prior to the Late Devonian intrusion. Because of the different peak metamorphic temperatures and pressures preserved in the Eagle Bay Formation and the Queest Mountain assemblage, the peak metamorphism recorded by the minerals in the metasedimentary rocks must have occurred before the Queest Mountain fault, and therefore is also pre-Late Devonian in age. If a metamorphic event after the Late Devonian had reequilibrated the metamorphic minerals in the Eagle Bay Formation and the Queest Mountain assemblage, then the two units should have the same temperature and pressure, therefore any metamorphic events after the Late Devonian must not have reequilibrated the Eagle Bay Formation or the Queest Mountain assemblage, and a record of pre-Late Devonian metamorphism is preserved in this area. As discussed in Chapter 2, the orientation of the fault implies that it has not been substantially deformed during the Columbian and Laramide orogenies. The timing of peak metamorphism could be tested by dating metamorphic minerals, for example monazite, from the Eagle Bay Formation and the Queest Mountain assemblage; this was beyond the scope of this study. The Queest Mountain fault must also have occurred after the deposition and syn-metamorphic deformation of the Eagle Bay Formation and of the Queest Mountain assemblage. If it is assumed, as discussed in Chapter 2, that the Eagle Bay Formation in the study area is Cambrian, the Queest Mountain fault must be post-Cambrian and pre-Late Devonian. The amount and sense of motion on this fault implies a normal detachment. The sense of motion implies extension parallel to the margin of Ancestral North America. The relationship of this fault to the evolution of the Ancestral Cordilleran margin will be discussed in Chapter 5.

Table 3-1: Mineral standards used for calibration of the electron microprobe

	Biotite	Muscovite	Garnet	Plagioclase
F	calbiotite	calbiotite		
Na_2O	kaersuitite	kaersuitite	kaersuitite	albite
K_2O	calbiotite	muscovite		sanidine
FeO	calbiotite	calbiotite	fayalite	osumite
Al_2O_3	muscovite	muscovite	rvgar1	plagioclase
Cl	tugtupite	tugtupite		
Cr_2O_3	chromite	chromite	chromite	
SiO_2	calbiotite	muscovite	rvgar1	sanidine
CaO	kaersuitite	kaersuitite	rvgar1	plagioclase
MnO	willemite	willemite	willemite	willemite
MgO	calbiotite	calbiotite	rvgar1	osumite
TiO_2	kaersuitite	kaersuitite	kaersuitite	

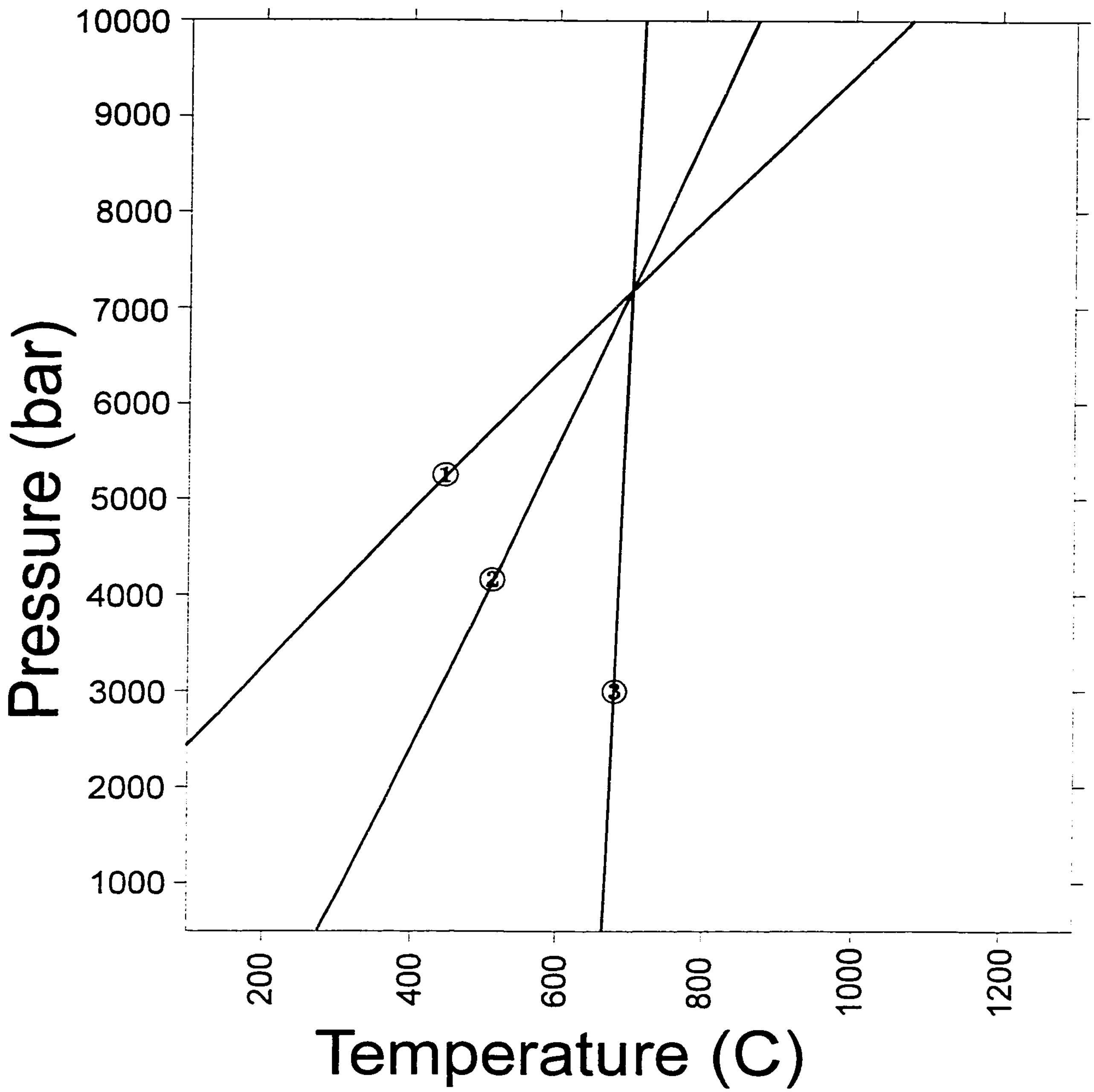

Reactions:	
1) Py + Ms + Gr ⇄ 3 An + Phl	Py = pyrope garnet
2) Alm + Gr + Ms ⇄ 3 An + Ann	Gr = grossular garnet
3) Phl + Alm ⇄ Ann + Py	Alm = almandine garnet
	Ms = muscovite
	Phl = phlogopite
	Ann = annite
(high pressure phases on left)	An = anorthite

Figure 3-1: Plot of pressure vs temperature reactions for sample NS97-340, Eagle Bay Formation.

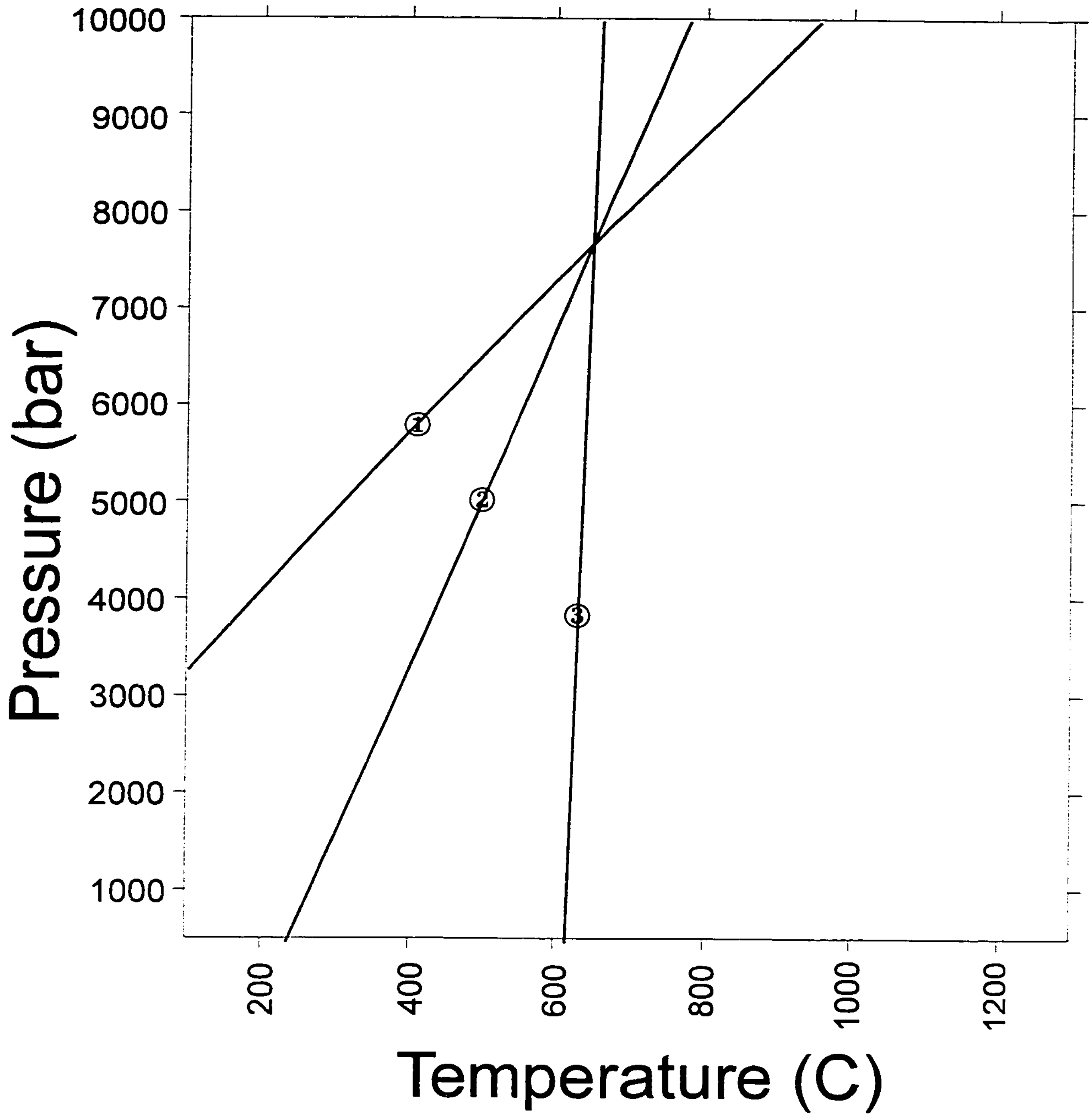

Reactions:	
1) Py + Ms + Gr ⇄ 3 An + Phl	Py = pyrope garnet
2) Alm + Gr + Ms ⇄ 3 An + Ann	Gr = grossular garnet
3) Phl + Alm ⇄ Ann + Py	Alm = almandine garnet
	Ms = muscovite
	Phl = phlogopite
	Ann = annite
(high pressure phases on left)	An = anorthite

Figure 3-2: Plot of pressure vs temperature reactions for sample NS97-82, Eagle Bay Formation.

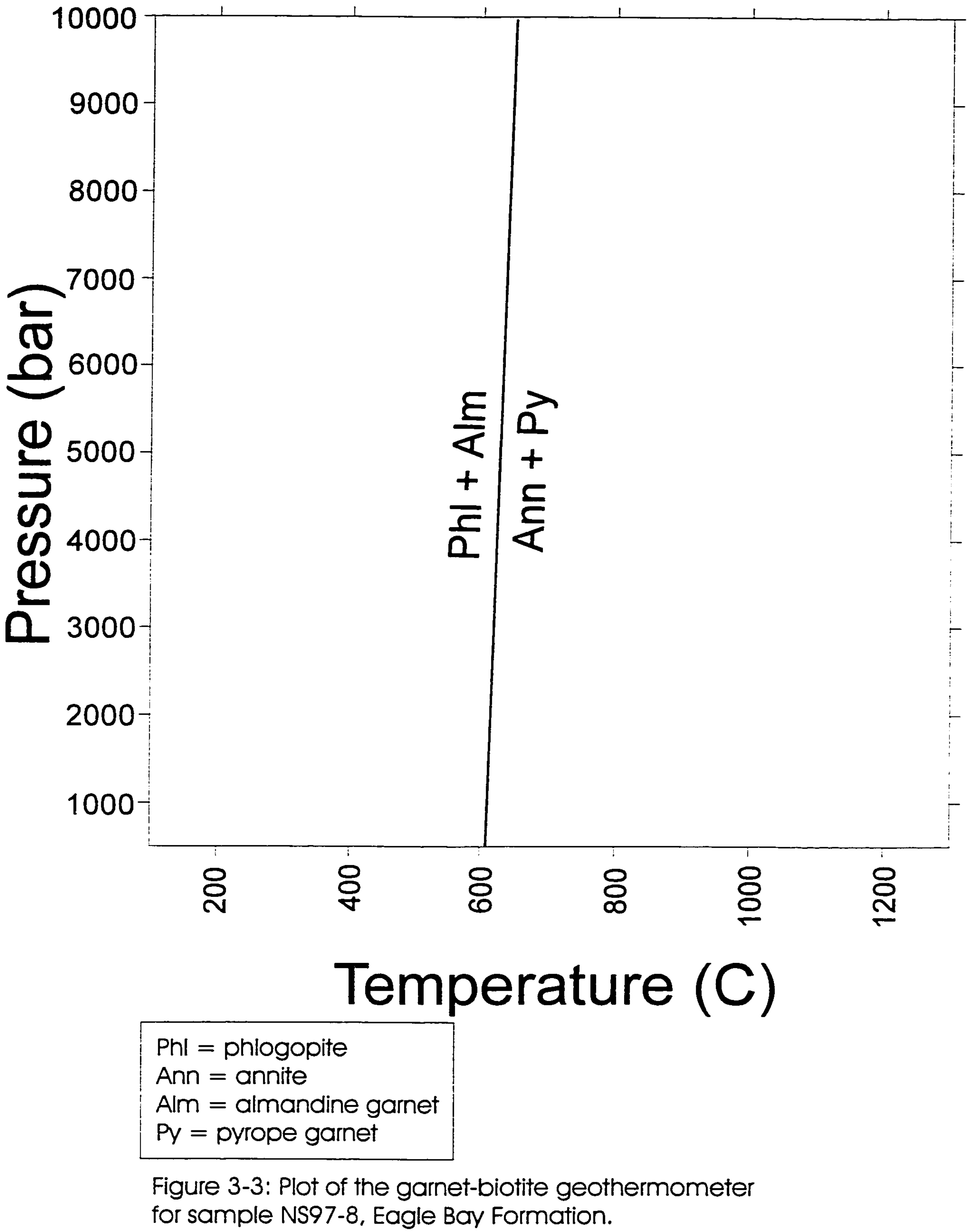

Figure 3-3: Plot of the garnet-biotite geothermometer for sample NS97-8, Eagle Bay Formation.

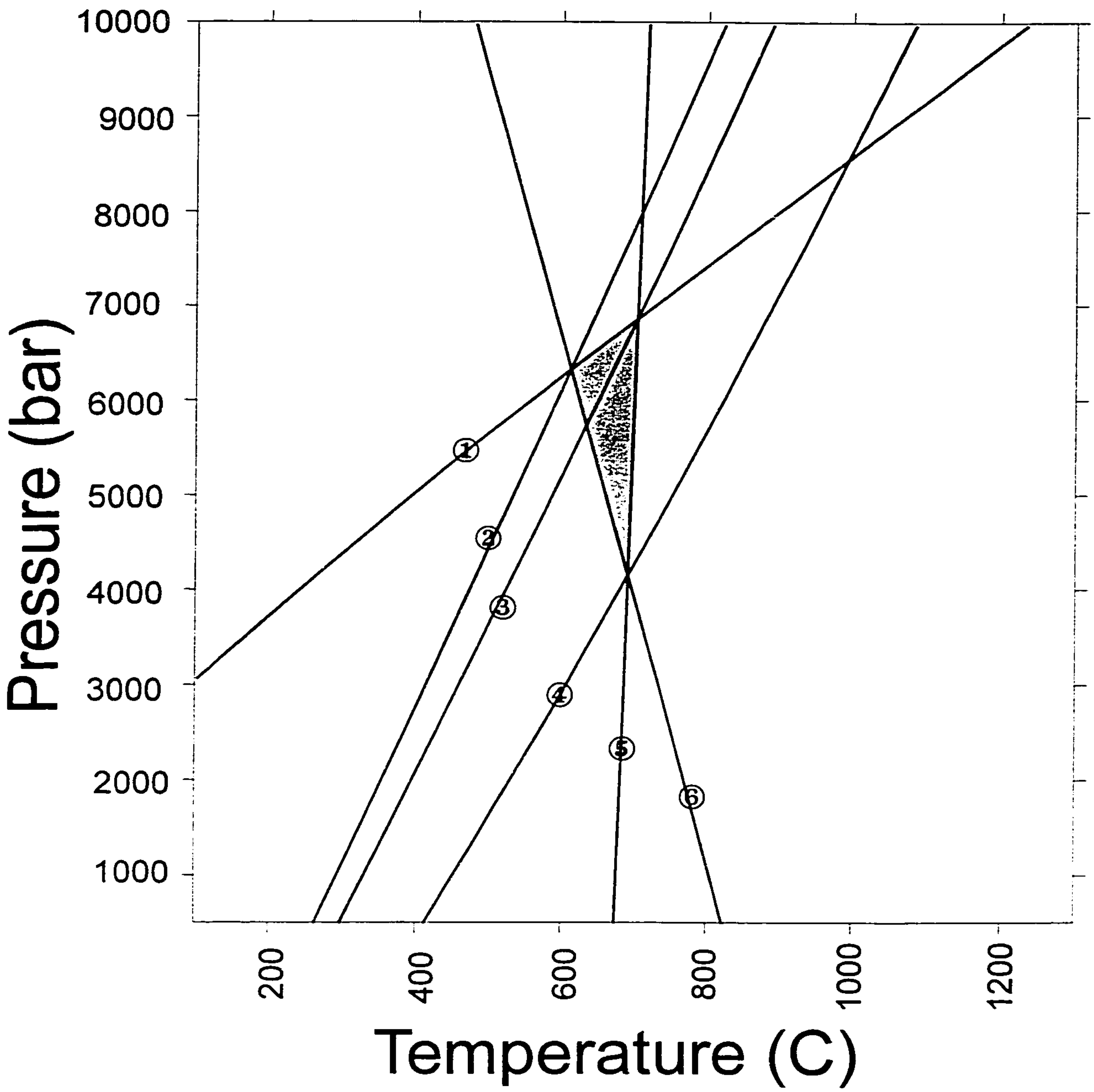

Reactions:	
1) Py + Ms + Gr ⇄ 3 An + Phl	Py = pyrope garnet
2) Gr + a-Qz + 2 Si ⇄ 3 An	Gr = grossular garnet
3) Alm + Gr + Ms ⇄ 3 An + Ann	Alm = almandine garnet
4) Alm + Ms ⇄ 2 Si + a-Qz + Ann	Ms = muscovite
5) Phl + Alm ⇄ Ann + Py	Phl = phlogopite
6) Py + Ms ⇄ Phl + a-Qz + 2 Si	Ann = annite
(high pressure phases on left)	a-Qz = alpha quartz
	An = anorthite
	Si = sillimanite

Figure 3-4: Plot of pressure vs temperature reactions for sample NS97-162, Eagle Bay Formation. Shaded area shows the possible P-T range for this sample.

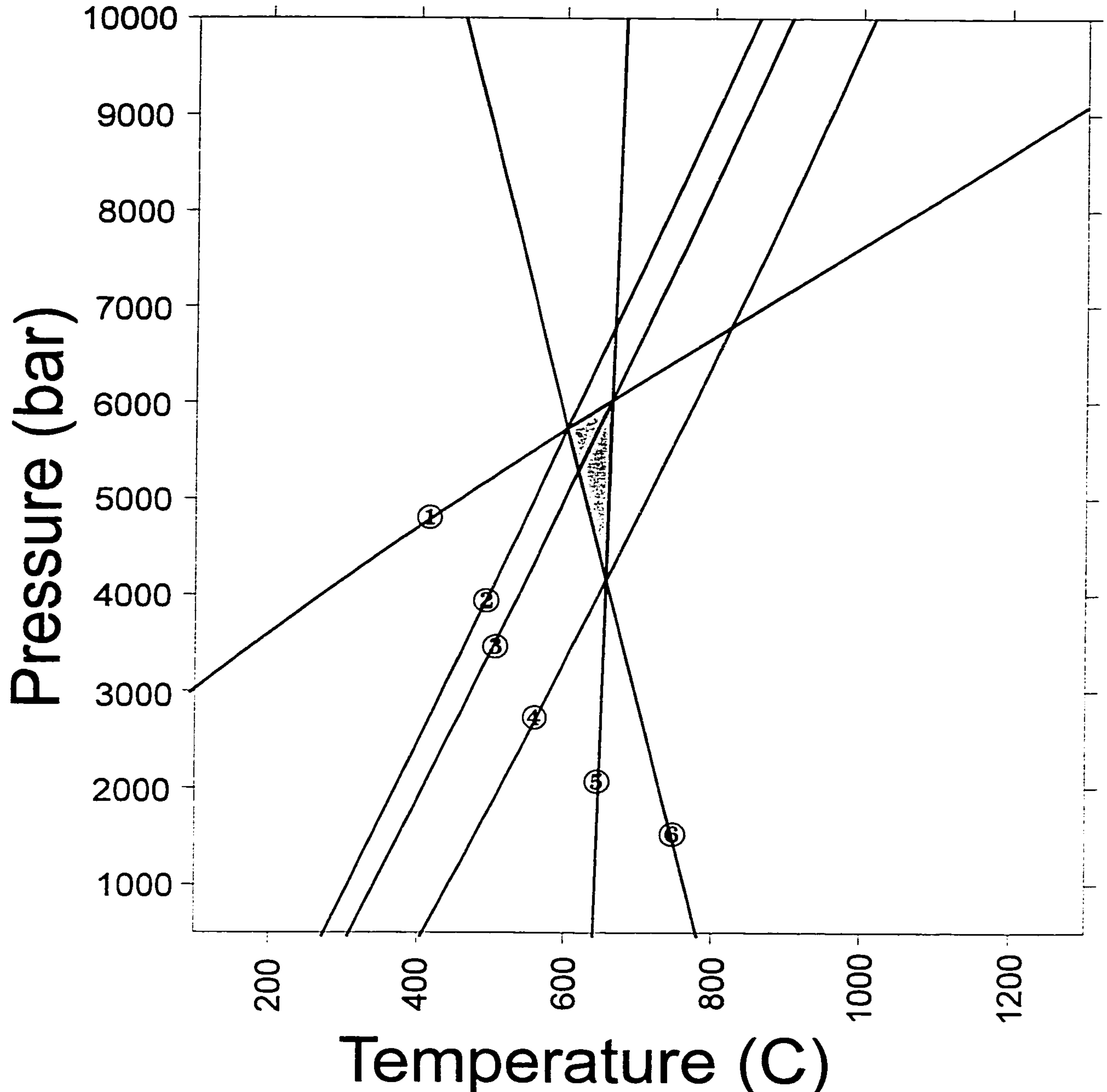

Reactions:	
1) Py + Ms + Gr ⇄ 3 An + Phl	Py = pyrope garnet
2) Gr + a-Qz + 2 Si ⇄ 3 An	Gr = grossular garnet
3) Alm + Gr + Ms ⇄ 3 An + Ann	Alm = almandine garnet
4) Alm + Ms ⇄ 2 Si + a-Qz + Ann	Ms = muscovite
5) Phl + Alm ⇄ Ann + Py	Phl = phlogopite
6) Py + Ms ⇄ Phl + a-Qz + 2 Si	Ann = annite
(high pressure phases on left)	a-Qz = alpha quartz
	An = anorthite
	Si = sillimanite

Figure 3-5: Plot of pressure vs temperature reactions for sample NS97-387, Eagle Bay Formation. Shaded area shows the possible P-T range for this sample.

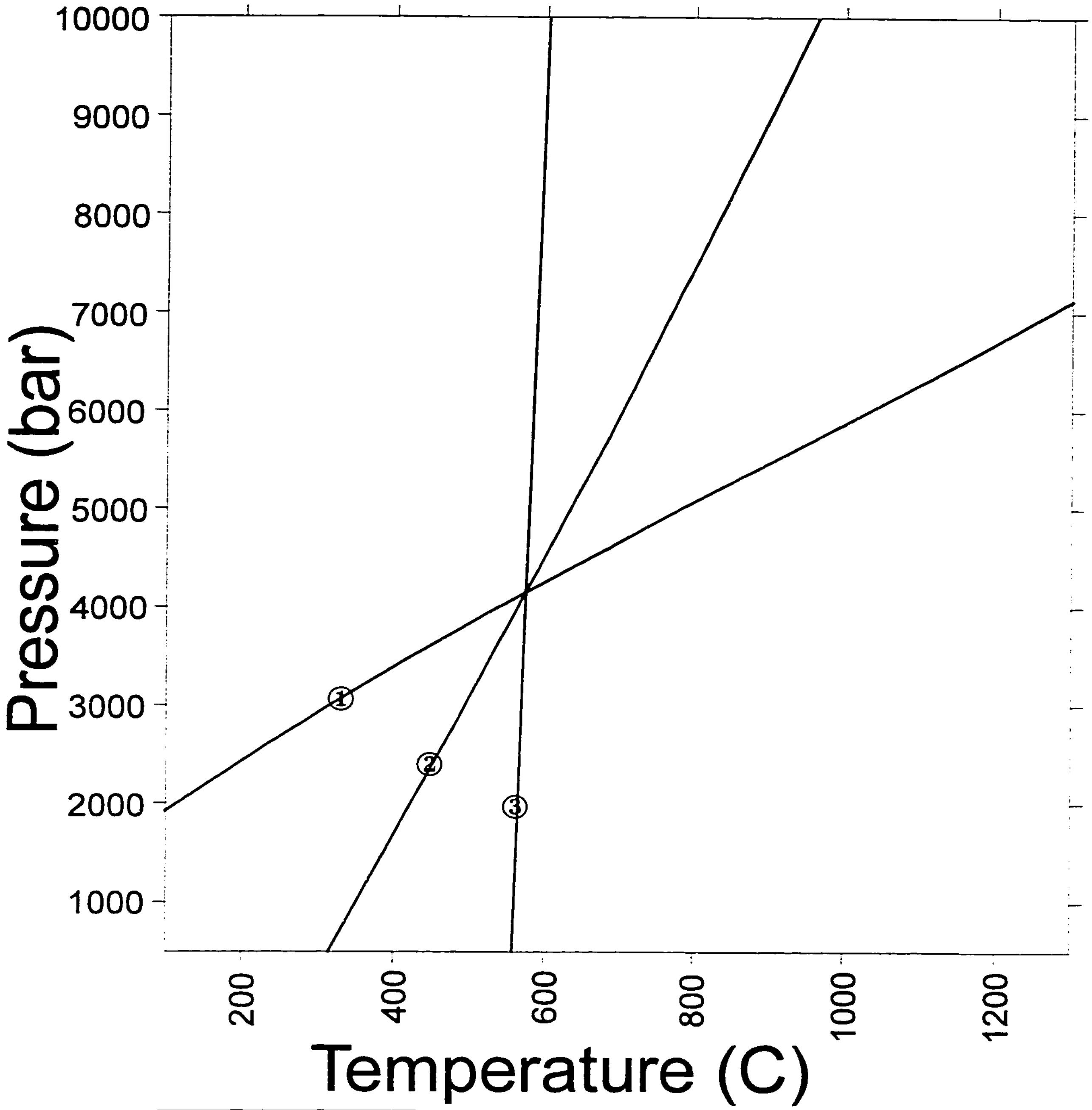

Reactions:	
1) Py + Ms + Gr ⇄ 3 An + Phl	Py = pyrope garnet
2) Alm + Gr + Ms ⇄ 3 An + Ann	Gr = grossular garnet
3) Phl + Alm ⇄ Ann + Py	Alm = almandine garnet
	Ms = muscovite
	Phl = phlogopite
	Ann = annite
(high pressure phases on left)	An = anorthite

Figure 3-6: Plot of pressure vs temperature reactions for sample NS97-75, Queest Mountain assemblage.

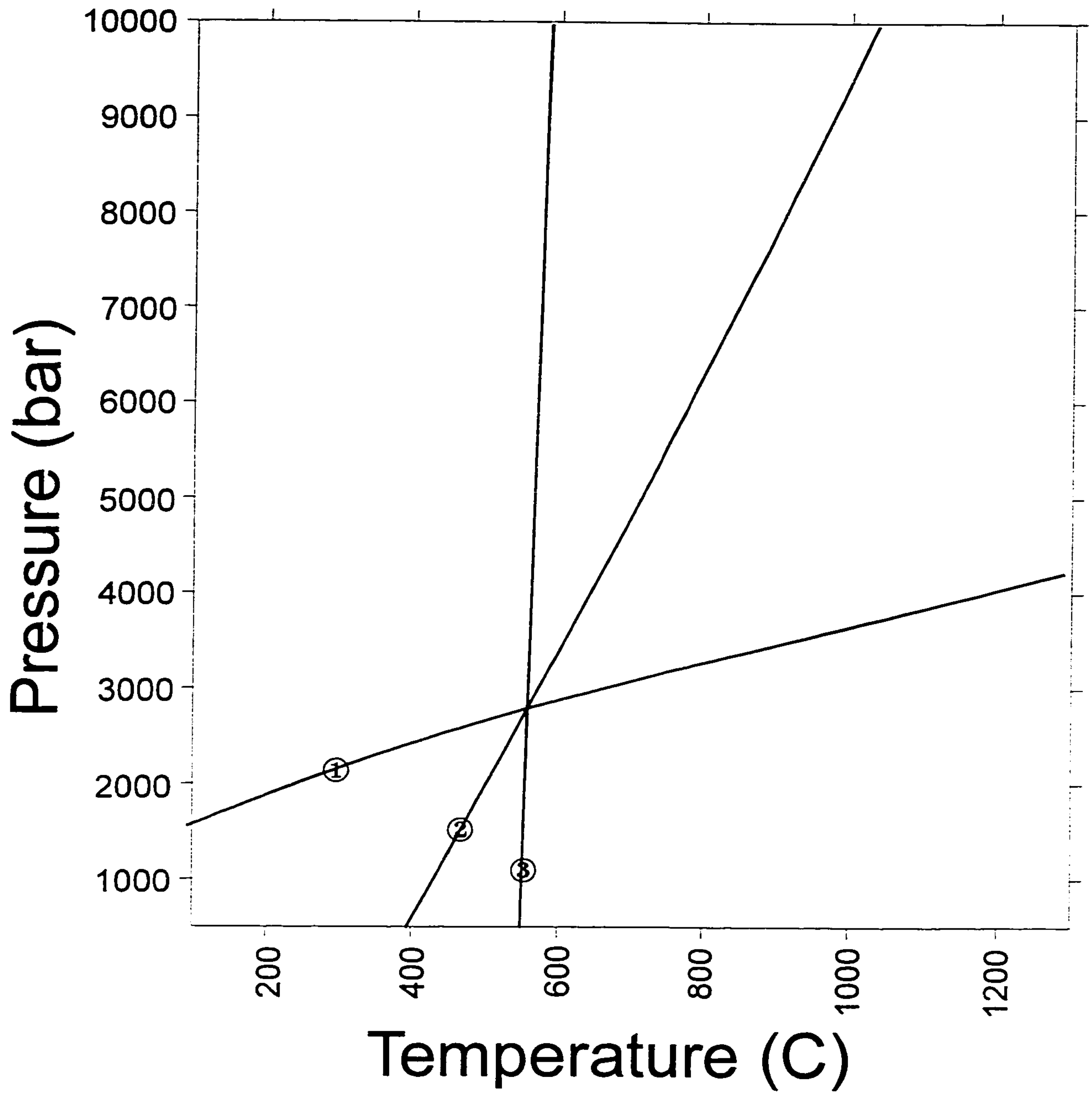

Reactions:	
1) Py + Ms + Gr ⇄ 3 An + Phl	Py = pyrope garnet
2) Alm + Gr + Ms ⇄ 3 An + Ann	Gr = grossular garnet
3) Phl + Alm ⇄ Ann + Py	Alm = almandine garnet
	Ms = muscovite
	Phl = phlogopite
(high pressure phases on left)	Ann = annite
	An = anorthite

Figure 3-7: Plot of pressure vs temperature reactions for sample NS97-91A, Queest Mountain assemblage.

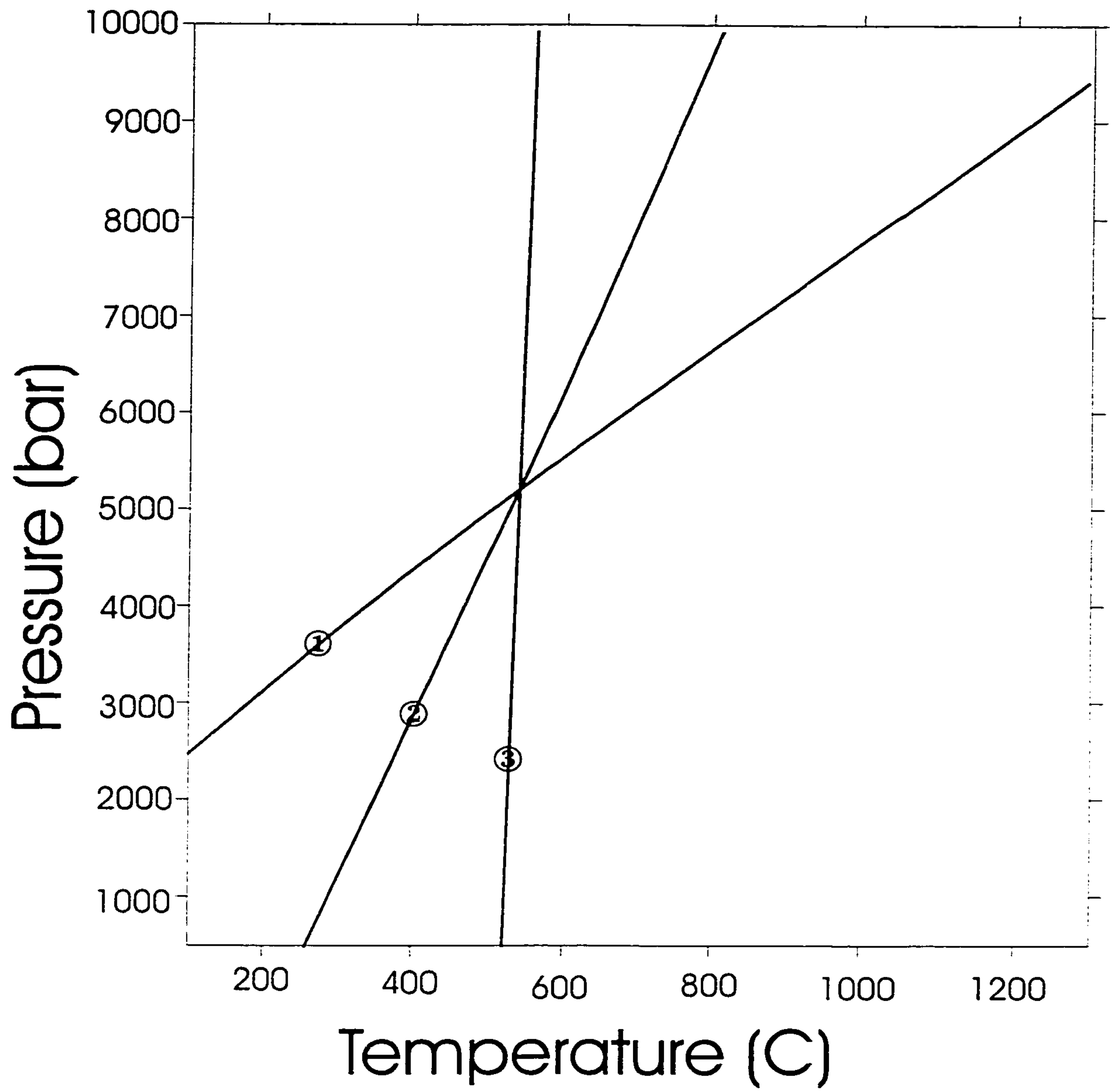

Reactions: 1) Py + Ms + Gr $\rightleftarrows$ 3 An + Phl 2) Alm + Gr + Ms $\rightleftarrows$ 3 An + Ann 3) Phl + Alm $\rightleftarrows$ Ann + Py (high pressure phases on left)	Py = pyrope garnet Gr = grossular garnet Alm = almandine garnet Ms = muscovite Phl = phlogopite Ann = annite An = anorthite

Figure 3-8: Plot of pressure vs temperature reactions for sample NS97-74, Queest Mountain assemblage.

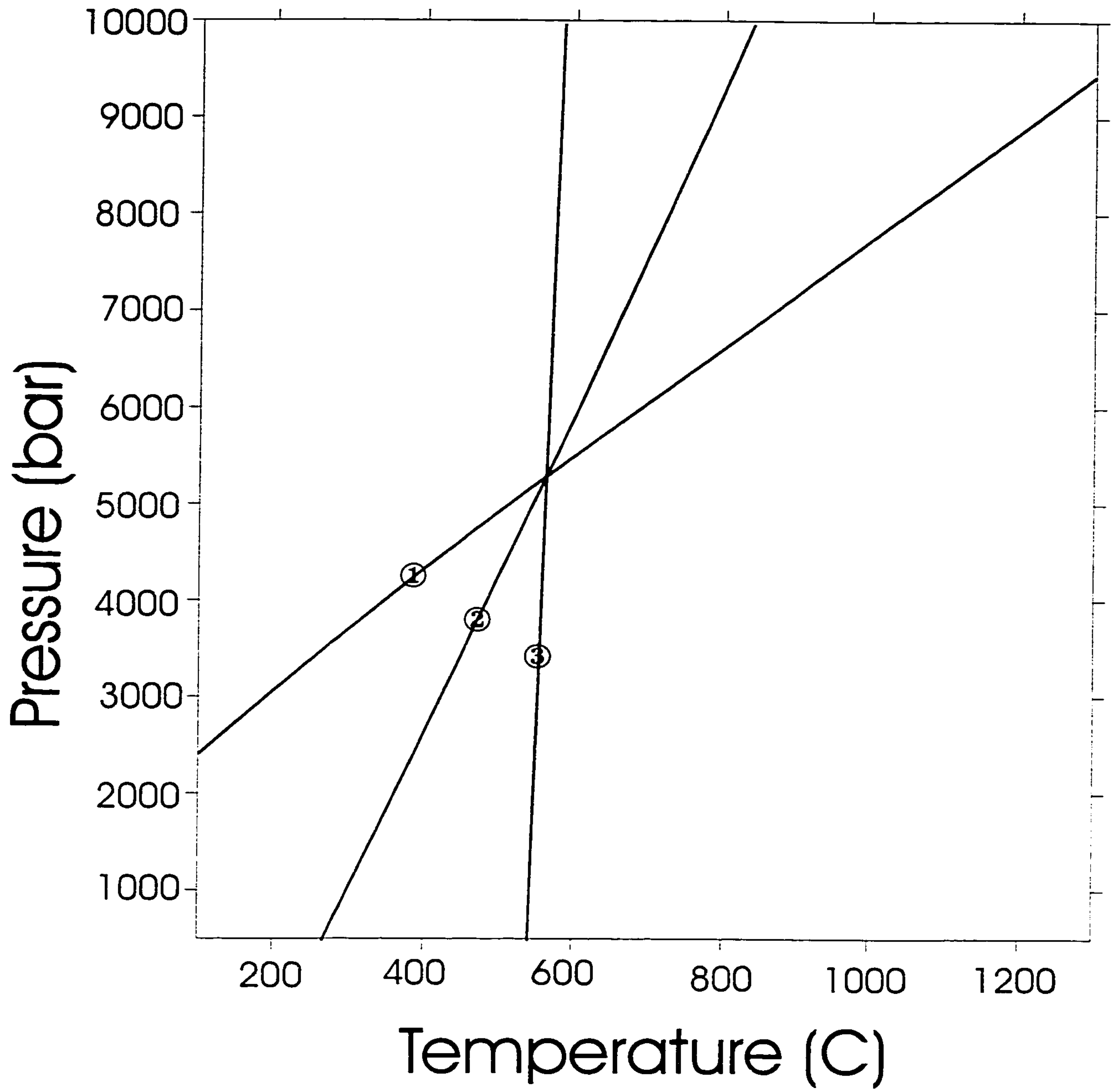

Reactions:	
1) Py + Ms + Gr ⇄ 3 An + Phl	Py = pyrope garnet
2) Alm + Gr + Ms ⇄ 3 An + Ann	Gr = grossular garnet
3) Phl + Alm ⇄ Ann + Py	Alm = almandine garnet
	Ms = muscovite
	Phl = phlogopite
	Ann = annite
(high pressure phases on left)	An = anorthite

Figure 3-9: Plot of pressure vs temperature reactions for sample NS97-326, Queest Mountain assemblage.

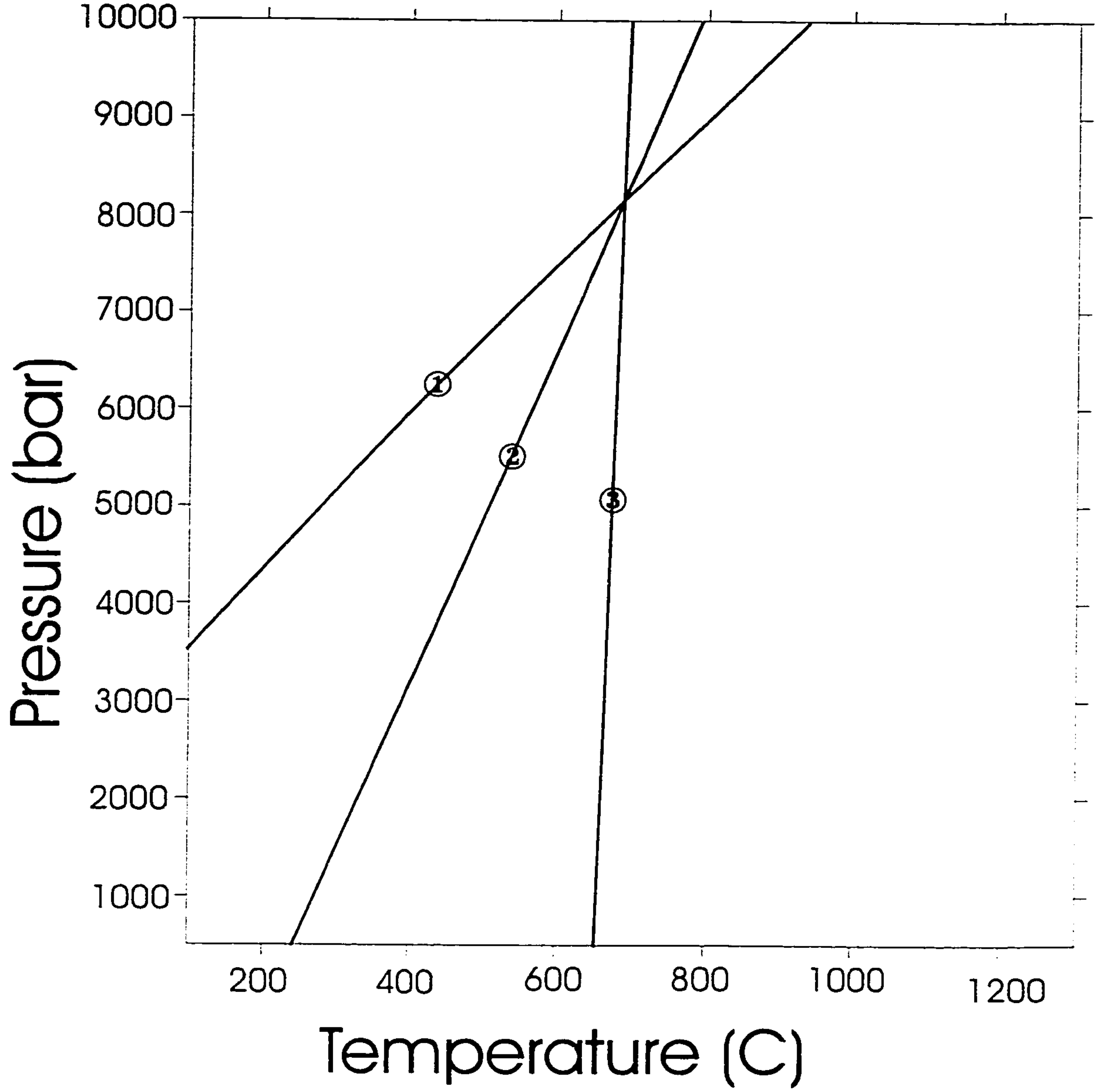

Reactions:	Py = pyrope garnet
1) Py + Ms + Gr ⇄ 3 An + Phl	Gr = grossular garnet
2) Alm + Gr + Ms ⇄ 3 An + Ann	Alm = almandine garnet
3) Phl + Alm ⇄ Ann + Py	Ms = muscovite
	Phl = phlogopite
	Ann = annite
(high pressure phases on left)	An = anorthite

Figure 3-10: Plot of pressure vs temperature reactions for sample NS97-119, Queest Mountain assemblage.

**Figure 3-11:
Pressure vs Temperature**

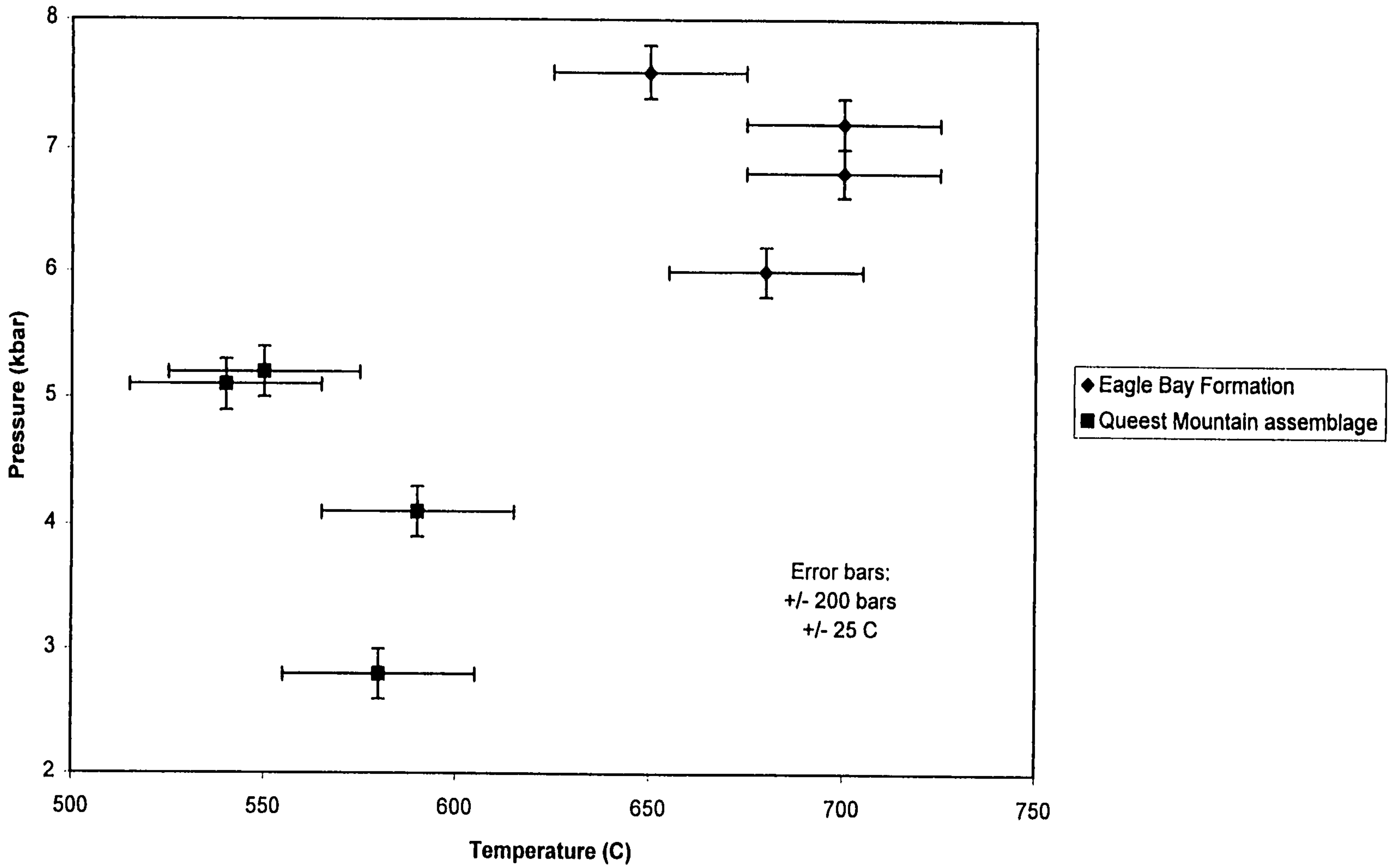

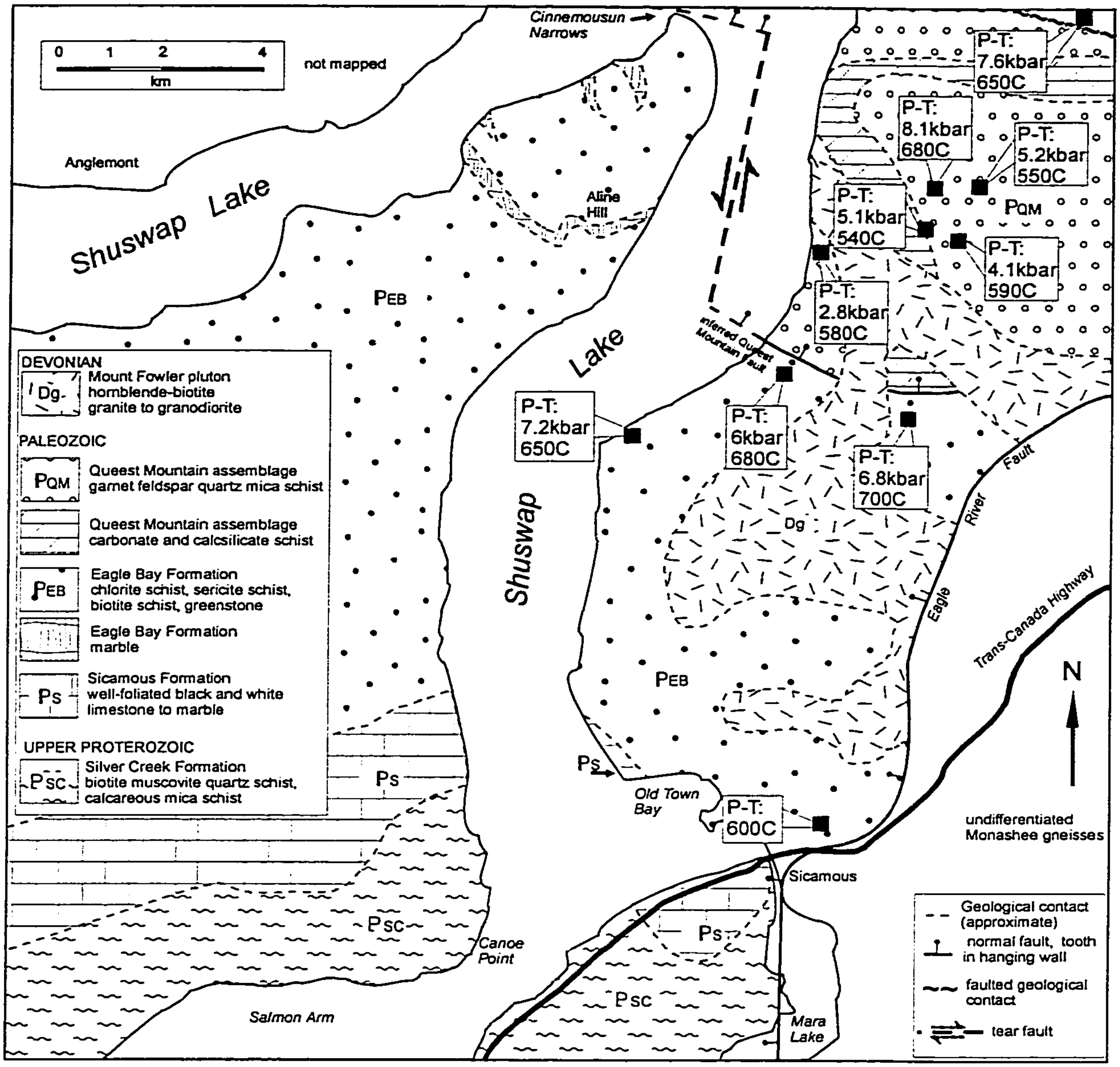

Figure 3-12: Generalized geological map of the Shuswap Lake area showing locations and data from geothermobarometry.

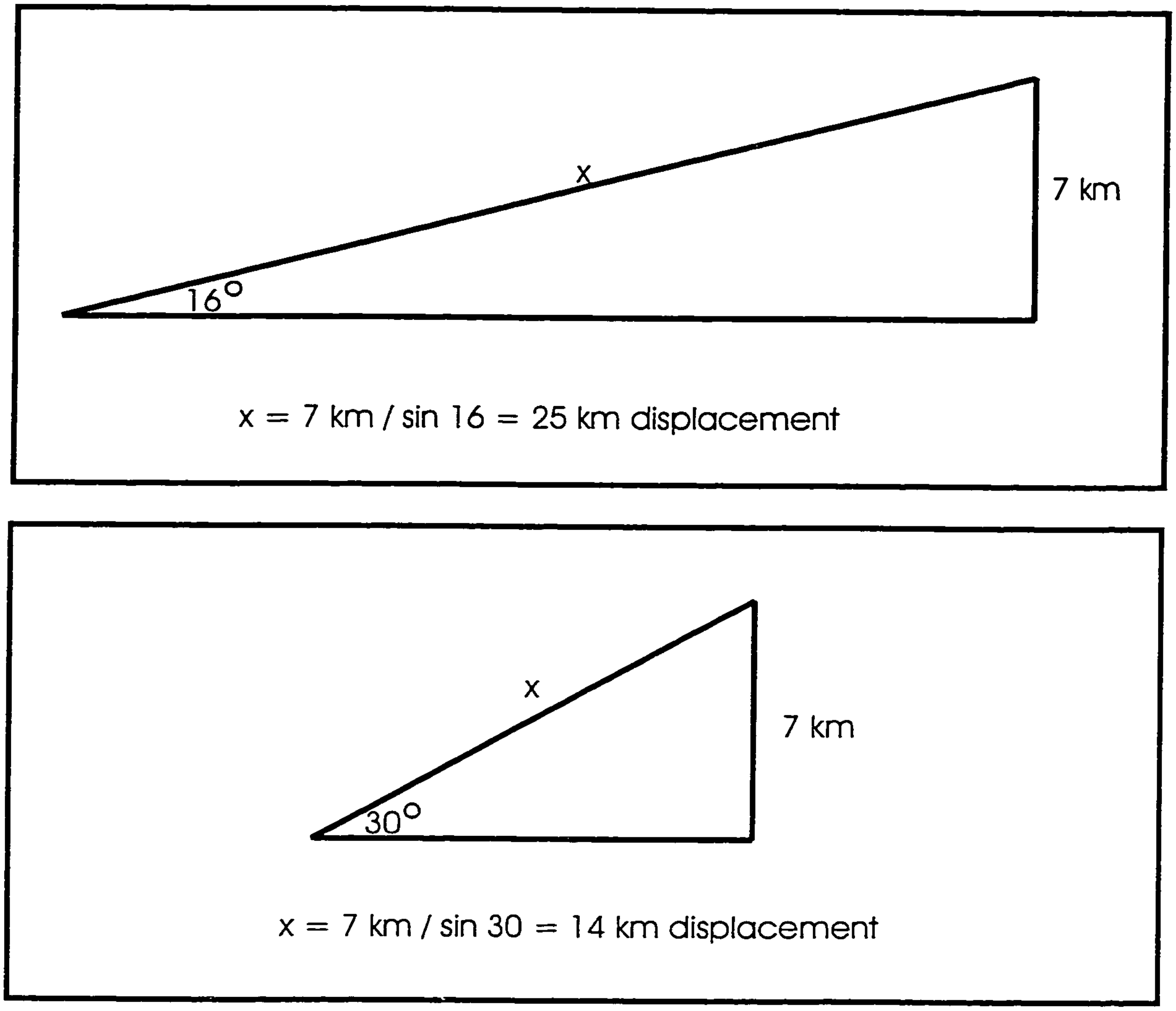

Figure 3-13: Displacement on the Queest Mountain fault.
Dip of the fault is constrained by outcrop locations to between 16 and 30 degrees. Differences in metamorphic pressures imply a difference of 7km depth between the Eagle Bay Formation and the Queest Mountain assemblage. The amount of displacement on the fault, x, is between 14 and 25 km.

CHAPTER 4

Geochronology of Units Dg and Dgm in the Study Area

INTRODUCTION

As described in Chapter 2, a granitoid pluton intrudes the Eagle Bay Formation and the Queest Mountain assemblage, and cuts the Queest Mountain fault and some foliation in the host rocks. The pluton has been previously dated at only one location within the field area, which yielded a $^{207}Pb/^{206}Pb$ zircon date of 376 ± 6 Ma (Okulitch *et al.*, 1975). This study has allowed for the detailed mapping of the boundary of the pluton on the east side of Shuswap Lake. Geochronological work for this thesis aims to more accurately and precisely determine the age of the pluton within the study area, using current geochronological techniques. Also, this study will date three samples within the study area to confirm the regional extent of the pluton. If the Late Devonian age of the pluton is confirmed, the correlation of the pluton with the Mount Fowler suite (Okulitch *et al.*,1975) will be substantiated, and the age of the pluton can be used to determine the relative ages of other structures.

There are two unstable nuclides of uranium, ^{238}U and ^{235}U, that decay to ^{206}Pb and ^{207}Pb respectively. The decay constant for ^{238}U is 1.55125×10^{-10} y^{-1} and the decay constant for ^{235}U is 9.8485×10^{-10} y^{-1} (Jaffey *et al.*, 1971). Uranium-lead geochronology allows for the determination of two apparent U-Pb ages, providing a test as to whether the mineral has behaved as a closed system. U-Pb analyses can be plotted on a graph of $^{206}Pb/^{238}U$ vs. $^{207}Pb/^{235}U$, termed a concordia diagram. A concordia curve on this diagram shows the location of identical U-Pb ages throughout time. Deviance from the concordia line is termed discordance. A best-fit line through several discordant analyses from the same unit is termed a discordia line. The upper intercept of the discordia line with the concordia curve is commonly interpreted as the age of the dated event, for example the age of intrusion of a pluton (Heaman and Parrish, 1991).

Zircon fractions were analysed using U-Pb geochronology (described in Heaman and Parrish, 1991) from three samples from the pluton on the east side of Shuswap Lake. These samples were chosen from two different phases, Dg, a medium-grained biotite-hornblende granite that comprises most of the pluton and is possibly the youngest phase, and Dgm, a fine-grained mafic biotite-hornblende granite to granodiorite that may be the oldest phase, in order to determine if different phases of the pluton are the same age. Also, samples were chosen from either side of the Queest Mountain fault to test the hypothesis that the pluton is the same unit across the fault. One of the zircon fractions analysed is from an outcrop where an intrusive contact is exposed between Unit Dgm and the Queest Mountain assemblage; this sample will be used to investigate whether foliation in the host rocks is older than Late Devonian.

This work was done using the rock crushing equipment, mineral separation equipment, the ultra-clean chemistry lab, and the mass spectrometers at the University of Alberta.

ANALYTICAL METHODS

Large (5-10 kg) samples were collected in the field. The samples were chosen to avoid weathering where possible. Samples were then broken into fist sized pieces using a sledge hammer. A jaw-crusher was used to break the pieces into pea-sized fragments, and samples were then reduced to powder with a disc-mill.

Mineral separation techniques were then used to separate zircons. The powdered sample was passed over a Wilfley table. The heavy fraction was passed over the Wilfley table a second time, dried, and retained for further processing. The heavy fraction from the Wilfley table was sieved through a 70 mesh (0.210 mm) screen. The <70 mesh fraction was then passed twice vertically by a Frantz isodynamic magnetic separator to remove magnetic minerals and steel particles originating from the crushing equipment. The non-magnetic portion was passed through the Frantz (forward tilt of 10° and side tilt of 15°) for several passes of increasing amperage between 0.25A and 1.1A (i.e. the non-magnetic portion from each step was passed through the Frantz again with increased amperage) to remove minerals (garnet, hornblende) with magnetic properties. The non-magnetic portion from this step, which would contain the zircons, was put in a separatory funnel with Methylene iodide (specific gravity = 3.32 g/cm^3). Zircon, which has a specific gravity of 4.5 to 4.7 g/cm^3, will be found in the heavy fraction. This heavy fraction was then passed through the Frantz a second time, with a constant amperage of 1.8 A and decreasing side tilt between 15° and 0° (i.e. the non-magnetic portion from each step was passed through the Frantz again with decreased side tilt). Zircons from the least magnetic fractions are better for U-Pb analysis as they contain fewer inclusions.

The zircons were then hand-picked using ethanol and small tweezers. The zircons were separated into populations based on size, colour, shape, and quality (amount of inclusions). All samples had several populations of zircon.

For the first pass, two fractions from each of two samples (i.e., four fractions) were analysed without abrasion. After this, two poorer-quality fractions from one sample were abraded to attempt to remove surface contamination and areas of lead loss near the edges of grains. Two other samples were not abraded due to their size and shape (small prismatic zircons from NS97-14 and needle-like grains from NS97-13B). Fractions were abraded with pyrite in a small air chamber at ~ 3 psi for ~ 4 hours. Details of the abrasion process can be found in Krogh (1982). The samples were then cleaned in warm 4N HNO_3 for ~ ½ hour to dissolve the pyrite. The acid was then replaced with ethanol and the zircons were picked out and transferred to a small beaker. Samples (abraded or not) were washed in warm 4N HNO_3. Each sample was rinsed with de-ionized water to remove the acid, the beaker was immersed in an ultrasonic bath for one minute, and then the sample was rinsed again with de-ionized water and acetone.

The samples were weighed on a small boat made of aluminum foil. The boat and zircons were weighed together on a microbalance, then the zircons were transferred to small ultraclean Teflon bombs (cleaned by repeated HF + HNO_3 / HCl washing at high temperature). The empty aluminum boat was then weighed; this mass was subtracted from the total mass to determine the mass of the zircons.

In the ultra-clean laboratory at the University of Alberta, the zircons were dissolved and U and Pb were extracted from the samples (see Krogh, 1973). To dissolve the zircons, HF and HNO_3, as well as a ^{205}Pb - ^{235}U tracer solution, were added to the bombs. The bombs were put in a teflon jacket and a metal jacket and heated at 220 °C for ~96 hours. The bombs were then removed from the oven, cooled, opened, and dried. To convert the sample to a chloride, 3.1N HCl was added and the bombs were resealed and heated at 200 °C for at least 8 hours.

While the sample was being dissolved and converted to a chloride, columns containing anion-exchange resin were set up and cleaned using at least 3 cycles of alternating 6.2N HCl and de-ionized water. The columns were then cleaned with 3.1N HCl. The sample was added to the column, and Pb was eluted into a clean beaker using 6.2N HCl. U was eluted into the same beaker using de-ionized water. Then, 2 drops of 0.125N H_3PO_4 were added to the beaker and it was evaporated to dryness.

The sample was then mixed with 3.5 µl of H_3PO_4 and 2.5 µl of silica gel and loaded onto a pre-cleaned Re filament. Details of this method were given in Cameron *et al.* (1969). The samples were analysed by thermal ionization mass spectrometry on either the VG-354 or the Micromass Sector 54 mass spectrometers in operation at the University of Alberta. In this technique, atoms of the sample are evaporated from a heated metal surface, producing a beam of positive ions. Depending on the amperage of the ionized beam, either the Daly or the Faraday detector was used. The Daly detector is used to detect low ion currents ($< 1 \times 10^{-13}$ A), because it has a low noise level (as low as 4×10^{-20} A). At higher amperages, data on the Daly detector becomes non-linear, so the Faraday detector is used. Corrections were made to the data to remove biases depending on which detector was used.

Mass bias corrections were also made for the mass spectrometer used, because every mass spectrometer is slightly different. In order to standardize data, data is calibrated against a standard, called NBS981, to obtain globally accepted values. For the VG-354, NBS981 $^{207}Pb/^{206}Pb$ runs at 0.91364472 ± 0.00021 and $^{208}Pb/^{206}Pb$ 2.1616264 ± 0.001. The accepted values for these ratios are 0.914585 and 2.16701 respectively. The correction factor for these values is then taken into account in the age calculation software program ROMAGE43.BAS (modified by Larry Heaman, 1992), which was used to calculate dates from the raw mass spectrometer data. Results are presented in Table 4-1. Calculations of the discordia line were made using the program MLKFIT.BAS (the in-house error propagation program described in Heaman and Machado, 1992), with lower intercepts forced through 0 Ma assuming recent lead loss.

SAMPLE NS97-14

Sample NS97-14 is from the medium-grained granite (Dg) phase of the pluton, south of the Queest Mountain fault (Map 2-1). Three zircon populations were obtained from this sample; none were abraded. NS97-14-1, composed of 40 colourless fragments (Plate 4-1), was slightly discordant (3.39%) and yielded a $^{207}Pb/^{206}Pb$ date of 366.4 ± 1.5 Ma (1 sigma errors are given for $^{207}Pb/^{206}Pb$ ages) (Table 4-1). NS97-14-2, a fraction containing 27 pink euhedral grains, was 2.19% discordant and yielded a $^{207}Pb/^{206}Pb$ date of 364.7 ± 1.3 Ma. The third fraction, NS97-14-3, 29 small colourless prismatic grains, was nearly concordant (0.38 % discordance) and yielded a $^{207}Pb/^{206}Pb$ date of 365.3 ± 1.4 Ma. These three analyses plot on a discordia line with an upper intercept of 365.4 ± 3.7

Ma (2 sigma errors are given for upper intercept ages), with a lower intercept forced through 0 Ma (assuming recent Pb loss) (Figure 4-1). The upper intercept is interpreted to be the age of crystallization of Unit Dg. The mean squared weighted deviance (MSWD) of the discordia line is 0.087 (Figure 4-1), which means that the line is a good fit to all the data.

SAMPLE NS97-83

Sample NS97-83 is from the Dgm (fine-grained mafic) phase of the pluton north of the Queest Mountain fault (Map 2-1). Four populations of zircon were analysed from this sample; the last two were abraded. NS97-83-1 consisted of 30 small yellow subhedral grains (Plate 4-2), is 4.21% discordant, and yielded a $^{207}Pb/^{206}Pb$ date of 362.6 ± 1.7 Ma (1 sigma error) (Table 4-1). NS97-83-2, containing 20 colourless subhedral grains with some inclusions, showed discordance of 3.67% and yielded a $^{207}Pb/^{206}Pb$ date of 355.2 ± 1.9 Ma. Fraction NS97-83-3, which consisted of 34 small colourless grains with inclusions (Plate 4-3), was abraded. This fraction was 1.40% discordant and yielded a $^{207}Pb/^{206}Pb$ date of 359.8 ± 3.3 Ma. Fraction NS97-83-4 was also abraded, and consisted of 34 small colourless grains with inclusions. This fraction showed discordance of 4.24% and yielded a $^{207}Pb/^{206}Pb$ date of 357.9 ± 1.5 Ma. These four fractions plot on a discordia line with an upper intercept of 366.2 ± 10 Ma (2 sigma error), and a lower intercept forced through 0 Ma (Figure 4-2). The upper intercept is considered to be the crystallization age of the Dgm phase of the pluton. The MSWD of the discordia line is 3.4 (Figure 4-2), which means that the line is not as good a fit to the data as sample

NS97-14. Fraction NS97-83-4 does not seem to fit the discordia line very well; this fraction had numerous inclusions and is more discordant than the other samples.

SAMPLE NS98-13B

Sample NS97-13B is from an outcrop north of the Queest Mountain fault where a contact between the pluton and calcsilicate rocks of the Queest Mountain assemblage is exposed (Map 2-1). This rock was taken from the Dgm (fine-grained mafic) phase of the intrusion. Only one zircon fraction from this sample was analysed, consisting of ~45 colourless needle-like grains. This fraction showed discordance of 1.37% and yielded a $^{207}Pb/^{206}Pb$ date of 365.6 ± 1.9 Ma (1 sigma error).

DISCUSSION

The two phases of the pluton that were dated represent most of the pluton, and are possibly the oldest and youngest phases. The dates obtained for Samples NS987-14 (Dg) and NS97-83 (Dgm) are identical within error, although NS97-14 may be slightly younger than NS97-83 as predicted by outcrop relationships. The analysis from NS98-13B would plot on a discordia line with the other analyses, implying that the pluton also has the same age at that outcrop. If all fractions from the three samples are plotted on a single diagram, an age of 365.9 ± 2.7 Ma is obtained, which is interpreted to be the crystallization age of the pluton. The results show that at least two phases (Dg and Dgm) of the pluton are essentially the same age, and that the pluton is the same age on both sides of the fault. As described in Chapter 2, the pluton appears to cut the Queest

Mountain fault and some foliation in the host rocks, implying a pre- 366 Ma age for these structures.

Okulitch *et al.* (1975) determined an upper intercept age of 372 ±6 Ma for the entire pluton. The 365.9 ± 2.7 Ma date from this study is identical within error to that age, confirming that the pluton within the study area is part of the Late Devonian Mount Fowler suite as suggested by Okulitch *et al.* (1975). Recent advances in geochronology, for example substantial decreases in amounts of blanks (Krogh, 1973) have allowed for more accurate and precise U-Pb dating. Ages obtained from this study have smaller errors than those of Okulitch *et al.* (1975) and are therefore more precise. This study dated three samples within the study area, compared to the one sample within this study area that was dates by Okulitch *et al.* (1975). The three samples have ages that are identical within error, and are likely more accurate than that of Okulitch *et al.* (1975). Therefore, the age of intrusion of the pluton is interpreted to be 365.9 ± 2.7 Ma.

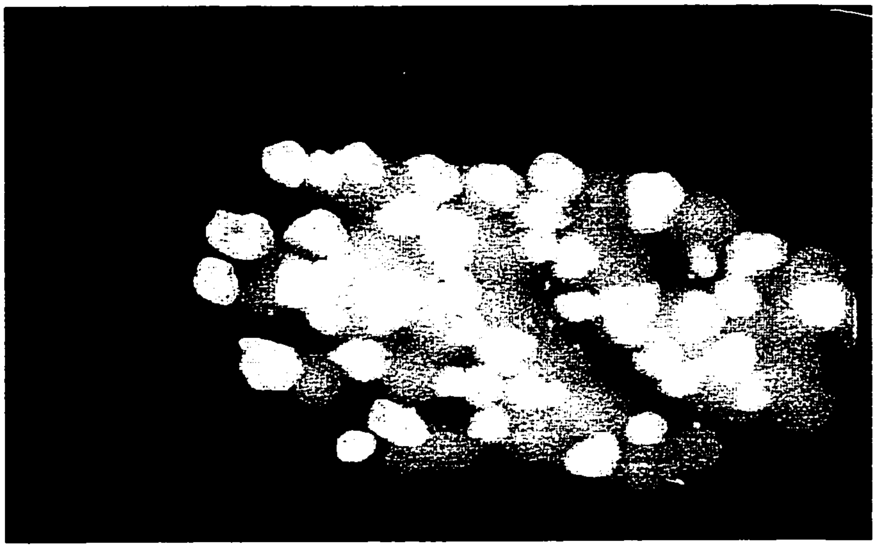

Plate 4-1:
Zircons of
sample NS97-14-1
Magnification 42X

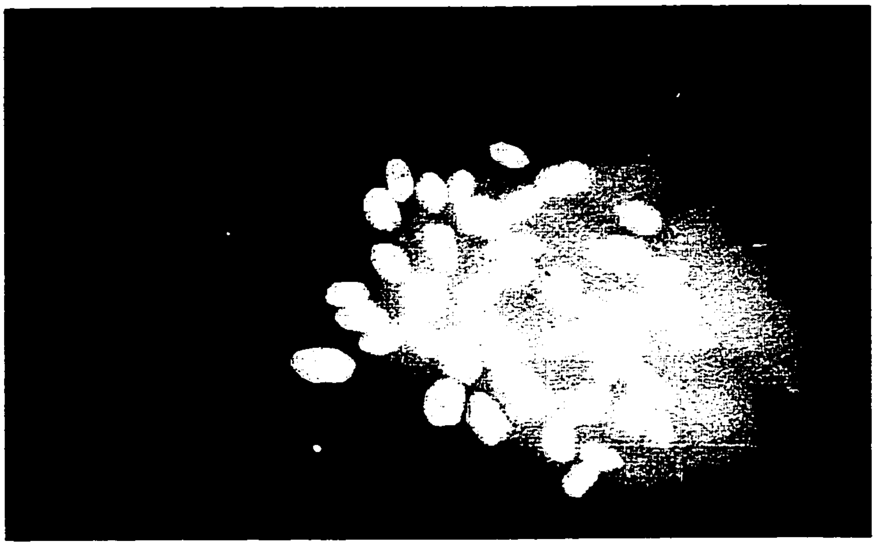

Plate 4-2:
Zircons of
sample NS97-83-1
Magnification 50X

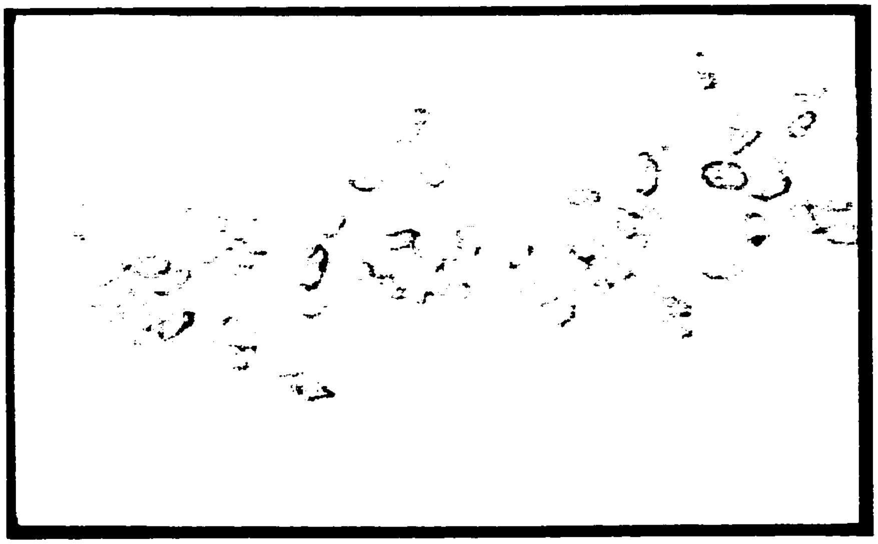

Plate 4-3:
Zircons of
sample NS97-83-3
Magnification 45X

Table 4-1: U-Pb analyses of zircon from the Mount Fowler Batholith

Unit/ Fraction	Magnetic fraction	Description	Grains (#)	Mass (mg)	U (ppm)	Pb rad (ppm)	Pb C tot (pg)	Th/U
Dgg/								
NS97-14-1	0°M	cless frag nabr	40	0.204	603	38	11	0.705
NS97-14-2	0°M	pink ehdrl incl nabr	27	0.288	1133	70	50	0.629
NS97-14-3	0°M	sm cless pr nabr	29	0.076	321	20	10	0.548
Dgm/								
NS97-83-1	2°M	sm yellow subhdrl nabr	30	0.072	492	29	8	0.569
NS97-83-2	2°M	cless subhdrl incl nabr	20	0.033	453	27	12	0.550
NS97-83-3	2°M	cless incl abr	30	0.014	428	26	16	0.579
NS97-83-4	2°M	sm cless incl poor qual abr	34	0.029	558	34	9	0.606
NS98-13B-1	1°NM	cless ndl nabr	~45	0.039	339	21	16	0.579

continued on next page

Table 4-1 continued

	$^{206}Pb/^{238}U$	$^{207}Pb/^{235}U$	$^{207}Pb/^{206}Pb$	apparent ages (Ma) $^{206}Pb/^{238}U$	$^{207}Pb/^{235}U$	$^{207}Pb/^{206}Pb$	Disc (%)
Dgg/							
NS97-14-1	0.05650 +/- 0.00026	0.41984 +/- 0.00199	0.05389 +/- 0.00004	354.3 +/- 1.6	355.9 +/- 1.4	366.4 +/- 1.5	3.39
NS97-14-2	0.05692 +/- 0.00022	0.42262 +/- 0.00168	0.05385 +/- 0.00003	356.9 +/- 1.3	357.9 +/- 1.2	364.7 +/- 1.3	2.19
NS97-14-3	0.05808 +/- 0.00013	0.43135 +/- 0.00104	0.05386 +/- 0.00003	364.0 +/- 0.8	364.1 +/- 0.7	365.3 +/- 1.4	0.38
Dgm/							
NS97-83-1	0.05543+/- 0.00014	0.41116 +/- 0.00105	0.0538 +/- 0.00004	347.8 +/- 0.8	349.7 +/- 0.8	362.6 +/- 1.7	4.21
NS97-83-2	0.05636 +/- 0.00015	0.41881 +/- 0.00119	0.05389 +/- 0.00005	353.5 +/- 0.9	355.2 +/- 0.9	366.6 +/- 1.9	3.67
NS97-83-3	0.05730 +/- 0.00011	0.42531 +/- 0.00112	0.05383 +/- 0.00008	359.2 +/- 0.7	359.8 +/- 0.8	364.1 +/- 3.3	1.40
NS97-83-4	0.05675 +/- 0.00013	0.42257 +/- 0.00108	0.05400 +/- 0.00004	355.8 +/- 0.8	357.9 +/- 0.8	371.2 +/- 1.5	4.24
NS98-13B-1	0.05755 +/- 0.00016	0.42741 +/- 0.00125	0.05387 +/- 0.00005	360.7 +/- 0.9	361.3 +/- 0.9	365.6 +/- 1.9	1.37

$^{206}Pb/^{238}U$, ^{207}Pb/235U, and $^{207}Pb/^{206}Pb$ ratios corrected for fractionation, blank (0.5pg Pb, 2.0pg U), spike, and initial common Pb.
206Pb/238U, 207Pb/238U, and 207Pb/206Pb ages calculated using the software ROMAGE.
Pb rad = radiogenic Pb
Pb C = total common Pb in sample
Magnetic fractions: M=magnetic, NM=nonmagnetic, degree is the side tilt of the chute in the Fratz magnetic separator.
Description abbreviations: cless=colourless, frag=fragments, ehdrl=euhedral, incl=inclusions, sm=small, pr=prismatic, subhdrl=subhedral, ndl=needle-shaped, nabr=non-abraded, abr=abraded.
Disc=discordance
Errors are one sigma

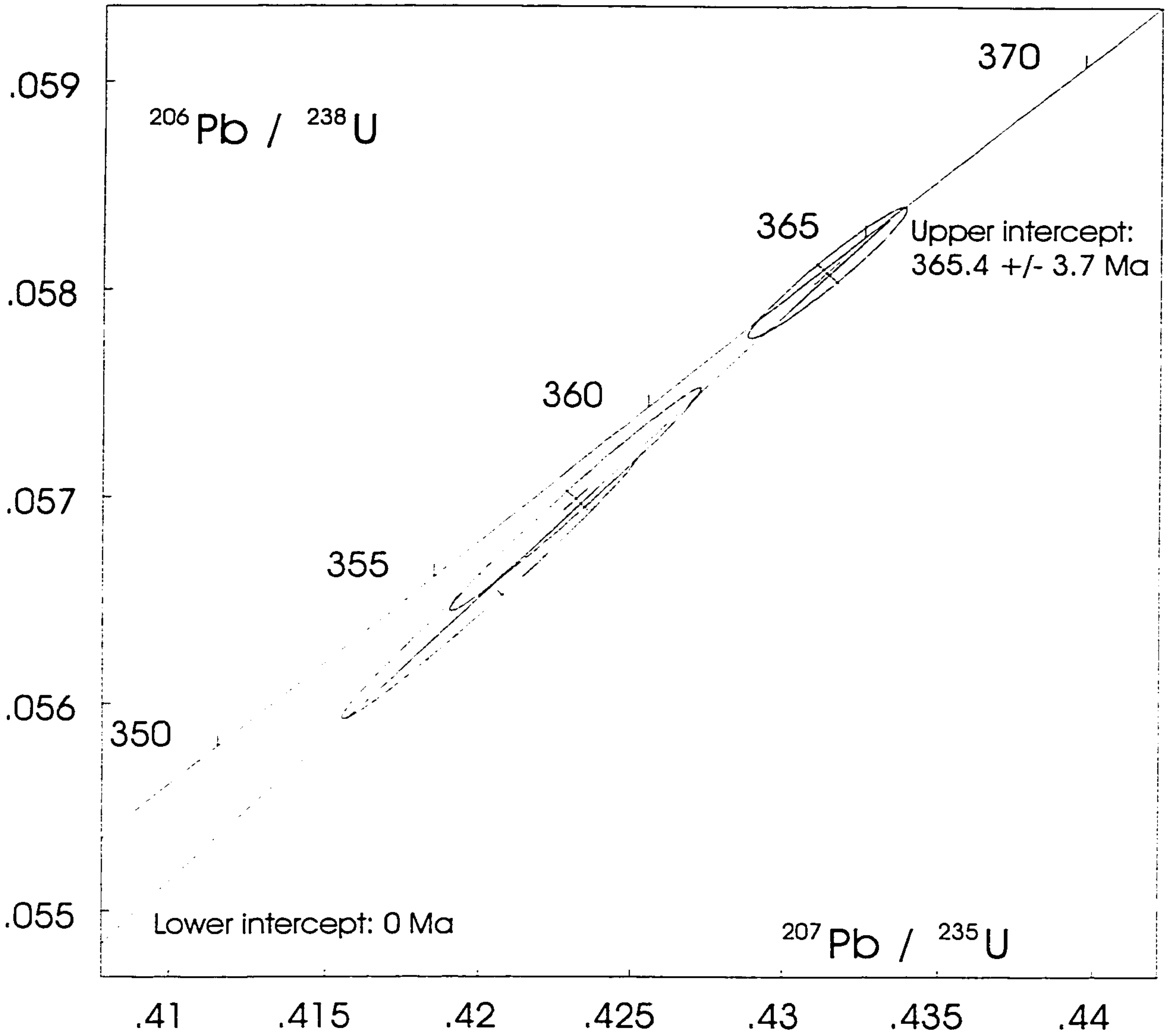

Figure 4-1: Concordia diagram for Sample NS97-14.
Error ellipses are 2 sigma.
MSWD (mean squared weighted deviance) = 0.087

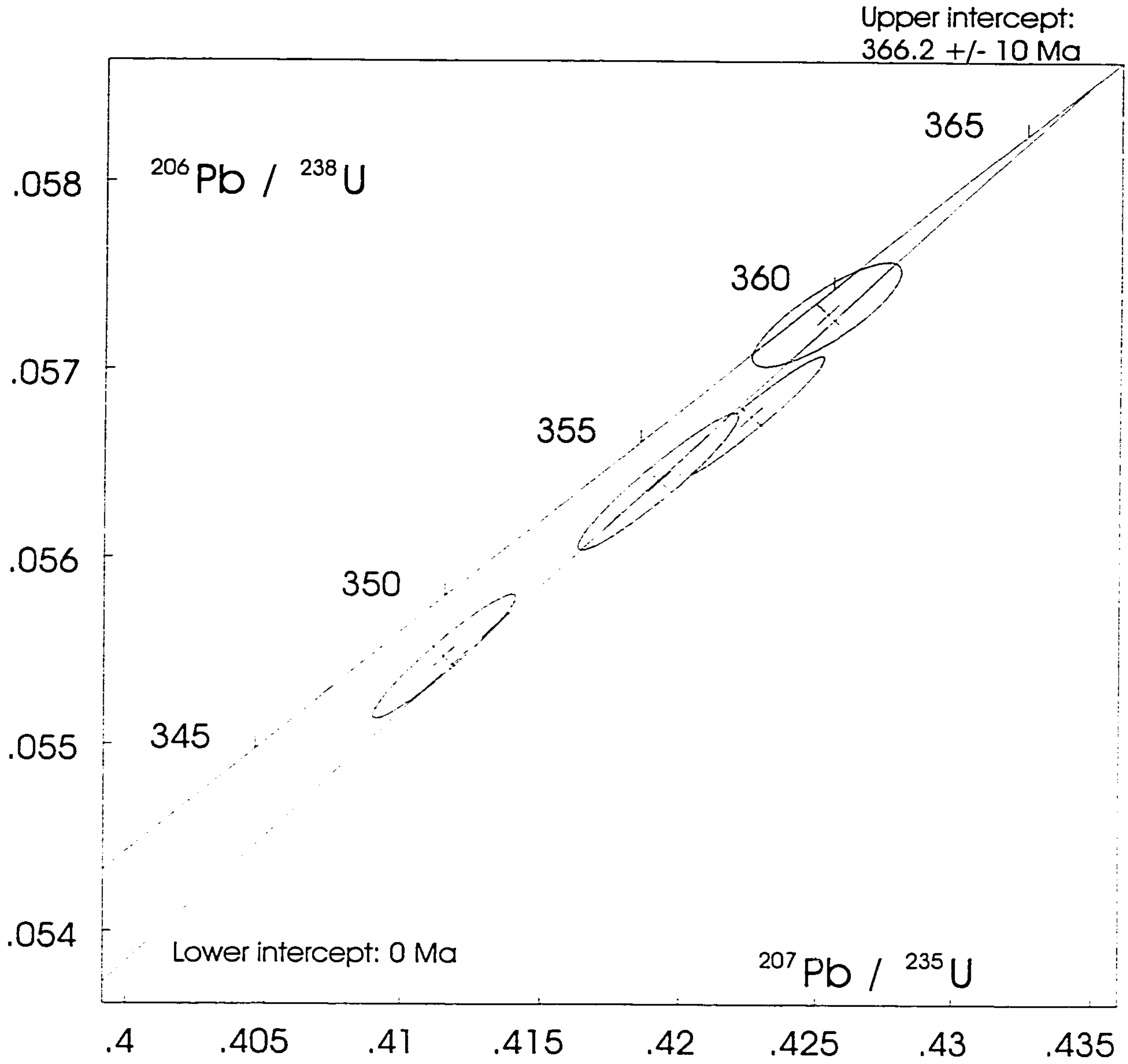

Figure 4-2: Concordia diagram for Sample NS97-83.
Error ellipses are 2 sigma.
MSWD = 3.4

CHAPTER 5

Discussion and Conclusions

DISCUSSION

Stratigraphy of the Mount Ida Group

The Mount Ida Group has been subdivided into the Silver Creek, Sicamous, and Eagle Bay formations (Jones, 1959). However, this early work was regional and at a 1 inch = 4 miles scale, and therefore did not focus on details of the internal stratigraphy of the three formations. Also, there has been substantial debate (Campbell and Okulitch, 1973; Schiarizza and Preto, 1987; Okulitch, 1989; Johnson, 1990, 1994) about the relationships between these units and their regional correlatives. This study examined the Silver Creek, Sicamous, and Eagle Bay formations in detail in order to better understand the past evolution of the Cordilleran margin in this area.

Regionally, the Eagle Bay Formation includes rocks of several types and of various ages. It includes Eocambrian archaeocyathid fossils (B.S. Norford, unpublished internal report, Geological Survey of Canada, 1985), mid-Devonian felsic volcanic units (Preto, 1981), and Mississippian conodonts (Campbell and Okulitch, 1973). Within the study area, the Eagle Bay Formation is intruded by a Late Devonian granitoid pluton, and is therefore older than Late Devonian. As discussed in Chapter 1, there is likely an unconformity between the Cambrian Eagle Bay Formation and younger rocks (Schiarizza and Preto, 1987). Further regional work is needed to accurately subdivide this unit. The original type section of the Eagle Bay Formation (Jones, 1959), from the town of Eagle

Bay near the study area, consists of Cambrian rocks below the unconformity, so the younger Devonian and Mississippian rocks near Adams Lake (Schiarizza and Preto, 1987) should likely be assigned to a separate unit.

Within the study area, rocks of the Silver Creek, Sicamous, and Eagle Bay formations have gradational contacts, which are interpreted as stratigraphic. The Silver Creek Formation is Neoproterozoic in age (Johnson, 1994) and the Sicamous and Eagle Bay formations are Early Proterozoic (Johnson, 1994). The orientation of contacts between units implies that these units are right-way-up within the study area, although regional studies of the genesis of mineral deposits in the Eagle Bay Formation (K.L. Daughtry, personal communication, 1997) have suggested that the Eagle Bay Formation is overturned.

The Silver Creek Formation has been subdivided into two units, a biotite-muscovite schist that comprises the majority of the unit and a calcareous mica schist that is present in layers within the biotite-muscovite schist. The Eagle Bay Formation has been subdivided into greenstones (chlorite schist, chlorite-sericite schist, and amphibolite), several layers of biotite-muscovite schist, and several marble marker horizons. No way-up indicators are observed in these subunits.

These changes in lithology within the Mount Ida Group are due to changes in the environment of deposition. First, the clastic sediments that were metamorphosed to form the Silver Creek Formation were deposited. Then, the carbonates of the Sicamous Formation were deposited, including significant organic input to account for the presence of graphite. Finally, the environment changed to a combination of volcanic, clastic, and carbonate deposition to form the Eagle Bay Formation.

The Queest Mountain assemblage

In the northeast part of the study area, garnet-biotite-muscovite schist and grossular-tremolite-diopside calcsilicate and marble have been previously (Okulitch, 1989; Johnson, 1990, 1994) mapped as part of the Eagle Bay Formation. Based on protolith composition, metamorphic grade, and fabric orientations, these rocks have been assigned to a new unit termed the Queest Mountain assemblage (Slemko and Thompson, 1998). This thesis provides a description of the Queest Mountain assemblage and its relationship to other units in the area, in order to determine its regional affinity.

The contact between the Eagle Bay Formation and the Queest Mountain assemblage is sharp and, as described in Chapters 2 and 3, constitutes a structural and metamorphic break. The contact is interpreted as a fault, termed the Queest Mountain fault. The fault dips to the north at between 16 and 30 degrees, placing the Queest Mountain assemblage above the Eagle Bay Formation.

Geothermobarometry, described in Chapter 3, shows that the Eagle Bay Formation was metamorphosed at an average of ~2.1 kbar higher pressure and ~123 °C higher temperature than the Queest Mountain assemblage. Thus, the fault is interpreted as a normal fault with between 14 and 25 km of displacement.

Within a few kilometers to the north of the area mapped for this study, Johnson (1994) mapped a group of rocks termed the Lichen assemblage, consisting of sillimanite-garnet-biotite-muscovite schist, calcsilicate gneiss, and impure marble. These rock types are similar to those of the Queest Mountain assemblage, in particular the calcsilicate gneiss and impure marble, which, within the study area, are unique to the Queest Mountain assemblage. The Queest Mountain assemblage and the Lichen assemblage of Johnson (1994) are likely correlative; further study, for example geothermobarometry of the Lichen assemblage, could be used to confirm this postulate. The Lichen assemblage lies just to the north of the Queest Mountain assemblage, meaning that these two units may potentially be traced into each other and therefore may be the same unit. Further field work to the north of the study area is needed to evaluate this possibility. Johnson (1994) provides no suggestions for regional correlatives of the Lichen assemblage, other than that Lichen assemblage mica schist lithologically resembles parts of the Silver Creek Formation. Thompson and Daughtry (1997) suggest that rocks now mapped as part of the Queest Mountain assemblage may also be correlative to the Silver Creek Formation.

Within the southern Omineca Belt, calcsilicate gneiss is present in both the Monashee Complex and the Hunters Range assemblage of the Shuswap Complex (Johnson, 1990, 1994; see Figure 1-8, this thesis). However, calcsilicate schist and/or gneiss is not prevalent in other units of the Omineca Belt. Johnson (1994) correlates the Hunters Range assemblage with the Silver Creek Formation. The suggestion (Johnson, 1994) that the Lichen assemblage may be correlative to the Silver Creek Formation implies that the Lichen assemblage may also be correlative to the Hunters Range assemblage. Correlation of the Queest Mountain assemblage with the Lichen assemblage, as well as the correlation of the Queest Mountain assemblage with the Silver Creek Formation (Thompson and Daughtry, 1997) means that the Queest Mountain assemblage may be correlative with the Hunters Range assemblage, as lithological similarities described above suggest. This implies that the Queest Mountain assemblage is more likely correlative to the Hunters Range assemblage than to the Monashee Complex, although either correlation remains tenable.

Correlation of the Queest Mountain assemblage with either the Hunters Range assemblage or the Monashee Complex creates problems with the interpretation of the contact between the Eagle Bay Formation and the Queest Mountain assemblage as a normal fault. Regional correlations suggest that the Queest Mountain assemblage is older than the Eagle Bay Formation. Geothermobarometry (Chapter 3) shows that the Eagle Bay Formation was metamorphosed at conditions that would place it ~ 7 km deeper that the Queest Mountain assemblage, implying that the Queest Mountain assemblage is younger than the Eagle Bay Formation. One solution is that the units were overturned before being metamorphosed; however this is unlikely due to the right-side-up relationships within the Mount Ida Group. Another possibility is that the Queest Mountain fault first experienced reverse motion, placing the Queest Mountain assemblage at a higher structural level than the Eagle Bay Formation before the units were metamorphosed, and the Queest Mountain fault was subsequently reactivated as a normal fault. Alternatively, the geothermobarometry could be incorrect; however textural relationships indicate that the minerals are at equilibrium and that the pressure and temperature differences between the units are real. It is also possible that correlation of the Queest Mountain assemblage with the Hunters Range assemblage or Monashee Complex is incorrect; however other potential correlatives for the calcsilicate rocks are unknown. Further study of the Queest Mountain assemblage and Lichen assemblage to the north of the study area may help to determine their regional affinity and solve the problem of the relationship of the Queest Mountain assemblage to the Eagle Bay Formation.

Contact relationships of the pluton

As described in Chapter 2, the Eagle Bay Formation and the Queest Mountain assemblage are intruded by a pluton correlated (Okulitch *et al.*, 1975) with the Late Devonian Mount Fowler suite. Inclusions of foliated Eagle Bay Formation schist are present within the pluton, and foliation in the host rock is cut by the pluton. As well, foliation is strongly penetrative in the host rock, but variable in the pluton. Metamorphic mineral growth is pre- or syn-tectonic with this foliation development. Folding of the Queest Mountain assemblage also appears to pre-date the intrusion. This implies that the metasedimentary rocks were metamorphosed and deformed prior to the intrusion.

This is in contrast to the work of Johnson (1994), which suggested three post-intrusion episodes of deformation. Johnson's (1994) oldest episode of deformation apparently produced a schistosity (S_1) parallel to compositional layering (S_0) in metasedimentary rocks, and a parallel gneissosity in the pluton, implying that all deformation post-dates the intrusion. In this study, schistosity in the metasedimentary rocks, which is parallel to compositional layering and to unit contacts and therefore equivalent to S_1 of Johnson (1994), is shown to be discordant to gneissosity in the pluton, meaning that the deformation event that produced the schistosity in the metasedimentary rocks pre-dated the intrusion. Johnson's (1994) second episode of deformation, which apparently folded S_0S_1 and produced a schistosity (S_2) that is essentially parallel to S_0S_1

except in hinges of F_2 folds, was not observed in this study. Johnson (1994) mapped large open folds that folded S_0S_1 and S_2, and were therefore produced by a third episode of deformation, which regionally has been shown to pre-date the intrusion of the Baldy batholith west of Adams Lake (Schiarizza and Preto, 1987) that has been dated at 116 ± 5 Ma (Calderwood *et al.*, 1990). In this study, these folds were mapped in the Queest Mountain assemblage in the northeast part of the map area. The Mount Fowler suite appears to cut these fold, so they are interpreted to have occurred prior to the intrusion of the Mount Fowler suite. This study suggests that metamorphic growth was syntectonic with S_1 foliation development, and therefore also pre-dates the intrusion.

Geochronology of the pluton

As described in Chapter 4, the granitoid pluton was dated using U-Pb zircon geochronology, in order to accurately and precisely determine the age of the pluton. This was done both to confirm the correlation of the pluton with the Mount Fowler Batholith (Okulitch *et al.*, 1975) and to use the age of the pluton to determine a relative age for other events.

Three samples, of two different phases of the pluton, from different sides of the Queest Mountain fault, were dated. The samples all have the same age within error, and all samples together have an age of 365.9 ± 2.7 Ma, confirming that this pluton is part of the Late Devonian Mount Fowler Batholith as mapped by Okulitch *et al.* (1975).

The granitoid pluton cuts foliation in the country rock, implying a pre- 366 Ma age for the foliation. The pluton also crosses the Queest Mountain fault without offset, implying a pre- 366 Ma age for this structure as well.

Geological history of the study area

The Silver Creek Formation is interpreted as a miogeoclinal succession (Thompson and Daughtry, 1997) and has been correlated (Okulitch, 1979; Johnson, 1990, 1994; Thompson and Daughtry, 1996) with the Lardeau Group or the Windermere Supergroup. These correlations imply that the Silver Creek Formation has a strong affinity to Ancestral North America. The Sicamous and Eagle Bay formations are eugeoclinal assemblages that were described as pericratonic (Monger *et al.*, 1991), which means that their association with Ancestral North America was unknown. However, detrital zircon ages of between 3.0 Ga and 750 Ma suggest that these eugeoclinal sediments were derived from Ancestral North America (Gehrels *et al.*, 1995). It has been suggested (Thompson and Daughtry, 1997) that the eugeoclinal rocks stratigraphically overly the miogeoclinal rocks, and therefore were deposited at the margin of Ancestral North America. These units were deposited during the Precambrian and Cambrian, and represent changes from a time of deposition of miogeoclinal clastic rocks, to a mixture of clastic, carbonate, and volcanic eugeoclinal rocks. The contact between miogeoclinal and eugeoclinal sediments occurs at the boundary between the Silver Creek Formation and the Sicamous Formation. The Queest Mountain assemblage is lithologically similar to, and possibly correlative to, the miogeoclinal rocks of the Silver Creek Formation.

In the Devonian to Mississippian Exshaw Formation of the Rocky Mountains, a ~364 Ma volcanic tuff layer has been dated using U-Pb geochronology (G.M. Ross, personal communication, 1999). The similar ages of this tuff and Late Devonian plutonism to the west, in particular the Mount Fowler suite, suggests that the tuff may be the volcanic equivalent of plutonic rocks to the west (B.C. Richards, personal communication, 2000). Since the Exshaw Formation is unequivocally North American, the correlation between volcanic and plutonic events of the same age provides additional evidence for the North American affinity of the eugeoclinal strata the Mount Fowler suite intrudes.

Between the Cambrian, when the youngest Eagle Bay Formation rocks were deposited in the area, and the Late Devonian, when the formations were intruded by granite of the Mount Fowler suite, several tectonic events occurred in the area. Metamorphism and deformation of the Eagle Bay Formation and the Queest Mountain assemblage, as well as folding in the Queest Mountain assemblage, occurred prior to the Late Devonian. Motion on the Queest Mountain fault occurred after metamorphism and deformation of the Eagle Bay Formation and Queest Mountain assemblage, as it juxtaposes rocks with different metamorphic histories, but before the intrusion of the pluton, which cuts the fault. The Queest Mountain fault is interpreted to be a normal fault with between 14 and 25 km of displacement. Its orientation suggests that extension on the Queest Mountain fault took place parallel to the margin of Ancestral North America. The study area was intruded by a granitoid pluton at 365.9 ± 2.7 Ma. This pluton is interpreted to be part of the Late Devonian Mount Fowler suite. In the Tertiary, the area was affected by extensional faulting on the Eagle River fault that exhumed rocks to the east of the study area, juxtaposing the Mount Ida Group and the Monashee Group (Johnson, 1990, 1994). Regionally, the area may have been deformed and metamorphosed during the mid-Jurassic to mid-Cretaceous Columbian Orogeny or the

Late Cretaceous to Paleocene Laramide Orogeny; however the only evidence for this in the study area is the variable (i.e. absent to penetrative) foliation in the Mount Fowler Batholith. And post-Late Devonian orogenesis has not overprinted the earlier deformation and metamorphism in the Eagle Bay Formation and Queest Mountain assemblage.

The geological history suggested by this thesis is in contrast to other studies that have proposed predominantly Mesozoic compressional orogenesis for the region, followed by Tertiary extension. In the Monashee Complex, zircon geochronology of leucosome melts and metamorphic monazite (Journeay and Parrish, 1989; Coleman, 1990; Carr, 1992; Johnson, 1994; Parrish, 1995) suggests the peak of metamorphism and deformation was Late Cretaceous to Paleocene. In the Shuswap Complex, geochronology (Carr, 1990, 1992; Heaman and Parrish, 1991; Parkinson, 1992; Johnson, 1994; Parrish, 1995) indicates that peak metamorphism and deformation was Middle Cretaceous to Paleogene in age. The lack of Jurassic and Early Cretaceous metamorphism in these rocks has been interpreted to mean that these rocks were east of the metamorphic front during the Columbian Orogeny and therefore only experienced the Laramide Orogeny (Carr, 1995). Johnson (1994) suggested that deformation and metamorphism of the Eagle Bay Formation in and near the study area post-dated the intrusion of the Mount Fowler suite, due to the apparent presence of similarly-oriented fabrics in the metasedimentary rocks and the Mount Fowler gneiss. This study, however, has shown that gneissosity in the Mount Fowler suite is discordant with schistosity in the host rock, implying that deformation of the host rock occurred before the intrusion of the Mount Fowler suite.

Hornblende $^{40}Ar/^{39}Ar$ and K-Ar dates of rocks in the hanging wall of the Eagle River Fault are Late Cretaceous (Johnson, 1994), suggesting that metamorphism may have occurred during this time. These dates, however, represent the time at which hornblende cooled through its closure temperature of ~ 500°C (Hanes, 1991), and the peak metamorphism at a higher temperature would have occurred before this time. Also, none of these samples are from within the study area of this thesis; they are from north and west of the study area, from the Mount Fowler Batholith or rocks that may not be part of the Cambrian Eagle Bay Formation. Much of the evidence to suggest that rocks of the Mount Ida Group were deformed and metamorphosed in the Mesozoic is derived from correlations of these rocks with rocks on the east side of the Eagle River Fault (e.g. Johnson, 1994). Although these rocks may be correlative, Okulitch (1984) suggested that there are many regional differences in the timing and preservation of metamorphism and deformation of rocks in this region, and studies from one area cannot necessarily be applied to adjacent areas. Therefore, evidence of Mesozoic orogenesis from surrounding areas cannot be applied to the study area unless independent evidence from within the study area is also found. Little evidence of Mesozoic metamorphism or deformation within the study area was found by this study; instead Early to Middle Paleozoic deformation and metamorphism is preserved.

In the Omineca Belt of the southern Canadian Cordillera, there is evidence of Middle Paleozoic deformation preserved in some areas. In the Kootenay Arc (Figure 1-5) to the east of this study area, cobbles of foliated clasts of Early Paleozoic Lardeau Group are found in the Lower Mississippian Milford Group, implying that deformation, uplift, and erosion occurred prior to the early Mississippian (Read and Wheeler, 1976; Klepacki, 1985). As well, folds, thrust faults, and foliations that are present in the Lardeau Group cannot be traced into the younger Milford Group (Read and Wheeler, 1976; Klepacki, 1985). In the Purcell Mountains, Middle to Upper Devonian limestone, dolomite, conglomerate, and volcanic rocks have been interpreted as foreland basin deposits related to a tectonic event (Root, 1992). Root (1987) documents nine episodes of deformation in the Purcell Anticlinorium (Figure 1-5) before the Late Devonian, including folding prior to the Middle Devonian and Middle Devonian extension.

Okulitch (1984) suggests that Mesozoic metamorphism and deformation may not have been pervasive in the Monashee Complex, and that structures instead may be related to an older event, such as pre-Mississippian orogenesis as is seen in the Kootenay Arc (Read and Wheeler, 1976) or to older events such as Proterozoic (1300 - 1350 Ma and 800 - 900 Ma) events in the Belt Purcell Supergroup (McMechan and Price, 1982). This suggests that, in certain areas, older deformation was not overprinted during the Columbian and Laramide orogenies. Further regional study is required to determine why certain areas escaped Mesozoic orogenesis.

There is also evidence in the Omineca Belt of Middle Paleozoic plutonic activity that may be related to a Devonian tectonic event. The Clachnacudainn Gneiss in the Kootenay Arc has been dated at 422 +124/-46 Ma, suggesting a Devonian age for the intrusion (Okulitch, 1985). Dating of the Quesnel Lake Gneiss resulted in six 207Pb/206Pb ages ranging between 516 and 369 Ma, suggesting a maximum age of 350-400 Ma for the intrusion (Okulich, 1985). The Mount Fowler suite has been dated at 372

± 6 Ma (Okulitch *et al.*, 1975) and 365.9 ± 2.6 Ma (this study). It has been suggested (Okulitch, 1985; Gehrel and Smith, 1987) that these plutonic suites may be related to Paleozoic tectonism.

There is evidence in Nevada (Silberling and Roberts, 1962) and Idaho (Roberts and Thomasson, 1964) for a Devonian to Mississippian orogenic event, termed the Antler Orogeny. Originally, this event was defined as the emplacement of the Roberts Mountains allochthon onto the North American continent (Roberts *et al.*, 1958). Subsequent work has shown that the Roberts Mountains allochthon is miogeoclinal in nature (Finney, 1998) and has been transported only a short distance (Noble and Finney, 1999). This orogeny resulted in an influx of clastic sediments, derived from the overthrust allochthon, into a foreland basin (Dickinson *et al.*, 1983). There is no evidence of Devonian- or Mississippian-aged volcanic or plutonic rocks in the United States that could be associated with the Antler orogeny. It has been suggested that compressional structures in the Kootenay Arc, described above, are related to the Antler Orogeny (Gehrels and Smith, 1987; Smith *et al.*, 1993). Ordovician and Devonian plutonic rocks, including the Mount Fowler suite, were interpreted to be part of a magmatic arc that evolved along the North American margin prior to Antler orogenesis (Gehrels and Smith, 1987).

The regional evidence discussed above implies that a Paleozoic tectonic event did occur in the Southern Canadian Cordillera. Deformation of the Eagle Bay Formation and the Queest Mountain assemblage, and the subsequent folding of this foliation, occurred prior to the Late Devonian. The Mount Fowler gneiss mapped by this study is part of a large suite of Devonian intrusions that are interpreted to be related to Devonian tectonism. This tectonic event may be correlative with the Antler orogeny in the United States.

There are, however, differences between data presented in this study and previous theories of Antler orogenesis in Canada. First, this study shows that deformation and metamorphism of the Eagle Bay Formation and the Queest Mountain assemblage occurred before the intrusion of the Mount Fowler suite, so if the deformation and metamorphism is related to the Antler Orogeny, the Mount Fowler suite cannot be part of a magmatic arc that formed prior to the orogeny. Instead, Devonian plutonism was likely late-orogenic or post-orogenic, resulting from a release of pressure on rocks that were deeply buried during orogenesis. Second, this study provided evidence for the existence of a normal fault, the Queest Mountain fault, that also occurred prior to the intrusion of the Mount Fowler suite in the Late Devonian. The orientation of this fault suggests that margin-parallel extension occurred. There is no other evidence of this type of extension during the Paleozoic in the southern Canadian Cordillera; however more recent examples of this type of motion exist. In the northern Cascadia forearc of southwestern British Columbia, there is evidence for a transition between margin-normal shortening and margin-parallel extension associated with strike-slip faulting (Journeay and Morrison, 1999). This transition is associated with subduction and northeasterly underplating along the Cascadia subduction zone (Journeay and Morrison, 1999). A similar event could have occurred in the Paleozoic.

Although evidence from this thesis supports the idea of a Paleozoic tectonic event in the southern Canadian Cordillera, data does not fit with previous workers (Gehrels and Smith, 1987; Smith *et al.*, 1993) ideas of the Antler orogeny. Instead, this study suggests that both compressional and extensional deformation occurred, followed by Late Devonian plutonism. Colpron *et al.* (2000) proposed a model of subduction and intra-arc tectonism to explain similar tectonic events in the Middle Paleozoic in the Yukon; this model could also apply to this study.

CONCLUSIONS

1) Regionally, rocks mapped as the Eagle Bay Formation should be divided into two units, one which is Cambrian and the other which is Devonian and Mississippian. The type section of the Eagle Bay Formation (Jones, 1959) consists of Cambrian rocks, so the younger rocks should be assigned to another unit.

2) An assemblage of biotite-muscovite schist ± staurolite ± garnet ± sillimanite and grossular-diposide-tremolite calcsilicate and marble, termed the Queest Mountain assemblage, occurs in the northeastern part of the study area. These rocks were previously mapped as part of the Eagle Bay Formation but are separated based on lithology, structural history, and metamorphic grade.

The contact between the Eagle Bay Formation and the Queest Mountain assemblage is interpreted as a fault, termed the Queest Mountain fault, which strikes approximately east-west and dips to the north at between 16 and 30 degrees. Pressure and temperature differences between the Eagle Bay Formation and the Queest Mountain assemblage suggest that it is a normal fault with between 14 and 25 km displacement.

Based on lithological similarities, the Queest Mountain assemblage may be correlative with the Lichen assemblage of Johnson (1994), and therefore may also be correlative with the Silver Creek Formation and the Hunters Range assemblage of proposed Windermere age.

3) A granitoid pluton intrudes the Eagle Bay Formation and the Queest Mountain assemblage, cutting foliation and folds in the host rocks as well as the Queest Mountain fault. The pluton also contains inclusions of foliated Eagle Bay Formation schist. Foliation is strongly penetrative in the Eagle Bay Formation and the Queest Mountain assemblage, but is variable in the pluton.

4) The pluton has been dated at 365.9 ± 2.7 Ma, confirming its correlation (Okulitch *et al.*, 1975) with the Late Devonian Mount Fowler Batholith. A record of Early to Middle Paleozoic compression and margin-parallel extension is preserved.

5) This thesis provides evidence of Early to Middle Paleozoic compression, extension, and plutonism. This tectonic activity may be related to the Devonian to Mississippian Antler orogeny or more likely to subduction and intra-arc tectonism. The main tectonic fabric and metamorphism seen in the Shuswap Lake region is the result of Early to Middle Paleozoic tectonism; the influence of Mesozoic orogenesis may not be as widespread as previously thought. Evidence of deformation and metamorphism in one

area cannot be applied to the entire Omineca Belt.

REFERENCES

Archibald, D.A., Glover, J.K., Price, R.A., Farrar, E., and Carmichael, D.M. (1983) Geochronology and tectonic implications of magmatism and metamorphism, southern Kootenay Arc and neighboring regions, southeastern British Columbia. Part I: Jurassic to mid-Cretaceous; *in* Canadian Journal of Earth Sciences, v. 20, p. 1891-1913.

Archibald, D.A., Krough, T.E., Armstrong, R.L., and Farrar, E. (1984) Geochronology and tectonic implications of magmatism and metamorphism, southern Kootenay Arc and neighboring regions, southeastern British Columbia. Part II: mid-Cretaceous to Eocene; *in* Canadian Journal of Earth Sciences, v. 21, p. 567-583.

Armstrong, R.L., Parrish, R.R., van der Heyden, P., Scott, K., Runkle, D., and Brown, R.L. (1991) Early Proterozoic basement exposures in the southern Canadian Cordillera: core gneiss of Frenchman Cap, Unit I of the Grand Forks Gneiss, and the Vaseaux Formation; *in* Canadian Journal of Earth Sciences, v. 28, p. 1169-1201.

Berman, R.G. (1988) Internally-consistent thermodynamic data for stoichiometric minerals in the system Na_2O-K_2O-CaO-MgO-FeO-Fe_2O_3-Al_2O_3-SiO_2-TiO_2-H_2O-CO_2; *in* Jounral of Petrology, vol.29, p. 445-522.

Berman, R.G. (1990) Mixing properties of Ca-Mg-Fe-Mn garnets; *in* The American Mineralogist, vol. 75, p. 328-344.

Berman, R.G. (1991) Thermobarometry using multi-equilibrium calculations: a new technique, with petrological application; *in* Canadian Mineralogist, vol. 29, p. 833-855.

Brock, R.B. (1934) The metamorphism of the Shuswap Terrane of British Columbia; *in* Journal of Geology, v. 42, p. 673-699.

Brown, R.L., Carr, S.D., Johnson, B.J., Coleman, V.J., Cook, F.A., and Varsek, J.L. (1992) The Monashee décollement of the southern Canadian Cordillera: a crustal scale shear zone linking the Rocky Mountain Foreland Belt to lower crust beneath accreted terranes; *in* Thrust Tectonics, *edited by* K. McClay; Chapman and Hall Ltd., London, p. 357-364.

Brown, R.L., Journeay, J.M., Lane, L.S., Murphy, D.C., and Rees, C.J. (1986) Obduction, backfolding, and piggyback thrusting in the metamorphic hinterland of the southeastern Canadian Cordillera; *in* Journal of Structural Geology, vol. 8, p. 255-268.

Calderwood, A.R., van der Heyden, P., and Armstrog, R.L. (1990) Geochronology of the Thuya, Takomkane, Raft, and Baldy batholiths, south-central British Columbia; *in* Geological Association of Canada Program with Abstracts, v. 15, p. A-19.

Cameron, A.E., Smith, D.H., and Walker, R.L. (1969) Mass spectrometry of nanogram-size samples of lead; *in* Analytical Chemistry, vol. 41, p. 525-526.

Campbell, R.B. and Okulitch, A.V. (1973) Stratigraphy and structure of the Mount Ida Group, Vernon (82L) Adams Lake (82M W1/2), and Bonaparte (92P) map-areas; *in* Report of Activities, Part A: April to October 1972, Geological Survey of Canada, Paper 73-1, p. 21-23.

Carr, S.D. (1991) Geology of the Thor-Odin-Pinnacles area, southern Omineca Belt, British Columbia; *in* Canadian Journal of Earth Sciences, v. 28, p. 2003-2023.

Carr, S.D. (1992) Tectonic setting and U-Pb geochronology of the early Tertiary Ladybird leucogranite suite, Thor-Odin-Pinnacles area, southern Omineca Belt, British Columbia; *in* Tectonics, v. 11, p. 258-278.

Carr, S.D. (1995) The southern Omineca Belt, British Columbian: new perspectives from the Lithoprobe Geoscience Program; *in* Canadian Journal of Earth Science, v. 32, p. 1720-1739.

Carr, S.D., Ghent, E.D., Simony, P.S., and Digel, S. (1997) U-Pb geochronology constraints on Early Cretaceous and Paleocene metamorphism in the Mount Cheadle area, Shuswap Complex, southern British Columbia; *in* F. Cook and P. Erdmer (compilers), Slave-Northern Cordillera Lithospheric Evolution (SNORCLE) Transect and Cordilleran Tectonics Workshop Meeting (March 7-9), University of Calgary, Lithoprobe Report No. 56, 245 p.

Coleman, V.J. (1990) The Monashee décollement at Cariboo Alp, southern British Columbia; M.Sc. Thesis, Carleton University, Ottawa.

Colpron, M., Murphy, D., and Mortensen, J. (2000) Mid-Paleozoic tectonism in Yukon-Tanana terrane, northern Canadian Cordillera: record of intra-arc deformation; *in* F. Cook and P. Erdmer (compilers), Slave-Northern Cordillera Lithospheric Evolution (SNORCLE) Transect and Cordilleran Tectonics Workshop Meeting (February 25-27), University of Calgary, Lithoprobe Report No. 72, 257 p.

Coney, P.J., Jones, D.L., and Monger J.W.H. (1980) Cordilleran suspect terranes; *in* Nature, v. 288, p. 329-333.

Cook, F.A., Varsek, J.L., Clowes, R.M., Kanasewich, E.R., Spencer, C.S., Parrish, R.R., Brown, R.L., Carr, S.D., Johnson, B.J., and Price, R.A. (1992) Lithoprobe crustal reflection cross section of the southern Canadian Cordillera, 1, foreland thrust and fold belt to Fraser River fault; *in* Tectonic, v. 11, p. 12-35.

Crowley, J.L. (1997) U-Pb geochronology in Frenchman Cap dome of the Monashee complex, southern Canadian Cordillera: Early Tertiary tectonic overprint of a Proterozoic history; Ph.D. thesis, Carleton University, Ottawa, Ontario.

Crowley, J.L. (1999) U-Pb geochronologic constraints on Paleoproterozoic tectonism in the monashee compex, Canadian Cordillera: Elucidating an overprinted geologic history; *in* Geological Society of America Bulletin, vol. 111, no. 4, p. 560-577.

Daly, R.A. (1915) A geological reconnaissance between Golden and Kamloops B.C., along the Canadian Pacific Railway; Geological Survey of Canada, Memoir 68, 260 p.

Dawson, G.M. (1898) Shuswap Sheet; Geological Survey of Canada, Map 604.

Dickinson, W.R., Harbaugh, D.W., Saller, A.H., Heller, P.L., and Snyder, W.S. (1983) Detrital modes of upper Paleozoic sandstones derived from the Antler orogen in Nevada: Implications for the nature of the Antler orogeny; *in* American Journal of Science, v. 283, p. 481-509.

Duncan, I.J. (1984) Structural evolution of the Thor-Odin gneiss dome; *in* Tectonophysics, v. 101, p. 87-130.

Finney, S.C. (1998) The Laurentian affinity of the Roberts Mountains Allochthon; *in* Abstracts with Programs - Geological Society of America, v. 30, no. 7, p. 150.

Gabrielse, H., Monger, J.W.H., Wheeler, J.O., and Yorath, C.J. (1991) Part A. Morphogeological belts, tectonic assemblages, and terranes; *in* Chapter 2 of Geology of the Cordilleran Orogen in Canada, H. Gabrielse and C.J. Yorath (ed.); Geological Survey of Canada, Geology of Canada, no. 4, p. 15-28.

Gehrels, G.E. and Smith, M.T. (1987) "Antler" allochthon in the Kootenay arc?; *in* Geology, v. 15, p. 769-770.

Gehrels, G.E., Dickinson, W.R., Ross, G.M., Stewart, J.H., and Howell, D.G. (1995) Detrital zircon reference for Cambrian to Triassic miogeoclinal strata of western North America; *in* Geology, v. 23, no. 9, p. 831-834.

Hanes, J.A. (1991) Chapter 2: K-Ar and 40Ar/39Ar geochronology: methods and applications; *in* Mineralogical Association of Canada Short Course Handbook on Applications of Radiogenic Isotope Systems to Problems in Geology, Toronto, May 1991, ed. L. Heaman and J.N. Ludden, p. 27-57.

Heaman, L.M. and Machado, N. (1992) Timing and origin of midcontinent rift alkaline magmatism, North America: evidence from the Coldwell Complex; *in* Contributions to Mineral Petrology, v. 110, p. 289-303.

Heaman, L. and Parrish, R. (1991) U-Pb geochronology of accessory minerals; *in* Mineralogical Association of Canada Short Course Handbook on Applications of Radiogenic Isotope Systems to Problems in Geology, Toronto, May 1991, ed. L. Heaman and J.N. Ludden, p. 59-102.

Höy, T. and Godwin, C.I. (1988) Significance of a Cambrian date from galena lead-isotope data for the stratiform Cottonbelt deposit in the Monashee Complex, southeastern British Columbia; *in* Canadian Journal of Earth Sciences, v. 25, p. 1534-1541.

Jaffey, A.H., Flynn, K.F., Glendenin, L.E., Bentley, W.C., and Essling, A.M. (1971) Precision measurement of half-lives and specific activities of ^{235}U and ^{238}U; *in* Physical Review, v. 4, p. 1889-1906.

Johnson, B.J. (1989) Geology of the western margin of the Shuswap terrane near Sicamous, implications for Tertiary extensional tectonics (82L, M); *in* British Columbia Ministry of Energy, Mines and Petroleum Resources, Geological Fieldwork, 1998, Paper 1989-1, p. 49-54.

Johnson, B.J. (1990) Geology adjacent to the western margin of the Shuswap metamorphic complex (Parts of 82L, M); British Columbia Ministry of Energy, Mines and Petroleum Resources Open File 1990-30.

Johnson, B.J. (1994) Structure and tectonic setting of the Okanagan Valley fault system in the Shuswap Lake area, southern British Columbia; Ph.D. thesis, Carleton University, Ottawa, Ontario.

Johnson, B.J. and Brown, R.L. (1996) Crustal structure and early Tertiary extensional tectonics of the Omineca belt at 51°N latitude, southern Canadian Cordillera; *in* Canadian Journal of Earth Science, vol. 33, p. 1596-1611.

Jones, A.G. (1959) Vernon Map-Area, British Columbia; Geological Survey of Canada, Memoir 296, 186p.

Jones, D.L., Howell, D.G., Coney, P.J., and Monger, J.W.H. (1983) Recognition, character, and analysis of tectonostratigraphic terranes in western North America; *in* Accretion Tectonics in the Circum-Pacific Regions; H. Hashimoto and S. Uyeda (ed.), Terra Scientific Publishing Co., Tokyo, p. 21-35.

Journeay, J.M. and Morrison, J. (1999) Field investigation of Cenozoic structures in the northen Cascadia Forearc, southwestern British Columbia; *in* Corrent Research 1999-A/B, Geological Survey of Canada, p. 239-250.

Journeay, J.M. and Parrish, R.R. (1989) The Shuswap thrust, sole fault to a metamorphic-plutonic complex of Late Cretaceous - Early Tertiary age, southern Omineca Belt, British Columbia; *in* Geological Society of America, Abstracts with Programs, v. 20, A19.

Klepacki, D.W. (1985) Stratigraphy and structural geology of the Goat Range area, southeastern British Columbia; Ph.D. thesis, Cambridge, Massachusetts Institute of Technology, 286 p.

Krogh, T.E. (1973) A low-contamination method for hydrothermal decomposition of zircon and extraction of U and Pb for isotopic age determinations; *in* Geochimica et Cosmochimica Acta, vol. 37, p. 485-494.

Krogh, T.E. (1982) Improved accuracy of U-Pb zircon ages by the creation of more concordant systems using an air abrasion technique; *in* Geochimica et Cosmochimica Acta, vol. 46, p. 637-649.

McMechan, M.E. and Price, R.A. (1982) Superimposed low-grade metamorphism in the Mount Fisher area, southeastern British Columbia - implications for the East Kootenay orogeny; *in* Canadian Journal of Earth Sciences, v. 19, p. 476-489.

McMillan, W.J. (1973) Petrology and structure of the west flank, Frenchman's Cap dome, near Revelstoke, British Columbia; Geological Survey of Canada, Paper 71-29.

McNicoll, V.J. and Brown, R.L. (1995) The Monashee décollement at Cariboo Alp, southern flank of the Monashee complex, southern British Columbia, Canada; *in* Journal of Structural Geology, v. 17, p. 17-30.

Monger, J.W.H. (1977) Upper Paleozoic rocks of the western Canadian Cordillera and their bearing on Cordilleran evolution; *in* Canadian Journal of Earth Sciences, v. 14, p. 1832-1859.

Monger, J.W.H. and Berg, H.C. (1984) Lithotectonic terrane map of western Canada and southeastern Alaska; *in* Lithotectonic Terrane Maps of the North American Cordillera; N.J. Silberling and D.L. Jones (ed.), United States Geological Survey, Open File Report 84-523.

Monger, J.W.H., Price, R.A., and Tempelman-Kluit, D.J. (1982) Tectonic accretion and the origin of the two major metamorphic and plutonic welts in the Canadian Cordillera; *in* Geology, v. 10, p. 70-75.

Monger, J.W.H., Wheeler, J.O., Tipper, H.W., Gabrielse, H., Harms, T., Struik, L.C., Campbell, R.B., Dodds, C.J., Gehrels, G.E., and O'Brien, J. (1991) Part B. Cordilleran terranes; *in* Upper Devonian to Middle Jurassic assemblages, Chapter 8 of Geology of the Cordilleran Orogen in Canada, no. 4, p. 281-327.

Nicholls, J., Stout, M.Z., and Ghent, E.D. (1991) Characterization of partly-open-system chemical variations in clinopyroxene amphibolite boudins, Three Valley Gap, British Columbia, using Thompson space calculations; *in* Canadian Mineralogist, v. 29, p. 633-653.

Noble, P.J. and Finney, S.C. (1999) Recognition of fine-scale imbricate thrusts in lower Paleozoic orogenic belts; an example from the Roberts Mountains Allochthon, Nevada; *in* Geology, v. 27, no. 6, p. 543-546.

Okulitch, A.V. (1974) Stratigraphy and structure of the Mount Ida group, Vernon (82L), Seymour Arm (82M), Bonaparte Lake (92P) and Kettle River (82E) map-areas, British Columbia; *in* Report of Activities: Part A, April to October 1973, Geological Survey of Canada Paper 74-1, Part A, p. 25-30.

Okulitch, A.V. (1979) Lithology, stratigraphy, structure and mineral occurrences of the Thompson-Shuswap-Okanagan area, British Columbia; Geological Survey of Canada, Open File 637.

Okulitch, A.V. (1984) The role of the Shuswap Metamorphic Complex in Cordilleran tectonism: a review; *in* Canadian Journal of Earth Sciences, v. 21, p. 1171-1193.

Okulitch, A.V. (1985) Paleozoic plutonism in southeastern British Columbia; *in* Canadian Journal of Earth Sciences, v. 22, p. 1409-1424.

Okulitch, A.V. (1989) Revised stratigraphy and structure in the Thompson-Shuswap-Okanagan map area, southern British Columbia; *in* Current Research, Part A, Geological Survey of Canada, Paper 89-1A, p. 51-60.

Okulitch, A.V., Loveridge, W.D., and Sullivan, R.W. (1981) Preliminary radiometric analyses of zircons from the Mount Copeland syenite gneiss, Shuswap Metamorphic Complex, British Columbia; *in* Current Research, Part A, Geological Survey of Canada, Paper 81-1A, p. 33-36.

Okulitch, A.V., Wanless, R.K., and Loveridge, W.D. (1975) Devonian plutonism in south-central British Columbia; *in* Canadian Journal of Earth Sciences, vol. 12, p. 1760-1769.

Parkinson, D.L. (1992) Age and tectonic evolution of the southern Monashee complex, southeastern British Columbia; a window into the deep crust; Ph.D. thesis, University of California, Santa Barbara, Calif.

Parrish, R.R. (1995) Thermal evolution of the southeastern Canadian Cordillera; *in* Canadian Journal of Earth Sciences, v. 32, p. 1618-1642.

Parrish, R.R. and Armstrong, R.L. (1983) U-Pb zircon age and tectonic significance of gneisses in structural culminations of the Omineca Crystalline Belt, British Columbia; *in* Geological Society of America, Abstracts with Programs, v. 15, p. 324.

Parrish. R.R. and Scammell, R.J. (1988) The age of the Mount Copeland syenite gneiss and its metamorphic zircons, Monashee Complex, southeastern British Columbia; Geological Survey of Canada, Paper 88-2, p. 21-28.

Preto, V.A. (1981) Barriere Lakes - Adams Plateau Area (82M/4, 5W; 92P/1E); *in* Geological Fieldwork 1980, B.C. Ministry of Energy, Mines and Petroleum Resources, Paper 1981-1, p. 15-23.

Preto, V.A. and Schiarizza, P. (1985) Geology and mineral deposits of the Adams Plateau - Clearwater region; *in* Field Guides to Geology and Mineral Deposits in the Southern Canadian Cordillera, edited by D.J. Tempelman-Kluit, Geological Society of America, Cordilleran Section Annual Meeting, Vancouver, B.C., p. 16.1 - 16.11.

Read, P.B. and Brown, R.L. (1981) Columbia River fault zone: southeastern margin of the Shuswap and Monashee complexes, southern British Columbia; *in* Canadian Journal of Earth Sciences, v. 18, p. 1127-1145.

Read, P.B. and Wheeler, J.O. (1976) Geology, Lardeau west half, British Columbia; Geological Survey of Canada Open-File Map 432, scale 1:125,000.

Reesor, J.E. (1965) Valhalla gneiss complex, British Columbia; Geological Survey of Canada, Bulletin 129.

Reesor, J.E. (1970) Some aspects of structural evolution and resional settingin part of the Shuswap Metamorphic Complex; *in* Structure of the southern Canadian Cordillera; J.O. Wheeler (ed.), Geological Association of Canada, Special Paper No. 6, p. 73-86.

Roberts, R.J., Hotz, P.E., Gilluly, J., and Ferguson, H.G. (1958) Paleozoic rocks of north-central Nevada; *in* American Association of Petroleum Geologists Bulletin, v. 42, p. 2813-2857.

Roberts, R.J. and Thomasson, M.R. (1964) Comparison of late Paleozoic depositional history of northern Nevada and central Idaho; U.S. Geological Survey Professional Paper 475-D, p. D1-D6.

Root, K.G. (1987) Geology of the Delphine Creek area, southeastern British Columbian: implications for the Proterozoic and Paleozoic development of the Cordilleran divergent margin; Ph.D. thesis, University of Calgary, Calgary, Alberta, 446 p.

Root, K.G. (1992) Middle Devonian thrustbelt and foreland basin development, southeastern British Columbia; *in* Annual Meeting Abstracts - American Association of Petroleum Geologists and Society of Economic Paleontologists and Mineralogists, p. 111.

Root, K.G. (1993) Devonian and Mississippian thrust belt and foreland basin development in western Canada: implications for tectonics and diagenesis in the plains; *in* Lithoprobe, Alberta basement transects, report of transect workshop, G.M. Ross (ed.), Lithoprobe Report 31, p. 92-95.

Scammell, R.J. (1993) Mid-Cretaceous to Tertiary thermotectonic history of former mid-crustal rocks, southern Omineca Belt, Canadian Cordillera; Ph.D. thesis: Kingston Ontario, Queen's University, 576p.

Scammell, R.J. and Brown, R.L. (1990) Cover gneisses of the Monashee Terrane; a record of synsedimentary rifting in the North American Cordillera; *in* Canadian Journal of Earth Sciences, v. 27, p. 712-726.

Scammell, R.J. and Parrish, R.R. (1993) U-Pb zircon chronometry from a metamorphosed felsic volcaniclastic rock in cover gneisses, Monashee Terrane, southeastern British Columbia; *in* Geological Association of Canada, Program with Abstracts, v. 18: A93.

Schiarizza, P. and Preto, V.A. (1987) Geology of the Adams Plateau-Clearwater-Vanenby Area; British Columbia Ministry of Energy, Mines, and Petroleum Resources, Paper 1987-2, 88 p.

Silberling, N.J. and Roberts, R.J. (1962) Pre-Tertiary stratigraphy and structure of northwest Nevada; Geological Society of America Special Paper 72, 53 p.

Slemko, N.M. and Thompson, R.I. (1998) A re-evaluation of the geology adjacent to Shuswap Lake, Vernon map area, British Columbia; *in* Current Research 1998-A, Geological Survey of Canada, p. 175-179.

Smith, M.T., Dickinson, W.R., and Gehrels, G.E. (1993) Contractional nature of Devonian-Mississippian Antler tectonism along the North American continental margin; *in* Geology, v. 21, p. 21-24.

Spear, F.S. (1995) Metamorphic Phase Equilibria and Pressure-Temperature-Time Paths; Mineralogical Society of America Monograph.

Thompson, R.I and Daughtry, K.L. (1996) New stratigraphic and tectonic interpretations, north Okanagan Valley, British Columbia; *in* Current Research 1996-A, Geological Survey of Canada, p. 135-141.

Thompson, R.I and Daughtry, K.L. (1997) Anatomy of the Neoproterozoic-Palaeozoic continental margin, Vernon map area, British Columbia; *in* Current Research 1997-A, Geological Survey of Canada, p. 145-150.

Wanless, R.K. and Reesor, J.E. (1975) Precambrian zircon age of orthogneiss in the Shuswap Metamorphic Complex, British Columbia; *in* Canadian Journal of Earth Sciences, v. 12, p. 326-331.

Wanless, R.K., Stevens, R.D., Lachance, G.R., and Delabio, R.N. (1978) Age determinations and geological studies, K-Ar isotopic ages, report 13, Geological Survey of Canada, Paper 77-2.

Yardley, B.W.D. (1989) An Introduction to Metamorphic Petrology; Longman Scientific & Technical, UK.

Appendix A: Outcrop Locations, descriptions, structural measurements

Legend:

Lithology: gar=garnet, bt=biotite, musc=muscovite, plag=plagioclase, kspar=k-feldspar, qtz=quartz, feld=feldspar, sill=sillimanite, di=diopside, ol=olivine, hbl=hornblende, ser=sericite, chl=chlorite, cc=calcite, gross=grossular, trem=tremolite, staur=staurolite (minerals listed in order of increasing abundance)

Unit: SCs=Silver Creek mica schist, SCc=Silver Creek calcareous schist, Sm=Sicamous marble, EBg=Eagle Bay greenstone (chlorite schist and amphibolite), EBq=Eagle Bay quartzite and mica-quartz schist, EBm=Eagle Bay marble, QMs=Queest Mountain mica schist, QMmc=Queest Mountain marble and calcsilicate, Dg=Devonian Mount Fowler, Dgm=mafic Devonian Mount Fowler, Dgf=felsic Devonian Mount Fowler, DGp=pegmatitic Devonian Mount Fowler, ERFZ=Eagle River Fault Zone, M=Monashee gneisses

HS/TS=hand sample/thin section: H=hand sample, T=thin section

Type of Lineation: cren=crenulation, min=mineral lineation, FA=minor fold axis

Station	Lithology	Unit	HS/TS	Strike	Dip	Trend	Plunge	Type	Easting	Northing
NS97-1	dark bt-hbl schist	EBg	H	321	73	191	10	FA	359011	5635210
NS97-2A	cc-chl-bt-feld-qtz schist	EBq	H,T	284	47					
NS97-2B	actinolite-chl-ser-feld-qtz schist	EBg	H			322	83	cren		
NS97-3	cc-bt-chl-ser-feld-qtz schist	EBg	H	264	74					
NS97-4	gar-cc-bt-musc-chl-qtz schist	EBq	H,T							
NS97-5	dk grey and white marble	EBm	H,T	304	64					
NS97-6	sugary marble	EBm	H,T	176	62	320	17	FA		
NS97-7	grey marble	EBm		315	59					
NS97-8	gar(?)-hbl-bt-feld-qtz-chl schist	EBq	H,T	278	18					
NS97-9	ser-chl-hbl schist	EBg								
NS97-10	chl-musc-hbl-qtz-feld schist	EBq	H	143	69					
NS97-11	bt-hbl-qtz-kspar-plag, felsic	Dgf	H,T						361516	5636340
NS97-12	bt-qtz-feld, felsic	Dgf		316	68				361661	5636377
NS97-13	musc-bt-feld-qtz schist	EBq	H	346	37					
NS97-14	kspar-plag-chl-qtz-hbl m.g. granite	Dg	H,T	321	42				360696	5636412
NS97-15	hbl diorite	Dgm		246	37					
NS97-16	bt-hbl diorite	Dgm		210	48	56	22	min	359571	5636219

NS97-17	hbl-musc-bt-feld-qtz schist	EBq	H	214	24				359231	5636622
NS97-18	chl-bt-feld-musc-qtz granite, pegmatitic	Dgp	H,T	217	42	345	36	min	357898	5639002
NS97-19	f.g. granite to aplite	SC							350478	5631270
NS97-20	musc schist	SCs		214	31	10	24	cren	350362	5631375
NS97-21	bt-musc schist	SCs		240	32	344	22	cren	350103	5631462
NS97-22	mica schist	SCs							349930	5630681
NS97-23	mica schist	SCs		344	24					
NS97-24	granite	SC							350020	5631472
NS97-25	granite-schist contact	SCs							350027	5631857
NS97-26	granite	SC								
NS97-27	granite	SC							350428	5631723
NS97-28		Dgf?		349	17				361978	5636574
NS97-29		Dgf?		210	40	20	13	min	362119	5636852
NS97-30		Dgf?							362098	5637335
NS97-31	sill-bt-feld-qtz mylonite	ERFZ	H	322	33	115	19	cren		
NS97-32A	musc granite	?	H						364546	5640052
NS97-32B	foliated marble	EBm?	H	244	32				364546	5640052
NS97-33A	cc-chl-hbl schist ("greenstone")	EBg	H	328	56				360884	5636819
NS97-33B	ep-qtz-hbl schist	EBg	H,T						360884	5636819
NS97-34	chl-bt-musc-qtz schist	EBq	H,T	260	47				361053	5637297
NS97-35	cc-qtz-musc-bt-chl-hbl schist ("greenstone")	EBg	H	200	30				361658	5638328
NS97-36		Dg		68	35	160	31	min	361427	5639245
NS97-37	feld-qtz-bt-hbl schist (f.g.)	Dgm	H	242	25				361876	5640023
NS97-38	massive qtz	EBq							362062	5641042
NS97-39	bt-chl-plag-qtz schist	EBq	H,T	280	12				362226	5641910
NS97-40A	f.g. massive greenstone	EBg	H						362270	564094
NS97-40B	big musc granite	?	H						362270	564094
NS97-40C	bt-musc-plag-qtz schist	EBq	H,T	5	50				362270	564094
NS97-41A	bt-feld-qtz-schist : mylonite?	ERFZ?	H							
NS97-41B	plag-qtz-bt-sill schist	ERFZ	H,T							
NS97-42	amphibolite	?	H	254	23				362777	5636101
NS97-43	hbl-gar-bt schist			165	31				363045	5636889

NS97-44	sill-qtz-bt schist								363888	5638479
NS97-45	qtz-musc schist	SCs		160	50				354577	5629864
NS97-46	qtz-musc schist + granite	SCs							354723	5630140
NS97-47	qtz-musc schist + granite	SCs							355014	5630439
NS97-48	qtz-musc schist + granite	SCs							355902	5631162
NS97-49	cc-qtz-musc schist	SCc		288	48				356097	5631354
NS97-50	cc-qtz-musc schist	SCc		302	53				356224	5631489
NS97-51	sill-bt-musc-feld-qtz mylonite	ERFZ	H,T	120	25	106	10	min	359740	5630935
NS97-52	musc schist	SCs							359317	5631025
NS97-53	musc schist	SCs		315	65				359500	5632042
NS97-54	musc schist	SCs		135	69				359590	5632604
NS97-55	white + grey marble	EBm		98	40					
NS97-56	sericitic marble	EBm	H	35	13					
NS97-57	sericitic marble	EBm		88	21					
NS97-58	sericitic marble	EBm		355	35				359149	5635413
NS97-59	sericitic marble	EBm		17	17				359217	5635497
NS97-60	grey marble	EBm							359180	5635728
NS97-61	sericitic marble	EBm		336	49				359141	5635537
NS97-62	sericitic marble	EBm							359169	5635556
NS97-63	sericitic marble	EBm	H	0	40				359133	5635551
NS97-64	massive grey marble	EBm							359176	5635695
NS97-65	plag-bt-graphite-musc-qtz schist	EBq	H,T							
NS97-66	black + white marble	EBm							359356	5635739
NS97-67	cc-musc schist	EBq		39	20				359292	5635863
NS97-68	grey marble w. graphite, musc, phlog, qtz	EBm	H,T	139	45				359421	5635743
NS97-69	cc-musc schist	EBq		135	78					
NS97-70	musc-chl-bt-qtz-plag schist	EBq	H,T	350	5				362312	5642579
NS97-71A	qtz-di-gross marble	QMmc	H,T	351	65				362338	5643854
NS97-71B	trem-di-feld-bt-qtz schist	QMmc	H,T						362338	5643854
NS97-72	qtz-feld-hbl-bt m.g., big amph blades	Dgm	H	340	53				362595	5644972
NS97-73	white marble	QMmc	H						362903	5646212
NS97-74	gar-feld-musc-bt-qtz schist	QMs	H	310	53				363375	5646705

NS97-75	gar-plag-musc-bt-qtz schist	QMs	H,T						363597	5646826
NS97-76	gar-amph-bt-musc schist	QMs							363907	5647258
NS97-77	gar-musc-bt schist	QMs							364393	5647751
NS97-78	gar-musc-bt schist	QMs							364675	5647739
NS97-79A	white marble	QMs	H	79	70				365095	5650075
NS97-79B	granitoid (kspar, plag, qtz)	?	H,T						365095	5650075
NS97-80	gar-hbl-bt-musc-qtz schist	QMs	H,T	110	70				365291	5650610
NS97-81	kspar-plag-qtz-hbl granitoid	Dgm	H,T						365535	5650799
NS97-82	gar(?)-plag-bt-musc-qtz schist	EBq	H,T	95	67				365761	5651383
NS97-83	ep-musc-kspar-bt-plag-qtz granitoid	Dg	H,T	330	75	0	55	min	362425	5645811
NS97-84A	bt-actinolite-qtz schist	QMs	H,T	311	39				362421	5646619
NS97-84B	sill-chl-hbl-plag-bt-qtz schist	QMs	H,T							
NS97-85	white marble	QMmc	H						362449	5646724
NS97-86	diopside marble	QMmc	H							
NS97-87A	bt-qtz-feld-hbl, m.g., big amph blades	Dgm	H						362278	5646745
NS97-87B	feld-phlog-qtz marble	QMmc	H,T	10	21				362278	5646745
NS97-88	bt-hbl-qtz-plag	Dg		204	20				361956	5646331
NS97-89	qtz-feld-bt-hbl, f.g., mafic	Dgm	H						362032	5646573
NS97-90	felsic granite	Dgf		320	65				362025	5646830
NS97-91A	cc-bt-musc-plag-qtz schist	QMs	H,T							
NS97-91B	bt-musc-qtz schist + gar	QMs	H	270	10				360602	5646518
NS97-92	bt-hbl-qtz-feld	Dgg	H						361593	5648097
NS97-93	hbl-qtz-feld, pegmatitic	Dgp	H	326	61				361472	5648032
NS97-94	lt grey, weakly fol. marble	QMmc	H						361275	5648484
NS97-95	trem-ol-di marble	QMmc	H,T	320	34				361061	5648678
NS97-96	di-qtz marble	QMmc	H						361023	5649169
NS97-97	gar(?)-chl-feld-bt-qtz schist	QMs	H,T						361275	5649546
NS97-98	bt-ol-cc-chl-feld-qtz-hbl granitoid	Dgm	H						361748	5649962
NS97-99	massive grey qtzite	QM?	H						361891	5650213
NS97-100	quartzite	QM?							361945	5650418
NS97-101	cc-bt-ol-plag-qtz-hbl	?	H,T	110	62				361962	5650507
NS97-102	gar-qtz-bt-musc schist	QMs							361462	5649688

NS97-103	musc-bt-qtz schist	QM?	H						361531	5649851
NS97-104	plag-amph	Dgm		115	13				361544	5650029
NS97-105	bt-qtz-plag-amph schist	Dgm		86	40				361572	5650705
NS97-106	white tremolite marble	QMmc	H							
NS97-107	trem-phlog-ol-di-qtz-plag	QMmc	H,T						361687	5648276
NS97-108	calsilicate	QMmc							361747	5648341
NS97-109	gar-chl-plag-musc-bt-qtz schist	QMs	H,T						361822	5648659
NS97-110	calcareous qtzite	QMmc	H						361846	5648822
NS97-111	gar-qtz-musc-bt schist	QMs		300	45				362431	5648382
NS97-112	gar-qtz-musc-bt schist	QMs							362305	5648079
NS97-113	gar-staur-chl-bt-qtz-musc schist	QMs	H,T						362511	5648015
NS97-114	bt-gar-qtz-plag schist	QMs							362587	5647645
NS97-115	musc schist	QMs		335	57				362711	5647955
NS97-116	bt-gar-qtz-plag schist	QMs							362840	5647852
NS97-117	bt-qtz schist	QMs	H							
NS97-118		QMs							362973	5647897
NS97-119	bt-qtz schist + gar	QMs	H	305	50				363113	5647663
NS97-120	garnetiferous schist	QMs							363158	5647718
NS97-121	garnetiferous schist	QMs		293	60				363127	5648384
NS97-122	garnetiferous schist	QMs		358	28	90	25	min	363126	5648982
NS97-123	mica schist	QMs		140	58				363545	5649299
NS97-124	chl-bt-qtz-hbl-plag	?	H,T						363699	5649621
NS97-125	gar-musc-qtz-feld schist	QMs							362379	5648973
NS97-126	garnet-mica schist	QMs	H						362721	5649140
NS97-127		QMs		97	9				362547	5649568
NS97-128	bt-musc-qtz schist	QMs	H,T	95	57				362848	5649932
NS97-129	musc-bt-qtz schist	QMs							363134	5650281
NS97-130	gar-bt-musc-feld-qtz schist	QMs							363292	5646274
NS97-131A	cc-mica-hbl-feld-qtz schist	QMs	H						363327	564652
NS97-131B	gar(?)-chl-qtz-bt-musc schist	QMs	H,T						363327	564652
NS97-132	gar-qtz-feld-bt-musc schist	QMs							364007	5647774
NS97-133	gar-musc schist	QMs							364304	5649718

NS97-134	musc bt schist	SCs		290	26				356288	5633025
NS97-135	di-microcline-hbl conglomerate	SC	H,T						356575	5631909
NS97-136	ep-actinolite-feld marble	SCc	H,T	305	47				356773	5631984
NS97-137	cc-bt-musc schist	SCc							356920	5632171
NS97-138	grey + white marble	Sm	H	260	41				357392	5632607
NS97-139	grey + white marble	Sm							358018	5632902
NS97-140	grey + white marble	Sm		135	80				359121	5633143
NS97-141	greenstone	EBg							361670	5634658
NS97-142	qtz-hbl-feld, m.g. granite	Dg	H	339	56				361470	5635754
NS97-143	mica schist	Dg	H						361149	5635704
NS97-144	bt-hbl-qtz-plag	Dg							361418	5636588
NS97-145	feld-qtz-hbl schist	EBg	H,T	150	33				362116	5638133
NS97-146	grey marble	EBm	H						362161	5638197
NS97-147	hbl-plag	Dg							362128	5638596
NS97-148	hbl-plag, felsic	Dgf							362234	5638940
NS97-149	chl schist	EBg		265	25				359470	5637490
NS97-150	grey+ white limestone	EBm	H	260	26				359574	5637588
NS97-151A	bt-chl-plag-musc-qtz schist	EBq	H,T	243	40				357700	5638785
NS97-151B	greenstone	EBg	H						357700	5638785
NS97-152		Dg		350	30				359067	5641256
NS97-153	mica schist?	?							359565	5641803
NS97-154		Dg								
NS97-155	bt-qtz-feld, m.g. granite, felsic	Dgf	H						359783	5642015
NS97-156	hbl-qtz-feld, m.g. granite, felsic	Dgf	H						359779	5642074
NS97-157	hbl-bt-feld-qtz, m.g. granite, felsic	Dgf	H	105	9				360198	5642238
NS97-158	bt-musc-hbl-plag-kspar-qtz	Dgf?							361986	5636918
NS97-159	greenstone	EBg	H						362070	5637384
NS97-160A	bt-musc-qtz schist, f.g. mafic	Dgm	H						361557	5639421
NS97-160B	chl-musc-kspar-plag-kspar-bt-qtz granitoid	Dgf	H,T						361557	5639421
NS97-161	bt-musc-qtz-plag-kspar	Dg							361952	5639728
NS97-162	sill-mus-feld-bt-qtz schist	EBq	H,T						362274	5642372
NS97-163	bt-musc-qtz schist	EBq		346	50				362315	5642371

NS97-164	grey marble	EBm							361900	5642240
NS97-165	bt-hbl-plag-kspar-qtz	Dg							361822	5642063
NS97-166	hbl-qtz-feld, m.g. granite, felsic	Dg	H						361799	5641928
NS97-167	musc-bt-qtz-feld schist	EBq	H,T						361735	5641754
NS97-168	bt-qtz-feld, f.g. mafic	Dgm	H						361452	5641606
NS97-169	bt-hbl-plag-kspar-qtz	Dg							361367	5641514
NS97-170	hbl-feld-qtz, m.g. granite	Dg	H						362709	5643653
NS97-171	hbl-feld-qtz, m.g. granite	Dg	H						362979	5643713
NS97-172	ol-plag-chl-hbl-kspar-bt-qtz granite	Dgf	H,T						363321	5644148
NS97-173A	hbl-feld-qtz, m.g. granite	Dg	H						363210	5644433
NS97-173B	musc granite	?	H						363210	5644433
NS97-174A	felsic granite	?	H						363390	5644592
NS97-174B	bt-qtz-hbl-feld, f.g. mafic	Dgm	H						363390	5644592
NS97-175	bt-hbl-qtz-feld, f.g. mafic	Dgm	H						362906	5644141
NS97-176	bt-musc-qtz-chl-ser schist	EBg	H	247	55				358898	5636527
NS97-177	bt-musc-cc-qtz-chl-ser schist	EBg	H	325	20				358817	5636528
NS97-178	bt-musc-cc-qtz-chl-ser schist	EBg		345	39				358710	5636535
NS97-179	sericitic marble	EBm	H						358655	5636558
NS97-180	bt-musc-qtz schist	EBq							358667	5636567
NS97-181	felsic Dg	Dgf							359520	5636083
NS97-182	bt-qtz-feld-hbl, f.g. mafic	Dgm	H						359553	5636147
NS97-183A	qtz-feld-bt-hbl schist, f.g. mafic	Dgm	H							
NS97-183B	greenstone w. marble layer	EBg	H							
NS97-184A	hbl-qtz-feld, m.g. granite	Dg	H	235	10				359049	5636972
NS97-184B	hbl-qtz-feld, m.g. granite	Dg	H						359049	5636972
NS97-185	mica qtz schist	EBq							358889	5636860
NS97-186	bt-musc-qtz schist								358880	5636949
NS97-187	calcareous greenstone	EBg	H	270	5				358819	5636915
NS97-188	musc granite	?							362762	5643018
NS97-189	qtz-bt-musc schist	EBq							362851	5642893
NS97-190	musc-bt-qtz schist	EBq							363187	5642505
NS97-191A	hbl-qtz-feld, m.g. granite	Dg	H						364205	5643570

NS97-191B	feld-qtz-hbl, f.g. mafic	Dgm	H	330	52	150	5	min	364205	5643570
NS97-191C	feld-qtz schist ; v. weathered	?	H						364205	5643570
NS97-192	hbl-qtz-feld, m.g. granite	Dg	H						361820	5640302
NS97-193	qtz-hbl-bt-feld, m.g. granite	Dg	H						361795	5640295
NS97-194	hbl-bt-qtz-feld, m.g. granite	Dg	H						361734	5640348
NS97-195	hbl-qtz-feld, m.g. granite	Dg	H						361622	5640399
NS97-196	hbl-qtz-feld, m.g. granite	Dg	H						361401	5640430
NS97-197	qtz-bt schist			330	30				361792	5640490
NS97-198	bt-chl-plag-qtz-musc schist	SCs	H,T						348176	5630531
NS97-199	calcareous schist	SCc	H	140	47				349425	5630915
NS97-200A	cc-musc-bt-qtz schist	SCc	H	270	42				350583	5631085
NS97-200B	bt-musc-kspar-plag-qtz	SC	H,T							
NS97-201	bt-cc-qtz schist	SCc	H						353735	5633203
NS97-202	cc-bt-qtz schist	SCc		240	37				353829	5633638
NS97-203	gar-bt-musc-cc-qtz schist	SCc	H						353640	5633684
NS97-204	bt-musc-qtz schist (assoc. intrusions)	SCs	H						353286	5633645
NS97-205	plag-bt-chl-musc-kspar-qtz schist	SCs	H,T	255	37				353081	5633515
NS97-206	bt-musc-qtz schist (assoc. intrusions)	SCs							353081	5633844
NS97-207	calcareous schist	SCc	H						351825	5631155
NS97-208	calcareous greenstone	EBg	H						345444	5644683
NS97-209	grey marble	EBm	H						346139	5644855
NS97-210	cc-chl schist	EBg	H						346623	5645055
NS97-211	grey marble	EBm							346139	5644855
NS97-212	cc-chl schist	EBg	H						346623	5645055
NS97-213	greenstone	EBg		275	24				347502	5644975
NS97-214	cc-chl schist	EBg	H						247831	5644933
NS97-215	greenstone	EBg	H						348411	5645375
NS97-216	sericitic marble	EBm	H	255	27				350280	5646069
NS97-217	ser-qtz schist	EBq	H						352063	5646941
NS97-218	greenstone	EBg								
NS97-219	grey massive marble (dol?)	EBm	H						345855	5641197
NS97-220	sericitic marble	EBm	H						346122	5641376

NS97-221	greenstone w. cc veins	EBg	H						347826	5641956
NS97-222	greenstone	EBg	H						349419	5640868
NS97-223	greenstone	EBg	H	250	20				351716	5641456
NS97-224	dk grey marble	EBm	H						352045	5641423
NS97-225	greenstone	EBg							352280	5640460
NS97-226	sericitic marble	EBm	H						352663	5641093
NS97-227	chl schist w py	EBg							353251	5641864
NS97-228	chl schist	EBg		250	25				352866	5643022
NS97-229	white, sugary, slightly fol. marble	EBm	H						353049	5643442
NS97-230	chl schist	EBg		195	37				352690	5641645
NS97-231	greenstone	EBg							352039	5642934
NS97-232	chl schist	EBg							352075	5643550
NS97-233A	greenstone	EBg	H						352702	5640955
NS97-233B	sericitic marble	EBm	H	245	33				352702	5640955
NS97-234	chl schist	EBg							351661	5640449
NS97-235	chl schist	EBg							351928	5639287
NS97-236	chl schist	EBg							350754	5640655
NS97-237	chl schist	EBg							350707	5640280
NS97-238	sericitic marble	EBm	H						351364	5639434
NS97-239	marble + chl schist	Sm + EBg		255	47				351202	5639574
NS97-240A	ser-qtz schist	EBq	H						351025	5639361
NS97-240B	malachite	EB?	H						351025	5639361
NS97-241	musc-qtz schist	EBq		260	54				350805	5639304
NS97-242	ser-qtz schist	EBq	H						350463	5638413
NS97-243	chl schist	EBg		290	57				350255	5638438
NS97-244	greenstone w. cc veins	EBg	H						349211	5638391
NS97-245	greenstone w. cc veins	EBg	H						350108	5637843
NS97-246	chl schist	EBg		270	28	70	12	cren	349884	5637116
NS97-247	cc-ser-qtz schist	EBq	H						349596	5636322
NS97-248	grey + white fol. graphitic marble	EBm	H						348311	5634828
NS97-249	grey + white fol. graphitic marble	EBm							348100	5634772
NS97-250	grey + white fol. graphitic marble	EBm		190	25				349080	5634579

NS97-251	grey + white fol. graphitic marble	EBm							349804	5633368
NS97-252	grey + white fol. graphitic marble	EBm							351534	5633843
NS97-253	grey + white fol. graphitic marble	EBm		250	37				351881	5633874
NS97-254	aplite sill in SC	SCs	H							
NS97-255	cc-qtz-musc-bt schist	SCs	H	240	40					
NS97-256	aplite intrustion									
NS97-257	chl schist	EBg							350463	5638314
NS97-258	bt-feld-qtz schist, m.g. granite	Dg	H						364287	5643462
NS97-259	qtz musc schist	EBq		200	33				367059	5642889
NS97-260	qtz-musc-bt schist	EBq		270	31				368229	5642395
NS97-261	greenstone	EBg	H	166	20				368980	5642504
NS97-262	cc-bt-musc-qtz schist	EBq	H						369430	5642770
NS97-263	greenstone w. cc vug	EBg	H						369731	5642926
NS97-264	b+w limestone	EBm	H						369996	5642924
NS97-265	aplite?	?							370348	5642308
NS97-266	qtz-bt schist	EBq							370531	5642441
NS97-267	qtz-feld-musc intrusion	?							370660	5642692
NS97-268	qtz-bt-musc schist	EBq							362201	5643001
NS97-269	qtz-feld	Dg?							361701	5643024
NS97-270	qtz-feld-bt-hbl	Dg							361039	5642502
NS97-271	tuff	Eocene?	H						361927	5640889
NS97-272	aplite?	?							361792	5640977
NS97-273	qtz-feld-bt-hbl	Dg							361738	5640761
NS97-274	bt-qtz-feld, m.g. granite, felsic	Dg	H						361627	5640698
NS97-275	bt-qtz-feld, m.g. granite, felsic	Dg							361426	5640888
NS97-276	qtz-feld-bt	Dgm	H						361319	5640825
NS97-277	qtz-feld-bt	Dgm							361241	5641033
NS97-278	qtz-feld-bt, pegmatitic	DGp							361318	5641157
NS97-279	grey+white fol. qtzite	EBq	H						356487	5641822
NS97-280	qtz-feld-bt-hbl, f.g. mafic	Dgm	H						359630	5638900
NS97-281	cc-musc-bt-qtz schist	EBq	H						359805	5639544
NS97-282		Dg							359958	5639484

NS97-283	musc-bt-hbl-qtz schist, m.g. granite	Dg	H	12	60				360311	5640137
NS97-284	musc-bt-hbl-qtz schist, m.g. granite	Dg							360411	5640205
NS97-285	musc-qtz-feld	Dg?							360497	5640509
NS97-286A	bt-hbl-qtz-feld, m.g. granite	Dg	H						360679	5640707
NS97-286B	bt-hbl-qtz-feld. m.g. granite	Dg	H						360679	5640707
NS97-287		Dg							360773	5640814
NS97-288	hbl-qtz-plag-ksap	Dg							360850	5641292
NS97-289	black + white marble	Sm		290	38				356818	5635298
NS97-290	black + white marble	Sm		300	35				356593	5635432
NS97-291	black + white marble	Sm		320	41				356430	5636125
NS97-292	cc-bt-musc-qtz schist	EBq	H,T	270	35				356127	5636617
NS97-293	hbl-chl-ser schist	EBg	H						356028	5636933
NS97-294	cc-hbl-chl-ser schist	EBg	H	290	45				355699	5637379
NS97-295A	grey + white marble	EBm	H	313	69				356021	5638509
NS97-295B	b + w marble	EBm	H						356021	5638509
NS97-296	b + w marble	EBm		81	39				356095	5638809
NS97-297	cc-mica schist	EBm		192	16				356567	5640500
NS97-298	cc-mica schist	EBm							356347	5640592
NS97-299	cc-mica schist	EBm		333	20				356391	5640724
NS97-300	gar-bt-musc-qtz schist	EBq	H	56	33				356485	5641530
NS97-301	pinkish, massive quartzite	EBq	H						356510	5642023
NS97-302	qtz-bt schist	EBq	H						356491	5642348
NS97-303	bt-musc schist	?		5	15	120	12	min	356656	5642551
NS97-304	gar(?)-ser-qtz schist	EBq	H	48	4				356958	5642724
NS97-305	bt-musc-qtz schist								357996	5643246
NS97-306	bt-musc-qtz schist	EBq?							358380	5643492
NS97-307	gar-musc-qtz schist								358659	5643541
NS97-308	bt-hbl-qtz-feld, m.g. granite	Dg	H							
NS97-309	feld-qtz-hbl, f.g. mafic	Dgm	H						360635	5647918
NS97-310	bt-hbl-feld-qtz, m.g. granite	Dg	H							
NS97-311A	ep-phlog-cc-calcsilicate	QMmc	H	329	60				360757	5649064
NS97-311B	qtz-feld-hbl, f.g. mafic	Dgm	H						360757	5649064

NS97-312	cc-chl-ser schist	EBg	H						361152	5637482
NS97-313	black + white marble	EBm	H,T	160	22				361602	5638369
NS97-314	tuff	Eocene?	H						361439	5638678
NS97-315	qtz-feld-hbl-bt	Dg							360723	5649287
NS97-316	qtz-feld-amph, f.g. mafic	Dgm	H						360540	5649190
NS97-317	calcsilicate schist	QMmc		316	56				360684	5649337
NS97-318	cc-bt-musc schist	QMmc		320	30				360855	5649689
NS97-319	bt-hbl-feld-qtz, m.g. granite	Dg	H						360912	5649847
NS97-320		Dg							360936	5650002
NS97-321	bt-hbl-feld-qtz, m.g. granite	Dg	H						361016	5650214
NS97-322	di(?)-gross(?) marble	QMmc	H	84	45				361055	5650384
NS97-323	bt-qtz-feld-hbl, m.g. granite	Dg	H						361195	5650859
NS97-324	feld-qtz-bt-hbl, f.g. mafic	Dgm	H						361447	5651069
NS97-325	gar-bt-musc-qtz schist	QMs	H						364860	5649787
NS97-326	gar-bt-musc-qtz schist	QMs	H						364311	5648155
NS97-327A	trem marble	QMmc	H						364454	5649918
NS97-327B	trem marble	QMmc	H						364454	5649918
NS97-328	undeformed f.g volcanic	Eocene?	H						364580	5650631
NS97-329	gar-bt-musc-qtz schist	QMs	H	104	26				364638	5650902
NS97-330	feld-qtz-bt-hbl, f.g. mafic + m.g. granite	Dgm + Dg	H	181	28				361327	5645563
NS97-331	bt-hbl-feld-qtz, m.g. granite	Dg	H	330	32				361502	5645196
NS97-332A	hbl-feld-qtz, m.g. granite	Dg	H						361427	5644858
NS97-332B	garnet-bearing granite?	?	H						361427	5644858
NS97-333	qtz-feld-bt-hbl, f.g. mafic	Dgm	H	175	45				361280	5644439
NS97-334	big musc + garnets	?							361328	5644322
NS97-335	sericitic marble	EBm	H						358422	5635696
NS97-336	garnet-bearing granite?	?	H						361541	5644584
NS97-337	felsic intrusion	?	H						361369	5644774
NS97-338	white qtzite								356650	5642639
NS97-339	pink quartzite	EBq	H	55	13				356693	5642845
NS97-340	gar(?)-qtz-bt-musc schist	EBq	H,T	65	18	315	5	min	356821	5642663
NS97-341		Dg		275	27	350	24	min	360180	5636178

NS97-342		Dg		315	18				358383	5640524
NS97-343		Dg		88	2				361567	5646813
NS97-344		Dg		33	5				361245	5646800
NS97-345	gar-musc-bt-qtz schist			110	35				361630	5649831
NS97-346	phlogopite cc marble	QMmc	H	70	23				362859	5649395
NS97-347	bt-hbl-qtz-feld, m.g. granite	Dg	H	318	47				362137	5645555
NS97-348		Dg							362093	5645529
NS97-349	calcsilicate schist	Lichen	H						359550	5652537
NS97-350	cc schist	Lichen	H						357914	5652853
NS97-351	cc-qtz-chl-ser schist	EBg	H	140	25	195	18	cren	359240	5651295
NS97-352	qtz-fel intrusion	?							359021	5650881
NS97-353	qtz-chl-bt-cc-ser schist	EBg	H	270	27				359024	5650869
NS97-354	bt-hbl-qtz-feld, m.g. granite	Dg	H	116	14				360817	5647571
NS97-355A	bt-hbl-feld-qtz, m.g. granite	Dg	H	127	81				361096	5648433
NS97-355B	feld-qtz-bt-hbl, f.g. mafic	Dgm	H						361096	5648433
NS97-356	bt-hbl-plag-qtz, m.g. granite	Dg	H	330	34				361912	5647674
NS97-357	hbl-bt-plag-qtz schist	QMs	H						361864	5647725
NS97-358	di(?)-gross(?) marble	QMmc	H	304	25				361781	5647664
NS97-359	musc-bt-qtz schist	EBq	H	306	29				367487	5642625
NS97-360	sericitic marble	EBm	H	321	11				367823	5642617
NS97-361	bt-ser-qtz schist	EBq	H	316	50	325	3	min	367957	5642898
NS97-362	white marble	EBm							354411	5648279
NS97-363	bt-ser-qtz schist	EBq	H	232	9	330	12	cren	354424	5648600
NS97-364	chl-bt-ser qtz schist	EBq		317	39	155	12	cren	355106	5649322
NS97-365	greenstone w. cc veins	EBg	H	319	51				356064	5649778
NS97-366	white massive marble	EBm	H	312	25				356602	5649793
NS97-367	chl-ser schist	EBg	H	320	77				356890	5649967
NS97-368	chl schist + cc	EBg	H	57	15	124	10	cren	354572	5648732
NS97-369	chl-bt-ser schist	EBg		329	27				354685	5648595
NS97-370	bt-ser-chl schist	EBg		289	13				354523	5647879
NS97-371	white weakly fol. marble	EBm	H	92	14				354594	5647479
NS97-372	white weakly fol. marble	EBm	H,T	150	9				355111	5646875

NS97-373A	f.g. felsic intrusion	Eocene?	H						351136	5647458
NS97-373B	cc-chl-ser schist	EBg	H	29	20				351136	5647458
NS97-374	hbl-bt-qtz-plag schist	near ERFZ	H	153	41				363016	5636413
NS97-375	cc-bt-qtz schist	near ERFZ	H						364171	5638726
NS97-376	hbl-plag-qtz gneiss	near ERFZ	H						364687	5639150
NS97-377	hbl-bt-feld-qtz	near ERFZ	H	325	25				365419	5639436
NS97-378	carbonate	near ERFZ	H	345	43				367833	5640224
NS97-379	gar-bt-plag-qtz schist			185	16				363321	5635661
NS97-380	bt-plag-qtz schist		H,T						364083	5636131
NS97-381	gar-bt-plag-qtz schist			179	26					
NS97-382	gar-chl-bt-qtz schist	SCs	H,T	281	25	31	23	min	354352	5632720
NS97-383	cc-qtz-bt-musc schist	SCs							354015	5633493
NS97-384	b + w marble	Sm	H	222	25				353805	5635674
NS97-385	chl-bt-qtz-feld schist	M	H,T	60	53	70	32	min	362457	5633481
NS97-386	chl-bt-musc-kspar-qtz schist	EBq	H,T						360242	5644046
NS97-387	sill-gar-plag-bt-musc-qtz schist	EBq	H,T	125	35					
NS97-388	calcareous sericitic quartzite	EBq	H	340	44				357970	5651125
NS97-389	bt-musc-chl-cc-feld-qtz schist	EBm	H,T	346	62	13	35	cren	357950	5651051
NS97-390	greenstone	EBg	H	334	84				357884	5650914
NS97-391	chl-ser marble	EBm		300	64				357710	5650738
NS97-392	grey weakly foliated marble	EBm	H	136	61				357261	5650669
NS97-393	greenstone (qtz+hbl)	EBg	H,T	124	84				357263	5650501
NS97-394	grey + white marble	EBm?		104	60				357153	5650587
NS97-395	chl-ser schist	EBg							356889	5650454
NS97-396	greenstone	EBg	H	307	34				356022	5650037
NS97-397	chl-ser schist	EBg	H	334	52				355141	5649826
NS97-398	musc-ser quartzite	EBg	H	332	30				355074	5649906
NS97-399A	bt-qtz-chl-cc-ser schist	EBg	H	340	39				354957	5649731
NS97-399B	bt-qtz-chl-cc-ser schist	EBg	H						354957	5649731
NS97-400	chl-ser schist	EBg							354840	5649702
NS97-401	felsic intrusion	Eocene?	H						354576	5649321
NS97-402	grey + white marble	EBm	H	173	5	160	3	cren	354397	5649095

NS97-403	cc-chl-ser schist	EBg				147	2	cren	354149	5648942
NS97-404	bt-qtz-cc-chl-ser schist	EBg	H						359026	5650754
NS97-405	greenstone w. cc	EBg	H						359168	5650587
NS97-406	f.g. granite intrusion	Eocene?	H	160	69				359118	5650445
NS97-407	granitoid intrusion	?							359142	5649777
NS97-408	cc-chl-ser schist	EBg	H						359322	5649538
NS97-409	chl schist	EBg		120	69				359061	5649300
NS97-410	greenstone	EBg							358876	5649299
NS97-411	massive white limestone	EBm	H						358001	5647686
NS97-412	ol-bt-cc-qtz-hbl schist	EBg	H,T	10	23	140	20	cren	357147	5646019
NS97-413	bt-chl schist	EBg							356826	5645730
NS97-414	bt-chl schist	EBg		304	19				356804	5645569
NS97-415	cc-chl-ser schist	EBg	H	246	29				356784	5645617
NS97-416	ser-chl schist	EBg	H						356481	5645124
NS97-417	cc-chl-ser schist	EBg							355958	5644941
NS97-418	cc-ser-chl-schist	EBg	H	245	28				355782	5644982
NS97-419	cc-chl-ser schist	EBg	H						355247	5644741
NS97-420	cc-chl-ser schist	EBg	H	213	19	293	18	cren	353815	5643036
NS97-421	grey and beige marble	EBm	H						356747	5639558
NS97-422	bt-musc-cc schist	EBm							356797	5639471
NS97-423	bt-musc-cc schist	EBm							356806	5639427
NS97-424	bt-chl-cc-feld-qtz-hbl schist	EBg	H,T	300	20	345	10	cren	353616	5642103
NS97-425	greenstone	EBg		268	35				353400	5640534
NS97-426	qtz-chl-ser schist	EBg	H	290	70				353478	5640104
NS97-427	sericitic marble	EBm	H						353648	5639690
NS97-428	bt-cc-ser-qtz schist	EBm	H,T	278	44				353641	5639561
NS97-429A	ser-chl schist	EBg	H	248	49				353601	5639047
NS97-429B	qtz-ser-chl schist	EBg	H						353601	5639047
NS97-430	qtz-chl-ser schist	EBg	H	280	52				353511	5638666
NS97-431	greenstone	EBg							353479	5637723
NS97-432	chl-ser schist	EBg							353521	5637245
NS97-433	qtz-chl-ser schist	EBg	H	278	44				353473	5637164

NS97-434	black + white marble	Sm	H,T	245	52				353531	5637072
NS97-435	amph-bt-musc schist	EB?							357218	5635225
NS97-436	bt-chl-ser schist	EBg							357364	5635306
NS97-437	hbl-feld-qtz, m.g. granite + f.g. mafic	Dg + Dgm	H						362444	5644352
NS97-438	chl-ser schist	EBg							357477	5635532
NS97-439	chl-ser-qtz schist	EBq							357444	5635534
NS97-440	chl-qtz-musc schist	EBq		310	74				357459	5635424
NS97-441	bt-chl-ser schist	EBg	H	330	35				357377	5635589
NS97-442	bt-chl-ser schist	EBg							357413	5634681
NS97-443	bt-chl-ser schist	EBg							357456	5635711
NS97-444	cc-qtz-chl-ser schist	EBg	H	295	46				357443	5635641
NS97-445A	lt grey marble	EBm	H						356086	5647366
NS97-445B	cc-ser-chl schist	EBg	H						356086	5647366
NS97-446	chl-ser schist	EBg	H						355919	5647202
NS97-447	grey dolomite	EBm	H						356306	5647639
NS97-448	ser-chl schist	EBg	H	345	5	121	5	cren	355671	5647121
NS97-449	grey marble	EBm	H	335	36				354535	5648750
NS97-450	bt-musc-qtz schist	QMs		340	35	150	6	min	360098	5645321
NS98-12A	sericitic quartzite		H	233	14				360870	5646109
NS98-12B	mafic dyke		H							
NS98-12C	bt-hbl-qtz-feld, m.g. granite	Dg	H,T	316	13				360999	5646298
NS98-12D	bt-hbl-qtz-feld, m.g. granite	Dg	H							
NS98-13A	di calcsilicate schist	QMmc	H,T	347	64					
				146	84					
NS98-13B	bt-cc-kspar-plag-qtz-hbl granitoid	Dgm	H,T	146	84					
NS98-14A	kspar-chl-qtz-ep-cc-plag schist	QMmc	H,T						362494	5650568
NS98-14B			H						362494	5650568
NS98-15	bt-hbl-qtz-feld, m.g. granite	Dg	H	90	39				362345	5651366
NS98-16A	bt-hbl-qtz-feld, m.g. granite	Dg	H						365550	5650816
NS98-16B	greenstone	EBg?	H						365550	5650816
NS98-16C	greenstone	EBg?	H						365550	5650816
NS98-16D	qtz-ser-chl schist	EBg?	H						365550	5650816

NS98-16E	bt-musc schist	EBq?	H						365550	5650816
NS98-17A	grey marble	QMmc	H						361311	5648615
NS98-17C	cc-di-ep schist	QMmc	H,T							
NS98-18	gar-feld-bt-qtz schist	QMs	H,T						362978	5647725
NS98-19	gar-musc-feld-qtz schist	QMs							364539	5647348
NS98-20	garnet-bt-musc schist	QMs	H	332	32	133	8	cren	364315	5647182
NS98-21	sill-gar(?)-feld-bt-musc-qtz schist	QMs	H,T	322	24					

Appendix B: Thin section descriptions

Sample/ Unit	Minerals	Mode %	Comments:
NS97-2A	quartz	30	-foliation defined by the alignment of micas
EBq	muscovite	20	-biotite retrograded to chlorite
	feldspar	20	
	biotite	15	
	chlorite	15	
	calcite	—	
	pyrite?	—	
NS97-4	quartz	60	-foliation defined by the alignment of micas
EBq	chlorite	20	-biotite retrograded to chlorite
	muscovite	10	
	biotite	10	
	garnet	—	
	graphite	—	
	calcite	—	
NS97-5	calcite	90	-fine-grained layers with graphite,
EBm	quartz	5	coarse-grained layers pure calcite
	graphite	5	
NS97-6	calcite	80	-elongate quartz and calcite define foliation
EBm	quartz	20	
	sphene	—	
	epidote?	—	
	tremolite?	—	
NS97-8	chlorite	35	-biotite retrograded to chlorite
EBq	quartz	20	-foliation defined by the alignment of micas
	feldspar	20	-plagioclase seriticized
	biotite	15	-biotite kinked - brittle deformation
	actinolite	10	
NS97-11	plagioclase	40	-plagioclase seriticized
Dgf	k-feldspar	20	-igneous texture
	quartz	20	
	hornblende	15	
	biotite	5	
NS97-14	hornblende	30	
Dg	quartz	20	
	chlorite	20	
	plagioclase	15	
	k-feldspar	15	
NS97-18	quartz	40	-biotite retrograded to chlorite
Dgp	muscovite	20	-plagioclase seriticized
	feldspar	20	-moderate foliation
	biotite	15	
	chlorite	5	
NS97-33B	hornblende	70	-weak foliation
EBg	quartz	15	
	epidote	15	

NS97-34 **EBq**	quartz muscovite biotite chlorite	40 30 20 10	-biotite retrograded to chlorite -crenulation -kinking of biotite
NS97-39 **EBq**	quartz plagioclase chlorite biotite	60 20 15 5	-biotite retrograded to chlorite
NS97-40C **EBq**	quartz feldspar muscovite biotite	70 20 5 5	-foliation defined by the alignment of micas
NS97-41B **ERFZ**	sillimanite biotite quartz feldspar	40 30 20 10	-synkinematic sillimanite growth -quartz shows mylonitic fabric
NS97-51 **ERFZ**	quartz feldspar muscovite biotite sillimanite	70 20 5 5 ---	-quartz shows mylonitic fabric
NS97-65 **EBq**	quartz muscovite graphite biotite plagioclase	40 30 15 10 5	-crenulation
NS97-68 **EBm**	calcite quartz phlogopite muscovite graphite	40 20 20 10 10	
NS97-70 **EBq**	plagioclase quartz biotite chlorite muscovite	30 20 20 20 10	-biotite retrograded to chlorite -layer of quartz mylonitized
NS97-71A **QMmc**	calcite diopside grossular quartz	30 30 25 15	
NS97-71B **QMmc**	quartz biotite feldspar diopside tremolite	30 20 20 20 10	-weak foliation

NS97-75 **QMs**	quartz biotite muscovite feldspar garnet	30 25 20 15 10	-moderate foliation -crenulation
NS97-79B **?**	quartz plagioclase k-feldspar	80 10 10	-igneous texture -plagioclase seriticized
NS97-80 **QMs**	quartz muscovite biotite hornblende garnet	70 10 10 10 —	-fine-grained micas
NS97-81 **Dgm**	hornblende quartz plagioclase k-feldspar	50 30 10 10	-foliation defined by the alignment of hornblende -slight chloritization, seritization
NS97-82 **EBq**	quartz muscovite biotite feldspar	35 30 20 15	-foliation defined by the alignment of micas -foliation wrapped around garnet
NS97-83 **Dg**	quartz plagioclase biotite k-feldspar muscovite epidote	30 25 20 15 10 —	
NS97-84A **QMs**	quartz actinolite biotite	50 30 20	-moderate foliation -crenulation
NS97-84B **QMs**	quartz biotite feldspar hornblende chlorite sillimanite	30 20 20 20 10 —	-moderate foliation -crenulation -biotite retrograded to chlorite
NS97-87B **QMmc**	calcite quartz phlogopite feldspar	50 20 20 10	-weak foliation
NS97-91A **QMs**	quartz feldspar muscovite biotite calcite	40 30 20 10 —	-foliation defined by the alignment of micas -quartz shows mylonitic fabric
NS97-95 **QMmc**	calcite diopside olivine tremolite	70 15 10 5	-weak foliation

NS97-97 **QMs**	quartz biotite feldspar chlorite	30 25 25 20	-weak foliation -biotite retrograded to chlorite
NS97-101 **?**	hornblende quartz feldspar chlorite calcite olivine biotite	25 20 20 10 10 10 5	-weak foliation -mylonitized
NS97-107 **QMmc**	feldspar quartz diopside olivine phlogopite tremolite	30 20 20 15 10 5	-weak foliation
NS97-109 **QMs**	quartz biotite muscovite feldspar chlorite graphite garnet	25 25 20 15 10 5 ---	-weak foliation -biotite retrograded to chlorite
NS97-113 **QMs**	muscovite quartz biotite chlorite staurolite garnet	30 20 20 20 10 ---	-moderate foliation -crenulation -biotite retrograded to chlorite
NS97-124 **?**	plagioclase hornblende quartz biotite chlorite olivine?	40 30 10 10 10 ---	-igneous texture
NS97-128 **QMs**	quartz muscovite biotite	70 15 15	-foliation defined by the alignment of micas
NS97-131B **QMs**	muscovite biotite quartz chlorite	40 30 20 10	-biotite retrograded to chlorite -moderate foliation -crenulation
NS97-135 **SC**	hornblende microcline diopside	60 30 10	-conglomerate - hornblende and diopside clasts, microcline matrix

NS97-136 **SCc**	calcite feldspar actinolite epidote olivine?	70 10 5 5 —	
NS97-145 **EBg**	hornblende quartz feldspar	70 15 15	-moderate foliation -crenulation
NS97-151A **EBq**	quartz muscovite feldspar chlorite biotite	40 25 20 15 —	-biotite almost completely retrograded to chlorite -foliation defined by the alignment of micas -plagioclase seriticized
NS97-160B **Dgf**	quartz biotite plagioclase k-feldspar muscovite chlorite	40 20 10 10 10 10	-weak foliation -biotite weakly chloritized
NS97-162 **EBq**	quartz biotite feldspar muscovite sillimanite	30 25 25 20 —	-plagioclase seriticized -sillimanite replacing biotite
NS97-167 **EBq**	feldspar quartz biotite muscovite	60 15 15 10	
NS97-172 **Dgf**	quartz biotite k-feldspar hornblende chlorite plagioclase olivine	20 20 20 15 10 10 5	-some biotite retrograded to chlorite
NS97-198 **SCs**	muscovite quartz feldspar chlorite biotite	40 20 15 15 10	-moderate foliation -crenulation
NS97-200B **SC**	quartz plagioclase k-feldspar muscovite biotite	50 25 25 — —	-igneous texture

NS97-205 **SCs**	quartz k-feldspar muscovite chlorite biotite plagioclase	30 20 15 15 10 10	-moderate foliation -compositional layering
NS97-292 **EBq**	quartz muscovite biotite calcite	40 40 10 —	-foliation defined by the alignment of micas
NS97-313 **EBm**	calcite graphite	80 20	-foliation defined by change in grain size, composition
NS97-340 **EBq**	muscovite biotite quartz	50 30 20	-moderate foliation -crenulation
NS97-372 **EBm**	calcite	100	-weak alignment of elongate calcite grains
NS97-380 **?**	quartz feldspar biotite	40 35 25	
NS97-382 **SCs**	quartz biotite chlorite garnet	80 15 5 —	-biotite retrograded to chlorite
NS97-385 **M**	feldspar quartz biotite chlorite garnet	40 30 20 10 —	
NS97-386 **EBq**	quartz k-feldspar muscovite biotite chlorite	40 30 15 10 5	-weak foliation -biotite retrograded to chlorite -plagioclase seriticized -quartz shows mylonitic fabric -micas are kinked - brittle deformation
NS97-387 **EBq**	quartz muscovite biotite feldspar sillimanite garnet	60 15 15 10 — —	-quartz shows mylonitic fabric -weak foliation
NS97-389 **EBm**	quartz feldspar calcite muscovite chlorite biotite	40 20 15 10 10 5	-moderate foliation
NS97-393 **EBg**	hornblende quartz cc	80 15 5	-foliation defined by the alignment of hornblende

NS97-412 **EBg**	hornblende quartz calcite biotite olivine?	40 30 15 10 5	
NS97-424 **EBg**	hornblende quartz feldspar biotite chlorite calcite	30 20 20 10 10 10	
NS97-428 **EBm**	quartz sericite calcite biotite	40 30 20 10	-foliation -crenulation
NS97-434 **Sm**	calcite muscovite	90 10	-foliation defined by elongate calcite
NS98-12C **Dg**	plagioclase hornblende quartz biotite k-feldspar epidote	25 20 20 15 15 5	
NS98-13A **QMmc**	plagioclase quartz sericite epidote calcite	30 20 20 20 10	-very altered - next to pluton?
NS98-13B **Dgm**	hornblende quartz plagioclase k-feldspar	50 20 20 10	-well foliated
NS98-14A **QMmc**	plagioclase calcite epidote quartz chlorite k-feldspar	30 20 20 10 10 10	-very altered - next to pluton?
NS98-17C **QMmc**	epidote diopside calcite	60 30 10	
NS98-18 **QMs**	quartz biotite feldspar garnet	60 20 20 —	-foliation -crenulation

NS98-21 **QMs**	quartz muscovite biotite feldspar sillimanite	40 20 20 20 ---	-foliation -crenulation

Appendix C-1: Electron Microprobe Data for garnet (weight percent)

#	Na2O	Al2O3	CaO	Cr2O3	MgO	SiO2	TiO2	MnO	FeO	Total	Comment	Loc.	?
1	0.005	20.995	2.123	0.018	1.871	37.209	0.002	0.339	38.401	100.963	NS-97-340c1-1	c	
2	0.000	20.989	2.477	0.000	1.598	37.160	0.046	1.520	36.607	100.397	NS-97-340c1-2	c	
3	0.024	20.849	2.327	0.020	1.924	37.311	0.000	0.215	38.268	100.938	NS-97-340c1-3	m	
4	0.026	21.111	2.168	0.035	1.988	37.312	0.000	0.143	38.185	100.968	NS-97-340c1-4	m	
5	0.003	21.049	1.299	0.000	2.177	37.153	0.048	0.281	38.834	100.844	NS-97-340c1-5	r	
6	0.013	21.017	1.213	0.013	2.167	37.403	0.000	0.276	38.855	100.957	NS-97-340c1-6	r	*
7	0.000	21.005	1.670	0.000	2.091	37.294	0.049	0.341	38.425	100.875	NS-97-340c1-7	r	
8	0.000	21.175	2.146	0.023	1.903	37.168	0.086	0.344	37.996	100.841	NS-97-340c2-1	c	
9	0.000	21.203	2.297	0.026	1.830	37.237	0.100	0.338	37.958	100.989	NS-97-340c2-2	c	
10	0.000	21.084	2.091	0.019	1.887	37.240	0.049	0.232	38.133	100.735	NS-97-340c2-3	m	
11	0.017	21.324	2.029	0.011	1.988	37.258	0.000	0.219	37.944	100.790	NS-97-340c2-4	m	
12	0.000	21.001	2.145	0.001	2.092	37.146	0.039	0.215	38.183	100.822	NS-97-340c2-5	r	
13	0.003	20.823	2.155	0.014	2.110	36.957	0.010	0.217	37.744	100.033	NS-97-340c2-6	r	
14	0.006	20.931	2.304	0.000	2.081	36.971	0.024	0.157	37.659	100.133	NS-97-340c2-7	r	*
15	0.026	21.346	2.323	0.001	1.639	37.251	0.055	0.956	37.397	100.994	NS-97-340c3-1	c	
16	0.013	21.135	2.228	0.007	1.658	36.880	0.000	0.891	37.734	100.546	NS-97-340c3-2	c	
17	0.019	20.783	2.534	0.007	1.649	37.085	0.016	1.270	36.964	100.327	NS-97-340c3-3	m	
18	0.009	20.979	2.426	0.039	1.554	37.250	0.054	1.210	37.423	100.944	NS-97-340c3-4	m	
19	0.010	21.283	1.108	0.000	2.148	37.073	0.000	0.294	38.525	100.441	NS-97-340c3-5	r	
20	0.016	21.020	2.060	0.032	2.096	37.235	0.000	0.255	38.106	100.820	NS-97-340c3-6	r	
21	0.018	21.279	1.066	0.010	2.161	37.243	0.055	0.254	38.614	100.700	NS-97-340c3-7	r	*
22	0.018	21.010	6.568	0.001	1.309	37.254	0.064	3.058	30.660	99.942	NS-97-75-c1-1	c	
23	0.020	21.228	6.710	0.002	1.316	37.554	0.065	2.975	30.634	100.504	NS-97-75-c1-2	c	
24	0.014	21.267	6.364	0.004	1.355	37.401	0.049	2.672	31.319	100.445	NS-97-75-c1-3	m	
25	0.027	21.112	6.299	0.032	1.301	37.225	0.042	2.648	31.194	99.880	NS-97-75-c1-4	m	
26	0.038	21.172	1.706	0.015	2.284	37.123	0.029	1.595	36.196	100.158	NS-97-75-c1-5	r	
27	0.022	21.184	1.844	0.000	2.280	37.154	0.036	1.541	36.064	100.125	NS-97-75-c1-6	r	
28	0.021	21.285	1.705	0.000	2.264	37.048	0.037	1.515	36.335	100.210	NS-97-75-c1-7	r	*
29	0.019	21.198	5.814	0.000	1.537	37.263	0.050	2.323	32.131	100.335	NS-97-75-c1-8	c	
30	0.019	21.242	6.181	0.000	1.445	37.422	0.049	2.477	31.584	100.419	NS-97-75-c1-9	c	
31	0.000	21.266	6.542	0.029	1.292	37.342	0.073	3.151	30.701	100.396	NS-97-75-c1-10	m	
32	0.000	21.235	6.469	0.044	1.275	37.318	0.034	3.161	30.823	100.359	NS-97-75-c1-11	m	
33	0.000	21.035	1.859	0.026	2.179	37.109	0.000	1.641	36.229	100.078	NS-97-75-c1-12	r	
34	0.000	21.293	2.060	0.023	2.219	37.223	0.050	1.627	35.909	100.404	NS-97-75-c1-13	r	
35	0.000	21.278	2.478	0.034	2.159	37.228	0.000	2.014	35.230	100.421	NS-97-75-c1-14	r	
36	0.002	21.351	1.878	0.020	2.958	37.363	0.047	2.186	34.340	100.145	NS-97-162-c2-1	c	
37	0.003	21.058	2.044	0.023	2.946	37.406	0.004	2.280	34.189	99.953	NS-97-162-c2-2	m	
38	0.000	21.586	2.206	0.011	2.849	37.699	0.050	1.563	34.458	100.422	NS-97-162-c2-3	r	
39	0.012	21.058	2.208	0.011	2.924	37.493	0.039	2.487	33.777	100.009	NS-97-162-c3-1	c	
40	0.010	21.152	2.131	0.036	2.875	37.417	0.016	2.418	34.013	100.068	NS-97-162-c3-2	m	
41	0.000	21.210	2.066	0.000	2.906	37.483	0.000	1.607	34.741	100.013	NS-97-162-c3-3	r	
42	0.008	21.243	2.464	0.000	2.729	37.175	0.000	1.593	34.665	99.877	NS-97-162-c3-4	r	
43	0.008	21.429	1.988	0.000	2.985	37.585	0.018	2.001	34.407	100.421	NS-97-162-c4-1	c	
44	0.000	21.124	2.126	0.000	2.946	37.196	0.028	1.872	34.443	99.735	NS-97-162-c4-2	c	
45	0.007	21.563	1.863	0.000	3.013	37.850	0.042	1.910	34.857	101.105	NS-97-162-c4-3	m	
46	0.008	21.094	1.861	0.026	3.004	37.240	0.016	1.746	34.811	99.806	NS-97-162-c4-4	m	

47	0.016	21.418	2.173	0.028	2.992	37.590	0.031	1.647	34.629	100.524	NS-97-162-c4-5	r	
48	0.000	21.470	2.119	0.019	2.918	37.664	0.018	1.597	34.855	100.660	NS-97-162-c4-6	r	
49	0.004	21.395	2.234	0.017	2.955	37.377	0.011	1.665	34.815	100.473	NS-97-162-c4-7	r	*
50	0.006	21.581	1.369	0.000	3.391	37.763	0.011	5.382	31.441	100.944	NS-97-387-c1-1	c	
51	0.031	21.454	1.405	0.000	3.309	37.555	0.008	5.345	31.244	100.351	NS-97-387-c1-2	c	
52	0.009	21.573	1.219	0.000	3.334	37.486	0.000	5.422	31.613	100.656	NS-97-387-c1-3	m	
53	0.000	21.721	1.429	0.000	3.344	37.676	0.003	5.407	31.355	100.935	NS-97-387-c1-4	m	
54	0.025	21.625	1.406	0.017	3.257	38.108	0.000	5.355	31.279	101.072	NS-97-387-c1-5	r	
55	0.054	21.611	1.455	0.008	3.297	38.097	0.000	5.259	31.513	101.294	NS-97-387-c1-6	r	
56	0.040	21.715	1.475	0.027	3.221	37.822	0.017	5.137	31.233	100.687	NS-97-387-c1-7	r	*
57	0.020	21.487	1.419	0.000	3.372	37.944	0.031	5.215	31.325	100.813	NS-97-387-c1-8	c	
58	0.037	21.403	1.312	0.006	3.328	37.718	0.008	5.296	31.394	100.502	NS-97-387-c1-9	m,	
59	0.031	21.716	1.444	0.000	3.307	37.898	0.013	5.198	31.341	100.948	NS-97-387-c1-10	r	
60	0.035	21.451	1.446	0.013	3.181	37.677	0.023	5.375	31.176	100.377	NS-97-387-c1-11	r	
61	0.017	21.594	1.220	0.009	3.338	37.790	0.009	5.180	31.658	100.815	NS-97-387-c2-1	c	
62	0.013	21.404	1.481	0.000	3.258	37.329	0.000	5.066	31.156	99.707	NS-97-387-c2-2	m	
63	0.019	21.475	1.329	0.020	3.104	37.529	0.001	5.296	31.123	99.896	NS-97-387-c2-3	r	
64	0.000	21.519	1.398	0.000	3.063	37.749	0.000	5.329	31.154	100.212	NS-97-387-c2-4	r	
65	0.035	21.620	1.363	0.000	3.207	37.808	0.005	5.115	31.321	100.474	NS-97-387-c2-5	c	
66	0.014	21.633	1.427	0.002	3.113	37.752	0.000	5.244	31.500	100.685	NS-97-387-c2-6	m	
67	0.032	21.527	1.320	0.000	3.059	37.880	0.000	5.252	31.593	100.663	NS-97-387-c2-7	r	
68	0.051	21.607	1.365	0.020	3.010	37.634	0.000	5.480	31.702	100.869	NS-97-387-c2-8	r	
69	0.055	21.497	1.363	0.001	3.115	37.523	0.025	5.345	31.345	100.269	NS-97-387-c2-9	c	
70	0.029	21.663	1.328	0.000	3.207	38.176	0.004	5.212	31.376	100.995	NS-97-387-c2-10	m	
71	0.029	21.780	1.480	0.000	3.080	37.839	0.000	5.258	31.050	100.516	NS-97-387-c2-11	r	
72	0.044	21.309	1.477	0.016	3.017	37.669	0.000	5.435	31.415	100.382	NS-97-387-c2-12	r	
73	0.019	21.148	1.690	0.012	1.638	36.834	0.071	11.768	27.546	100.726	NS-97-91A-c5-1	c	
74	0.000	21.186	1.555	0.000	1.679	37.015	0.030	11.870	27.508	100.843	NS-97-91A-c5-2	m	
75	0.000	21.229	1.038	0.000	1.700	37.447	0.009	11.887	27.919	101.229	NS-97-91A-c5-3	r	
76	0.000	21.229	1.335	0.014	1.553	37.188	0.038	12.023	27.272	100.652	NS-97-91A-c5-4	r	*
77	0.031	21.082	1.561	0.015	1.611	36.953	0.058	11.632	27.327	100.270	NS-97-91A-c5-5	c	
78	0.033	21.262	1.465	0.017	1.574	36.935	0.000	11.866	27.528	100.680	NS-97-91A-c5-6	m	
79	0.038	21.210	1.478	0.019	1.679	37.037	0.000	11.582	27.583	100.626	NS-97-91A-c5-7	r	
80	0.024	21.258	2.228	0.000	1.355	37.158	0.007	12.024	26.581	100.635	NS-97-91A-c5-8	r	
81	0.027	21.206	0.899	0.008	1.590	36.822	0.066	12.018	27.455	100.091	NS-97-91A-c5-9	c	
82	0.010	21.265	0.812	0.000	1.481	36.852	0.012	12.182	27.841	100.455	NS-97-91A-c5-1	m	
83	0.000	21.467	1.329	0.005	1.527	37.151	0.004	12.136	27.366	100.985	NS-97-91A-c5-1	r	
84	0.014	21.241	1.697	0.000	1.525	37.042	0.000	11.961	27.394	100.874	NS-97-91A-c6-1	c	
85	0.015	21.439	1.423	0.011	1.510	37.268	0.040	12.267	27.462	101.435	NS-97-91A-c6-2	m	
86	0.012	21.282	1.131	0.000	1.575	37.296	0.070	12.279	27.510	101.155	NS-97-91A-c6-3	r	
87	0.028	21.204	1.027	0.007	1.498	36.799	0.000	12.385	27.746	100.694	NS-97-91A-c6-4	r	
88	0.027	21.427	1.707	0.000	1.400	37.158	0.000	12.307	26.956	100.982	NS-97-91A-c6-5	1	
89	0.046	21.223	1.137	0.000	1.487	36.561	0.135	12.455	27.495	100.539	NS-97-91A-c6-6	2	
90	0.031	21.255	1.168	0.024	1.521	37.167	0.002	12.312	27.365	100.845	NS-97-91A-c6-7	1	
91	0.041	21.246	1.294	0.000	1.500	37.137	0.007	12.539	27.091	100.855	NS-97-91A-c6-8	2	

92	0.039	21.399	1.244	0.000	1.684	36.967	0.078	11.783	28.087	101.281	NS-97-91A-c7-1	c	
93	0.009	21.388	1.523	0.001	1.707	36.617	0.046	11.441	27.684	100.416	NS-97-91A-c7-2	c	
94	0.000	21.495	1.317	0.000	1.721	36.959	0.023	11.864	27.908	101.287	NS-97-91A-c7-3	m	
95	0.010	21.292	1.039	0.031	1.726	36.703	0.031	11.750	28.043	100.625	NS-97-91A-c7-4	r	
96	0.012	21.132	1.334	0.000	1.686	36.676	0.063	11.453	27.926	100.282	NS-97-91A-c7-5	r	
97	0.000	21.316	1.326	0.000	1.646	37.030	0.017	11.759	28.044	101.138	NS-97-91A-c7-6	r	
98	0.013	21.161	0.471	0.014	1.691	36.656	0.042	11.956	28.510	100.514	NS-97-91A-c7-7	c	
99	0.026	21.218	0.910	0.000	1.731	37.014	0.018	11.940	28.035	100.892	NS-97-91A-c7-8	m	
100	0.028	21.490	1.297	0.011	1.414	37.355	0.000	12.314	27.560	101.469	NS-97-91A-c7-9	r	
101	0.001	21.213	1.435	0.000	1.512	37.330	0.009	12.029	27.500	101.029	NS-97-91A-c7-1	r	
102	0.025	21.340	1.230	0.008	1.646	36.781	0.000	12.062	27.603	100.695	NS-97-91A-c7-1	c	
103	0.012	21.390	1.007	0.000	1.627	37.024	0.008	12.043	27.783	100.894	NS-97-91A-c7-1	m	
104	0.035	21.185	0.845	0.000	1.584	36.881	0.000	12.313	27.761	100.604	NS-97-91A-c7-1	r	
105	0.014	21.206	1.258	0.000	1.619	36.690	0.000	11.949	27.366	100.102	NS-97-91A-c7-1	r	
106	0.028	21.266	3.667	0.014	2.048	37.347	0.036	2.951	32.881	100.238	NS-97-82-c1-1	c	
107	0.019	21.298	3.022	0.010	2.151	37.551	0.018	2.213	34.273	100.555	NS-97-82-c1-2	c	
108	0.002	21.407	5.202	0.008	1.895	37.727	0.020	1.451	32.974	100.686	NS-97-82-c1-3	m	
109	0.003	21.092	3.374	0.000	2.136	37.269	0.038	1.079	35.128	100.119	NS-97-82-c1-4	r	
110	0.007	21.124	3.478	0.000	2.173	37.445	0.008	0.793	34.876	99.904	NS-97-82-c1-5	r	*
111	0.008	21.354	3.657	0.000	1.924	37.572	0.014	1.957	33.923	100.409	NS-97-82-c1-6	r	
112	0.003	21.285	5.562	0.011	1.384	37.373	0.031	1.527	33.192	100.368	NS-97-82-c4-1	c	
113	0.019	21.292	5.543	0.000	1.420	37.321	0.025	1.291	33.754	100.665	NS-97-82-c4-2	c	
114	0.000	21.280	4.305	0.000	2.119	37.540	0.031	0.416	34.858	100.549	NS-97-82-c4-3	m	
115	0.026	21.466	3.335	0.000	2.250	37.402	0.021	0.764	35.803	101.067	NS-97-82-c4-4	r	
116	0.015	21.357	4.727	0.005	2.008	37.475	0.030	1.294	33.628	100.539	NS-97-82-c4-5	r	
117	0.018	21.450	4.198	0.000	2.178	37.690	0.041	1.016	34.281	100.872	NS-97-82-c4-6	r	
118	0.007	21.348	5.545	0.033	1.534	37.467	0.016	1.208	33.536	100.694	NS-97-82-c4-7	c	
119	0.030	21.327	5.476	0.008	1.869	37.544	0.047	0.999	33.384	100.684	NS-97-82-c4-8	c	
120	0.016	21.579	6.247	0.026	1.724	38.024	0.072	0.929	32.822	101.439	NS-97-82-c4-9	m	
121	0.003	21.444	4.956	0.031	1.876	37.509	0.016	1.206	33.601	100.642	NS-97-82-c4-10	r	
122	0.000	21.271	3.103	0.021	2.283	37.496	0.014	1.596	35.105	100.889	NS-97-82-c4-11	r	*
123	0.016	21.449	3.752	0.050	2.297	37.510	0.003	0.570	35.163	100.810	NS-97-82-c4-12	r	
124	0.044	21.346	4.982	0.030	2.093	37.278	0.050	0.560	34.123	100.506	NS-97-82-c5-1	c	
125	0.041	21.345	3.881	0.043	2.393	37.469	0.059	0.515	34.879	100.625	NS-97-82-c5-2	m	
126	0.002	21.392	3.112	0.015	2.453	37.980	0.046	0.406	35.357	100.763	NS-97-82-c5-3	r	
127	0.025	21.374	3.428	0.042	2.386	37.511	0.024	0.673	34.754	100.217	NS-97-82-c5-4	r	
128	0.032	21.582	5.369	0.045	2.809	37.957	0.054	1.179	31.995	101.022	NS-97-8-c4-1	c	
129	0.032	21.638	4.942	0.061	3.052	37.920	0.092	1.052	32.251	101.040	NS-97-8-c4-2	c	
130	0.015	21.857	4.634	0.031	3.203	38.023	0.011	0.965	32.095	100.834	NS-97-8-c4-3	m	
131	0.030	21.746	4.470	0.016	3.223	37.958	0.001	0.962	32.438	100.844	NS-97-8-c4-4	m	
132	0.000	21.918	2.300	0.056	4.261	38.185	0.008	0.548	33.884	101.160	NS-97-8-c4-5	r	
133	0.023	21.807	3.924	0.035	3.700	38.215	0.041	0.857	32.721	101.323	NS-97-8-c4-6	r	
134	0.010	21.657	4.449	0.028	3.296	38.248	0.043	0.986	32.395	101.112	NS-97-8-c4-7	r	
135	0.032	21.800	2.195	0.021	4.428	38.026	0.000	0.645	33.405	100.552	NS-97-8-c5-1	c	
136	0.053	21.847	2.027	0.028	4.510	38.113	0.003	0.652	33.353	100.586	NS-97-8-c5-2	c	
137	0.048	21.970	2.094	0.014	4.536	38.365	0.000	0.672	33.868	101.567	NS-97-8-c5-3	m	
138	0.004	21.677	2.191	0.005	4.551	36.155	0.000	0.688	33.452	100.723	NS-97-8-c5-4	r	

139	0.006	21.804	2.190	0.015	4.454	38.163	0.000	0.775	33.533	100.940	NS-97-8-c5-5	r	
140	0.043	21.978	2.172	0.013	4.369	38.030	0.029	0.799	33.464	100.897	NS-97-8-c5-6	r	
141	0.008	21.756	2.327	0.009	3.965	37.665	0.000	1.190	33.889	100.809	NS-97-8-c5-7	c	
142	0.005	21.651	3.327	0.003	4.185	38.319	0.000	0.931	32.416	100.837	NS-97-8-c5-8	m	
143	0.050	21.867	2.392	0.002	3.850	37.805	0.006	1.189	33.723	100.884	NS-97-8-c5-9	r	
144	0.012	21.774	2.276	0.027	3.996	37.827	0.000	1.210	33.609	100.731	NS-97-8-c5-10	r	
145	0.017	21.841	2.391	0.051	4.531	38.043	0.037	0.824	32.918	100.653	NS-97-8-c5-11	c	
146	0.062	21.802	2.442	0.031	4.521	37.958	0.000	0.863	32.740	100.419	NS-97-8-c5-12	m	
147	0.009	21.825	2.454	0.041	4.193	38.249	0.000	0.984	33.240	100.995	NS-97-8-c5-13	r	
148	0.061	21.735	2.532	0.027	4.435	37.904	0.000	0.964	33.280	100.938	NS-97-8-c5-14	r	
149	0.026	21.486	5.010	0.006	3.111	37.935	0.036	0.971	32.340	100.921	NS-97-8-c5-15	c	
150	0.032	21.645	5.297	0.045	2.981	38.103	0.127	1.148	32.114	101.492	NS-97-8-c5-16	c	
151	0.046	21.707	4.817	0.054	3.329	38.171	0.111	1.003	32.152	101.390	NS-97-8-c5-17	m	
152	0.010	21.594	4.626	0.000	3.066	37.931	0.051	1.072	32.309	100.659	NS-97-8-c5-18	m	
153	0.050	21.550	2.736	0.023	3.931	37.874	0.016	1.002	33.355	100.537	NS-97-8-c5-19	r	
154	0.045	21.700	2.116	0.014	4.278	37.952	0.024	0.811	33.815	100.755	NS-97-8-c5-20	r	
155	0.030	21.610	2.184	0.059	4.211	37.800	0.095	0.950	33.795	100.734	NS-97-8-c5-21	r	*
156	0.036	21.696	2.491	0.037	4.304	38.037	0.042	0.774	33.509	100.926	NS-97-8-c5-22	r	
157	0.005	20.987	4.263	0.037	1.126	36.837	0.135	8.004	28.362	99.756	NS97-74-c1-1	c	
158	0.021	21.004	4.227	0.019	1.168	37.048	0.120	7.903	28.682	100.192	NS97-74-c1-2	c	
159	0.007	21.075	7.639	0.032	0.949	37.499	0.117	4.829	28.081	100.228	NS97-74-c1-3	m	
160	0.047	20.981	7.874	0.017	0.970	37.379	0.115	4.935	27.699	100.017	NS97-74-c1-4	m	
161	0.018	21.231	1.968	0.007	2.063	37.113	0.000	3.880	33.828	100.108	NS97-74-c1-5	r	
162	0.039	21.147	2.523	0.008	1.997	37.020	0.000	4.067	33.427	100.228	NS97-74-c1-6	r	
163	0.022	21.056	7.518	0.018	0.924	37.369	0.065	5.051	28.194	100.217	NS97-74-c2-1	c	
164	0.027	21.304	7.339	0.008	0.978	37.339	0.089	5.151	28.104	100.339	NS97-74-c2-2	c	
165	0.047	21.119	7.483	0.005	0.938	37.467	0.057	5.305	27.888	100.309	NS97-74-c2-3	m	
166	0.016	21.033	7.853	0.014	1.004	37.041	0.129	4.619	28.105	99.814	NS97-74-c2-4	m	
167	0.004	21.138	4.647	0.059	1.803	37.181	0.021	3.781	31.679	100.313	NS97-74-c2-5	r	
168	0.000	21.373	1.906	0.022	2.143	37.161	0.000	4.185	33.917	100.707	NS97-74-c2-6	r	
169	0.031	21.086	3.962	0.021	1.153	36.894	0.086	7.297	29.578	100.108	NS97-74-c1-1	c	
170	0.008	21.151	4.386	0.006	1.157	37.035	0.072	7.124	29.380	100.319	NS97-74-c1-2	c	
171	0.014	21.304	7.494	0.036	1.102	37.340	0.072	4.616	28.628	100.606	NS97-74-c1-3	m	
172	0.010	21.237	7.258	0.044	1.192	37.266	0.016	4.027	29.009	100.059	NS97-74-c1-4	m	
173	0.000	21.420	2.777	0.000	1.940	37.235	0.050	3.926	33.044	100.392	NS97-74-c1-5	r	
174	0.005	21.350	2.107	0.000	1.921	37.190	0.024	3.908	33.972	100.477	NS97-74-c1-6	r	*
175	0.020	20.927	5.246	0.020	1.042	36.943	0.172	9.096	26.614	100.080	NS97-74-c4-1	c	
176	0.041	21.095	4.237	0.016	1.076	37.111	0.223	8.595	27.821	100.215	NS97-74-c4-2	c	
177	0.044	20.963	4.231	0.001	1.274	37.205	0.142	8.102	28.292	100.254	NS97-74-c4-3	m	
178	0.046	21.005	4.900	0.014	1.233	37.297	0.116	7.125	28.600	100.336	NS97-74-c4-4	m	
179	0.045	21.363	5.050	0.000	1.699	37.148	0.051	3.985	30.964	100.305	NS97-74-c4-5	r	
180	0.013	21.040	1.939	0.010	2.013	36.677	0.039	3.863	33.887	99.481	NS97-74-c4-6	r	
181	0.008	21.242	4.846	0.002	1.278	37.057	0.124	6.626	29.232	100.415	NS-97-326-c1-1	c	
182	0.000	20.983	4.850	0.034	1.233	36.909	0.152	6.506	29.086	99.753	NS-97-326-c1-2	c	
183	0.000	21.163	4.506	0.002	1.247	37.034	0.092	6.277	29.724	100.045	NS-97-326-c1-3	m	
184	0.024	20.852	4.674	0.033	1.247	36.935	0.098	6.382	29.633	99.878	NS-97-326-c1-4	m	
185	0.008	21.215	3.220	0.015	1.807	37.220	0.045	2.914	34.285	100.729	NS-97-326-c1-5	r	
186	0.000	21.129	1.875	0.000	1.843	36.952	0.029	2.875	35.629	100.332	NS-97-326-c1-6	r	

187	0.027	21.080	3.597	0.009	1.514	36.756	0.089	4.532	32.269	99.873	NS-97-326-c1-7	c	
188	0.000	21.071	3.725	0.000	1.596	37.030	0.061	3.749	32.628	99.860	NS-97-326-c1-8	m	
189	0.041	21.217	3.209	0.056	1.801	37.267	0.082	2.937	34.099	100.709	NS-97-326-c1-9	r	
190	0.005	21.275	3.214	0.045	1.754	36.956	0.071	2.913	34.279	100.512	NS-97-326-c1-1	r	
191	0.000	20.969	5.068	0.005	1.003	36.869	0.148	8.708	27.096	99.866	NS-97-326-c2-1	c	
192	0.000	21.116	5.097	0.021	1.028	36.991	0.143	8.414	27.249	100.059	NS-97-326-c2-2	c	
193	0.000	21.023	4.956	0.004	1.107	36.963	0.089	7.243	28.442	99.827	NS-97-326-c2-3	m	
194	0.005	21.147	4.595	0.000	1.236	37.259	0.116	6.254	29.760	100.372	NS-97-326-c2-4	m	
195	0.000	20.876	2.122	0.016	1.822	36.946	0.006	2.840	34.815	99.443	NS-97-326-c2-5	r	
196	0.020	21.194	2.227	0.006	1.850	37.143	0.000	2.796	35.170	100.406	NS-97-326-c2-6	r	*
197	0.024	20.898	4.020	0.037	1.370	36.981	0.142	5.352	31.127	99.951	NS-97-326-c3-1	c	
198	0.015	21.004	4.131	0.000	1.361	37.053	0.077	5.407	31.046	100.094	NS-97-326-c3-2	c	
199	0.001	21.139	3.704	0.020	1.450	36.956	0.064	4.843	32.024	100.201	NS-97-326-c3-3	m	
200	0.030	20.982	4.202	0.020	1.417	36.776	0.099	5.329	31.271	100.126	NS-97-326-c3-4	m	
201	0.040	20.970	2.033	0.020	1.848	36.672	0.000	2.760	35.021	99.364	NS-97-326-c3-5	r	
202	0.021	21.253	3.839	0.008	1.743	37.099	0.000	2.651	33.982	100.596	NS-97-326-c3-6	r	
203	0.005	20.965	4.259	0.030	1.370	36.900	0.213	5.380	30.880	100.002	NS-97-326-c4-1	c	
204	0.009	20.988	3.980	0.001	1.394	37.132	0.100	5.584	31.348	100.536	NS-97-326-c4-2	c	
205	0.004	21.228	3.731	0.000	1.566	36.980	0.088	3.788	33.080	100.465	NS-97-326-c4-3	m	
206	0.021	21.056	3.711	0.000	1.453	36.961	0.139	5.257	31.760	100.358	NS-97-326-c4-4	m	
207	0.000	21.206	3.352	0.032	1.857	36.897	0.049	2.731	34.169	100.293	NS-97-326-c4-5	r	
208	0.015	21.393	3.478	0.021	1.638	37.287	0.055	2.898	34.168	100.953	NS-97-326-c4-6	r	
209	0.029	21.164	4.070	0.000	1.625	37.244	0.058	4.643	31.678	100.511	NS97-119-c1-1	c	
210	0.005	20.958	3.927	0.043	1.646	37.020	0.070	4.647	31.960	100.276	NS97-119-c1-2	c	
211	0.022	21.122	6.918	0.000	1.238	37.058	0.117	4.859	28.268	99.602	NS97-119-c1-3	m	
212	0.000	20.828	3.686	0.000	1.617	37.144	0.000	4.911	31.568	99.754	NS97-119-c1-4	m	
213	0.000	21.105	3.890	0.030	1.391	37.157	0.023	5.158	31.240	99.994	NS97-119-c1-5	r	
214	0.049	21.128	3.096	0.000	1.649	36.920	0.000	5.030	32.082	99.954	NS97-119-c1-6	r	
215	0.000	21.184	5.001	0.027	1.387	37.103	0.025	5.438	29.464	99.629	NS97-119-c2-1	c	
216	0.001	21.138	4.961	0.028	1.414	37.041	0.050	5.236	29.812	99.681	NS97-119-c2-2	c	
217	0.000	20.952	5.417	0.010	1.442	36.989	0.093	5.077	29.302	99.282	NS97-119-c2-3	m	
218	0.000	21.113	4.408	0.000	1.603	36.893	0.027	5.001	30.786	99.831	NS97-119-c2-4	m	
219	0.001	21.213	3.518	0.021	1.624	36.867	0.047	4.996	31.595	99.882	NS97-119-c2-5	r	
220	0.000	21.139	4.551	0.032	1.600	37.229	0.065	4.520	31.079	100.215	NS97-119-c2-6	r	*
221	0.036	20.983	4.168	0.019	1.418	36.901	0.056	6.246	29.939	99.766	NS97-119-c3-1	c	
222	0.000	20.970	4.091	0.033	1.539	37.038	0.059	5.727	30.415	99.872	NS97-119-c3-2	c	
223	0.000	20.976	3.631	0.046	1.507	36.947	0.042	6.065	30.502	99.716	NS97-119-c3-3	m	
224	0.014	21.042	3.955	0.000	1.558	36.859	0.034	5.716	30.372	99.550	NS97-119-c3-4	m	
225	0.036	21.112	3.916	0.019	1.535	37.177	0.016	4.808	31.056	99.675	NS97-119-c3-5	r	
226	0.000	20.742	3.389	0.002	1.588	36.234	0.922	5.567	31.330	99.774	NS97-119-c3-6	r	
Legend:													
Loc. (Location): c=center, m=middle (between center and rim), r=rim of grain, blank means unknown													
? (Used?): *=data used in calculations													

Appendix C-2: Electron Microprobe Data for biotite (weight percent)

#	F	Na2O	K2O	FeO	Al2O3	Cl	Cr2O3	SiO2	CaO	MnO	MgO	TiO2	Total	Comment	Loc.	?
1	0.214	0.362	8.693	21.473	19.003	0.126	0.002	35.098	0.137	0.099	8.312	1.711	95.112	NS-97-82-c1-1	c	
2	0.220	0.346	8.901	22.058	19.130	0.129	0.000	35.317	0.131	0.078	8.460	1.739	96.387	NS-97-82-c1-2	m	
3	0.249	0.255	9.167	22.058	18.827	0.091	0.012	35.967	0.146	0.064	8.802	1.664	97.176	NS-97-82-c1-3	r	*
															c	
4	0.208	0.357	8.701	21.741	19.140	0.081	0.011	35.019	0.198	0.020	8.378	1.643	95.391	NS-97-82-c1-4	m	
5	0.149	0.347	8.831	22.015	19.250	0.079	0.000	35.294	0.101	0.066	8.440	1.714	96.205	NS-97-82-c1-5	r	
6	0.185	0.337	9.330	21.821	19.379	0.102	0.000	35.405	0.084	0.080	8.756	1.711	97.089	NS-97-82-c1-6		
7	0.189	0.187	7.981	21.469	19.333	0.094	0.012	35.393	0.350	0.052	8.471	1.767	95.197	NS-97-82-c2-1	c	
8	0.218	0.134	7.198	24.255	18.711	0.060	0.013	33.448	0.357	0.063	8.123	1.368	93.842	NS-97-82-c2-2	m	
9	0.285	0.093	7.350	22.778	20.403	0.086	0.006	35.010	0.396	0.052	7.443	1.003	94.766	NS-97-82-c2-3	r	
10	0.206	0.249	9.437	21.328	19.380	0.075	0.011	35.709	0.066	0.052	8.619	1.852	96.880	NS-97-82-c2-4	c	
11	0.232	0.266	8.419	21.753	18.974	0.066	0.025	35.190	0.218	0.041	8.558	1.827	95.456	NS-97-82-c2-5	m	
12	0.155	0.310	9.268	20.119	20.582	0.055	0.008	35.876	0.122	0.045	8.654	2.155	97.272	NS-97-82-c2-6	r	
13	0.163	0.260	8.050	21.620	19.287	0.060	0.045	35.936	0.309	0.038	8.480	1.831	95.996	NS-97-82-c3-1	c	
14	0.150	0.252	8.223	22.280	19.025	0.071	0.012	35.591	0.302	0.069	8.439	1.721	96.056	NS-97-82-c3-2	m	
15	0.209	0.173	8.089	22.165	18.761	0.043	0.000	35.558	0.247	0.069	8.268	1.623	95.107	NS-97-82-c3-3	r	
16	0.235	0.342	9.145	21.736	19.498	0.069	0.052	36.202	0.113	0.033	8.788	1.864	97.962	NS-97-82-c3-4	c	
17	0.201	0.303	9.475	22.212	19.463	0.091	0.030	35.818	0.079	0.057	8.904	1.792	98.319	NS-97-82-c3-5	m	
18	0.187	0.207	9.510	21.977	19.496	0.087	0.026	35.874	0.100	0.057	8.827	1.732	97.981	NS-97-82-c3-6	r	
19	0.183	0.223	8.107	21.791	19.345	0.046	0.033	35.893	0.272	0.082	8.487	1.761	96.136	NS-97-82-c4-1	c	
20	0.177	0.165	8.727	21.194	19.492	0.056	0.019	35.531	0.183	0.094	8.348	1.432	95.330	NS-97-82-c4-2	m	
21	0.203	0.122	8.925	20.970	20.750	0.070	0.000	35.860	0.201	0.092	8.582	0.764	96.438	NS-97-82-c4-3	r	*
22	0.225	0.192	9.690	24.126	19.157	0.062	0.041	35.949	0.053	0.110	8.094	1.440	99.030	NS-97-82-c4-4	c	
23	0.248	0.119	9.990	23.982	18.940	0.058	0.033	35.560	0.016	0.121	8.048	1.531	98.529	NS-97-82-c4-5	m	
24	0.201	0.191	9.692	23.876	18.907	0.067	0.055	35.388	0.083	0.093	7.976	1.282	97.711	NS-97-82-c4-6	r	
25	0.442	0.338	9.252	16.760	17.895	0.022	0.045	37.434	0.003	0.000	13.734	1.357	97.091	NS-97-8-c1-1	c	
26	0.260	0.354	9.066	16.589	17.809	0.014	0.042	37.438	0.003	0.014	13.766	1.335	96.578	NS-97-8-c1-2	c	
27	0.476	0.407	9.043	16.842	17.652	0.023	0.055	37.594	0.000	0.019	13.985	1.388	97.279	NS-97-8-c1-3	m	
28	0.741	0.325	9.287	17.284	17.257	0.029	0.036	37.271	0.011	0.018	13.567	1.401	96.908	NS-97-8-c1-4	r	*
29	0.596	0.413	9.120	17.378	17.765	0.020	0.006	37.581	0.000	0.000	13.713	1.415	97.751	NS-97-8-c1-5	r	
30	0.597	0.365	9.299	16.740	18.090	0.006	0.011	37.420	0.008	0.003	13.275	1.371	96.933	NS-97-8-c2-1	c	
31	0.576	0.313	7.227	19.306	17.747	0.016	0.032	35.618	0.019	0.000	13.903	1.121	95.631	NS-97-8-c2-2	c	
32	0.485	0.310	9.301	17.605	17.718	0.022	0.000	37.357	0.001	0.005	13.476	1.335	97.406	NS-97-8-c2-3	m	
33	0.732	0.173	9.351	18.148	17.357	0.013	0.029	36.518	0.000	0.016	13.707	1.455	97.188	NS-97-8-c2-4	r	
34	0.699	0.270	9.319	18.296	17.456	0.011	0.019	36.994	0.005	0.036	13.643	1.344	97.796	NS-97-8-c2-5	r	
35	0.616	0.385	8.919	16.642	17.535	0.031	0.035	37.515	0.051	0.033	14.007	1.360	96.863	NS-97-8-c3-1	c	
36	0.676	0.430	8.837	16.653	17.443	0.046	0.051	37.763	0.084	0.038	14.161	1.386	97.273	NS-97-8-c3-2	c	
37	0.694	0.343	9.018	16.536	17.326	0.022	0.045	37.395	0.044	0.041	14.105	1.340	96.612	NS-97-8-c3-3	m	
38	0.749	0.408	8.691	17.346	17.093	0.014	0.048	36.764	0.044	0.033	13.765	1.654	96.291	NS-97-8-c3-4	r	
39	0.765	0.241	8.415	18.823	17.229	0.028	0.040	36.216	0.044	0.033	13.308	1.350	96.164	NS-97-8-c3-5	r	
40	0.355	0.098	10.138	22.762	18.763	0.017	0.039	35.950	0.028	0.360	7.137	3.285	98.779	NS-97-91A-c1-1	c	
41	0.257	0.104	10.226	22.753	18.894	0.000	0.012	35.564	0.072	0.402	7.088	3.050	98.314	NS-97-91A-c1-2	m	
42	0.290	0.076	9.105	23.882	19.229	0.026	0.015	34.740	0.091	0.358	7.663	2.306	97.653	NS-97-91A-c1-3	r	*
43	0.251	0.097	10.242	22.594	18.541	0.031	0.025	35.489	0.000	0.361	7.428	3.370	98.316	NS-97-91A-c2-1	c	
44	0.270	0.068	10.200	22.293	18.499	0.026	0.028	35.707	0.018	0.401	7.535	3.512	98.437	NS-97-91A-c2-2	m	
45	0.267	0.100	10.115	22.164	18.213	0.033	0.022	35.549	0.000	0.414	7.476	3.573	97.807	NS-97-91A-c2-3	r	
46	0.256	0.105	10.176	21.700	19.046	0.044	0.037	35.701	0.002	0.377	7.826	2.830	97.982	NS-97-91A-c3-1	c	
47	0.293	0.079	10.283	21.970	18.778	0.044	0.038	35.674	0.014	0.414	7.827	2.805	98.086	NS-97-91A-c3-2	m	
48	0.303	0.075	10.285	22.027	18.889	0.026	0.041	35.798	0.007	0.427	7.717	3.130	98.591	NS-97-91A-c3-3	r	
49	0.230	0.077	9.895	21.801	18.791	0.020	0.054	35.340	0.101	0.387	6.920	3.595	97.109	NS-97-91A-c4-1	c	
50	0.277	0.059	9.837	22.640	18.320	0.017	0.050	35.516	0.113	0.400	7.111	3.549	97.768	NS-97-91A-c4-2	m	
51	0.225	0.065	9.002	21.647	18.393	0.013	0.036	35.521	0.280	0.353	7.189	3.170	95.796	NS-97-91A-c4-3	r	
53	0.227	0.322	9.565	25.033	18.656	0.029	0.003	34.856	0.025	0.011	5.956	2.529	97.109	NS-97-340-c1-1	c	

54	0.249	0.339	9.592	24.633	18.702	0.012	0.013	34.814	0.014	0.024	6.070	2.494	96.848	NS-97-340-c1-2	c	
55	0.294	0.300	9.544	25.150	18.887	0.016	0.000	34.897	0.000	0.017	5.897	2.576	97.450	NS-97-340-c1-3	m	
56	0.316	0.262	9.713	25.643	18.567	0.021	0.032	34.619	0.000	0.024	5.519	2.855	97.433	NS-97-340-c1-4	r	
57	0.271	0.212	9.709	25.455	18.994	0.007	0.007	34.732	0.000	0.036	5.893	2.403	97.603	NS-97-340-c1-5	r	
58	0.307	0.259	9.396	24.787	19.446	0.012	0.025	34.584	0.073	0.034	6.275	1.737	96.803	NS-97-340-c1-6	c	
59	0.356	0.296	9.371	24.931	19.558	0.000	0.033	34.505	0.071	0.046	6.121	1.637	96.775	NS-97-340-c1-7	c	
60	0.357	0.237	8.463	25.690	19.280	0.000	0.000	33.875	0.086	0.018	6.154	1.594	95.604	NS-97-340-c1-8	m	
61	0.349	0.144	9.290	25.156	19.406	0.009	0.025	34.360	0.057	0.008	6.165	1.694	96.514	NS-97-340-c1-9	r	*
62	0.421	0.167	9.079	25.310	19.476	0.000	0.035	34.522	0.067	0.000	6.278	1.463	96.641	NS-97-340-c1-10	r	
63	0.240	0.257	9.517	25.718	18.584	0.017	0.032	34.674	0.000	0.034	5.687	2.529	97.184	NS-97-340-c2-1	c	
64	0.293	0.234	9.828	25.927	18.631	0.010	0.026	34.672	0.003	0.025	5.621	2.448	97.593	NS-97-340-c2-2	c	
65	0.279	0.201	9.671	26.558	18.099	0.000	0.011	34.416	0.004	0.037	5.335	2.834	97.328	NS-97-340-c2-3	m	
66	0.268	0.273	9.535	25.480	19.333	0.017	0.001	34.894	0.002	0.047	5.675	2.450	97.858	NS-97-340-c2-4	r	
67	0.354	0.249	9.756	25.580	18.876	0.006	0.000	34.829	0.000	0.060	5.677	2.334	97.571	NS-97-340-c2-5	r	
68	0.304	0.285	9.837	24.261	19.581	0.015	0.042	34.615	0.007	0.006	6.155	2.302	97.279	NS-97-340-c2-6	c	
69	0.260	0.316	9.530	24.619	19.610	0.016	0.060	34.683	0.002	0.034	6.049	2.416	97.482	NS-97-340-c2-7	c	
70	0.253	0.325	9.549	23.876	19.550	0.015	0.029	35.144	0.000	0.006	6.660	2.241	97.538	NS-97-340-c2-8	m	
71	0.321	0.319	9.580	23.497	19.709	0.000	0.044	34.764	0.000	0.014	6.750	2.131	96.994	NS-97-340-c2-9	r	
72	0.313	0.241	9.623	24.777	19.371	0.017	0.002	34.374	0.013	0.000	6.541	2.212	97.348	NS-97-340-c2-10	r	
73	0.234	0.330	9.502	24.191	19.481	0.004	0.017	34.964	0.000	0.000	6.141	2.340	97.104	NS-97-340-c3-1	c	
74	0.264	0.308	9.574	24.373	19.473	0.000	0.005	35.051	0.000	0.001	6.213	2.247	97.398	NS-97-340-c3-2	c	
75	0.266	0.310	9.657	24.695	18.900	0.000	0.038	34.613	0.000	0.012	6.061	2.386	96.826	NS-97-340-c3-3	m	
76	0.346	0.061	9.400	25.584	19.169	0.004	0.058	34.295	0.005	0.034	6.254	1.849	96.912	NS-97-340-c3-4	r	
77	0.311	0.278	9.491	24.816	18.906	0.010	0.024	34.733	0.030	0.022	6.037	2.338	96.863	NS-97-340-c3-5	r	
78	0.304	0.182	9.636	25.264	19.132	0.014	0.036	34.630	0.016	0.010	5.990	2.216	97.299	NS-97-340-c3-6	c	
79	0.242	0.276	9.535	24.521	19.571	0.016	0.064	34.968	0.014	0.041	5.776	2.202	97.120	NS-97-340-c3-7	c	
80	0.265	0.347	9.351	24.871	19.275	0.003	0.014	34.895	0.023	0.020	5.804	2.371	97.126	NS-97-340-c3-8	m	
81	0.277	0.357	9.468	24.993	19.361	0.000	0.037	35.043	0.000	0.007	5.957	1.928	97.311	NS-97-340-c3-9	r	
82	0.255	0.362	9.361	24.552	19.346	0.011	0.006	34.623	0.014	0.010	5.915	2.204	96.550	NS-97-340-c3-10	r	
83	0.258	0.297	8.828	22.006	19.260	0.028	0.027	35.781	0.076	0.034	9.818	1.237	97.535	NS-97-75-c1-1	c	
84	0.257	0.229	9.392	21.392	19.654	0.038	0.050	35.863	0.062	0.050	9.068	1.819	97.757	NS-97-75-c1-2	c	
85	0.279	0.234	9.085	22.226	19.525	0.053	0.065	35.355	0.023	0.040	9.508	1.327	97.591	NS-97-75-c1-3	m	
86	0.263	0.266	9.572	21.008	20.095	0.059	0.026	36.074	0.031	0.048	9.201	1.675	98.194	NS-97-75-c1-4	r	
87	0.210	0.265	9.420	21.994	19.647	0.039	0.048	35.751	0.067	0.019	9.183	1.332	97.878	NS-97-75-c1-5	r	*
88	0.209	0.321	9.301	22.098	19.584	0.012	0.057	36.034	0.010	0.028	9.114	1.516	98.193	NS-97-75-c1-6	c	
89	0.222	0.323	9.399	21.889	19.522	0.050	0.031	36.201	0.000	0.062	9.100	1.637	98.332	NS-97-75-c1-7	c	
90	0.198	0.281	8.754	22.473	19.383	0.051	0.034	35.288	0.009	0.031	9.251	1.465	97.123	NS-97-75-c1-8	m	
91	0.194	0.281	9.227	21.931	19.950	0.030	0.067	36.112	0.045	0.075	8.169	2.165	98.157	NS-97-75-c1-9	r	
92	0.199	0.221	9.158	22.456	19.059	0.040	0.068	35.630	0.137	0.077	8.117	1.964	97.033	NS-97-75-c1-10	r	
93	0.210	0.318	9.245	22.157	19.150	0.033	0.033	35.764	0.036	0.078	9.054	1.574	97.557	NS-97-75-c1-11	c	
94	0.245	0.289	9.441	22.298	19.498	0.047	0.047	36.056	0.019	0.096	9.215	1.554	98.691	NS-97-75-c1-12	c	
95	0.221	0.335	9.409	22.258	19.132	0.040	0.038	35.809	0.009	0.087	8.963	1.558	97.757	NS-97-75-c1-13	m	
96	0.255	0.315	8.934	21.661	19.373	0.033	0.000	35.949	0.070	0.062	9.121	0.938	96.597	NS-97-75-c1-14	r	
97	0.195	0.388	9.130	21.076	20.247	0.014	0.021	36.309	0.028	0.056	8.681	1.902	97.962	NS-97-75-c1-15	r	
98	0.247	0.190	9.195	22.089	19.258	0.027	0.040	36.069	0.014	0.082	9.515	1.447	98.063	NS-97-75-c1-16	c	
99	0.276	0.257	9.444	21.461	19.384	0.026	0.053	36.036	0.025	0.115	9.626	1.557	98.138	NS-97-75-c1-17	c	
100	0.298	0.233	9.246	23.009	18.689	0.018	0.043	35.968	0.018	0.117	9.632	1.465	98.607	NS-97-75-c1-18	m	
101	0.213	0.266	8.605	23.701	19.086	0.008	0.009	34.750	0.015	0.125	9.470	1.434	97.590	NS-97-75-c1-19	r	
102	0.269	0.256	8.760	21.404	20.276	0.015	0.039	35.906	0.195	0.053	8.963	1.999	98.019	NS-97-162-c1-1	c	
103	0.180	0.272	8.983	21.352	20.047	0.000	0.004	35.749	0.114	0.030	8.886	1.839	97.380	NS-97-162-c1-2	c	
104	0.246	0.253	8.658	21.106	20.137	0.019	0.022	36.081	0.183	0.045	8.764	1.889	97.295	NS-97-162-c1-3	m	
105	0.254	0.240	8.310	21.355	20.192	0.028	0.032	35.712	0.174	0.024	8.954	1.816	96.978	NS-97-162-c1-4	r	
106	0.252	0.220	8.363	21.289	20.442	0.015	0.052	36.418	0.159	0.048	8.956	1.807	97.912	NS-97-162-c1-5	r	
107	0.232	0.252	8.202	21.242	19.975	0.031	0.015	35.587	0.257	0.020	8.663	2.076	96.447	NS-97-162-c1-6	c	
108	0.229	0.297	8.703	20.209	20.575	0.016	0.010	36.033	0.155	0.068	8.670	2.027	96.892	NS-97-162-c1-7	c	
109	0.165	0.281	8.034	21.434	19.902	0.039	0.020	35.899	0.415	0.045	8.614	2.028	96.798	NS-97-162-c1-8	m	
110	0.227	0.282	8.834	20.615	20.357	0.020	0.029	35.972	0.174	0.029	8.728	2.363	97.529	NS-97-162-c1-9	r	
111	0.245	0.236	8.650	20.837	20.083	0.034	0.016	35.801	0.219	0.031	8.890	2.160	97.091	NS-97-162-c1-10	r	

112	0.156	0.237	8.817	22.228	19.598	0.016	0.009	35.401	0.106	0.068	7.876	2.418	96.860	NS-97-162-c2-1	c	
113	0.249	0.257	8.748	22.226	19.820	0.033	0.011	35.724	0.148	0.110	7.775	2.591	97.580	NS-97-162-c2-2	c	
114	0.203	0.283	9.147	21.920	19.711	0.026	0.028	35.550	0.085	0.082	7.895	2.639	97.478	NS-97-162-c2-3	m	
115	0.177	0.254	8.770	21.722	19.990	0.000	0.000	35.827	0.178	0.044	7.854	2.521	97.262	NS-97-162-c2-4	r	
116	0.200	0.227	9.413	22.149	19.539	0.025	0.063	35.607	0.036	0.069	7.206	3.807	98.251	NS-97-162-c2-5	r	
117	0.269	0.268	9.402	21.805	20.849	0.000	0.032	35.942	0.043	0.084	8.241	1.487	98.309	NS-97-162-c2-6	c	
118	0.270	0.242	8.931	21.874	20.517	0.024	0.022	35.491	0.135	0.113	7.985	1.091	96.576	NS-97-162-c2-7	c	
119	0.238	0.246	9.224	21.597	21.136	0.031	0.024	35.803	0.039	0.081	8.192	1.176	97.680	NS-97-162-c2-8	m	
120	0.335	0.169	8.611	21.789	20.688	0.023	0.000	35.602	0.175	0.080	8.137	1.227	96.690	NS-97-162-c2-9	r	
121	0.276	0.265	9.531	21.652	21.251	0.036	0.046	35.706	0.045	0.082	8.190	1.324	98.280	NS-97-162-c2-10	r	
122	0.202	0.287	8.233	22.219	19.800	0.050	0.031	35.570	0.309	0.054	7.516	2.486	96.661	NS-97-162-c3-1	c	
123	0.194	0.286	8.786	22.793	19.840	0.000	0.070	35.593	0.157	0.087	7.633	2.557	97.914	NS-97-162-c3-2	c	
124	0.263	0.234	8.462	23.502	19.681	0.016	0.052	34.939	0.185	0.087	7.539	2.410	97.255	NS-97-162-c3-3	m	
125	0.241	0.260	8.709	22.336	20.076	0.054	0.030	34.330	0.191	0.084	7.167	2.034	95.399	NS-97-162-c3-4	r	
126	0.255	0.236	8.466	22.478	20.069	0.025	0.017	35.605	0.291	0.092	7.750	1.959	97.130	NS-97-162-c3-5	r	
127	0.219	0.319	9.041	21.235	19.970	0.009	0.021	36.031	0.139	0.052	8.999	2.100	98.041	NS-97-162-c3-6	c	
128	0.160	0.299	8.833	20.888	19.626	0.011	0.010	36.214	0.236	0.048	9.011	1.952	97.219	NS-97-162-c3-7	c	
129	0.268	0.276	8.850	20.784	19.923	0.030	0.015	35.725	0.159	0.039	8.780	1.800	96.529	NS-97-162-c3-8	m	
130	0.221	0.276	8.771	20.556	20.258	0.038	0.011	36.025	0.141	0.050	8.419	2.242	96.906	NS-97-162-c3-9	r	
131	0.231	0.278	8.731	20.789	20.262	0.023	0.000	35.673	0.211	0.036	8.559	1.773	96.464	NS-97-162-c3-10	r	
132	0.190	0.384	8.744	20.126	20.286	0.085	0.026	35.987	0.069	0.056	7.973	1.736	95.563	NS-97-162-c4-1	c	
133	0.208	0.297	8.905	20.784	20.363	0.043	0.003	36.674	0.097	0.062	7.941	1.576	96.855	NS-97-162-c4-2	c	
134	0.220	0.270	8.795	22.591	19.882	0.033	0.020	34.709	0.027	0.080	7.895	1.386	95.808	NS-97-162-c4-3	m	
135	0.302	0.181	9.229	22.475	20.058	0.040	0.000	34.622	0.039	0.089	7.589	1.610	96.098	NS-97-162-c4-4	r	
136	0.181	0.385	9.235	20.825	20.812	0.056	0.000	35.718	0.028	0.069	7.838	1.644	96.702	NS-97-162-c4-5	r	
137	0.277	0.267	9.448	20.700	20.052	0.030	0.044	35.722	0.023	0.040	8.424	2.356	97.259	NS-97-162-c4-6	c	
138	0.261	0.260	9.527	20.946	19.993	0.027	0.022	35.837	0.041	0.056	8.546	2.369	97.769	NS-97-162-c4-7	c	
139	0.240	0.287	9.471	21.174	20.058	0.027	0.067	35.752	0.052	0.065	8.581	2.396	98.063	NS-97-162-c4-8	m	
140	0.216	0.240	9.412	21.511	19.486	0.036	0.014	36.099	0.016	0.080	8.746	2.343	98.100	NS-97-162-c4-9	r	*
141	0.220	0.283	9.497	21.165	19.670	0.006	0.000	35.934	0.007	0.007	8.984	2.124	97.803	NS-97-162-c4-10	r	
142	0.136	0.439	9.272	19.016	19.746	0.106	0.039	36.503	0.041	0.138	9.954	2.621	97.930	NS-97-387-c1-1	c	
143	0.115	0.442	9.473	18.465	19.824	0.191	0.027	36.231	0.030	0.104	9.648	2.804	97.263	NS-97-387-c1-2	c	
144	0.105	0.401	9.212	19.673	19.713	0.072	0.000	36.062	0.044	0.127	10.017	2.540	97.906	NS-97-387-c1-3	m	
145	0.127	0.358	8.639	18.733	20.067	0.082	0.009	35.492	0.066	0.125	9.484	2.438	95.548	NS-97-387-c1-4	r	*
146	0.165	0.274	6.769	21.216	19.839	0.139	0.038	33.905	0.026	0.105	10.453	2.018	94.847	NS-97-387-c1-5	r	
147	0.144	0.354	9.495	19.076	19.994	0.053	0.035	36.281	0.031	0.119	9.842	2.622	97.973	NS-97-387-c1-6	c	
148	0.124	0.364	9.360	19.592	19.807	0.042	0.026	36.291	0.000	0.138	9.745	2.821	98.249	NS-97-387-c1-7	c	
149	0.163	0.394	9.352	19.179	20.023	0.050	0.032	36.559	0.001	0.143	9.723	2.545	98.084	NS-97-387-c1-8	m	
150	0.153	0.440	9.589	18.321	20.227	0.096	0.055	36.215	0.000	0.126	9.788	2.692	97.616	NS-97-387-c1-9	r	
151	0.251	0.222	9.449	19.143	20.165	0.031	0.027	35.718	0.000	0.126	9.806	2.394	97.219	NS-97-387-c1-10	r	
152	0.102	0.341	9.359	18.662	19.829	0.032	0.019	36.297	0.008	0.100	9.681	2.432	96.812	NS-97-387-c2-1	c	
153	0.122	0.334	9.434	19.119	20.142	0.035	0.033	36.483	0.002	0.137	9.685	2.568	98.035	NS-97-387-c2-2	c	
154	0.152	0.385	9.391	18.929	20.291	0.008	0.017	36.413	0.000	0.110	9.577	2.447	97.654	NS-97-387-c2-3	m	
155	0.169	0.359	9.370	18.423	20.441	0.047	0.005	35.992	0.000	0.078	9.538	2.451	96.791	NS-97-387-c2-4	r	
156	0.159	0.316	9.723	18.847	20.447	0.031	0.027	36.599	0.000	0.139	9.575	2.534	98.323	NS-97-387-c2-5	r	
157	0.174	0.278	9.242	19.013	20.120	0.045	0.012	36.229	0.012	0.141	9.868	2.270	97.321	NS-97-387-c2-6	c	
158	0.120	0.317	9.459	18.892	20.093	0.043	0.045	36.343	0.021	0.134	9.892	2.346	97.644	NS-97-387-c2-7	c	
159	0.125	0.348	9.541	18.866	20.068	0.049	0.042	36.485	0.008	0.136	9.921	2.425	97.950	NS-97-387-c2-8	m	
160	0.142	0.315	9.532	18.757	20.639	0.023	0.000	36.067	0.000	0.137	10.011	1.972	97.530	NS-97-387-c2-9	r	
161	0.251	0.271	9.338	18.947	19.500	0.047	0.030	33.390	0.000	0.128	9.414	2.337	93.536	NS-97-387-c2-10	r	
162	0.192	0.214	9.504	23.149	19.169	0.028	0.026	35.582	0.000	0.068	8.575	1.792	98.212	NS97-326-c1-1		
163	0.203	0.205	9.498	22.477	19.525	0.026	0.012	35.873	0.000	0.038	8.582	1.655	98.003	NS97-326-c1-2		
164	0.213	0.232	9.292	22.580	19.613	0.029	0.018	35.839	0.000	0.069	8.828	1.705	98.321	NS97-326-c1-3		
165	0.195	0.212	8.996	22.504	19.519	0.014	0.025	35.908	0.000	0.047	8.567	1.635	97.537	NS97-326-c1-4		
166	0.222	0.170	9.227	22.608	19.109	0.011	0.029	35.679	0.004	0.057	8.632	1.574	97.227	NS97-326-c1-5		
167	0.180	0.235	9.197	22.869	19.231	0.005	0.014	35.298	0.000	0.022	8.538	1.673	97.185	NS97-326-c1-6		
168	0.193	0.255	9.144	22.805	19.716	0.018	0.037	35.612	0.000	0.074	8.644	1.018	97.431	NS97-326-c2-1		

169	0.187	0.256	8.999	21.799	20.685	0.020	0.025	35.677	0.012	0.090	8.528	0.762	96.956	NS97-326-c2-2		
170	0.197	0.251	8.894	22.255	19.935	0.025	0.031	36.065	0.049	0.093	8.810	1.556	98.072	NS97-326-c2-3		
171	0.204	0.281	9.141	22.119	19.700	0.017	0.037	35.834	0.028	0.104	8.718	1.514	97.607	NS97-326-c2-4		*
172	0.180	0.279	9.184	22.131	19.574	0.029	0.045	35.587	0.000	0.058	8.229	1.558	96.771	NS97-326-c2-5		
173	0.209	0.188	9.048	22.939	19.511	0.026	0.013	35.266	0.020	0.071	7.938	1.287	96.422	NS97-326-c2-6		
174	0.170	0.249	9.570	23.163	19.191	0.000	0.028	35.387	0.000	0.039	8.472	1.701	97.898	NS97-326-c3-1		
175	0.195	0.209	9.494	23.020	19.233	0.026	0.016	35.258	0.002	0.039	8.085	1.728	97.217	NS97-326-c3-2		
176	0.161	0.269	9.205	22.740	19.385	0.011	0.027	35.460	0.000	0.042	8.528	1.454	97.212	NS97-326-c3-3		
177	0.152	0.285	9.154	22.289	19.655	0.018	0.015	35.456	0.002	0.079	8.865	1.301	97.203	NS97-326-c3-4		
178	0.180	0.213	9.235	24.415	19.229	0.030	0.004	35.376	0.055	0.112	7.212	1.594	97.572	NS97-326-c3-5		
179	0.190	0.189	8.977	24.821	19.232	0.042	0.024	35.159	0.048	0.095	6.865	1.541	97.094	NS97-326-c3-6		
180	0.148	0.288	8.965	22.398	19.727	0.009	0.005	35.609	0.051	0.044	8.467	1.521	97.168	NS97-326-c4-1		
181	0.203	0.162	9.559	22.369	19.594	0.006	0.017	35.271	0.058	0.035	8.336	1.613	97.136	NS97-326-c4-2		
182	0.205	0.140	9.312	22.529	19.666	0.020	0.002	35.302	0.033	0.075	8.221	1.826	97.240	NS97-326-c4-3		
183	0.176	0.182	9.056	22.521	19.521	0.028	0.020	35.359	0.018	0.095	8.661	1.762	97.319	NS97-326-c4-4		
184	0.142	0.316	9.212	22.591	19.729	0.030	0.049	35.345	0.007	0.064	8.789	1.592	97.799	NS97-326-c4-5		
185	0.169	0.268	9.352	22.434	19.591	0.028	0.025	35.922	0.000	0.050	8.521	1.680	97.963	NS97-326-c4-6		
186	0.269	0.108	9.546	21.210	18.973	0.021	0.037	35.185	0.022	0.107	8.948	1.438	95.746	NS97-74-c1-1		
187	0.243	0.112	9.267	20.401	19.208	0.024	0.013	35.410	0.082	0.078	9.089	1.260	95.080	NS97-74-c1-2		
188	0.269	0.130	8.517	19.743	19.145	0.034	0.044	36.047	0.186	0.093	9.127	1.513	94.727	NS97-74-c1-3		
189	0.292	0.108	9.606	20.520	18.973	0.042	0.063	34.707	0.041	0.087	8.654	1.598	94.559	NS97-74-c1-4		
190	0.248	0.254	8.648	20.688	19.221	0.027	0.026	35.656	0.130	0.055	9.136	1.487	95.466	NS97-74-c1-5		
191	0.267	0.180	9.573	21.187	19.175	0.004	0.022	35.608	0.024	0.074	9.046	1.970	97.017	NS97-74-c1-6		
192	0.282	0.160	9.315	22.075	19.011	0.032	0.029	35.385	0.065	0.046	9.192	1.456	96.922	NS97-74-c2-1		
193	0.223	0.118	9.804	20.851	20.960	0.015	0.007	35.402	0.052	0.076	8.931	0.911	97.253	NS97-74-c2-2		
194	0.234	0.136	9.244	21.110	19.237	0.012	0.041	35.250	0.083	0.066	9.556	1.546	96.413	NS97-74-c2-3		
195	0.299	0.082	9.648	20.800	19.226	0.000	0.035	35.604	0.070	0.073	10.005	1.395	97.111	NS97-74-c2-4		
196	0.275	0.192	9.278	21.539	19.484	0.006	0.024	35.946	0.103	0.092	9.233	1.636	97.691	NS97-74-c2-5		
197	0.241	0.157	9.900	21.345	19.641	0.004	0.031	36.241	0.032	0.110	8.506	2.155	98.261	NS97-74-c2-6		
198	0.251	0.164	9.836	21.245	19.290	0.016	0.033	35.753	0.000	0.055	9.245	1.837	97.615	NS97-74-c3-1		
199	0.202	0.117	9.636	20.978	19.147	0.021	0.056	35.593	0.009	0.062	8.801	1.929	96.461	NS97-74-c3-2		
200	0.285	0.161	9.311	20.883	19.420	0.014	0.005	35.611	0.066	0.064	9.662	1.517	96.876	NS97-74-c3-3		
201	0.253	0.123	9.763	20.633	19.606	0.042	0.015	35.525	0.058	0.064	9.143	1.444	96.553	NS97-74-c3-4		
202	0.239	0.197	9.221	20.859	19.486	0.027	0.044	35.941	0.082	0.072	9.460	1.418	96.939	NS97-74-c3-5		
203	0.290	0.092	9.054	21.521	19.464	0.027	0.039	35.450	0.030	0.048	9.733	1.501	97.121	NS97-74-c3-6		*
204	0.231	0.246	9.810	22.128	19.641	0.079	0.037	35.416	0.006	0.155	8.905	1.580	98.119	NS97-74-c4-1		
205	0.159	0.226	9.492	21.633	19.560	0.079	0.036	35.359	0.020	0.160	8.323	1.597	96.559	NS97-74-c4-2		
206	0.213	0.162	9.300	21.709	19.561	0.044	0.020	34.895	0.037	0.177	8.146	1.652	95.816	NS97-74-c4-3		
207	0.237	0.120	9.442	21.434	18.836	0.021	0.053	34.703	0.036	0.139	9.324	1.640	95.880	NS97-74-c4-4		
208	0.212	0.168	9.600	21.888	19.024	0.038	0.066	35.910	0.022	0.178	8.855	1.590	97.453	NS97-74-c4-5		
209	0.237	0.172	9.739	21.952	19.431	0.026	0.049	35.595	0.009	0.148	8.591	1.625	97.468	NS97-74-c4-6		
210	0.163	0.169	9.585	23.405	19.344	0.033	0.029	35.542	0.015	0.113	7.812	2.140	98.274	NS97-119-c1-1		
211	0.000	0.000	0.014	0.000	0.007	0.000	0.000	97.639	0.000	0.000	0.000	0.000	97.660	NS97-119-c1-2		
212	0.255	0.169	9.412	22.611	19.546	0.030	0.019	35.315	0.019	0.116	8.068	2.366	97.812	NS97-119-c1-3		
213	0.180	0.174	9.581	22.337	19.387	0.036	0.044	35.297	0.000	0.091	7.850	2.467	97.360	NS97-119-c1-4		
214	0.174	0.157	9.671	23.643	18.849	0.021	0.015	35.209	0.001	0.135	7.697	2.587	98.081	NS97-119-c1-5		
215	0.179	0.124	9.781	22.692	19.169	0.035	0.032	35.316	0.007	0.152	7.351	2.387	97.142	NS97-119-c1-6		

216	0.151	0.215	9.151	24.176	18.948	0.042	0.000	34.390	0.066	0.266	6.763	1.925	96.020	NS97-119-c2-1		
217	0.146	0.131	9.116	25.032	18.216	0.037	0.005	34.334	0.074	0.261	6.827	1.713	95.823	NS97-119-c2-2		*
218	0.130	0.019	2.787	34.572	19.976	0.027	0.029	27.563	0.008	0.430	7.239	0.191	92.910	NS97-119-c2-3		
219	0.108	0.030	3.632	33.389	20.573	0.030	0.026	28.348	0.026	0.407	6.814	0.294	93.625	NS97-119-c2-4		
220	0.112	0.173	9.698	25.866	19.610	0.037	0.042	34.698	0.012	0.324	4.855	2.476	97.848	NS97-119-c2-5		
221	0.124	0.123	8.896	26.311	12.287	0.040	0.048	18.434	0.000	0.365	3.560	1.712	71.839	NS97-119-c2-6		
222	0.116	0.185	8.771	23.814	19.407	0.032	0.038	34.842	0.026	0.173	7.758	2.154	97.260	NS97-119-c3-1		
223	0.223	0.193	9.411	23.425	18.760	0.027	0.054	35.194	0.051	0.153	7.863	1.942	97.196	NS97-119-c3-2		
224	0.140	0.239	9.489	23.042	18.862	0.034	0.036	35.316	0.013	0.109	8.148	2.110	97.471	NS97-119-c3-3		
225	0.177	0.191	9.667	22.685	18.863	0.023	0.017	35.226	0.000	0.090	8.116	1.989	96.964	NS97-119-c3-4		
226	0.166	0.233	9.729	22.508	19.349	0.035	0.032	35.596	0.000	0.074	7.829	2.170	97.643	NS97-119-c3-5		
227	0.166	0.202	9.714	23.086	19.065	0.059	0.016	35.253	0.000	0.096	7.784	2.272	97.630	NS97-119-c3-6		
Legend:																
Loc. (Location): c=center, m=middle (between center and rim), r=rim of grain, blank means unknown																
? (Used?): *=data used in calculations																

Appendix C-3: Electron Microprobe Data for plagioclase (weight percent

#	Na2O	SiO2	K2O	MnO	MgO	Al2O3	CaO	FeO	Total	Comment	Loc.	?
1	9.513	64.345	0.225	0.010	0.019	22.337	3.109	0.059	99.617	NS-97-340-c1-1	c	
2	9.369	63.775	0.237	0.007	0.012	22.786	3.626	0.033	99.845	NS-97-340-c1-2	c	
3	9.091	63.733	0.184	0.000	0.004	22.768	3.714	0.024	99.518	NS-97-340-c1-3	m	
4	9.397	64.447	0.175	0.006	0.012	22.617	3.376	0.028	100.058	NS-97-340-c1-4	r	
5	9.403	64.178	0.130	0.000	0.021	22.590	3.453	0.039	99.814	NS-97-340-c1-5	r	
6	9.300	64.430	0.175	0.000	0.000	22.727	3.396	0.043	100.071	NS-97-340-c1-6	r	*
7	9.199	64.071	0.171	0.000	0.003	22.855	3.582	0.047	99.928	NS-97-340-c1-7	m	
8	9.246	64.045	0.180	0.000	0.000	22.801	3.558	0.015	99.845	NS-97-340-c1-8	c	
9	9.169	64.186	0.191	0.000	0.009	22.859	3.512	0.012	99.938	NS-97-340-c1-9	c	
10	9.257	63.691	0.205	0.000	0.000	22.841	3.632	0.017	99.643	NS-97-340-c1-10	m	
11	9.277	64.232	0.190	0.012	0.000	22.611	3.378	0.035	99.735	NS-97-340-c1-11	m	
12	9.794	65.255	0.174	0.022	0.001	22.185	2.777	0.073	100.281	NS-97-340-c1-12	r	
13	9.545	64.753	0.150	0.007	0.000	22.540	3.084	0.200	100.279	NS-97-340-c1-13	r	
14	9.298	63.964	0.185	0.005	0.000	22.792	3.467	0.041	99.752	NS-97-340-c1-14	r	
15	9.615	64.853	0.158	0.018	0.008	22.488	3.118	0.047	100.305	NS-97-340-c2-1	c	
16	9.892	65.187	0.220	0.000	0.012	22.175	2.827	0.048	100.361	NS-97-340-c2-2	c	
17	9.813	65.002	0.218	0.000	0.003	22.263	2.769	0.019	100.087	NS-97-340-c2-3	m	
18	9.638	64.691	0.207	0.000	0.005	22.181	2.985	0.033	99.740	NS-97-340-c2-4	m	
19	9.414	64.373	0.193	0.000	0.006	22.778	3.334	0.050	100.148	NS-97-340-c2-5	r	
20	9.851	65.261	0.134	0.004	0.004	22.193	2.763	0.035	100.245	NS-97-340-c2-6	r	
21	9.667	65.010	0.204	0.007	0.008	22.342	2.955	0.017	100.210	NS-97-340-c2-7	r	
22	10.189	66.145	0.125	0.000	0.000	21.802	2.270	0.110	100.641	NS-97-340-c2-8	c	
23	10.299	65.973	0.132	0.000	0.004	21.616	2.269	0.095	100.388	NS-97-340-c2-9	c	
24	9.888	65.471	0.068	0.000	0.000	22.068	2.584	0.124	100.203	NS-97-340-c2-10	m	
25	10.075	65.417	0.097	0.000	0.000	21.869	2.179	0.089	99.726	NS-97-340-c2-11	m	
26	9.790	65.272	0.136	0.012	0.000	22.106	2.758	0.089	100.163	NS-97-340-c2-12	r	
27	9.930	65.224	0.079	0.001	0.003	21.911	2.480	0.113	99.741	NS-97-340-c2-13	r	
28	10.204	66.018	0.085	0.000	0.000	21.654	2.240	0.081	100.282	NS-97-340-c2-14	r	
29	9.415	64.998	0.124	0.005	0.000	22.494	2.991	0.017	100.044	NS-97-340-c3-1	c	
30	9.432	64.693	0.171	0.005	0.000	22.434	3.019	0.026	99.780	NS-97-340-c3-2	c	
31	9.467	64.902	0.211	0.000	0.003	22.544	3.022	0.029	100.178	NS-97-340-c3-3	m	
32	9.796	64.778	0.198	0.000	0.007	22.422	2.907	0.000	100.108	NS-97-340-c3-4	m	
33	9.662	64.431	0.137	0.000	0.005	22.740	3.214	0.071	100.260	NS-97-340-c3-5	r	
34	9.394	64.555	0.129	0.000	0.006	22.566	3.217	0.057	99.924	NS-97-340-c3-6	r	
35	9.539	64.289	0.109	0.000	0.015	22.576	3.052	0.057	99.637	NS-97-340-c3-7	r	
36	9.440	64.530	0.191	0.000	0.000	22.559	3.204	0.010	99.934	NS-97-340-c3-8	c	
37	9.519	64.152	0.206	0.000	0.000	22.599	3.264	0.009	99.749	NS-97-340-c3-9	c	
38	9.267	64.242	0.164	0.006	0.000	22.860	3.565	0.010	100.114	NS-97-340-c3-10	m	
39	9.302	63.883	0.206	0.000	0.003	22.903	3.642	0.000	99.939	NS-97-340-c3-11	m	
40	9.591	64.745	0.135	0.000	0.000	22.181	2.963	0.089	99.704	NS-97-340-c3-12	r	
41	9.577	64.561	0.156	0.000	0.000	22.715	3.393	0.061	100.463	NS-97-340-c3-13	r	
42	9.805	64.556	0.179	0.000	0.000	22.405	3.242	0.040	100.227	NS-97-340-c3-14	r	
43	8.799	62.599	0.122	0.000	0.006	23.474	4.643	0.029	99.672	NS-97-75-c1-1	c	
44	8.819	62.711	0.094	0.000	0.000	23.810	4.718	0.052	100.204	NS-97-75-c1-2	m	
45	7.574	60.320	0.074	0.000	0.000	25.083	6.619	0.043	99.713	NS-97-75-c1-3	r	*
46	8.119	61.421	0.087	0.000	0.004	24.405	5.735	0.043	99.814	NS-97-75-c1-4	r	

47	7.860	60.908	0.121	0.008	0.004	24.290	5.749	0.068	99.008	NS-97-75-c1-5	c	
48	8.005	61.206	0.105	0.000	0.000	24.568	5.695	0.085	99.664	NS-97-75-c1-6	c	
49	8.241	61.520	0.354	0.012	0.000	24.208	5.316	0.248	99.899	NS-97-75-c1-7	m	
50	8.070	61.304	0.082	0.005	0.000	24.977	6.024	0.182	100.644	NS-97-75-c1-8	r	
51	8.206	61.335	0.186	0.000	0.001	24.411	5.659	0.251	100.049	NS-97-75-c1-9	r	
52	7.519	60.404	0.112	0.003	0.011	25.276	6.474	0.189	99.988	NS-97-75-c1-10	r	
53	7.036	60.528	3.447	0.027	0.209	25.167	1.673	0.522	98.609	NS-97-75-c1-11	c	
54	8.492	62.385	0.103	0.012	0.000	24.055	5.062	0.143	100.252	NS-97-75-c1-12	m	
55	8.323	61.907	0.115	0.038	0.009	24.470	5.398	0.373	100.633	NS-97-75-c1-13	r	*
56	7.822	59.890	0.110	0.018	0.004	25.395	6.770	0.180	100.189	NS-97-75-c1-14	r	
57	7.481	59.912	0.245	0.012	0.000	25.193	6.786	0.060	99.689	NS-97-162-c4-1	c	
58	7.264	59.491	0.247	0.007	0.000	25.365	6.654	0.012	99.040	NS-97-162-c4-2	c	
59	7.305	59.757	0.219	0.000	0.000	25.351	6.884	0.088	99.604	NS-97-162-c4-3	m	
60	7.477	59.859	0.185	0.003	0.000	25.288	6.796	0.085	99.693	NS-97-162-c4-4	m	
61	7.913	60.725	0.223	0.000	0.000	24.769	6.183	0.054	99.867	NS-97-162-c4-5	r	
62	7.603	59.687	0.468	0.008	0.000	25.255	6.265	0.050	99.336	NS-97-162-c4-6	r	*
63	7.464	59.620	0.156	0.025	0.000	25.602	7.009	0.078	99.954	NS-97-162-c4-7	r	
64	8.959	62.948	0.107	0.010	0.000	23.469	4.342	0.013	99.848	NS-97-387-c1-1	c	
65	8.978	63.559	0.125	0.013	0.000	23.575	4.478	0.092	100.820	NS-97-387-c1-2	c	
66	8.593	62.681	1.254	0.027	0.028	24.059	2.766	0.105	99.513	NS-97-387-c1-3	m	
67	8.183	62.942	0.174	0.013	0.000	24.017	4.831	0.034	100.194	NS-97-387-c1-4	m	
68	8.783	63.397	0.177	0.037	0.000	23.924	4.564	0.122	101.004	NS-97-387-c1-5	r	
69	8.537	62.531	0.189	0.024	0.000	23.661	4.540	0.065	99.547	NS-97-387-c1-6	r	
70	8.649	63.097	0.146	0.008	0.000	24.154	4.955	0.017	101.026	NS-97-387-c1-7	r	*
71	8.160	62.500	1.074	0.000	0.000	25.013	3.903	0.044	100.694	NS-97-387-c1-8	c	
72	8.615	62.474	0.170	0.017	0.000	23.477	4.566	0.078	99.397	NS-97-387-c1-9	m	
73	9.985	65.606	0.629	0.000	0.027	22.079	1.481	0.071	99.878	NS-97-387-c1-10	r	
74	8.805	63.292	0.164	0.006	0.005	23.737	4.664	0.030	100.703	NS-97-387-c1-11	r	
75	9.148	63.542	0.140	0.000	0.000	23.258	3.805	0.004	99.897	NS-97-387-c1-12	r	
76	10.235	66.558	0.339	0.000	0.002	21.381	1.425	0.021	99.961	NS-97-387-c1-13	c	
77	8.851	63.268	0.214	0.000	0.007	23.364	4.451	0.006	100.161	NS-97-91A-c5-1	?	
78	8.995	62.710	0.279	0.018	0.000	23.609	4.579	0.045	100.235	NS-97-91A-c5-2	?	
79	8.615	62.858	0.214	0.009	0.000	23.796	4.603	0.010	100.105	NS-97-91A-c5-3	?	
80	8.625	62.834	0.279	0.000	0.001	23.686	4.712	0.001	100.138	NS-97-91A-c5-4	?	
81	8.616	62.715	0.182	0.000	0.006	23.453	4.643	0.011	99.626	NS-97-91A-c5-5	?	*
82	8.787	62.920	0.250	0.000	0.000	23.507	4.480	0.000	99.944	NS-97-91A-c6-1	c	
83	8.577	63.290	0.295	0.000	0.002	23.607	4.510	0.001	100.282	NS-97-91A-c6-2	c	
84	8.865	63.403	0.265	0.012	0.005	23.285	4.097	0.007	99.939	NS-97-91A-c6-3	m	
85	8.765	63.732	0.263	0.011	0.000	23.157	4.250	0.015	100.193	NS-97-91A-c6-4	m	
86	9.063	63.953	1.637	0.004	0.088	23.131	1.427	0.257	99.560	NS-97-91A-c6-5	r	
87	8.783	63.239	0.308	0.000	0.007	23.496	4.411	0.053	100.297	NS-97-91A-c6-6	r	
88	8.945	63.834	1.445	0.016	0.095	22.614	1.884	0.176	99.009	NS-97-91A-c6-7	r	
89	8.671	63.189	0.222	0.000	0.000	23.746	4.629	0.013	100.470	NS-97-91A-c7-1	c	
90	8.675	63.552	0.240	0.019	0.000	23.596	4.441	0.026	100.549	NS-97-91A-c7-2	c	
91	8.688	63.236	0.207	0.000	0.000	23.602	4.541	0.018	100.292	NS-97-91A-c7-3	m	
92	8.901	64.142	0.622	0.000	0.015	23.272	3.075	0.031	100.058	NS-97-91A-c7-4	r	
93	9.173	64.452	0.199	0.000	0.000	22.778	3.524	0.022	100.148	NS-97-91A-c7-5	r	
94	9.168	64.020	0.135	0.002	0.000	23.125	3.998	0.011	100.459	NS-97-91A-c7-6	r	

95	8.422	62.506	0.328	0.013	0.000	23.823	4.846	0.010	99.948	NS-97-91A-c9-1	c	
96	8.647	63.217	0.347	0.012	0.000	23.835	4.787	0.027	100.872	NS-97-91A-c9-2	m	
97	8.623	62.949	0.353	0.000	0.000	23.793	4.767	0.014	100.499	NS-97-91A-c9-3	r	
98	8.572	63.010	0.259	0.003	0.008	23.736	4.792	0.023	100.403	NS-97-91A-c9-4	r	
99	8.440	62.305	0.244	0.007	0.009	23.678	4.855	0.024	99.562	NS-97-91A-c9-5	r	
100	8.617	62.842	0.215	0.010	0.000	23.595	4.804	0.031	100.114	NS-97-91A-c9-6	r	
101	8.053	61.369	0.126	0.000	0.000	24.967	5.926	0.125	100.566	NS-97-82-c1-1	c	
102	7.862	60.996	0.078	0.015	0.000	25.106	6.110	0.137	100.304	NS-97-82-c1-2	m	
103	8.023	61.402	0.098	0.031	0.000	24.853	5.991	0.103	100.501	NS-97-82-c1-3	r	
104	7.983	61.217	0.138	0.002	0.000	24.893	5.969	0.146	100.348	NS-97-82-c1-4	r	
105	8.097	61.790	0.123	0.000	0.000	24.606	5.693	0.154	100.463	NS-97-82-c1-5	c	
106	8.135	61.750	0.131	0.010	0.000	24.589	5.738	0.160	100.513	NS-97-82-c1-6	m	
107	8.031	61.265	0.127	0.007	0.000	24.661	5.690	0.224	100.005	NS-97-82-c1-7	r	*
108	8.037	61.715	0.107	0.010	0.000	24.620	5.624	0.027	100.140	NS-97-82-c4-1	c	
109	8.295	61.935	0.111	0.000	0.000	24.532	5.516	0.017	100.406	NS-97-82-c4-2	c	
110	8.697	62.929	0.101	0.000	0.000	23.631	4.535	0.026	99.919	NS-97-82-c4-3	r	
111	7.999	61.773	0.086	0.006	0.000	24.657	5.755	0.013	100.289	NS-97-82-c4-4	r	
112	8.618	63.171	0.117	0.004	0.000	23.634	4.783	0.019	100.346	NS-97-82-c4-5	r	
113	8.661	63.217	0.089	0.000	0.000	23.563	4.482	0.015	100.027	NS-97-82-c4-6	c	
114	8.918	62.813	0.123	0.000	0.000	23.135	4.385	0.034	99.408	NS-97-82-c4-7	c	
115	8.775	62.871	0.099	0.000	0.002	23.601	4.693	0.047	100.088	NS-97-82-c4-8	m	
116	7.873	61.421	0.089	0.001	0.000	25.140	6.131	0.049	100.704	NS-97-82-c4-9	r	
117	8.348	61.691	0.093	0.000	0.000	24.404	5.488	0.041	100.065	NS-97-82-c4-10	r	
118	8.597	62.885	0.096	0.000	0.000	23.938	4.999	0.014	100.529	NS-97-82-c4-11	r	
119	8.487	62.601	0.093	0.000	0.000	24.078	5.045	0.100	100.404	NS-97-82-c4-12	c	
120	8.578	62.831	0.095	0.000	0.000	23.554	4.738	0.079	99.875	NS-97-82-c4-13	m	
121	7.990	61.418	0.078	0.002	0.004	24.756	5.884	0.046	100.178	NS-97-82-c4-14	r	
122	8.330	62.124	0.083	0.014	0.000	24.524	5.504	0.073	100.652	NS-97-82-c4-15	r	
123	7.877	61.469	0.142	0.000	0.012	24.214	5.721	0.039	99.474	NS-97-82-c5-1	m	
124	8.241	61.869	0.111	0.000	0.000	24.503	5.557	0.039	100.320	NS-97-82-c5-2	r	
125	8.149	61.757	0.131	0.010	0.015	24.502	5.549	0.064	100.177	NS-97-82-c5-3	r	
126	8.933	63.598	0.115	0.006	0.000	23.251	4.330	0.081	100.314	NS-97-8-c4-1	c	
127	7.875	60.801	0.076	0.000	0.000	25.496	6.790	0.033	101.071	NS-97-8-c4-2	c	
128	7.473	60.768	0.307	0.000	0.001	25.711	6.708	0.077	101.045	NS-97-8-c4-3	m	
129	9.040	63.558	0.093	0.002	0.000	23.873	4.650	0.099	101.315	NS-97-8-c4-4	m	
130	8.813	63.367	0.101	0.000	0.001	23.802	4.773	0.113	100.970	NS-97-8-c4-5	r	
131	8.160	61.238	0.279	0.000	0.000	24.176	5.428	0.090	99.371	NS-97-8-c4-6	r	
132	7.381	60.250	0.074	0.000	0.000	26.124	7.261	0.071	101.161	NS-97-8-c4-7	r	
133	7.594	60.509	0.084	0.000	0.003	25.796	6.832	0.127	100.945	NS-97-8-c5-1	c	
134	7.300	60.156	0.073	0.000	0.000	25.967	7.318	0.139	100.953	NS-97-8-c5-2	m	
135	7.397	59.685	0.091	0.000	0.008	26.025	7.386	0.157	100.749	NS-97-8-c5-3	r	
136	7.361	59.936	0.085	0.000	0.000	25.623	6.989	0.228	100.222	NS-97-8-c5-4	r	
137	7.498	60.300	0.092	0.031	0.004	25.579	6.778	0.239	100.521	NS-97-8-c5-5	r	
138	7.140	59.188	0.092	0.000	0.000	26.114	7.680	0.076	100.290	NS-97-8-c5-6	c	
139	7.054	59.695	0.128	0.000	0.000	26.397	7.591	0.111	100.976	NS-97-8-c5-7	m	
140	8.425	62.722	0.091	0.000	0.000	24.181	5.227	0.180	100.826	NS-97-8-c5-8	m	
141	7.621	60.484	0.087	0.000	0.000	25.256	6.493	0.096	100.037	NS-97-8-c5-9	r	

142	7.031	59.580	0.097	0.009	0.000	26.299	7.485	0.206	100.707	NS-97-8-c5-10	r	
143	7.244	59.917	0.057	0.016	0.000	26.031	7.420	0.158	100.843	NS-97-8-c5-11	r	
144	8.602	63.192	0.073	0.000	0.000	23.972	4.827	0.069	100.735	NS-97-8-c5-12	c	
145	7.292	60.161	0.978	0.008	0.001	26.229	5.437	0.118	100.224	NS-97-8-c5-13	m	
146	8.110	62.124	0.092	0.015	0.000	24.658	5.817	0.110	100.926	NS-97-8-c5-14	r	
147	7.693	60.896	0.090	0.002	0.007	25.440	6.675	0.187	100.990	NS-97-8-c5-15	r	
148	7.095	58.997	0.067	0.000	0.003	26.497	8.076	0.129	100.864	NS-97-8-c5-16	c	
149	7.039	59.363	0.077	0.006	0.000	26.584	7.940	0.099	101.108	NS-97-8-c5-17	c	
150	8.720	62.916	0.081	0.013	0.012	24.366	5.159	0.135	101.402	NS-97-8-c5-18	r	
151	7.596	60.382	0.083	0.000	0.001	25.471	6.585	0.174	100.292	NS-97-8-c5-19	r	
152	7.660	60.179	0.094	0.001	0.006	25.645	6.864	0.229	100.678	NS-97-8-c5-20	r	
153	8.410	60.959	0.108	0.025	0.013	24.476	5.467	0.044	99.502	NS97-74-c2-1	c	
154	8.078	60.453	0.073	0.000	0.003	24.788	5.857	0.080	99.332	NS97-74-c2-2	r	
155	8.717	61.559	0.119	0.014	0.002	24.057	5.142	0.087	99.697	NS97-74-c2-3	c	
156	8.601	61.661	0.103	0.000	0.000	23.991	5.085	0.071	99.512	NS97-74-c2-4	r	
157	8.624	61.499	0.101	0.001	0.000	24.391	5.335	0.041	99.992	NS97-74-c2-5	c	
158	8.788	61.893	0.163	0.011	0.053	24.400	5.049	0.101	100.458	NS97-74-c2-6	r	
159	8.837	62.071	0.101	0.000	0.000	24.045	4.873	0.355	100.282	NS97-74-c3-1		
160	8.925	63.122	0.116	0.000	0.000	23.890	4.458	0.220	100.731	NS97-74-c3-2	c	
161	8.772	62.079	0.143	0.027	0.000	23.789	4.733	0.256	99.799	NS97-74-c3-3	r	
162	9.030	63.175	0.136	0.007	0.006	23.568	4.485	0.295	100.702	NS97-74-c3-4	r	*
163	8.599	61.777	0.103	0.000	0.008	24.764	5.369	0.203	100.823	NS97-74-c3-5	c	
164	9.193	63.009	0.115	0.004	0.006	23.519	4.232	0.199	100.277	NS97-74-c3-6	r	
165	9.339	61.270	0.129	0.000	0.064	20.443	2.436	0.275	93.956	NS97-326-c1-1		
166	9.856	63.539	0.106	0.001	0.013	21.377	2.393	0.234	97.519	NS97-326-c1-2		
167	8.721	61.967	0.128	0.000	0.000	24.157	4.862	0.051	99.886	NS97-326-c5-1		
168	8.419	60.883	0.105	0.008	0.003	24.455	5.417	0.033	99.323	NS97-326-c5-2		
169	8.545	61.899	0.115	0.015	0.000	24.277	5.071	0.061	99.983	NS97-326-c5-3		*
170	8.592	61.809	0.110	0.010	0.000	24.081	5.049	0.043	99.694	NS97-326-c6-1		
171	8.382	61.403	0.097	0.000	0.002	24.103	5.208	0.041	99.236	NS97-326-c6-2		
172	8.371	60.931	0.102	0.025	0.004	24.695	5.660	0.096	99.884	NS97-326-c6-3		
173	9.246	62.897	0.120	0.000	0.009	23.223	4.177	0.060	99.732	NS97-326-c7-1	c	
174	8.519	61.644	0.095	0.018	0.000	24.093	5.044	0.036	99.449	NS97-326-c7-2	m	
175	8.286	60.951	0.089	0.017	0.000	24.436	5.619	0.064	99.462	NS97-326-c7-3		
176	9.274	62.934	0.090	0.010	0.009	23.147	4.050	0.149	99.663	NS97-326-c7-4		
177	9.135	63.242	0.105	0.018	0.000	23.657	4.321	0.131	100.609	NS97-326-c7-5		
178	8.209	60.754	0.107	0.023	0.000	24.577	5.939	0.298	99.907	NS97-119-c3-1	c	

179	8.189	60.933	0.126	0.041	0.013	24.683	5.943	0.419	100.347	NS97-119-c3-2	r	
180	7.956	60.517	0.147	0.077	0.000	25.333	6.219	0.581	100.830	NS97-119-c3-3	c	
181	7.917	60.458	0.136	0.073	0.014	25.098	6.261	0.583	100.540	NS97-119-c3-4	r	
182	7.953	60.464	0.113	0.048	0.001	25.146	6.136	0.353	100.214	NS97-119-c3-5	c	
183	8.080	61.147	0.157	0.065	0.000	24.347	5.538	0.389	99.723	NS97-119-c3-6	r	
184	8.045	60.228	0.138	0.017	0.000	24.896	6.052	0.155	99.531	NS97-119-c1-1	c	
185	8.209	61.294	0.638	0.030	0.000	24.319	4.585	0.199	99.274	NS97-119-c1-2	r	
186	8.006	60.700	0.130	0.016	0.000	24.861	5.929	0.151	99.793	NS97-119-c1-3	c	
187	8.177	60.673	0.115	0.047	0.000	24.692	5.736	0.197	99.637	NS97-119-c1-4	c	
188	8.172	61.301	0.177	0.001	0.016	24.758	5.506	0.059	99.990	NS97-119-c1-5	c	
189	8.195	61.121	0.155	0.000	0.004	24.299	5.583	0.164	99.521	NS97-119-c1-6	m	
190	8.230	61.476	0.135	0.044	0.009	24.506	5.598	0.254	100.252	NS97-119-c1-7	r	
191	8.130	61.053	0.123	0.005	0.012	24.503	5.559	0.202	99.587	NS97-119-c1-8	c	
192	8.182	61.380	0.129	0.030	0.000	24.855	5.765	0.344	100.685	NS97-119-c1-9	r	
193	8.145	61.131	0.151	0.005	0.000	24.532	5.768	0.064	99.796	NS97-119-c2-1	c	
194	7.909	60.891	0.125	0.011	0.000	24.825	5.999	0.125	99.885	NS97-119-c2-2	r	
195	8.400	61.819	0.138	0.027	0.000	24.189	5.194	0.098	99.865	NS97-119-c2-3	c	
196	8.233	61.120	0.135	0.041	0.012	24.504	5.632	0.235	99.912	NS97-119-c2-4	r	
197	8.061	60.912	0.134	0.060	0.000	24.778	5.995	0.240	100.180	NS97-119-c2-5	r	*
198	8.212	61.454	0.136	0.000	0.002	24.558	5.604	0.075	100.041	NS97-119-c2-6	c	
199	8.192	60.744	0.112	0.023	0.009	25.141	6.080	0.228	100.529	NS97-119-c2-7	r	

Legend:

Loc. (Location): c=center, m=middle (between center and rim), r=rim of grain, blank means unknown

? (Used?): *=data used in calculations

Appendix C-4: Electron Microprobe Data for muscovite (weight percent)

#	F	Na2O	K2O	FeO	Al2O3	Cl	Cr2O3	SiO2	CaO	MnO	MgO	TiO2	Total	Comment	Loc.	?
1	0.057	0.473	11.104	1.751	34.023	0.002	0.000	46.191	0.072	0.012	0.845	0.639	95.145	NS-97-91A-c5-1	c	
2	0.026	0.458	10.842	1.543	33.615	0.008	0.008	46.041	0.093	0.000	0.795	0.628	94.044	NS-97-91A-c5-2	c	
3	0.014	0.497	11.074	1.593	34.204	0.033	0.016	46.002	0.044	0.001	0.754	0.425	94.644	NS-97-91A-c5-3	m	
4	0.071	0.548	10.823	1.509	34.436	0.000	0.009	46.386	0.099	0.008	0.693	0.554	95.106	NS-97-91A-c5-4	r	
5	0.027	0.517	10.958	1.634	34.232	0.026	0.019	46.310	0.088	0.021	0.767	0.583	95.165	NS-97-91A-c5-5	r	*
6	0.017	0.446	11.047	1.346	34.631	0.000	0.000	45.814	0.071	0.017	0.645	0.392	94.419	NS-97-91A-c5-6	c	
7	0.010	0.441	10.891	1.519	33.884	0.003	0.033	45.946	0.086	0.000	0.771	0.537	94.116	NS-97-91A-c5-7	m	
8	0.059	0.384	10.990	1.570	33.735	0.032	0.015	46.318	0.065	0.000	0.805	0.380	94.321	NS-97-91A-c5-8	r	
9	0.048	0.493	11.303	1.433	34.320	0.007	0.003	46.537	0.013	0.029	0.671	0.358	95.193	NS-97-91A-c6-1	c	
10	0.053	0.482	11.131	1.497	34.362	0.000	0.025	46.266	0.043	0.011	0.711	0.374	94.933	NS-97-91A-c6-2	c	
11	0.041	0.471	11.011	1.527	34.791	0.019	0.000	46.523	0.090	0.003	0.623	0.440	95.518	NS-97-91A-c6-3	m	
12	0.052	0.325	11.690	1.361	34.680	0.004	0.000	46.298	0.018	0.000	0.566	0.491	95.462	NS-97-91A-c6-4	r	
13	0.081	0.318	11.393	1.305	34.200	0.015	0.006	46.986	0.020	0.007	0.761	0.415	95.470	NS-97-91A-c6-5	c	
14	0.067	0.434	11.260	1.469	34.006	0.002	0.004	46.217	0.000	0.041	0.689	0.662	94.823	NS-97-91A-c6-6	c	
15	0.074	0.315	11.582	1.712	34.073	0.006	0.000	46.658	0.000	0.016	0.787	0.661	95.852	NS-97-91A-c6-7	m	
16	0.096	0.478	11.224	1.604	33.293	0.015	0.000	46.830	0.030	0.015	0.898	0.721	95.161	NS-97-91A-c6-8	r	
27	0.035	0.460	10.918	1.677	34.148	0.012	0.000	46.443	0.087	0.029	0.785	0.304	94.880	NS-97-91A-c8-1	c	
28	0.024	0.473	10.914	1.627	34.648	0.015	0.000	46.502	0.099	0.020	0.744	0.245	95.298	NS-97-91A-c8-2	c	
29	0.032	0.462	10.985	1.695	34.419	0.000	0.001	46.676	0.051	0.037	0.773	0.253	95.371	NS-97-91A-c8-3	m	
30	0.020	0.388	11.402	1.343	35.136	0.002	0.006	46.458	0.051	0.048	0.594	0.213	95.653	NS-97-91A-c8-4	r	
31	0.027	0.497	10.979	1.649	34.301	0.012	0.012	46.862	0.074	0.030	0.810	0.278	95.517	NS-97-91A-c8-5	r	
32	0.038	0.375	11.027	1.597	33.488	0.014	0.000	46.570	0.120	0.030	0.903	0.358	94.501	NS-97-91A-c8-6	r	
33	0.027	0.322	11.341	1.306	34.974	0.000	0.016	46.740	0.059	0.027	0.591	0.344	95.736	NS-97-91A-c8-7	r	
34	0.057	0.461	11.020	1.529	34.465	0.009	0.028	46.447	0.106	0.045	0.696	0.224	95.061	NS-97-91A-c8-8	r	
35	0.040	0.448	11.080	1.462	34.762	0.008	0.019	46.858	0.075	0.000	0.675	0.281	95.689	NS-97-91A-c8-9	r	
36	0.031	0.491	11.299	1.628	34.923	0.000	0.021	46.546	0.047	0.000	0.691	0.185	95.849	NS-97-91A-c8-10	c	
37	0.045	0.503	11.238	1.576	35.117	0.000	0.008	47.086	0.071	0.006	0.691	0.325	96.647	NS-97-91A-c8-11	m	
38	0.039	0.462	11.165	1.673	34.011	0.000	0.011	46.956	0.079	0.001	0.815	0.398	95.594	NS-97-91A-c8-12	r	
39	0.064	0.468	11.327	1.787	34.028	0.000	0.000	47.060	0.054	0.048	0.860	0.491	96.160	NS-97-91A-c8-13	r	
40	0.000	1.018	10.333	1.169	33.945	0.032	0.000	45.545	0.020	0.017	0.649	0.152	92.873	NS-97-82-c1-1	c	
41	0.000	1.024	10.177	1.200	34.797	0.010	0.000	46.270	0.005	0.002	0.563	0.302	94.348	NS-97-82-c1-2	c	
42	0.000	1.049	10.417	1.156	34.505	0.026	0.000	45.894	0.022	0.006	0.581	0.216	93.866	NS-97-82-c1-3	m	
43	0.001	0.980	10.487	1.493	34.454	0.017	0.028	47.196	0.000	0.000	0.809	0.370	95.831	NS-97-82-c1-4	r	
44	0.000	1.076	10.097	1.277	34.601	0.044	0.000	45.778	0.011	0.000	0.564	0.221	93.659	NS-97-82-c1-5	r	
45	0.011	0.968	10.163	1.308	34.636	0.019	0.014	47.694	0.031	0.003	0.828	0.276	95.942	NS-97-82-c1-6	c	
46	0.005	0.951	10.425	1.337	34.500	0.009	0.025	47.464	0.011	0.008	0.803	0.279	95.813	NS-97-82-c1-7	m	
47	0.000	0.984	10.323	1.350	34.690	0.000	0.052	47.381	0.000	0.000	0.738	0.279	95.797	NS-97-82-c1-8	r	*
60	0.000	1.042	10.281	1.112	35.186	0.005	0.000	46.501	0.052	0.000	0.618	0.282	95.078	NS-97-82-c3-1	c	
61	0.000	1.015	10.212	1.039	35.500	0.000	0.045	46.902	0.027	0.000	0.641	0.467	95.848	NS-97-82-c3-2	c	
62	0.000	0.991	10.240	1.281	34.949	0.000	0.091	46.721	0.042	0.000	0.629	0.318	95.262	NS-97-82-c3-3	m	
63	0.016	1.071	10.245	1.369	35.623	0.000	0.019	46.334	0.001	0.000	0.485	0.349	95.505	NS-97-82-c3-4	r	
64	0.061	0.936	10.015	1.212	34.469	0.032	0.009	46.248	0.147	0.000	0.615	0.425	94.136	NS-97-82-c3-6	c	
65	0.000	1.050	10.020	1.108	35.010	0.012	0.021	46.854	0.106	0.000	0.633	0.417	95.228	NS-97-82-c3-7	c	
66	0.000	0.935	10.035	1.252	34.840	0.021	0.031	46.696	0.096	0.000	0.658	0.346	94.905	NS-97-82-c3-8	m	
67	0.000	1.065	9.855	1.197	35.599	0.013	0.030	47.118	0.075	0.000	0.588	0.450	95.987	NS-97-82-c3-9	r	
68	0.000	0.964	9.909	1.249	34.523	0.023	0.056	46.370	0.108	0.002	0.689	0.424	94.312	NS-97-82-c3-10	r	
69	0.000	1.040	10.379	1.217	35.290	0.000	0.002	46.249	0.032	0.000	0.596	0.432	95.237	NS-97-82-c4-1	c	
70	0.000	1.077	10.312	1.235	35.363	0.000	0.010	46.383	0.000	0.005	0.553	0.424	95.362	NS-97-82-c4-2	c	
71	0.001	1.130	10.315	1.214	35.222	0.000	0.039	46.483	0.007	0.000	0.590	0.426	95.427	NS-97-82-c4-3	m	
72	0.000	0.983	10.485	1.262	34.735	0.012	0.019	46.928	0.007	0.000	0.726	0.340	95.494	NS-97-82-c4-4	r	*
73	0.000	1.008	10.242	1.415	34.894	0.000	0.008	47.294	0.018	0.003	0.703	0.370	95.955	NS-97-82-c4-5	r	
74	0.009	0.940	9.990	1.359	34.463	0.000	0.013	47.364	0.092	0.008	0.812	0.402	95.448	NS-97-82-c4-6	c	
75	0.000	0.893	10.209	1.251	34.223	0.012	0.000	47.155	0.022	0.012	0.872	0.392	95.038	NS-97-82-c4-7	c	
76	0.000	1.008	10.045	1.186	35.195	0.014	0.000	46.905	0.086	0.014	0.657	0.419	95.526	NS-97-82-c4-8	m	
77	0.000	0.971	10.268	1.256	35.487	0.022	0.021	47.236	0.062	0.001	0.647	0.293	96.259	NS-97-82-c4-9	r	
78	0.005	0.977	10.199	1.392	35.075	0.013	0.000	46.900	0.078	0.010	0.706	0.280	95.630	NS-97-82-c4-10	r	

79	0.011	0.835	10.284	2.819	33.770	0.000	0.035	47.020	0.036	0.010	0.718	0.292	95.825	NS-97-340-c1-1	c	
80	0.022	0.916	10.161	2.856	33.794	0.008	0.038	46.631	0.036	0.000	0.672	0.255	95.378	NS-97-340-c1-2	c	
81	0.012	0.927	10.083	2.782	34.058	0.011	0.046	46.714	0.024	0.000	0.613	0.288	95.551	NS-97-340-c1-3	m	
82	0.000	0.962	9.966	2.725	34.644	0.008	0.018	45.926	0.027	0.003	0.454	0.423	95.154	NS-97-340-c1-4	r	
83	0.000	1.022	10.074	2.782	34.706	0.027	0.013	46.058	0.064	0.008	0.493	0.458	95.699	NS-97-340-c1-5	r	*
84	0.000	0.895	9.863	2.807	34.065	0.000	0.001	46.354	0.078	0.007	0.627	0.389	95.086	NS-97-340-c1-6	c	
85	0.000	0.847	9.743	2.702	34.460	0.000	0.000	46.765	0.097	0.000	0.619	0.402	95.635	NS-97-340-c1-7	c	
86	0.012	0.856	9.712	2.787	34.258	0.000	0.000	46.207	0.151	0.000	0.615	0.436	95.029	NS-97-340-c1-8	m	
87	0.069	0.889	9.831	2.731	34.535	0.023	0.019	46.614	0.145	0.000	0.506	0.437	95.765	NS-97-340-c1-9	m	
88	0.033	0.946	9.637	2.770	34.560	0.005	0.014	45.745	0.106	0.000	0.468	0.410	94.679	NS-97-340-c1-10	m	
89	0.000	0.887	9.943	2.722	34.002	0.000	0.000	46.139	0.026	0.006	0.613	0.408	94.746	NS-97-340-c2-1	c	
90	0.000	0.836	9.977	2.651	34.162	0.000	0.000	46.592	0.073	0.000	0.590	0.421	95.302	NS-97-340-c2-2	c	
91	0.000	0.964	10.031	2.719	34.653	0.007	0.000	46.210	0.052	0.012	0.550	0.457	95.653	NS-97-340-c2-3	m	
92	0.000	0.930	9.723	2.664	34.704	0.018	0.000	46.408	0.096	0.010	0.518	0.648	95.715	NS-97-340-c2-4	r	
93	0.000	0.934	9.834	2.631	34.831	0.013	0.019	46.356	0.161	0.012	0.533	0.591	95.912	NS-97-340-c2-5	r	
94	0.000	1.071	10.362	2.720	34.628	0.007	0.019	46.324	0.000	0.000	0.454	0.516	96.099	NS-97-340-c2-6	c	
95	0.050	1.040	10.310	2.774	34.995	0.016	0.026	46.740	0.000	0.008	0.452	0.484	96.870	NS-97-340-c2-7	c	
96	0.023	0.990	10.417	2.791	34.643	0.000	0.041	46.182	0.000	0.005	0.426	0.475	95.983	NS-97-340-c2-8	m	
97	0.002	0.942	10.465	2.836	34.734	0.003	0.026	46.195	0.020	0.000	0.407	0.550	96.178	NS-97-340-c2-9	r	
98	0.000	1.003	10.372	2.744	35.016	0.000	0.015	46.354	0.000	0.000	0.420	0.519	96.443	NS-97-340-c2-10	r	
99	0.016	0.959	9.721	2.606	34.597	0.015	0.000	45.924	0.053	0.000	0.471	0.527	94.879	NS-97-340-c3-1	c	
100	0.020	0.976	9.991	2.662	34.561	0.022	0.026	45.758	0.031	0.000	0.468	0.576	95.078	NS-97-340-c3-2	c	
101	0.000	1.009	10.127	2.755	34.925	0.015	0.023	46.204	0.020	0.003	0.487	0.549	96.114	NS-97-340-c3-3	m	
102	0.000	0.943	10.024	2.701	34.718	0.007	0.028	45.960	0.090	0.017	0.519	0.588	95.593	NS-97-340-c3-4	r	
103	0.000	1.020	10.197	2.684	34.916	0.018	0.000	46.272	0.060	0.017	0.492	0.541	96.213	NS-97-340-c3-5	r	
104	0.007	1.041	10.447	2.578	34.774	0.012	0.007	46.509	0.000	0.000	0.401	0.437	96.207	NS-97-340-c3-6	c	
105	0.000	1.049	10.301	2.682	34.918	0.000	0.046	46.610	0.000	0.019	0.458	0.575	96.658	NS-97-340-c3-7	c	
106	0.008	1.052	10.377	2.746	34.545	0.000	0.007	46.698	0.000	0.000	0.491	0.419	96.340	NS-97-340-c3-8	m	
107	0.000	0.975	10.498	2.733	34.714	0.005	0.020	46.248	0.000	0.008	0.457	0.477	96.134	NS-97-340-c3-9	r	
108	0.000	1.030	10.362	2.497	35.250	0.007	0.005	46.153	0.000	0.017	0.355	0.359	96.033	NS-97-340-c3-10	r	
109	0.000	1.102	9.963	1.319	35.622	0.001	0.036	46.104	0.016	0.019	0.462	0.307	94.951	NS-97-75-c1-1	c	
110	0.000	0.934	10.313	1.516	34.520	0.001	0.017	46.568	0.016	0.000	0.683	0.323	94.891	NS-97-75-c1-2	c	
111	0.000	1.028	10.240	1.412	35.025	0.000	0.014	46.503	0.010	0.012	0.584	0.340	95.168	NS-97-75-c1-3	m	
112	0.003	1.190	10.045	1.318	35.478	0.000	0.064	46.226	0.006	0.000	0.498	0.348	95.175	NS-97-75-c1-4	r	
113	0.011	0.813	10.637	1.673	34.627	0.000	0.009	46.621	0.012	0.000	0.724	0.245	95.367	NS-97-75-c1-5	r	
114	0.039	0.947	10.028	1.580	33.346	0.000	0.039	47.640	0.015	0.001	1.035	0.359	95.013	NS-97-75-c1-6	c	
115	0.000	1.146	9.920	1.442	35.228	0.000	0.021	46.945	0.004	0.010	0.691	0.412	95.819	NS-97-75-c1-7	c	
116	0.025	0.904	10.049	1.564	33.581	0.000	0.059	47.208	0.014	0.011	0.913	0.436	94.753	NS-97-75-c1-8	r	
117	0.000	0.993	10.006	1.451	35.196	0.000	0.021	46.503	0.028	0.000	0.579	0.334	95.111	NS-97-75-c1-9	r	
118	0.000	1.015	9.847	1.274	33.793	0.000	0.000	46.765	0.036	0.000	0.864	0.295	93.889	NS-97-75-c1-10	c	
119	0.000	1.138	9.975	1.181	34.513	0.021	0.028	47.442	0.034	0.000	0.807	0.296	95.430	NS-97-75-c1-11	c	
120	0.000	1.030	9.953	1.305	34.296	0.021	0.007	47.166	0.005	0.012	0.909	0.297	94.996	NS-97-75-c1-12	r	
121	0.000	1.086	10.007	1.206	34.687	0.000	0.055	46.920	0.051	0.002	0.695	0.246	94.955	NS-97-75-c1-13	r	*
122	0.000	1.188	10.004	1.151	34.880	0.000	0.035	46.720	0.032	0.018	0.586	0.329	94.943	NS-97-75-c1-14	c	
123	0.003	1.002	10.133	1.238	34.618	0.004	0.039	47.189	0.032	0.000	0.782	0.315	95.353	NS-97-75-c1-15	c	
124	0.000	0.916	10.398	1.283	35.025	0.023	0.050	46.335	0.037	0.005	0.613	0.313	94.993	NS-97-75-c1-16	r	
125	0.000	1.188	10.055	1.130	35.491	0.007	0.045	46.166	0.046	0.009	0.493	0.337	94.965	NS-97-75-c1-17	r	
126	0.000	0.829	10.190	1.153	35.755	0.000	0.012	47.189	0.000	0.008	0.643	0.524	96.303	NS97-162-1-1	c	
127	0.000	0.834	10.309	1.296	35.953	0.017	0.012	47.421	0.000	0.007	0.736	0.472	97.053	NS97-162-1-2	r	
128	0.000	0.767	10.465	1.322	35.132	0.000	0.057	46.234	0.063	0.000	0.798	0.411	95.249	NS97-162-2-1	c	
129	0.000	0.807	10.206	1.222	35.935	0.000	0.022	47.510	0.037	0.000	0.665	0.474	96.878	NS97-162-2-2	r	
130	0.000	0.879	10.223	1.244	35.777	0.000	0.021	47.316	0.015	0.000	0.689	0.403	96.567	NS97-162-3-1	c	
131	0.000	0.798	10.182	1.276	36.147	0.012	0.018	47.301	0.011	0.012	0.656	0.478	96.888	NS97-162-3-2	r	*
132	0.000	0.756	10.539	1.130	35.894	0.013	0.035	46.759	0.014	0.002	0.534	0.500	96.173	NS97-162-4-1	c	
133	0.000	0.808	10.569	1.156	35.574	0.009	0.021	46.849	0.002	0.008	0.651	0.533	96.178	NS97-162-4-2	r	

134	0.000	0.807	10.481	1.244	35.446	0.000	0.015	46.618	0.008	0.016	0.645	0.537	95.817	NS97-162-5-1	c	
135	0.000	0.798	10.320	1.263	35.743	0.001	0.023	47.113	0.031	0.014	0.662	0.491	96.459	NS97-162-5-2	r	
136	0.000	1.029	10.131	0.972	35.622	0.009	0.001	47.174	0.008	0.000	0.638	0.770	96.352	NS97-387-1-1	c	
137	0.000	0.882	10.242	1.003	35.229	0.000	0.033	47.819	0.036	0.011	0.746	0.743	96.744	NS97-387-1-2	r	
138	0.000	1.066	9.888	1.192	35.691	0.006	0.000	47.198	0.000	0.008	0.706	0.598	96.352	NS97-387-2-1	c	
139	0.000	1.080	9.996	1.275	35.534	0.017	0.013	47.383	0.016	0.003	0.721	0.724	96.758	NS97-387-2-2	r	*
140	0.000	1.110	10.136	1.020	35.125	0.001	0.011	46.773	0.000	0.011	0.669	0.723	95.579	NS97-387-3-1	c	
141	0.000	1.122	9.945	1.146	35.403	0.009	0.021	47.128	0.000	0.000	0.673	0.832	96.277	NS97-387-3-2	r	
142	0.000	1.033	9.865	1.096	35.454	0.016	0.052	47.067	0.000	0.021	0.701	0.821	96.122	NS97-387-4-1	c	
143	0.000	1.129	10.069	1.101	35.039	0.006	0.022	47.272	0.007	0.010	0.684	0.668	96.006	NS97-387-4-2	r	
144	0.000	1.003	9.862	1.152	35.740	0.000	0.035	47.497	0.025	0.003	0.691	0.774	96.782	NS97-387-5-1	c	
145	0.000	0.922	9.750	1.169	35.961	0.009	0.032	47.473	0.027	0.017	0.660	0.769	96.787	NS97-387-5-2	r	
146	0.000	1.176	10.060	1.081	35.493	0.000	0.016	47.139	0.007	0.000	0.704	0.856	96.532	NS97-387-6-1	c	
147	0.000	1.094	10.125	1.062	35.350	0.003	0.029	47.251	0.011	0.018	0.662	0.843	96.447	NS97-387-6-2	r	
148	0.000	1.102	8.873	1.122	35.200	0.040	0.016	46.115	0.067	0.015	0.569	0.430	93.540	NS97-74-c1-1		
149	0.000	1.067	9.020	1.203	35.384	0.021	0.001	46.275	0.068	0.011	0.536	0.462	94.043	NS97-74-c1-2		
150	0.000	1.189	9.148	1.403	35.718	0.002	0.011	47.098	0.000	0.036	0.557	0.352	95.514	NS97-74-c1-3		
151	0.000	1.197	8.975	1.380	35.927	0.002	0.027	47.229	0.000	0.011	0.515	0.394	95.657	NS97-74-c1-4		
152	0.000	1.057	9.170	1.383	34.338	0.009	0.033	47.377	0.000	0.018	0.795	0.276	94.454	NS97-74-c1-5		
153	0.003	0.822	9.316	1.653	33.920	0.003	0.033	48.065	0.023	0.022	1.021	0.322	95.201	NS97-74-c1-6		
154	0.000	1.112	9.015	1.181	35.236	0.006	0.044	47.088	0.000	0.013	0.636	0.322	94.652	NS97-74-c2-1		
155	0.000	1.010	9.086	2.396	34.448	0.024	0.034	45.722	0.021	0.021	0.943	0.326	94.026	NS97-74-c2-2		
156	0.000	1.129	9.341	1.164	35.361	0.012	0.000	46.594	0.000	0.000	0.517	0.318	94.433	NS97-74-c2-3		
157	0.000	1.209	9.164	1.208	35.195	0.007	0.031	46.077	0.000	0.004	0.507	0.374	93.774	NS97-74-c2-4		
158	0.000	1.189	8.935	1.219	35.779	0.006	0.013	48.325	0.068	0.000	0.678	0.310	96.521	NS97-74-c2-5		
159	0.000	1.124	9.089	1.161	35.308	0.000	0.053	48.067	0.002	0.000	0.723	0.345	95.872	NS97-74-c2-6		
160	0.000	1.057	9.208	1.393	35.016	0.000	0.037	46.998	0.000	0.009	0.663	0.318	94.699	NS97-74-c3-1		
161	0.000	1.072	9.210	1.460	34.899	0.013	0.061	47.248	0.000	0.024	0.716	0.264	94.964	NS97-74-c3-2		
162	0.000	1.007	9.244	1.491	33.733	0.000	0.031	47.994	0.000	0.020	0.940	0.267	94.727	NS97-74-c3-3		
163	0.000	1.006	9.351	1.544	34.250	0.000	0.022	48.348	0.000	0.039	0.964	0.293	95.817	NS97-74-c3-4		*
164	0.000	1.177	9.041	1.312	35.805	0.000	0.049	46.832	0.024	0.003	0.508	0.476	95.227	NS97-74-c3-5		
165	0.000	1.085	8.816	1.356	35.065	0.000	0.029	47.066	0.000	0.008	0.581	0.359	94.365	NS97-74-c3-6		
166	0.000	0.868	9.439	1.482	34.694	0.018	0.017	46.914	0.008	0.038	0.686	0.280	94.440	NS97-74-c4-1		
167	0.000	1.054	9.167	1.587	34.528	0.000	0.041	46.956	0.026	0.046	0.722	0.321	94.448	NS97-74-c4-2		
168	0.000	1.109	9.138	1.473	34.665	0.100	0.044	46.146	0.036	0.000	0.666	0.310	93.664	NS97-74-c4-3		
169	0.000	1.249	9.201	1.430	34.926	0.087	0.039	46.804	0.027	0.045	0.630	0.239	94.657	NS97-74-c4-4		
170	0.000	1.125	9.361	1.332	35.795	0.055	0.065	46.903	0.014	0.000	0.535	0.341	95.514	NS97-74-c4-5		
171	0.000	0.906	9.636	1.531	34.524	0.030	0.039	47.497	0.000	0.000	0.739	0.339	95.234	NS97-74-c4-6		
172	0.000	1.032	9.038	1.489	35.605	0.027	0.007	47.905	0.022	0.028	0.726	0.333	96.206	NS97-326-c1-1		
173	0.000	1.014	9.239	1.661	35.300	0.000	0.000	47.660	0.000	0.027	0.661	0.302	95.864	NS97-326-c1-2		
174	0.000	1.153	9.014	1.408	36.003	0.000	0.018	46.865	0.000	0.008	0.508	0.372	95.349	NS97-326-c1-3		
175	0.000	1.093	9.283	1.364	35.302	0.002	0.023	47.414	0.032	0.006	0.602	0.212	95.333	NS97-326-c1-4		
176	0.000	0.938	9.495	1.535	34.653	0.012	0.000	47.375	0.004	0.044	0.726	0.274	95.053	NS97-326-c1-5		
177	0.000	0.936	9.470	1.816	34.990	0.006	0.029	48.044	0.005	0.025	0.775	0.313	96.408	NS97-326-c1-6		
178	0.000	1.217	9.130	1.325	36.257	0.000	0.035	47.203	0.004	0.009	0.481	0.374	96.035	NS97-326-c2-1		
179	0.000	1.097	9.264	1.493	35.651	0.013	0.029	47.396	0.000	0.000	0.534	0.315	95.789	NS97-326-c2-2		*
180	0.000	1.035	9.172	1.338	34.481	0.000	0.044	46.898	0.000	0.000	0.727	0.358	94.053	NS97-326-c2-3		

181	0.000	0.921	9.265	1.397	33.931	0.000	0.011	45.676	0.025	0.000	0.623	0.328	92.177	NS97-326-c2-4		
182	0.000	1.045	9.091	1.432	34.712	0.014	0.000	47.675	0.062	0.013	0.759	0.287	95.087	NS97-326-c2-5		
183	0.000	1.085	9.237	1.348	35.414	0.017	0.000	47.079	0.008	0.018	0.609	0.314	95.125	NS97-326-c2-6		
184	0.000	1.093	9.261	1.204	35.447	0.013	0.020	46.871	0.028	0.004	0.611	0.296	94.845	NS97-326-c3-1		
185	0.000	1.050	9.450	1.287	35.821	0.000	0.012	46.339	0.007	0.000	0.433	0.293	94.692	NS97-326-c3-2		
186	0.000	0.944	9.429	1.443	34.996	0.008	0.017	47.166	0.044	0.004	0.706	0.286	95.041	NS97-326-c3-3		
187	0.000	1.026	9.333	1.738	34.972	0.009	0.037	47.179	0.004	0.015	0.663	0.304	95.278	NS97-326-c3-4		
188	0.000	1.023	9.347	1.310	35.241	0.000	0.044	47.367	0.000	0.000	0.685	0.355	95.372	NS97-326-c3-5		
189	0.000	1.156	9.253	1.280	35.999	0.000	0.050	47.215	0.033	0.000	0.595	0.317	95.898	NS97-326-c3-6		
190	0.000	1.154	9.242	1.446	35.841	0.000	0.041	47.338	0.007	0.005	0.632	0.323	96.029	NS97-326-c4-1		
191	0.000	1.120	9.246	1.543	36.516	0.000	0.036	47.955	0.007	0.006	0.557	0.291	97.277	NS97-326-c4-2		
192	0.000	1.130	9.138	1.297	35.827	0.018	0.044	47.712	0.000	0.000	0.595	0.274	96.031	NS97-326-c4-3		
193	0.000	0.844	9.613	1.351	35.368	0.011	0.016	46.710	0.021	0.022	0.602	0.529	95.085	NS97-326-c4-4		
194	0.000	1.169	9.389	1.210	35.915	0.000	0.030	47.099	0.000	0.003	0.491	0.319	95.625	NS97-326-c4-5		
195	0.000	1.108	9.477	1.366	35.369	0.002	0.012	46.612	0.000	0.022	0.582	0.253	94.803	NS97-326-c4-6		
196	0.000	0.598	10.084	1.558	34.249	0.000	0.016	46.898	0.001	0.016	0.828	0.371	94.619	NS97-119-c1-1		
197	0.000	0.713	10.073	1.411	35.237	0.007	0.063	46.999	0.000	0.031	0.598	0.400	95.530	NS97-119-c1-2		
198	0.000	0.476	10.230	1.737	33.051	0.000	0.004	48.518	0.000	0.015	1.148	0.578	95.757	NS97-119-c1-3		
199	0.000	0.610	9.982	1.522	34.715	0.004	0.058	46.884	0.050	0.023	0.739	0.475	95.061	NS97-119-c1-4		
200	0.000	0.537	9.870	1.618	34.313	0.000	0.022	47.908	0.042	0.008	0.929	0.365	95.612	NS97-119-c1-5		
201	0.000	0.614	9.894	1.494	34.616	0.000	0.027	46.950	0.007	0.000	0.676	0.491	94.769	NS97-119-c1-6		
202	0.000	0.718	9.993	1.384	35.468	0.008	0.011	46.842	0.036	0.000	0.548	0.379	95.385	NS97-119-c2-1		
203	0.000	0.718	9.985	1.506	35.429	0.000	0.035	47.029	0.017	0.003	0.600	0.430	95.752	NS97-119-c2-2		*
204	0.000	0.709	9.754	1.454	34.622	0.008	0.006	46.438	0.030	0.000	0.638	0.339	93.996	NS97-119-c2-3		
205	0.000	0.645	9.738	1.550	34.593	0.000	0.032	46.715	0.032	0.000	0.757	0.368	94.430	NS97-119-c2-4		
206	0.000	0.668	9.910	1.398	34.906	0.002	0.044	46.670	0.035	0.005	0.618	0.535	94.791	NS97-119-c2-5		
207	0.000	0.613	9.482	1.518	33.963	0.002	0.032	46.279	0.084	0.000	0.712	0.452	93.137	NS97-119-c2-6		
208	0.000	0.295	15.562	0.259	17.995	0.002	0.000	66.093	0.000	0.047	0.000	0.004	100.257	NS97-119-c3-1		
209	0.000	0.197	16.033	0.235	18.269	0.000	0.002	65.354	0.000	0.013	0.021	0.009	100.133	NS97-119-c3-2		
210	0.000	0.661	9.943	1.524	34.844	0.000	0.027	46.600	0.017	0.000	0.657	0.559	94.832	NS97-119-c3-3		
211	0.000	0.683	9.955	1.471	35.435	0.000	0.041	46.752	0.000	0.009	0.688	0.575	95.609	NS97-119-c3-4		
212	0.000	0.647	10.094	1.570	35.338	0.000	0.018	46.559	0.007	0.059	0.577	0.513	95.382	NS97-119-c3-5		
213	0.000	0.697	9.968	1.556	34.873	0.012	0.000	46.976	0.003	0.034	0.632	0.411	95.159	NS97-119-c3-6		

Legend:
Loc. (Location): c=center, m=middle (between center and rim), r=rim of grain, blank means unknown
? (Used?): *=data used in calculations

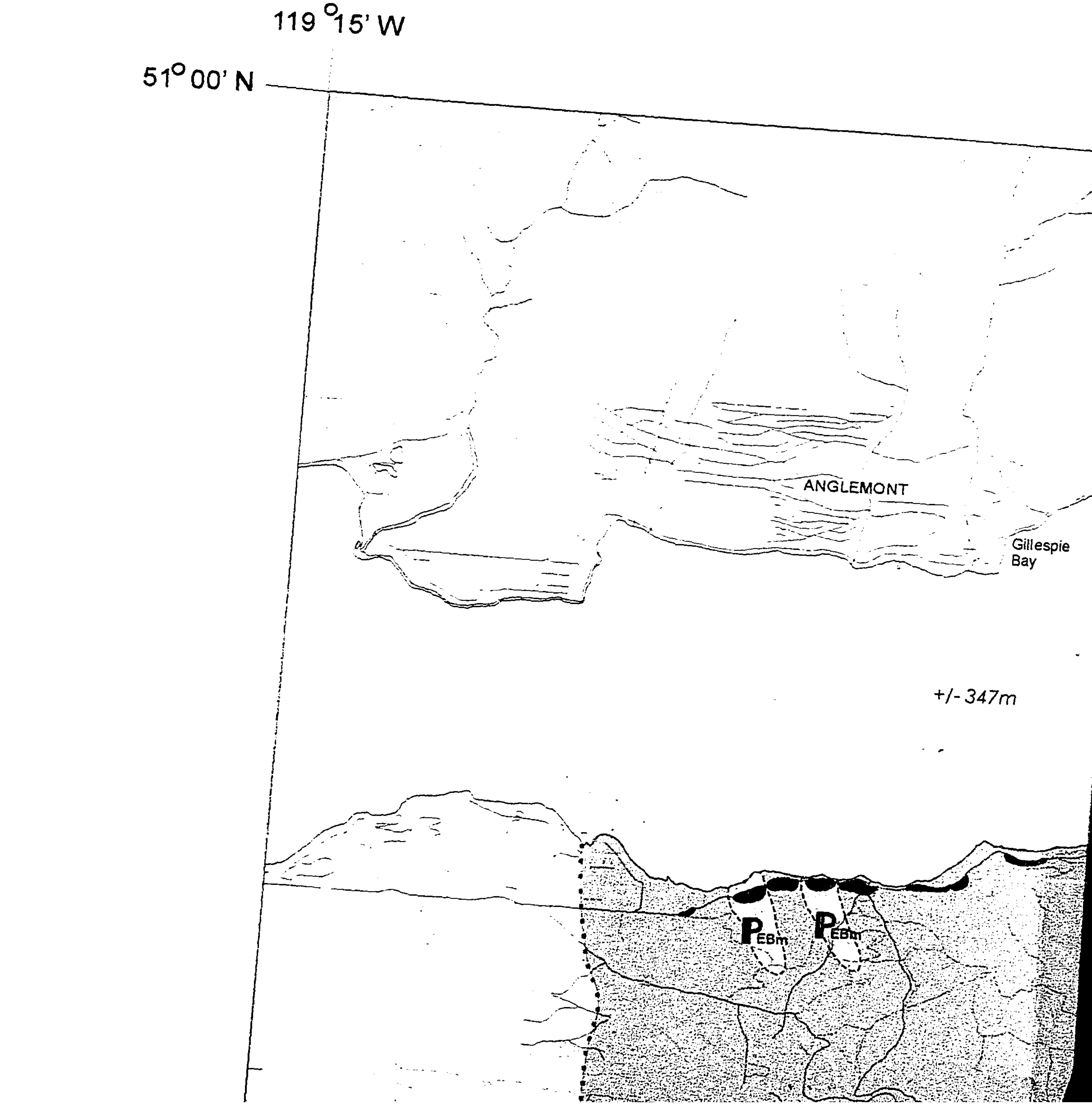

119°15' W
51°00' N
ANGLEMONT
Gillespie Bay
+/- 347m
PEBm
PEBm

Geological Map of the Shuswap La

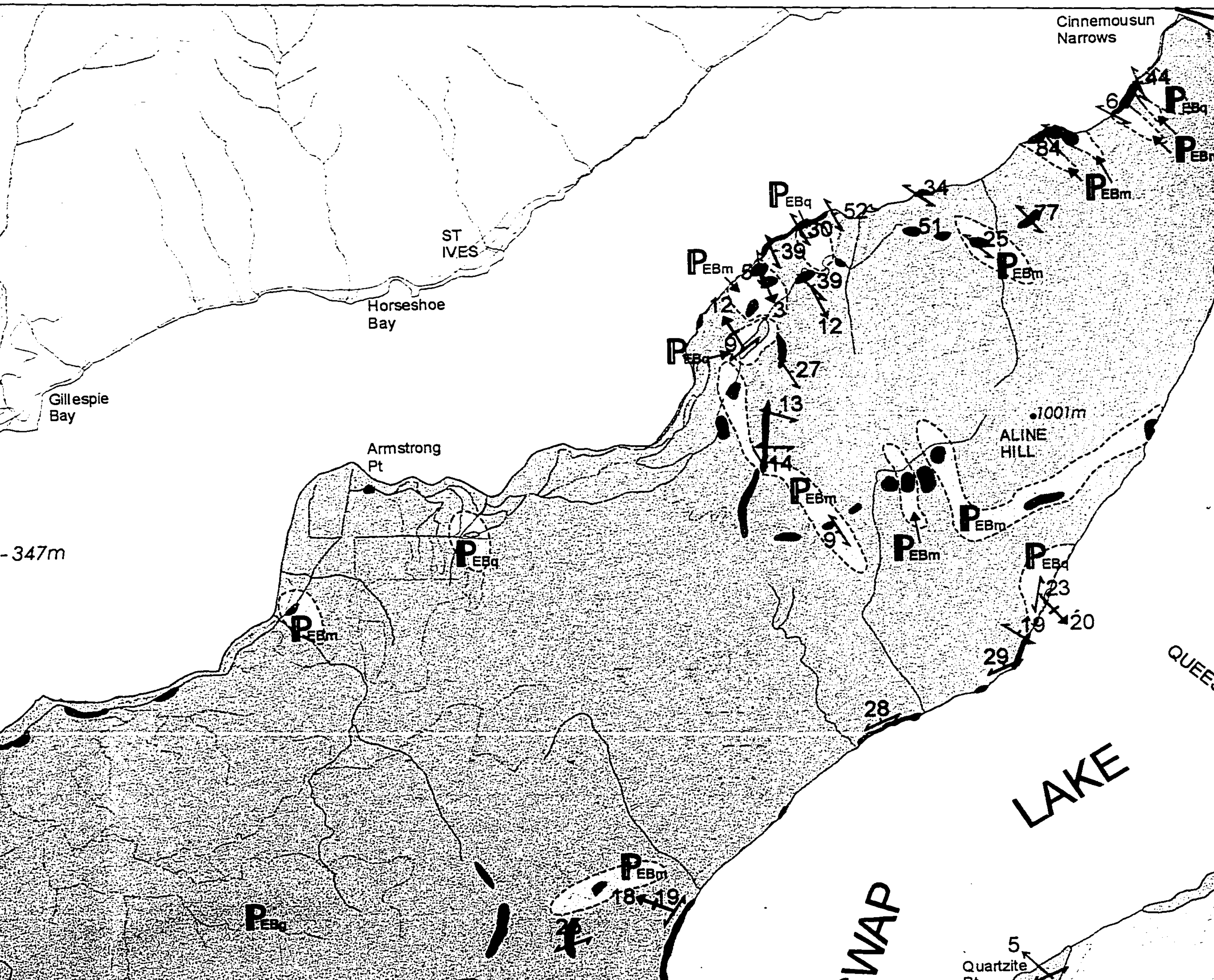

British Columbia

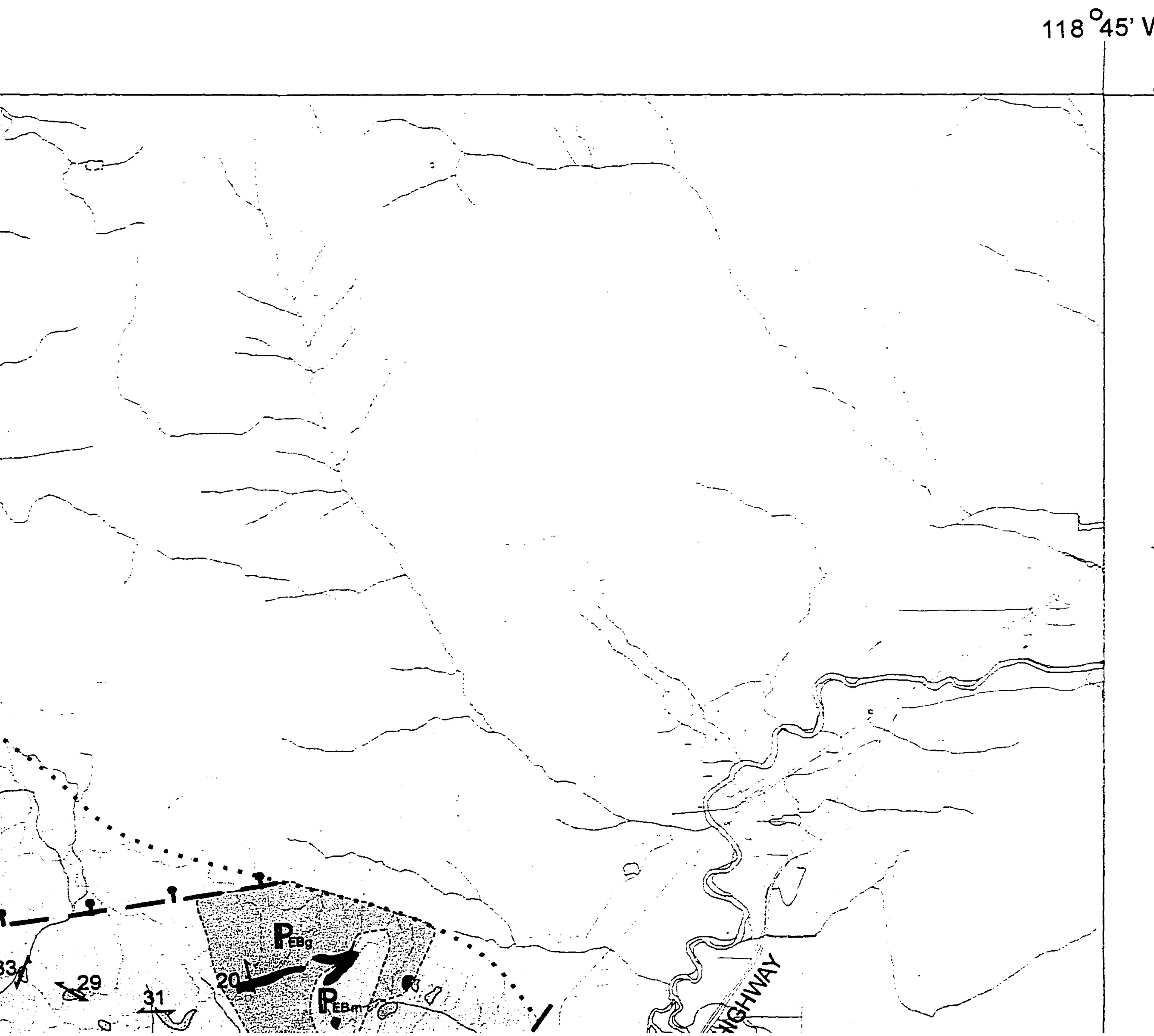

45' W

51° 00' N

GEOLOGICAL UNITS

DEVONIAN

Mount Fowler Batholith

hornblende-biotite granite to granodiorite
Phases (marked on map with letters):
Dg - medium grained hornblende-biotite granite
Dgm - (mafic) fine grained hornblende-biotite granite to granodiorite
Dgf - (felsic) medium grained granite +/- hornblende, +/- biotite
Dgp - pegmatitic granite +/- hornblende, +/- biotite

PALEOZOIC

Queest Mountain assemblage

P(?)QMs — garnet-biotite-muscovite-feldspar-quartz schist +/- staurolite

QMmc — calcsilicate schist +/- garnet, +/- tremolite, +/- diopside and marble

Mount Ida Group

Eagle Bay Formation

EBg — greenstones: chlorite schist, chlorite-sericite schist, amphibolite

PEBq — biotite-muscovite-feldpar-quartz schist, quartzite

EBm — calcareous mica schist, marble

Sicamous Formation

S — black and white graphitic marble

PROTEROZOIC

Silver Creek Formation

muscovite-biotite-feldspar-quartz schist

766m
PEBm
PEBg
1230m
47
PEBq
PEBq
1639m
PSC
24
24
31
42
PSCc
47
SALMON ARM

SHUSWAP
Quartzite Pt
TILLI LANDING
Hermit Bay
+/- 347m
Hungry Cove
Old Town Bay
937m
Bastion Bay
EAGLE RIVER
SICAMOUS
Canoe Pt
1005m
MARA LAKE
+/- 347m
+/- 348m

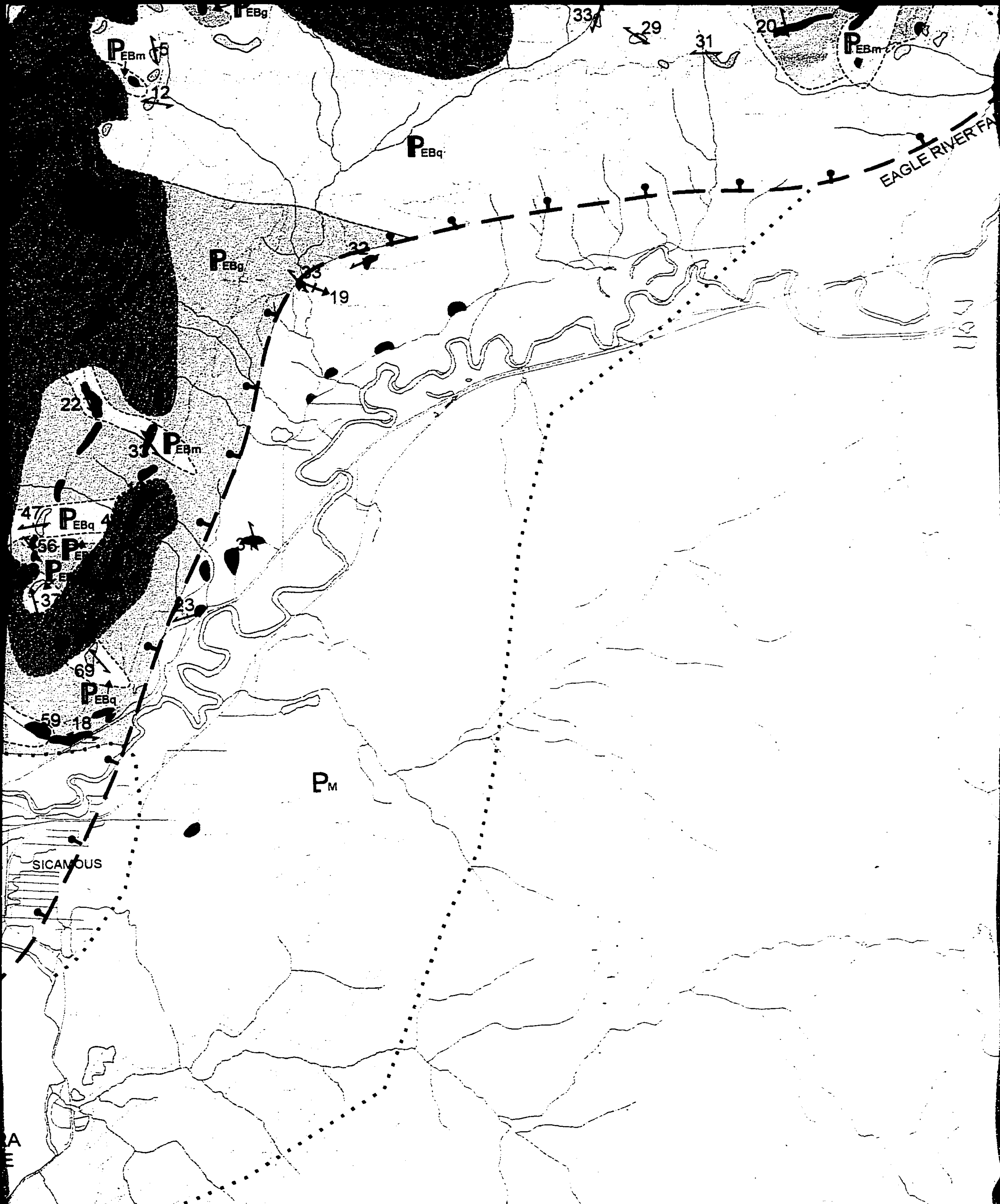

PEBg
PEBm
PEBq
EAGLE RIVER FA
SICAMOUS
PM
33
29
31
20
12
32
23
19
22
47
56
37
69
59
18

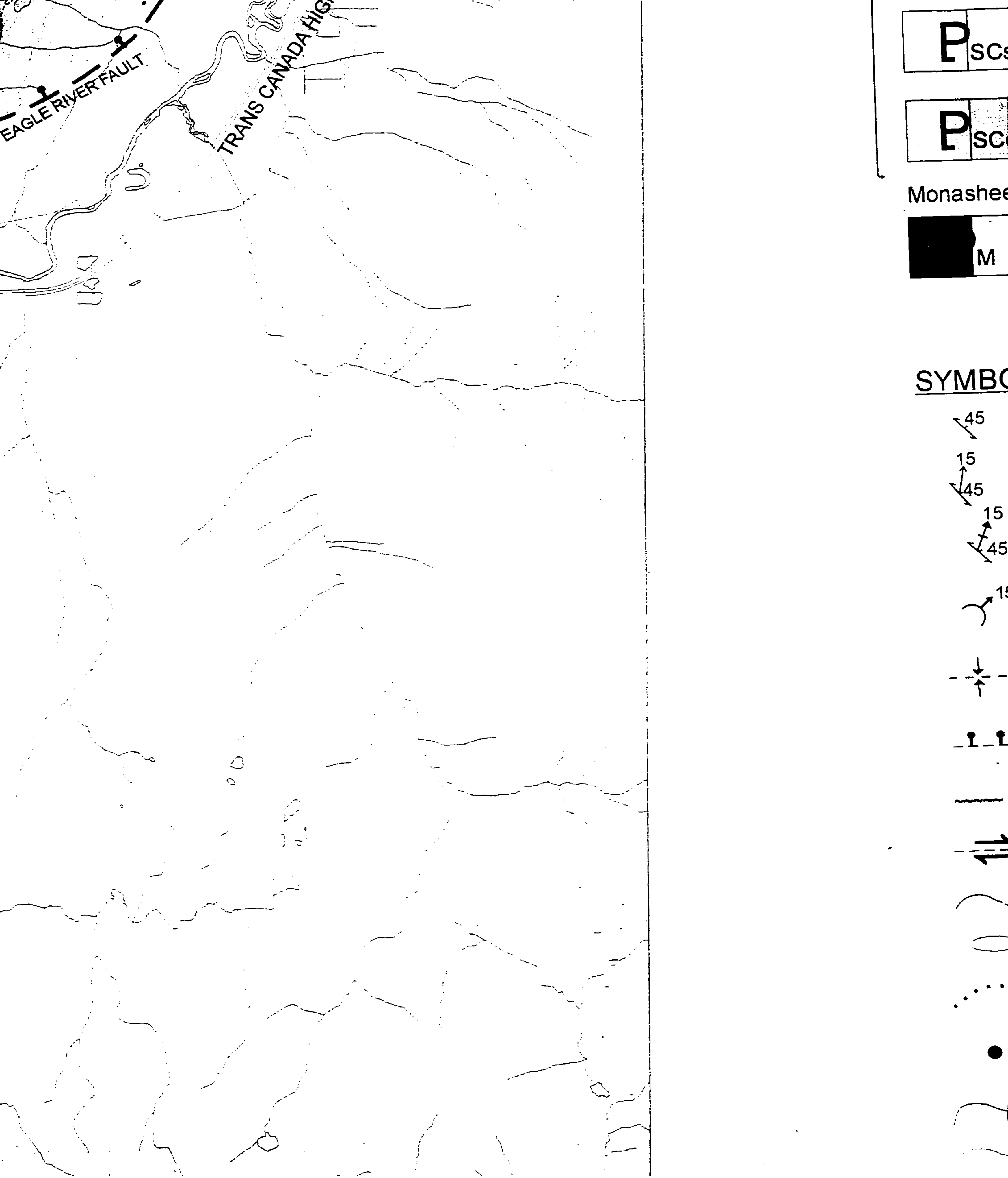

EAGLE RIVER FAULT
TRANS CANADA HIG
Monashee
SYMBO

PROTEROZOIC
Silver Creek Formation

PSCs	muscovite-biotite-feldspar-quartz schist, with abundant aplite and pegmatite sills and dykes
PSCc	calcareous mica schist

Monashee Group

M	undifferentiated Monashee gneisses

SYMBOLS

45	Strike of foliation with dip
15, 45	Trend of mineral lineation with plunge, on foliation
15, 45	Trend of crenulation lineation with plunge, on foliation
15	Trend of minor fold axis with plunge
	Axial trace of regional syncline
	Normal fault, approximate or assumed; circles in hanging wall
	Faulted geological contact, approximate or assumed
	Tear fault, assumed; arrows show direction of movement
	Geological contact, known, approximate or assumed
	Outcrop
	Boundary of mapped area
	Uranium - Lead zircon age
	Road

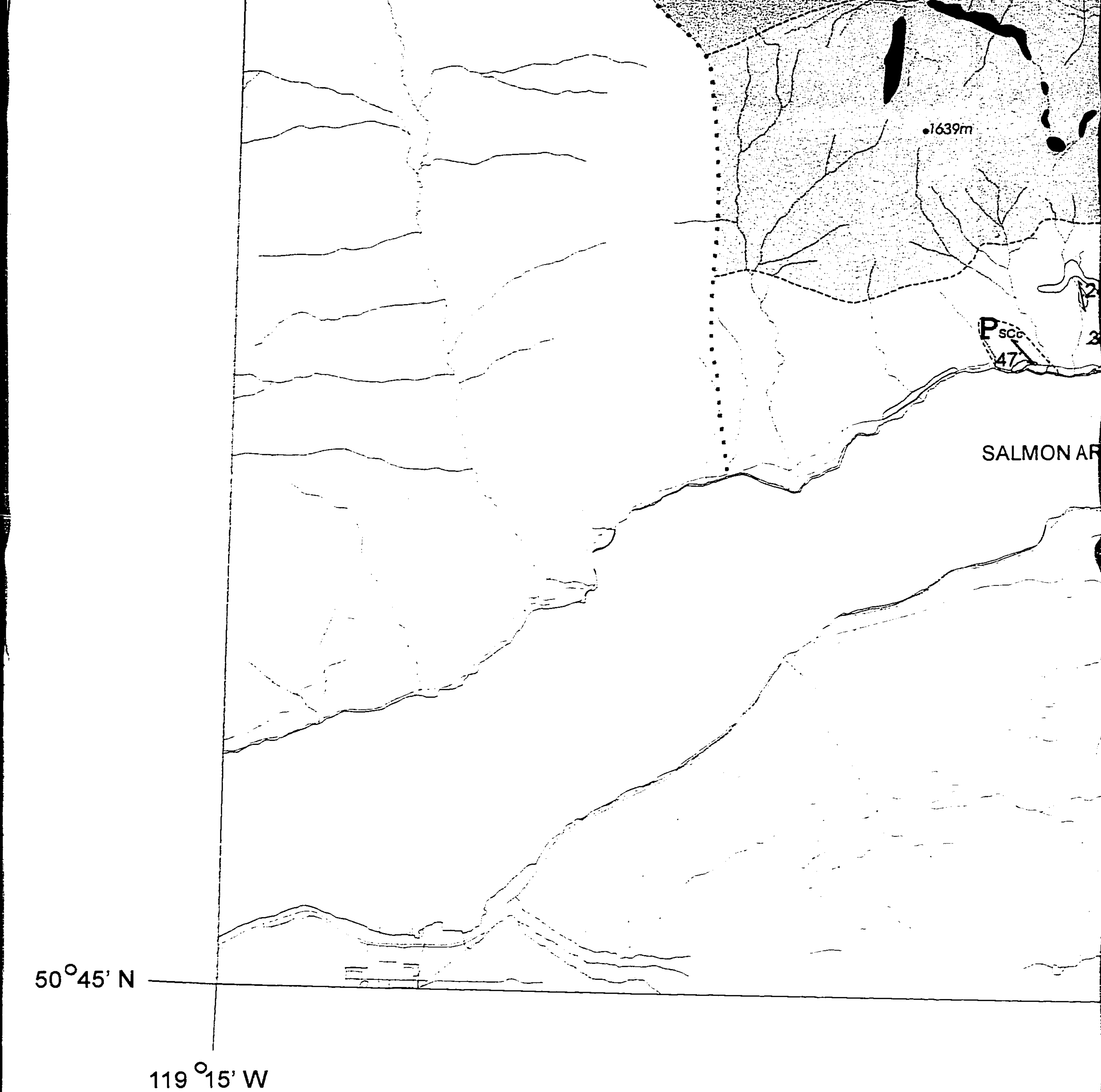

1639m
Pscc
47
SALMON AR
50°45' N
119°15' W

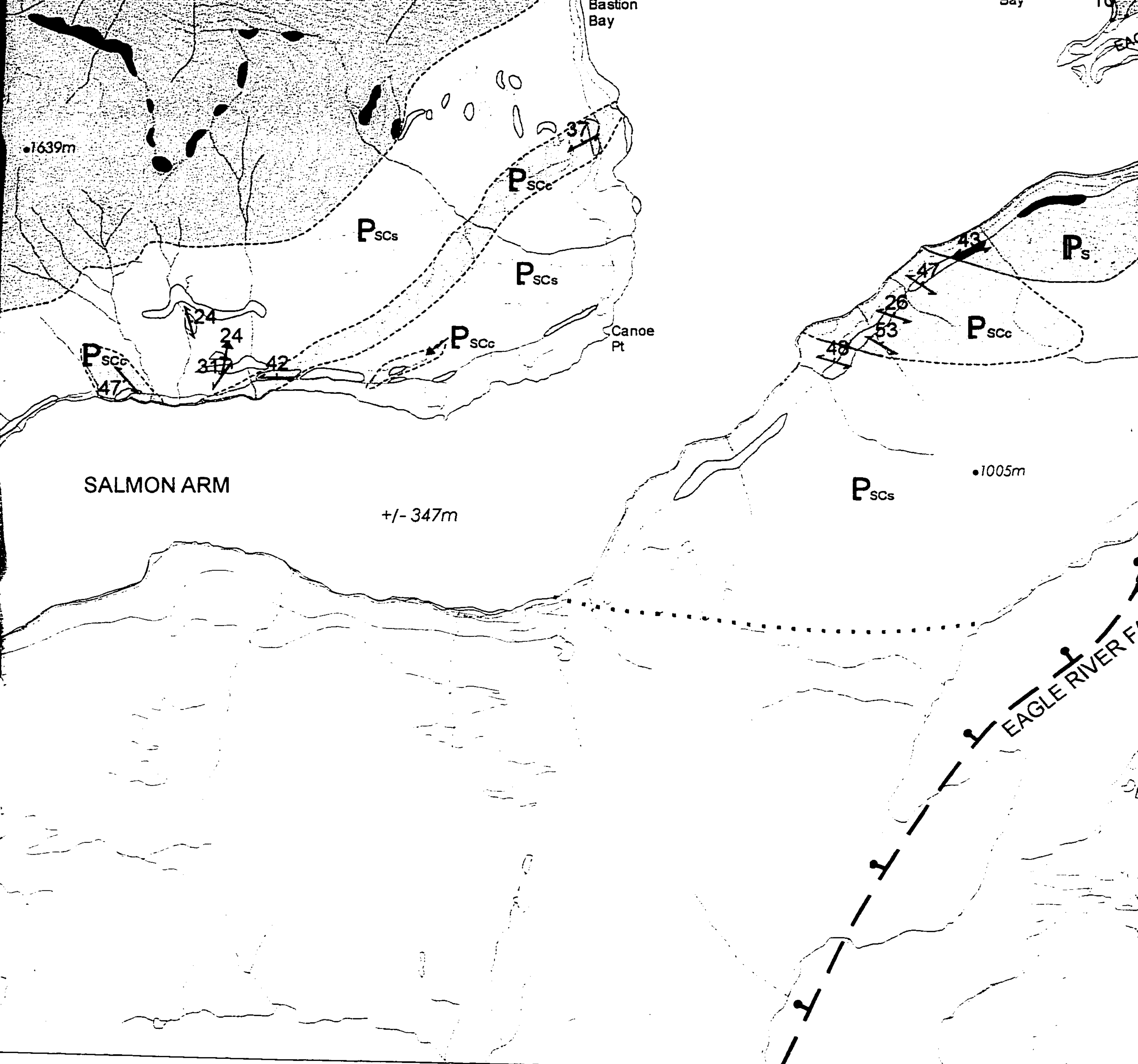
Bastion
Bay
•1639m
PSCc
PSCs
37
PSCs
24
24
31
42
PSCc
PSCc
47
Canoe
Pt
43
47
Ps
26
53
48
PSCc
SALMON ARM
+/- 347m
•1005m
PSCs
EAGLE RIVER

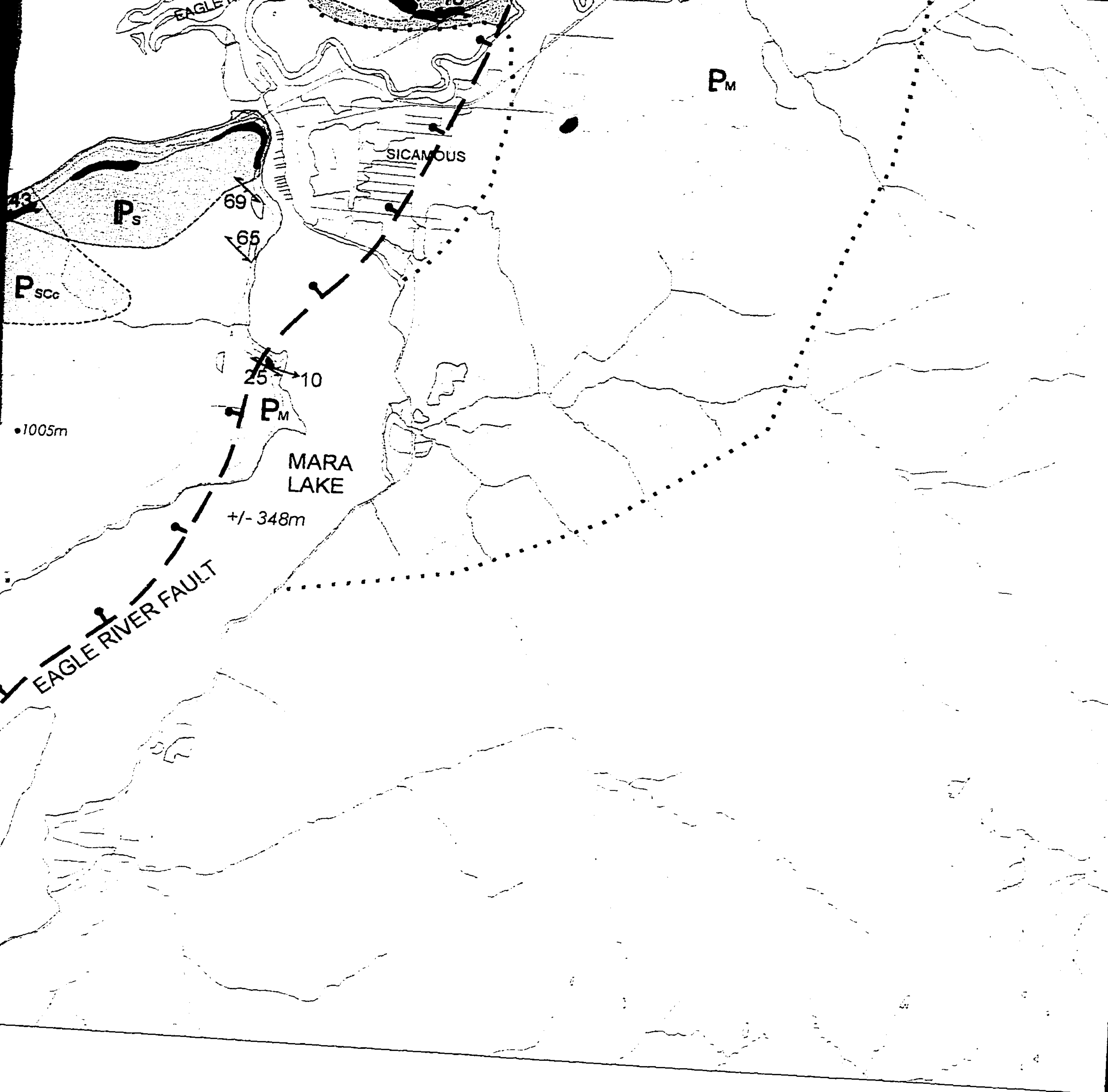

SICAMOUS
PM
Ps
PSCc
69
65
43
25
10
•1005m
MARA
LAKE
+/- 348m
EAGLE RIVER FAULT

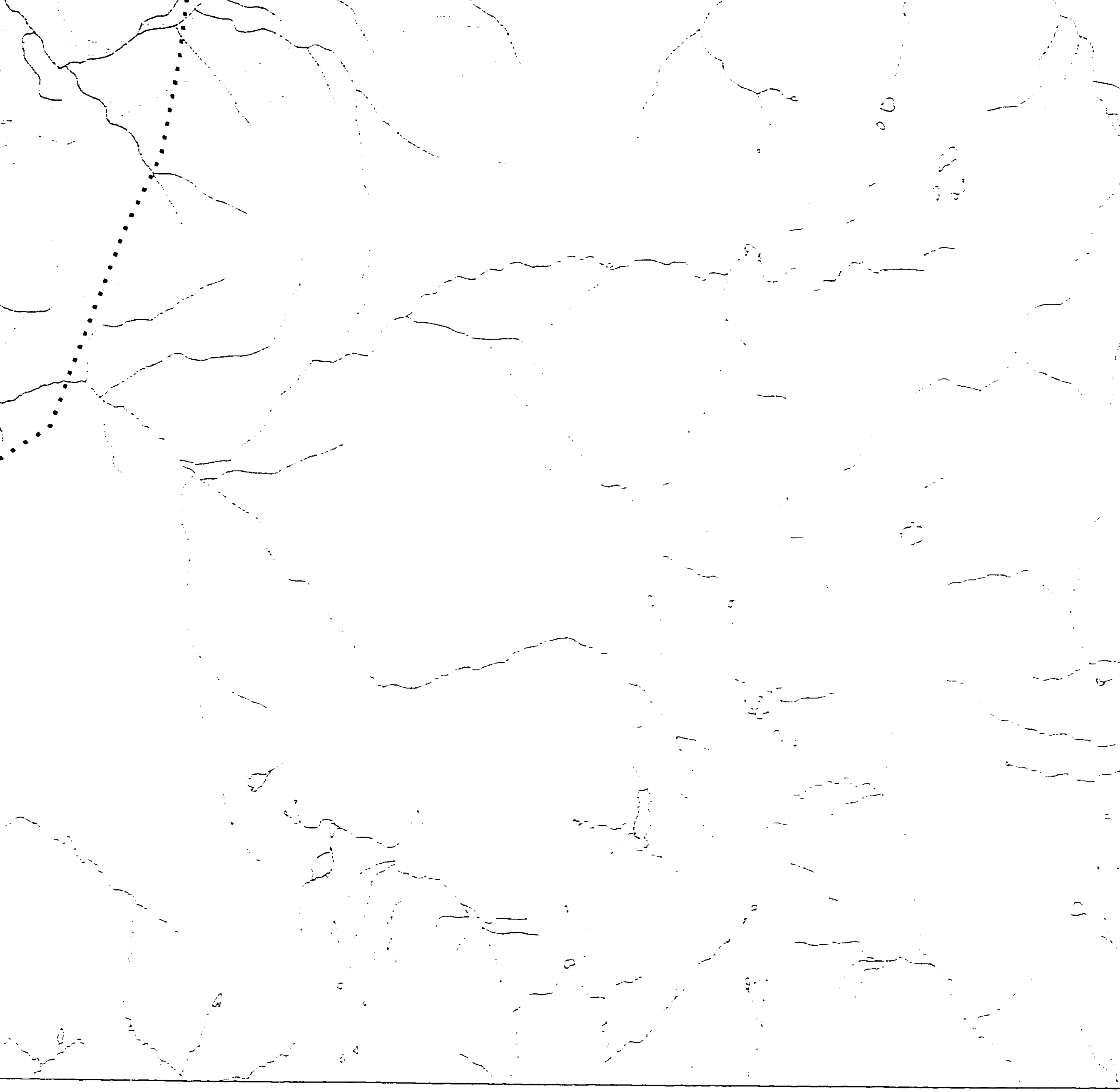

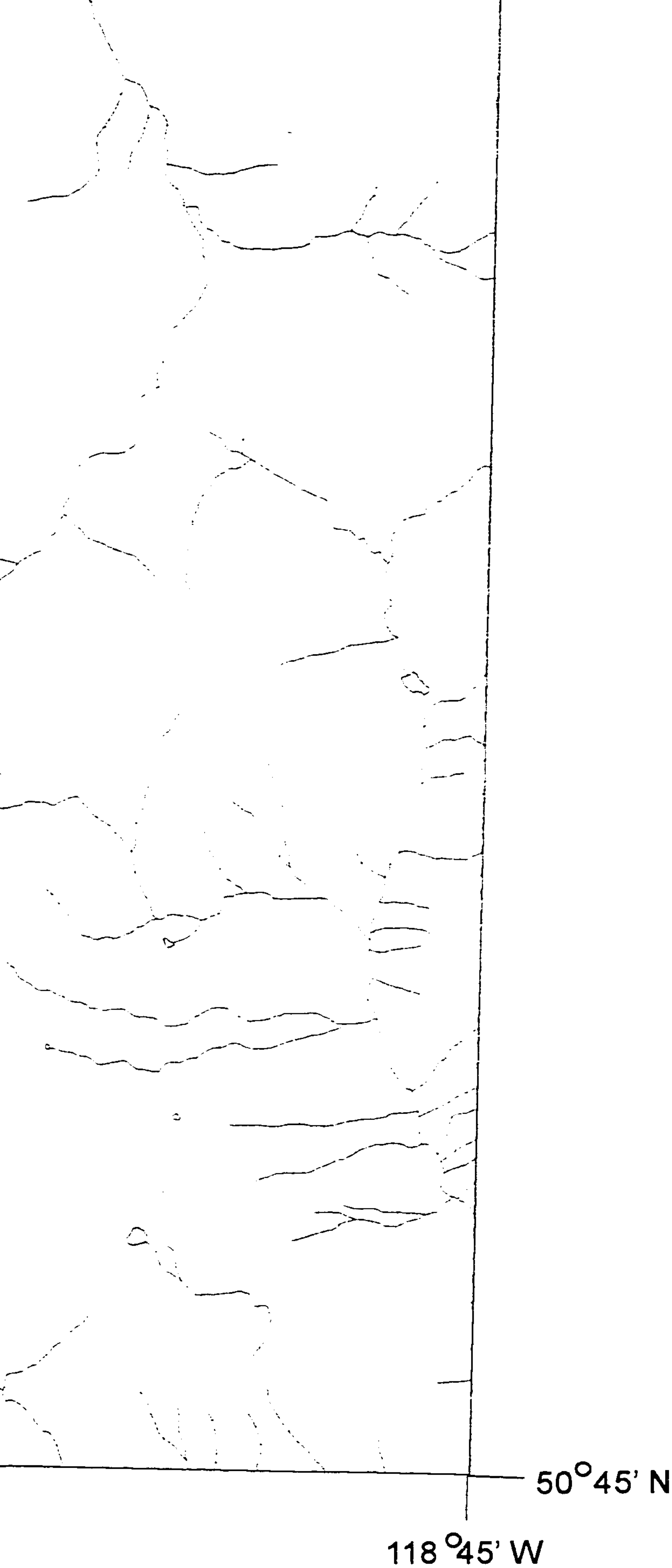

Axial trace of regional syncli

Normal fault, approximate or

Faulted geological contact, a

Tear fault, assumed; arrows

Geological contact, known, a

Outcrop

Boundary of mapped area

Uranium - Lead zircon age

Road

Limited access road, tracks,

Topographic contours (40 m

River or stream

Lake

Scale: 1:50 000

0 1 2

km

Geology by Nadya M. Slemko
University of Alberta
2000

15 Trend of minor fold axis with plunge

Axial trace of regional syncline

Normal fault, approximate or assumed; circles in hanging wall

Faulted geological contact, approximate or assumed

Tear fault, assumed; arrows show direction of movement

Geological contact, known, approximate or assumed

Outcrop

Boundary of mapped area

Uranium - Lead zircon age

Road

Limited access road, tracks, trails

Topographic contours (40 m interval)

River or stream

Lake

Scale: 1:50 000

0 1 2 4

km

Geology by Nadya M. Slemko
University of Alberta
2000

Map 2-1